



Magnetic Measurements and Imaging

J. McCord

Institute for Materials Science, Kiel University, Germany

- **Magnetic material properties (integral)**

■ Saturation magnetization	M_s	}	Static
■ Magnetic anisotropy constant(s)	K		
■ Magnetostriction constants	$\lambda_{100}, \lambda_{111}, \lambda_s$		
■ Precessional frequency	f_{res}	}	Dynamic
■ Magnetic damping parameter	α		

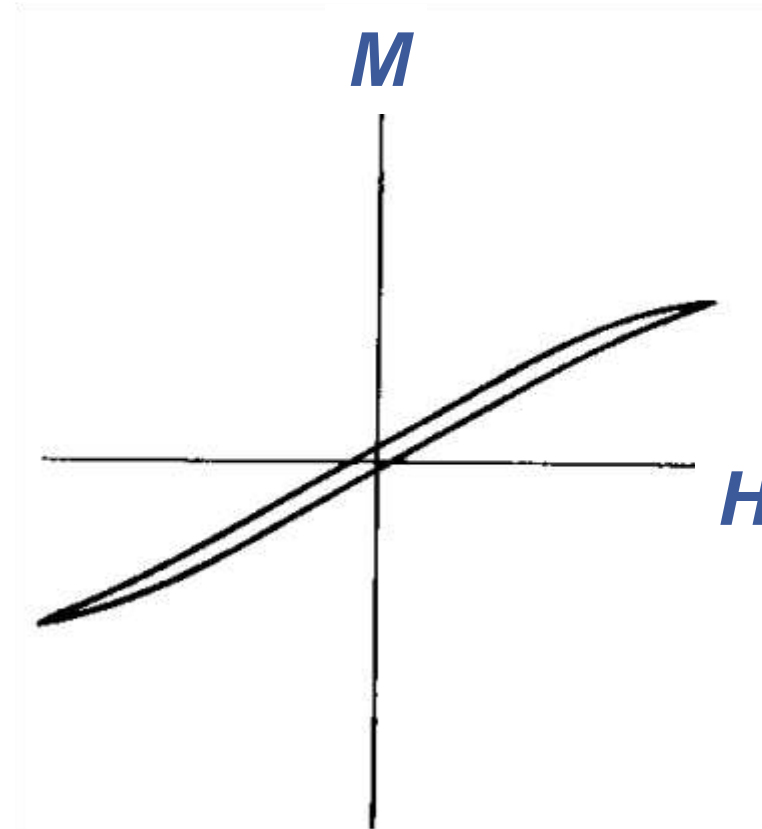
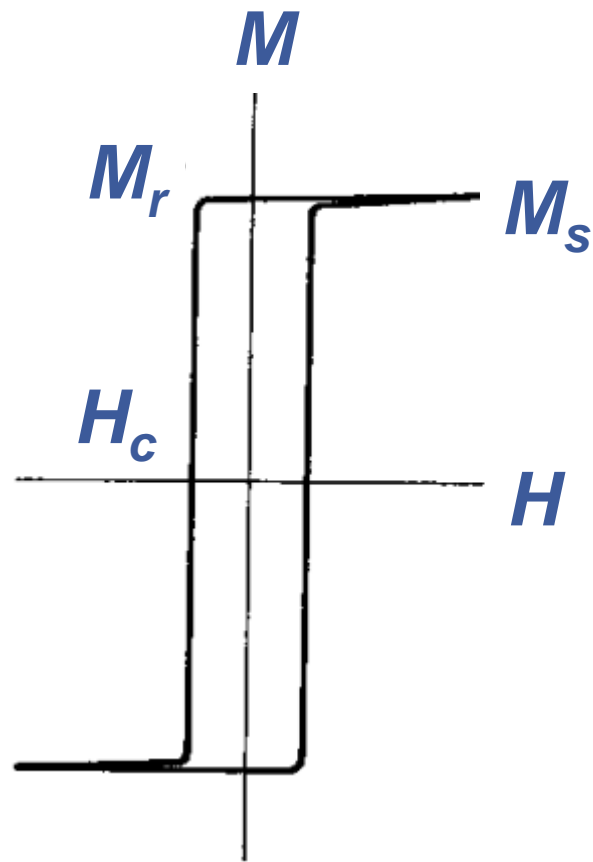
- **Magnetic imaging (spatial)**



- **Magnetic fields**
- **Quasi-static measurements**
- **Dynamic measurements**

Far from being complete!

- Quasi-static magnetic domain imaging
- Imaging of magnetization dynamics

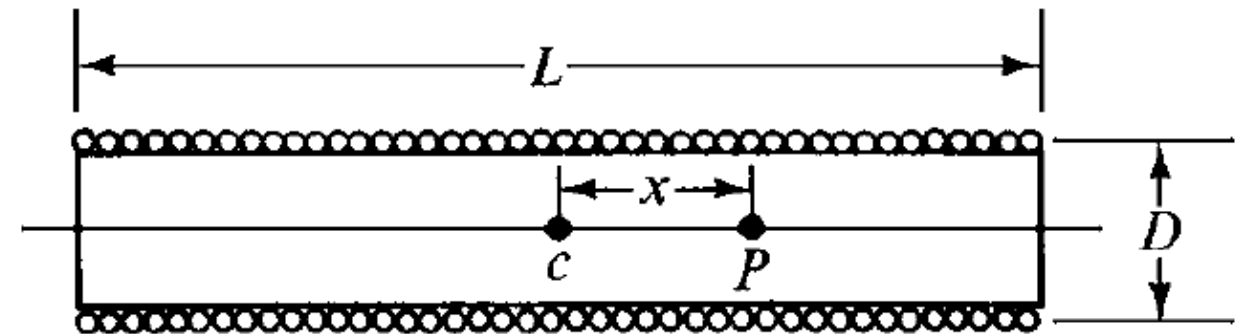


- **Magnetic field H**
- **Magnetization $M(H)$ (or flux density $B(H)$)**
 - Not an intrinsic property of the material
 - Character of $M(H)$ loop changes with sample preparation and shape

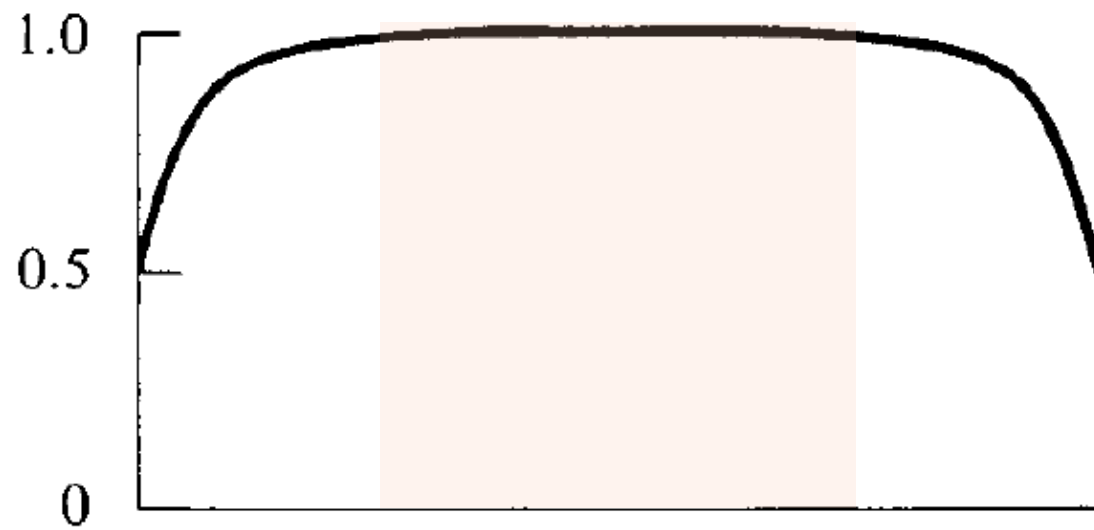


- **Various methods of producing magnetic fields**
- **Important parameters**
 - Field intensity (what kind of sample is investigated)
 - Volume (depending on sample)
 - Uniformity
- **Resistive solenoids**
- **Electromagnets**
- **Superconducting coils**
- **Pulsed magnetic fields**
- **Permanent magnets**

Solenoids



$$\frac{H}{H_{inf}}$$



Position P

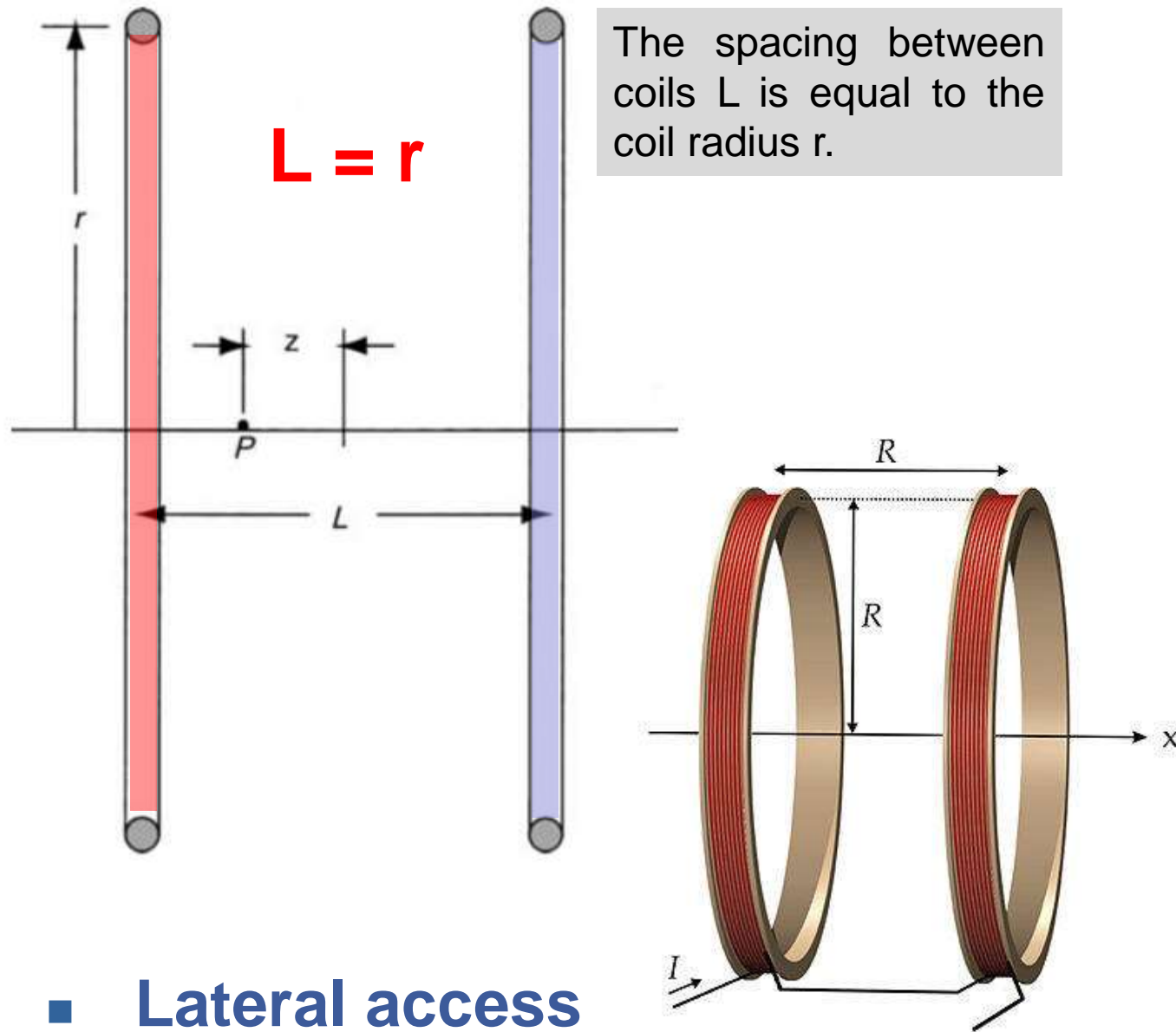
Single-layer solenoid and its magnetic field distribution.

L/D	H at Center	H at Edge of Middle Half
5	$0.9806 H_{inf}$	$0.9598 H_{inf}$
10	0.9950	0.9892
20	0.9987	0.9972
50	0.9996	0.9994

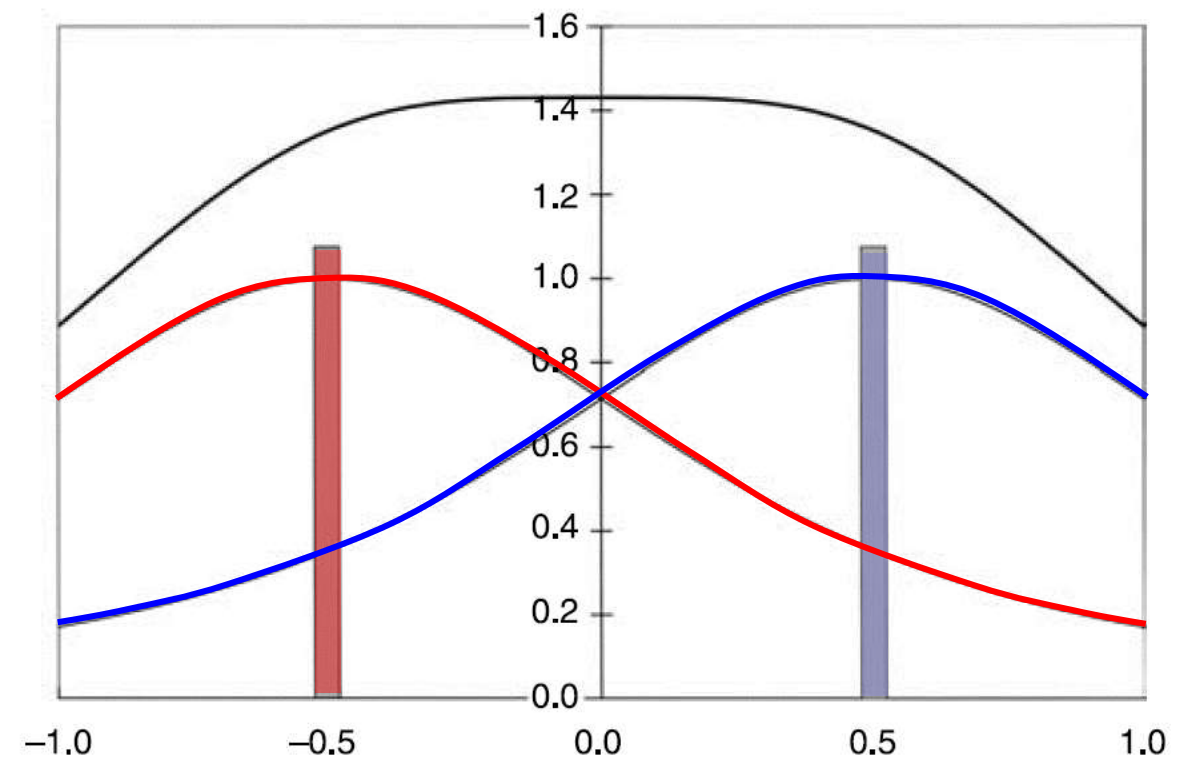
$$H = \frac{n \cdot I}{L} \left[\frac{L + 2x}{2\sqrt{D^2 + (L + 2x)^2}} + \frac{L + 2x}{2\sqrt{D^2 + (L - 2x)^2}} \right]$$

$$H_{center} (x = 0) = \frac{n \cdot I}{L} \left[\frac{L}{\sqrt{D^2 + L^2}} \right] \approx \frac{n \cdot I}{L}$$

Helmholtz coils



The spacing between coils L is equal to the coil radius r .

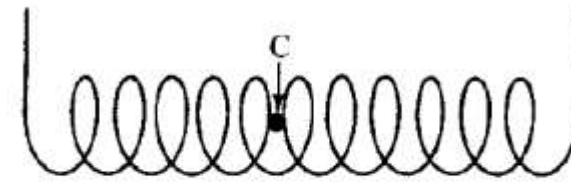


Magnetic field distribution in Helmholtz coils. Position is specified in units of the coil radius r .

- Lateral access
- High magnetic field homogeneity over large volume
- Usually small fields (smaller than solenoid)
- Investigations of soft magnetic materials

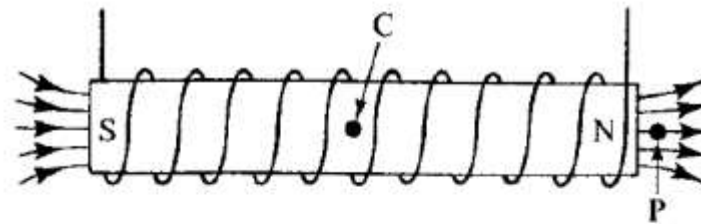
- Increasing fields of solenoids

$$B = \mu_0 H$$

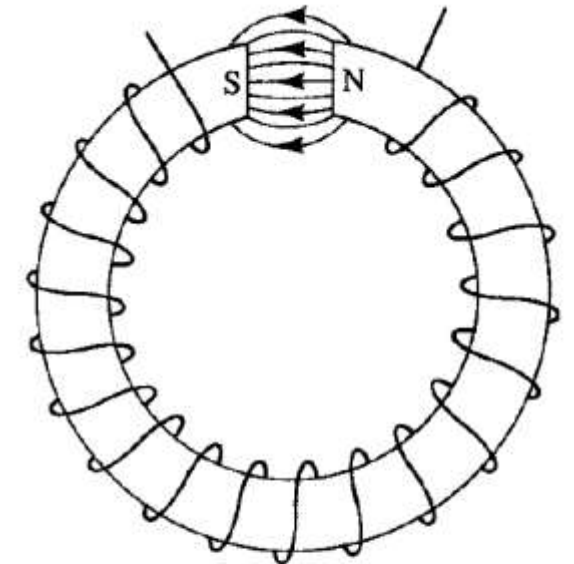


(a)

$$B = \mu_0 \mu_r H$$

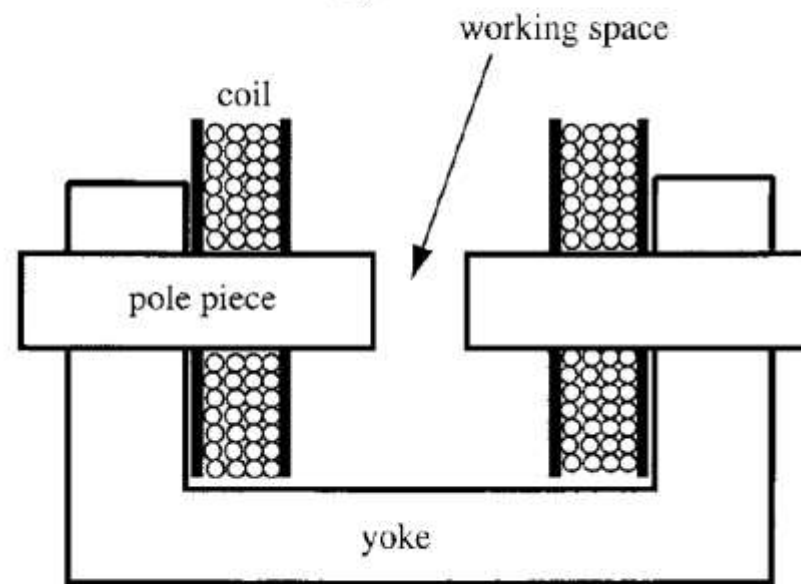


(b)

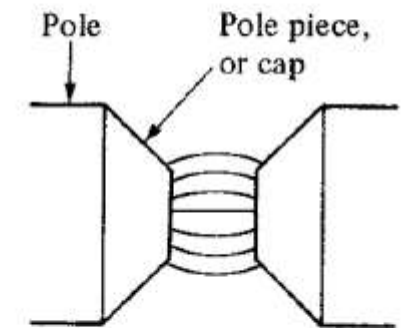


(c)

- Magnetic circuit with a yoke and two pole pieces



(d)



(e)

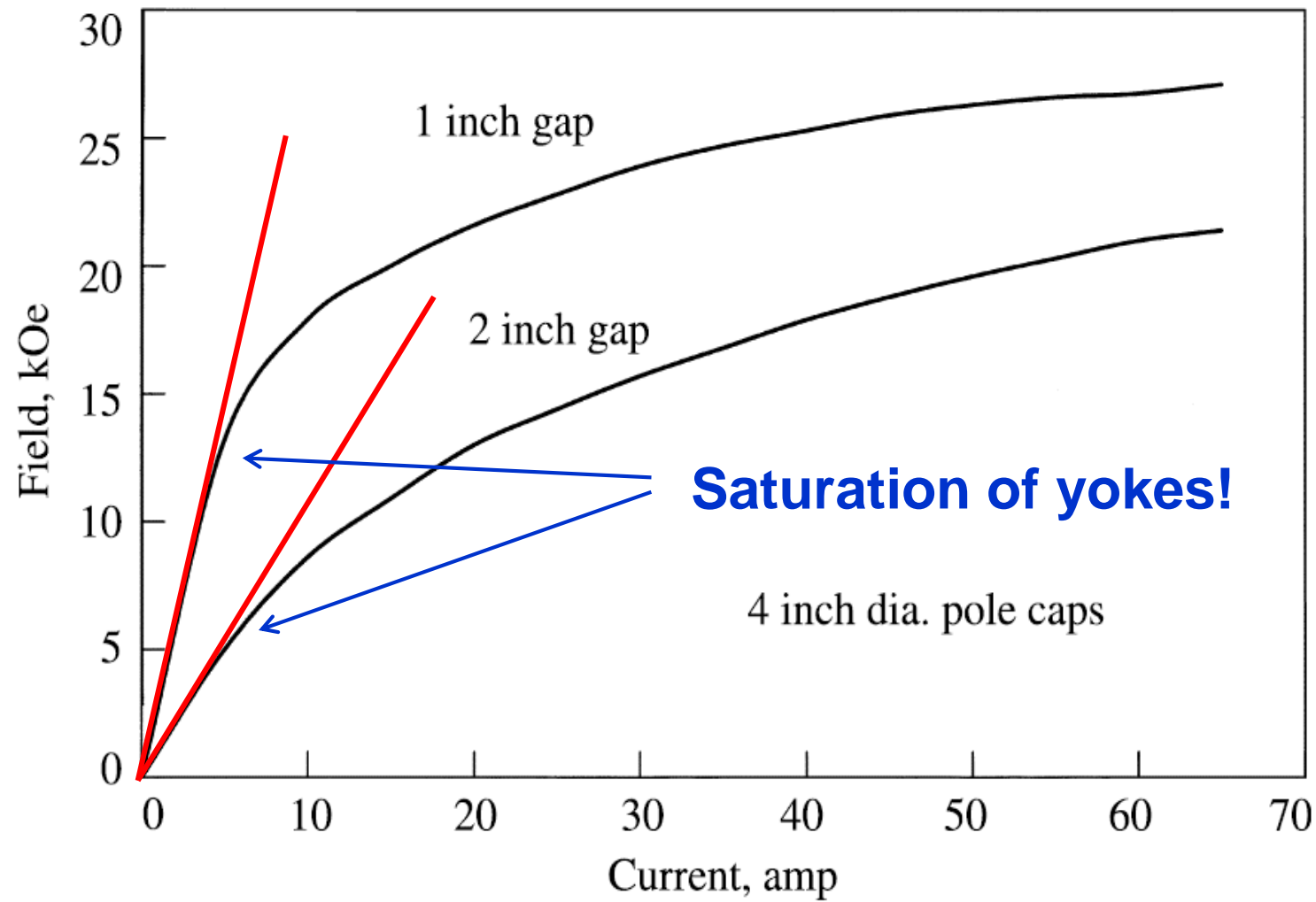
- Magnetic field generated in air gap

- **Magnetic DC fields up to 30 kOe (3 T)**
 - Higher than saturation polarization of yokes
- **Magnetic field depends on**
 - Current
 - Permeability and saturation magnetization of yoke and pole tips
 - Gap width
- **Joule heating**
 - Limited by insulation of copper wires of coils
 - Cooling of coils (water cooling)

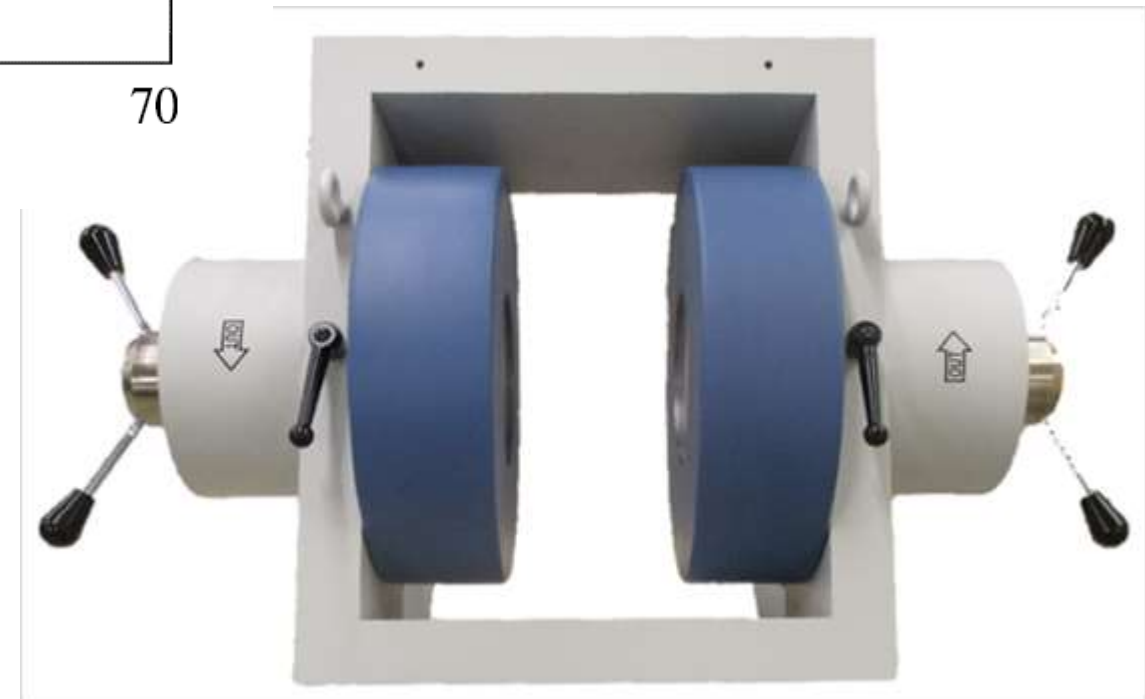
<http://www.gmw.com>



Limitations of electromagnets



Magnetic field vs. current in an electromagnet for two different gap widths.

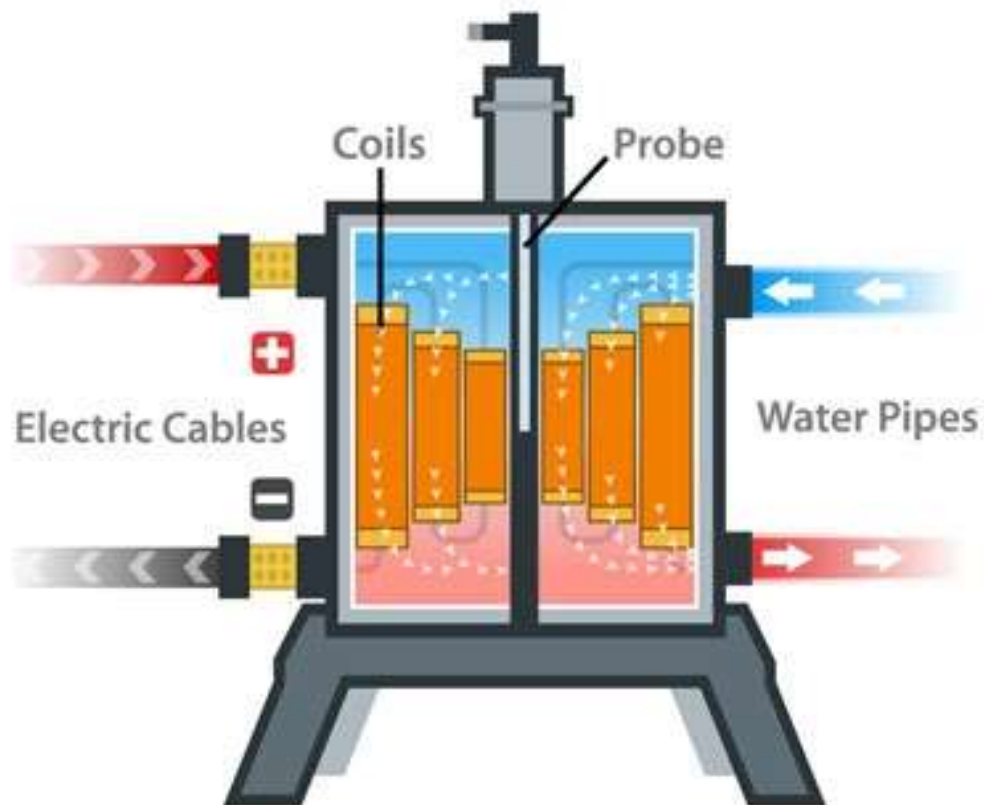


<http://www.technicoil.com>

High field solenoids (up to 45 T)



- **Magnetic DC fields up to 450 kOe (45 T)**
 - Stacked Bitter plates
 - High strength low resistivity Cu alloys
 - Axial water flow
 - Resistance to Lorentz force and magnetic clamping



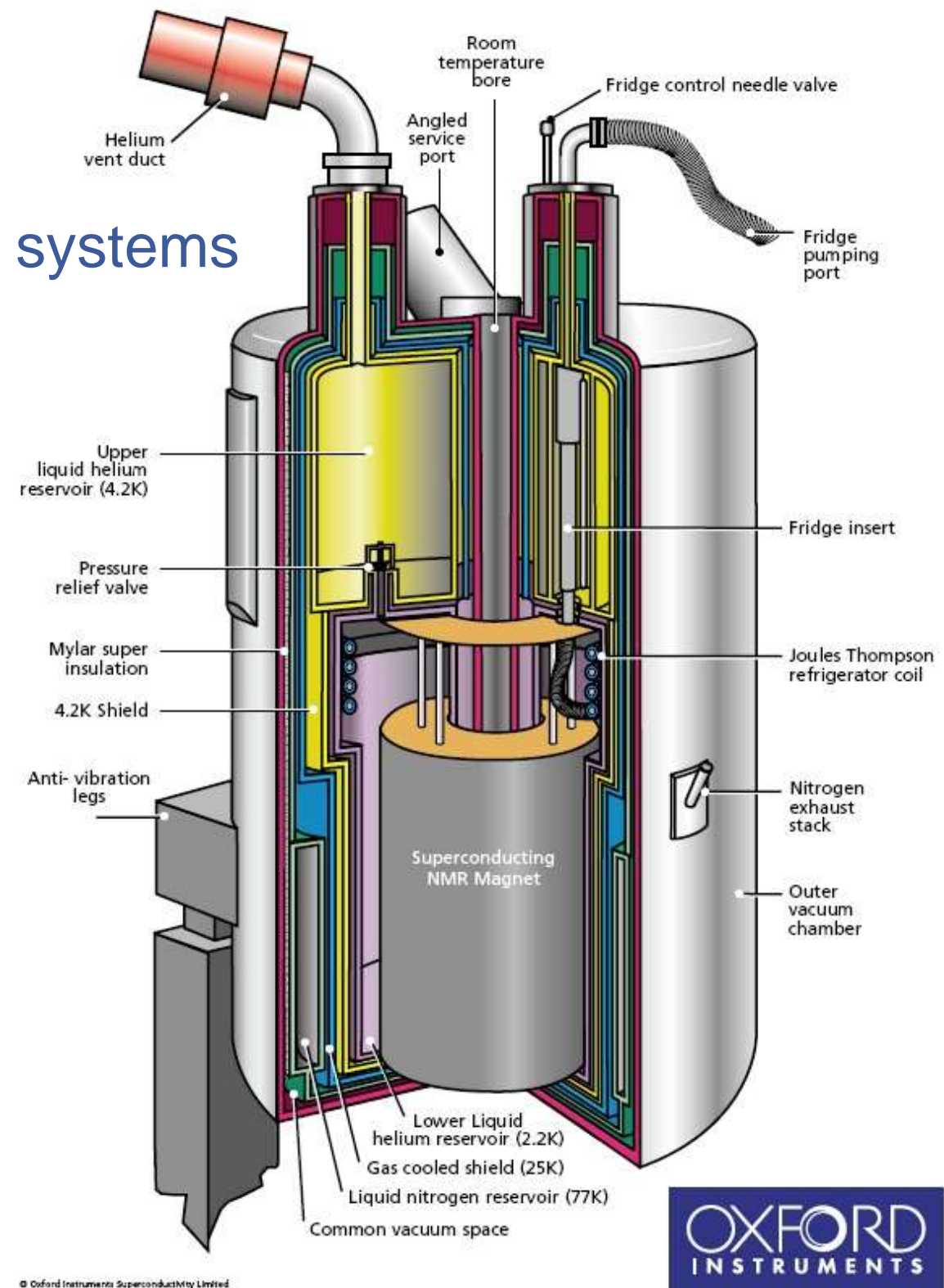
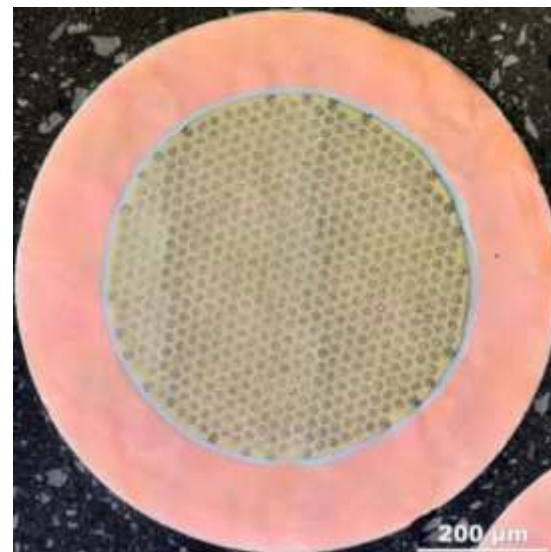
<https://nationalmaglab.org/>

Superconducting solenoids

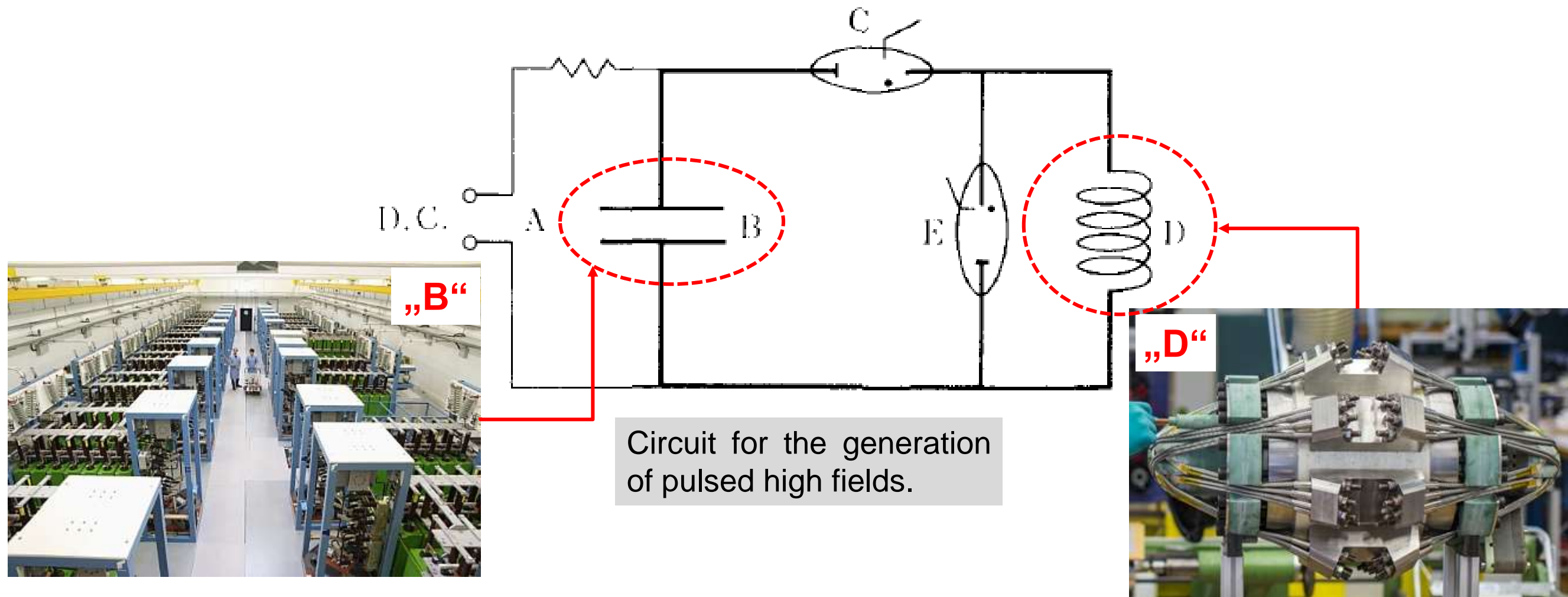


- Elimination of Joule heating
- Applications (incl. cryostats)
 - Nuclear magnetic resonance (NMR) systems
 - Scientific magnetometers (SQUID)
- Low power to maintain magnetic field
- High inductance – slow ramp rates
- Materials (high critical field H_c !)
 - Nb_3Sn – $H_c = 22 \text{ T}$ @ 4.2 K
 - NbZr or NbTi

20 T @ 4.2 K
Current 120 A
Voltage < 10 V
Inductance $L \approx 240 \text{ H}$

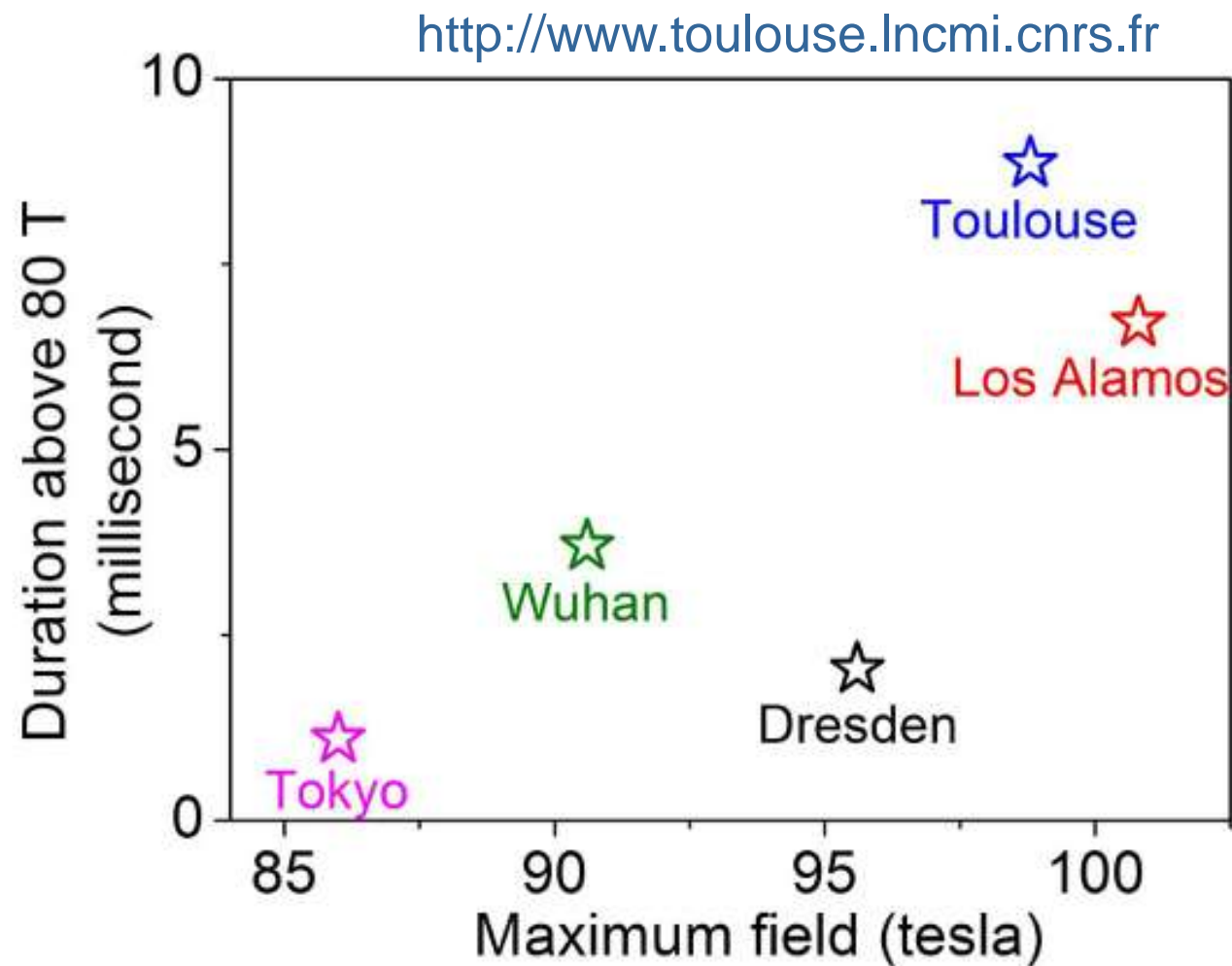


Pulsed magnetic field magnets (100 T)



- Large capacity discharge – RLC circuit
 - Stored energy of capacity bank (“B”)
- Pulsed field with short duration (typ. milliseconds)
- High mechanical strength of coil (“D”) needed

$$E_{\text{tot}} = 50 \text{ MJ}$$
$$I_{\text{max}} = 100 \text{ kA}$$



- Non-destructive short pulses
- Mechanically reinforced magnet design

10^4 T/s

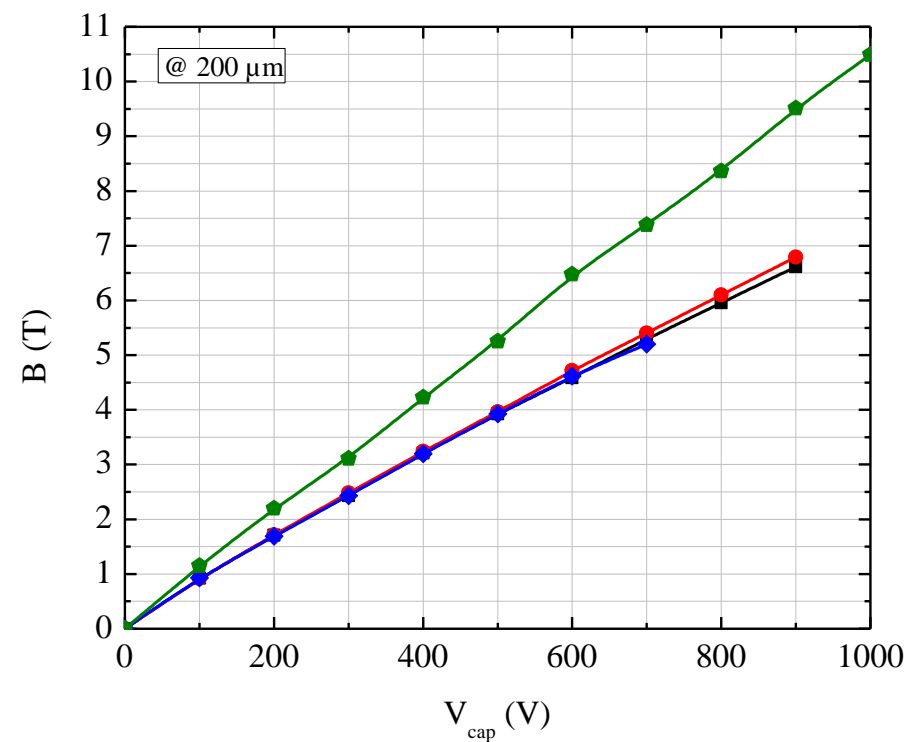
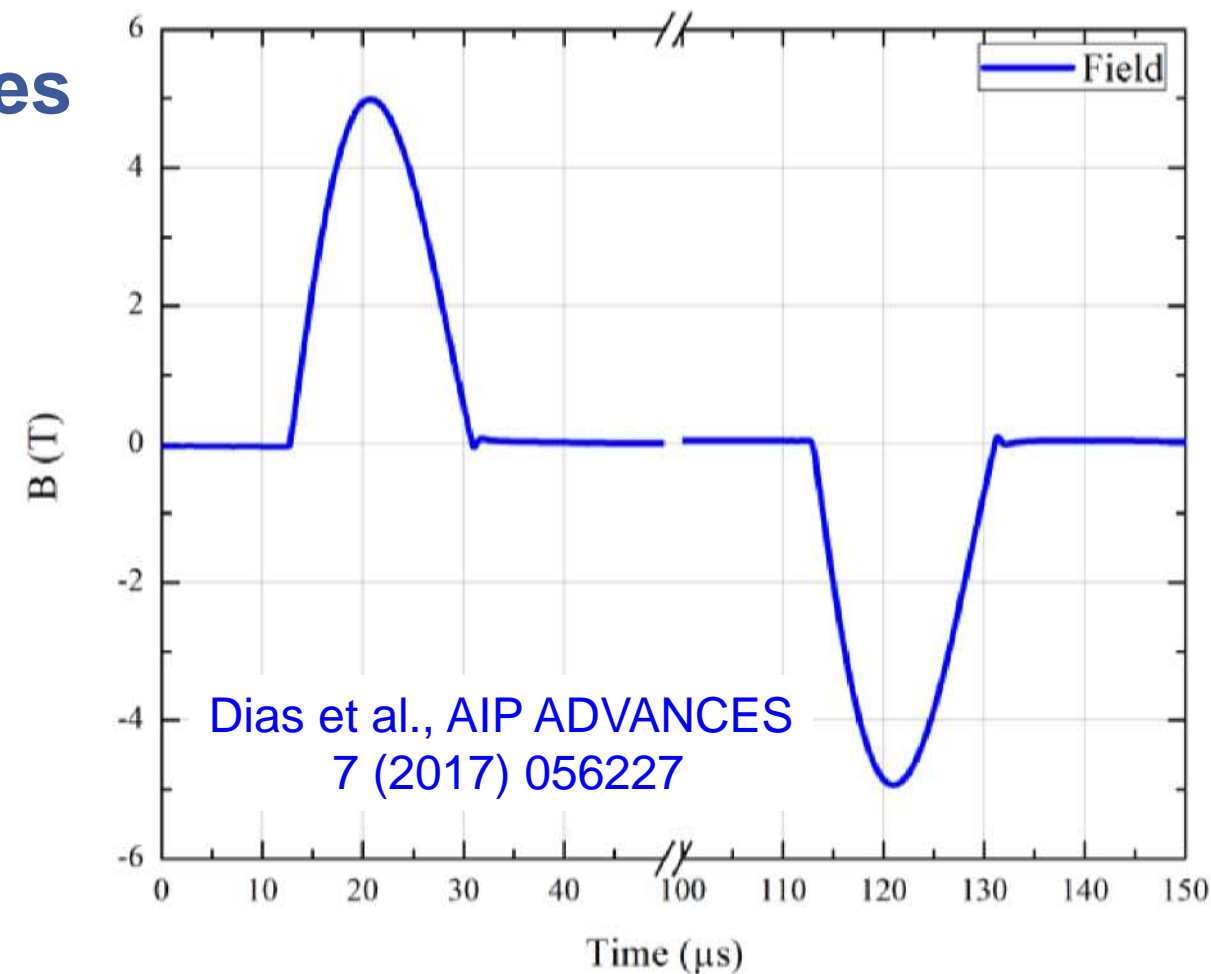
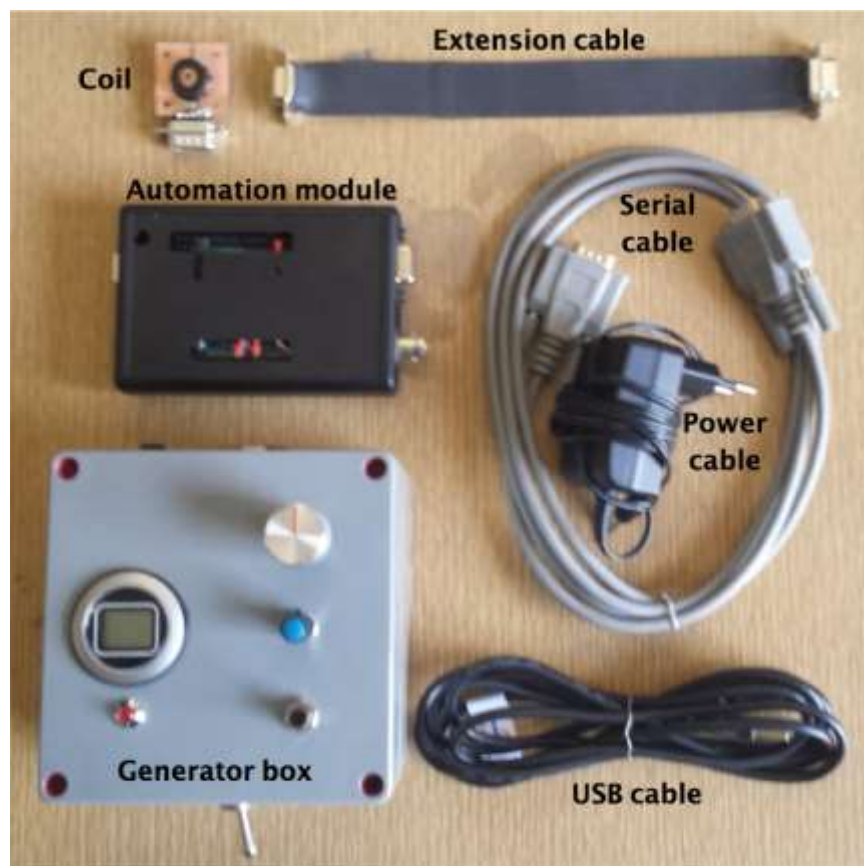


Small coils – high pulsed fields



- Bi-polar pulsed magnetic field sources
- Coolant-free
- Compact in size: cm³
- High working field: 10 T

■ Works in your laboratory!

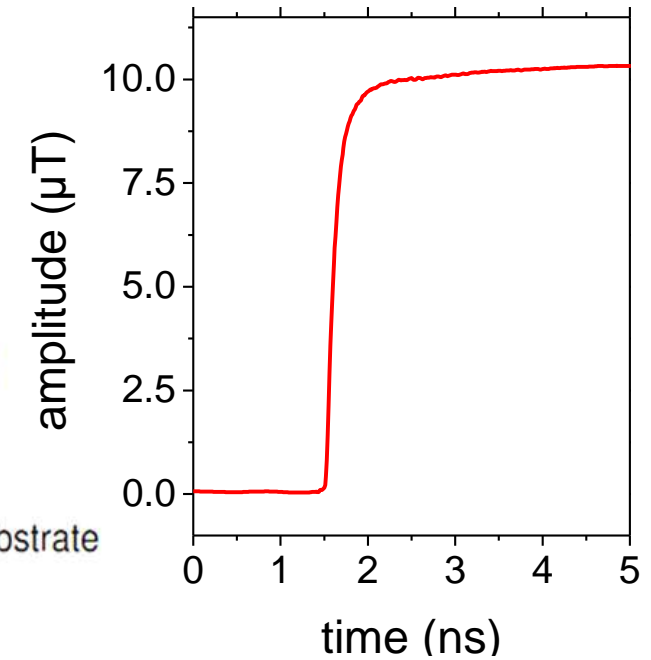
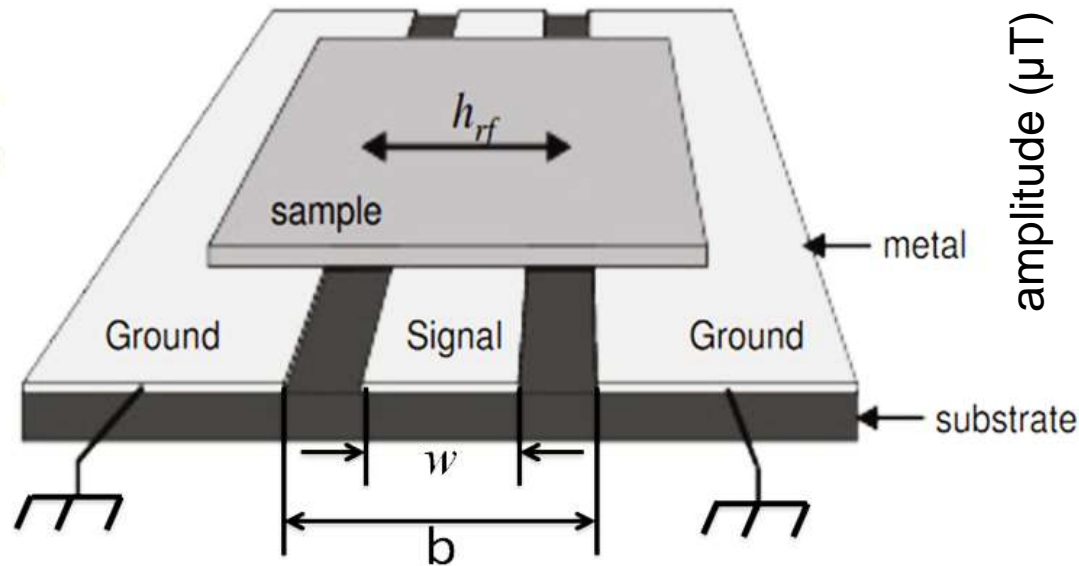
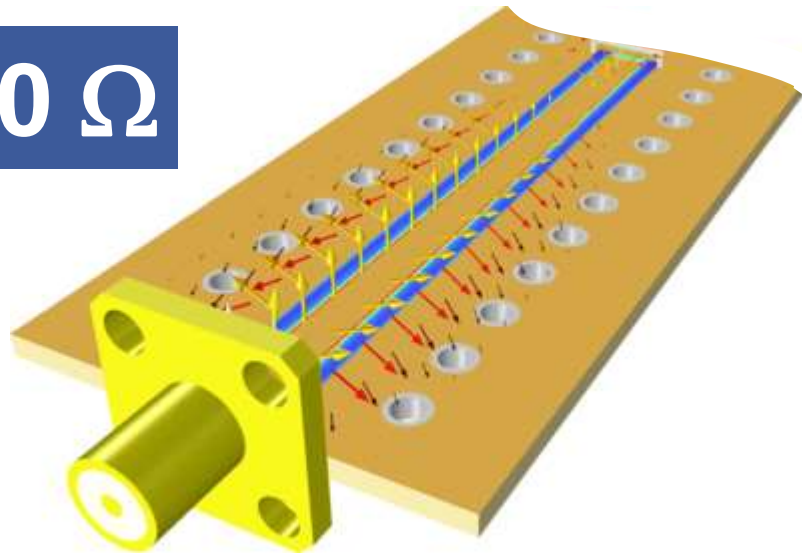


5 · 10⁵ T/s



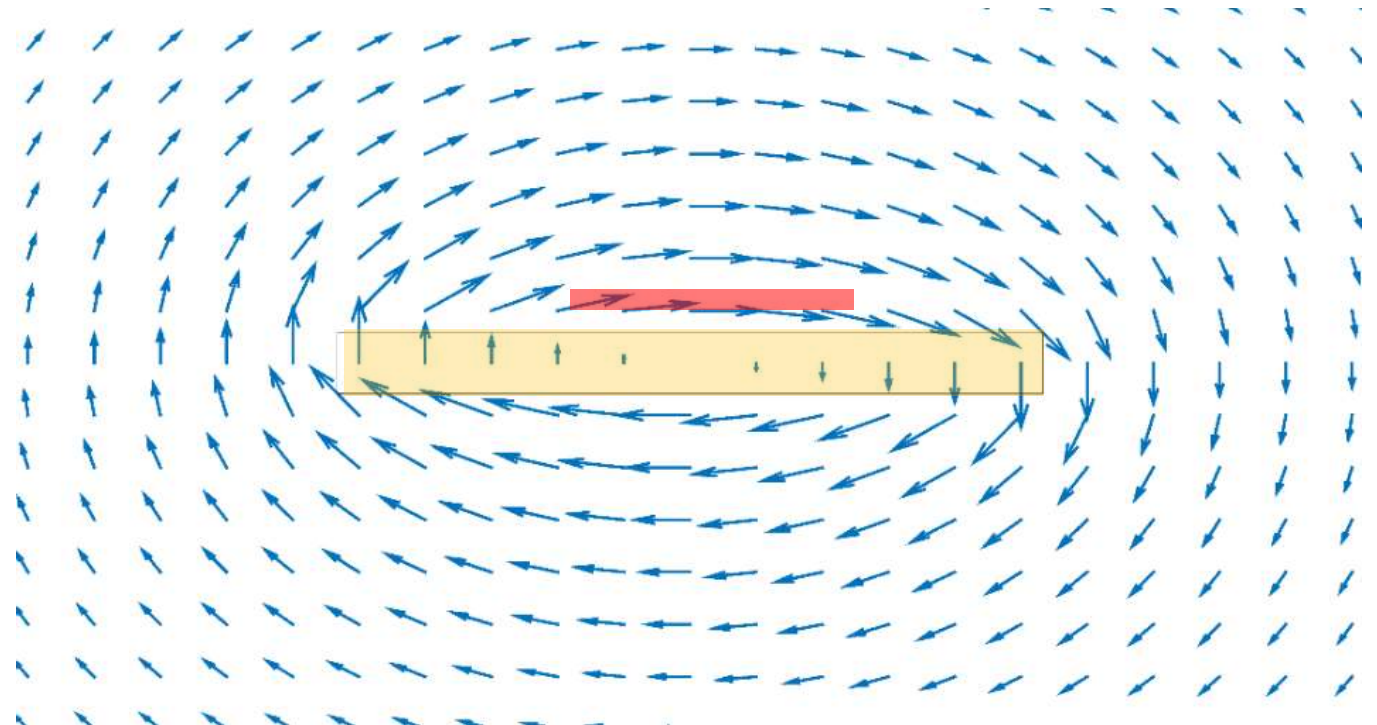
- Magnetization dynamics

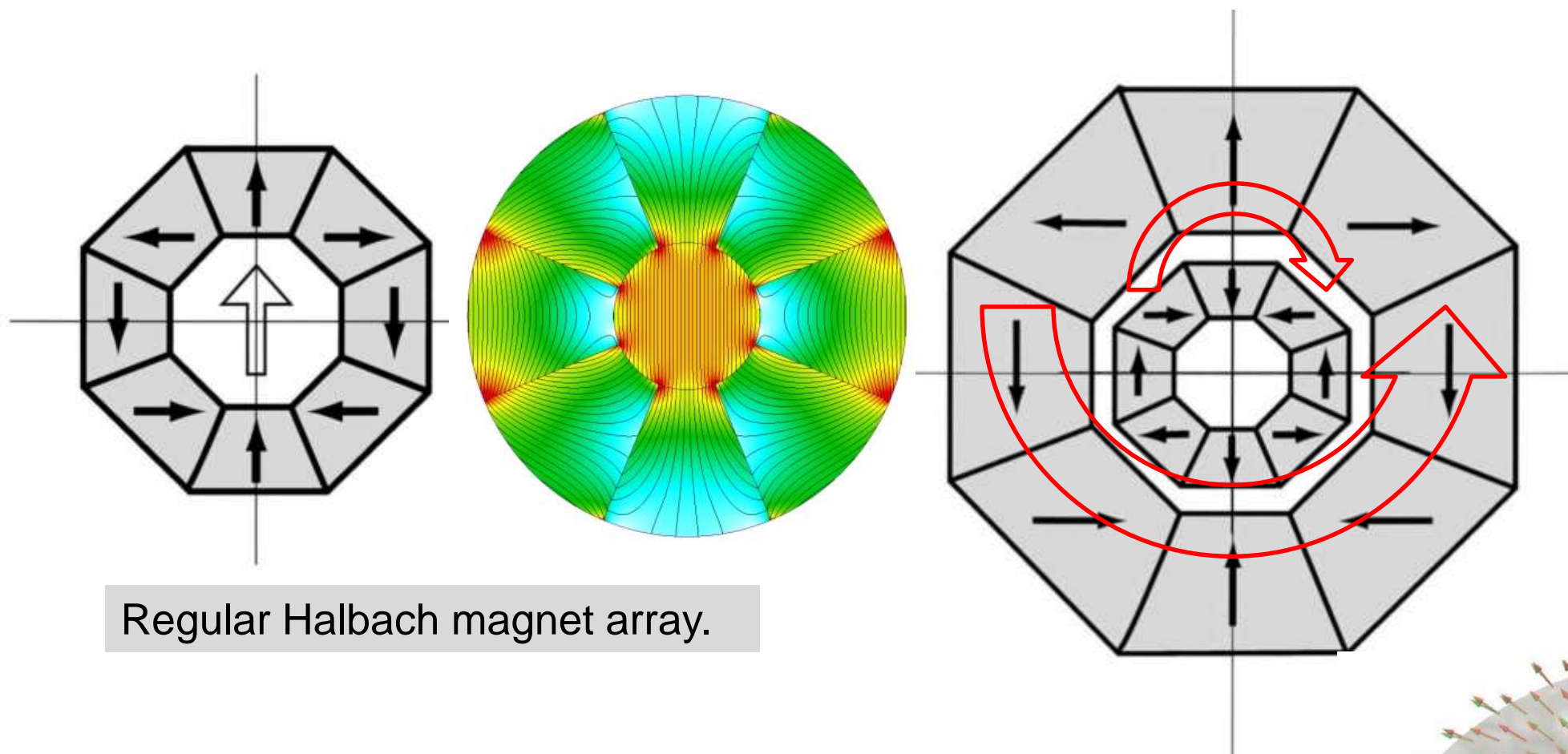
50 Ω



10⁶ T/s

- Impedance matched coplanar waveguide (or similar)
- Local magnetic rf field sources

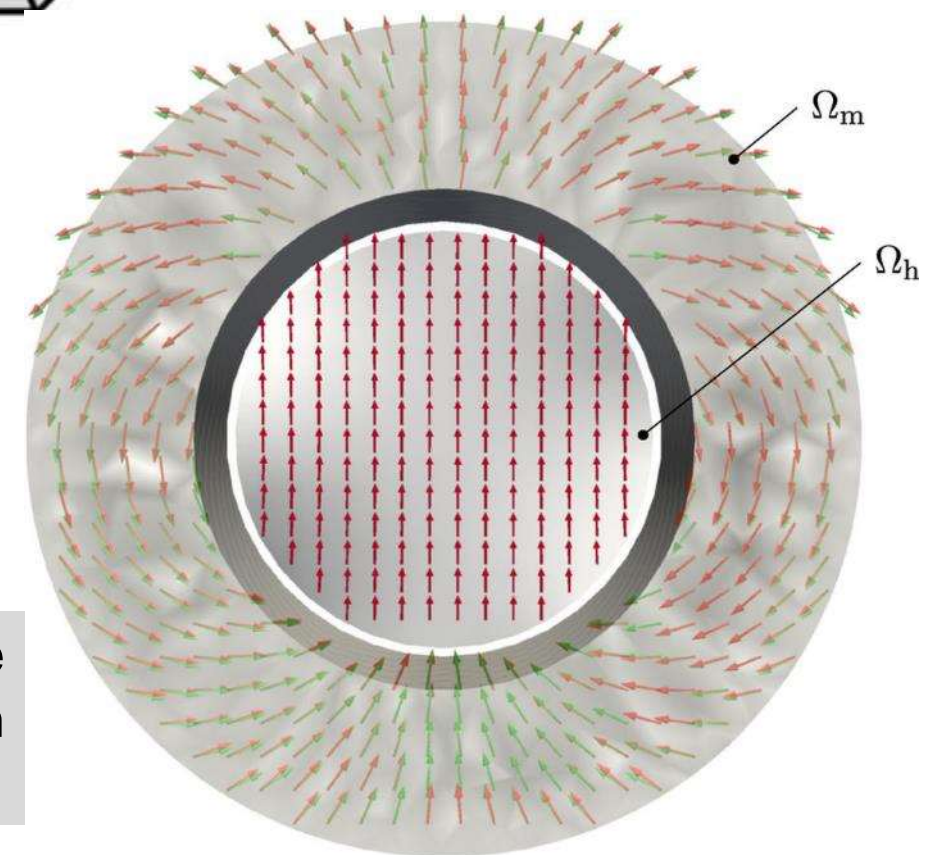




Regular Halbach magnet array.

Pair of concentric Halbach arrays. Each array can be rotated independently.

- Halbach cylinders
- Homegenous magnetic fields over large area



Optimized Halbach like magnetization configuration (Scientific Reports 7, 40816 (2017))

Overview on magnetic field generation



	Maximum field	Duration	High field laboratories
Electromagnetic flux compression	600 T	10^{-6} s	Tokyo
Pulsed coils (destructive)	300 T	10^{-6} s	Tokyo, Toulouse, Los Alamos
Pulsed coils	> 100 T	10^{-3} to 1 s	Los Alamos
Hybrid magnet (resistive + superconducting)	45 T	static	Tallahassee
Superconducting magnets (conventional)	22 T	static	commercial
Pulsed magnetic field coils	10 T	10^{-5} s	commercial
Coils with yoke, Halbach cylinders	2 T - 3 T	static	commercial
Helmholtz coils	≈ 0.2 T	static	commercial
Micro strip lines	0.1 T	<100 psec	commercial

Comparison of the generation of magnetic fields.

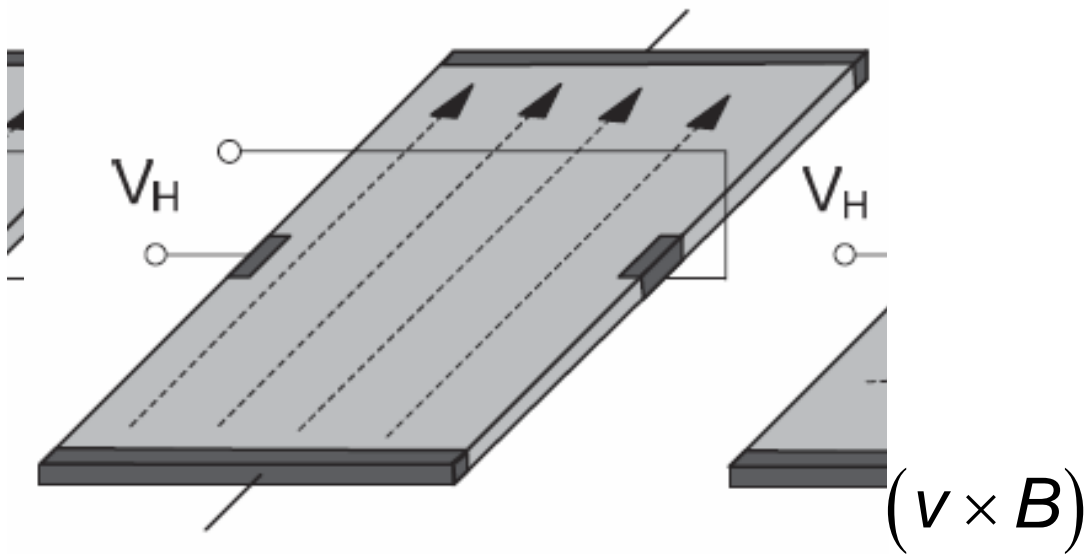
Laboratory



- **Measurement of magnetic field strengths**
 - **Hall probes („Gaussmeters“)**
 - Magneto-resistive devices
 - Flux gate sensors
 - Induction coils
 - SQUID sensors

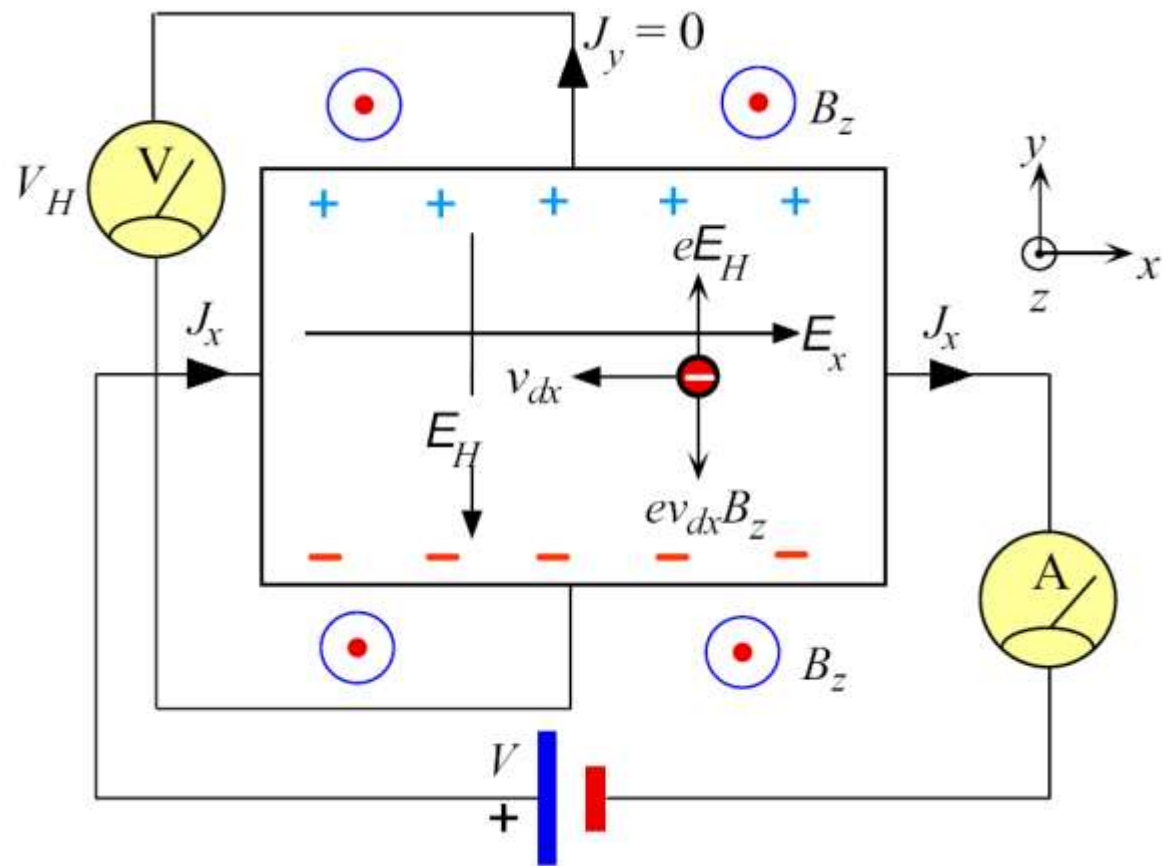
- **Only very rarely the magnetic field can be calculated!**
- **Most apparatus need to be calibrated!**

Hall probes



$$V_H = \mu \frac{w}{l} V_0 B_z$$
 carrier mobility μ
 length l
 width w
 supply voltage V_0

	carrier mobility
InSb	80.000 cm ² /Vs
InAs	33.000 cm ² /Vs
GaAs	8.500 cm ² /Vs
Si	2.000 cm ² /Vs



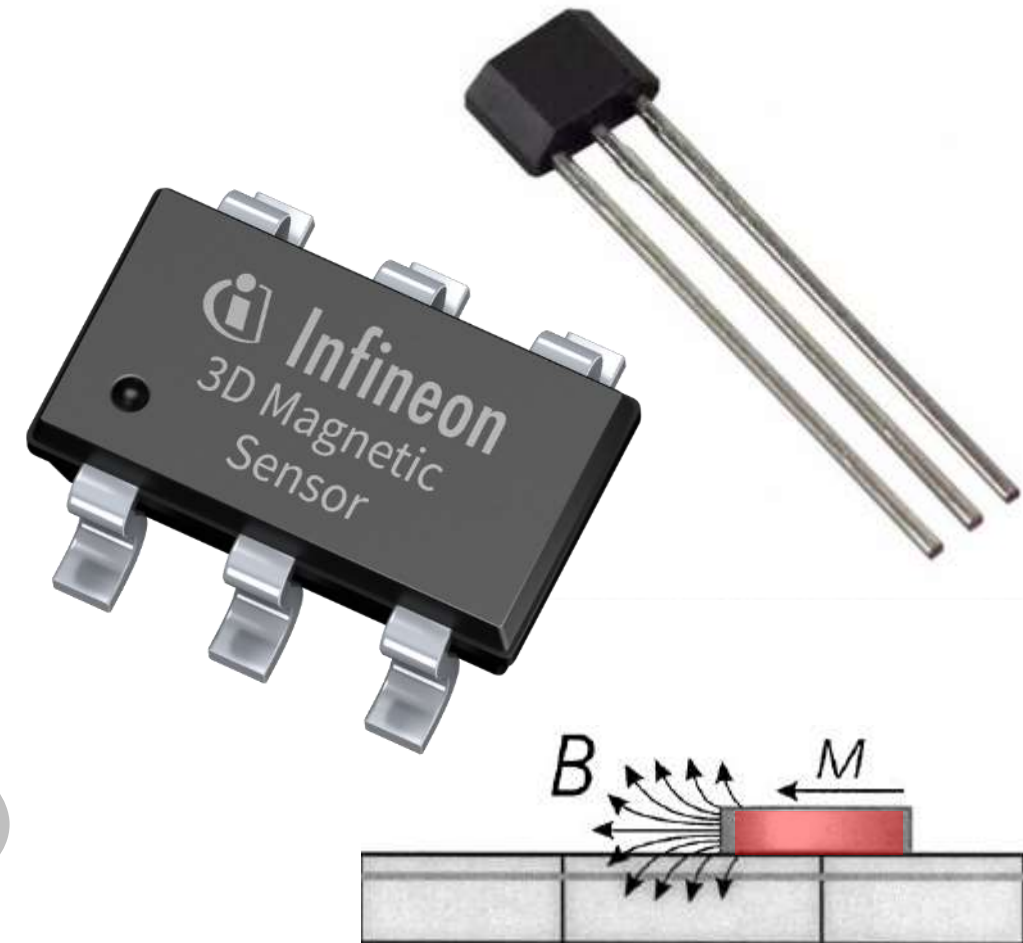
- Experience Lorentz force at charge carriers with perpendicular magnetic field
 - Results in Voltage V_H perpendicular to current and field
 - Temperature dependent
 - High spatial resolution

■ Specs

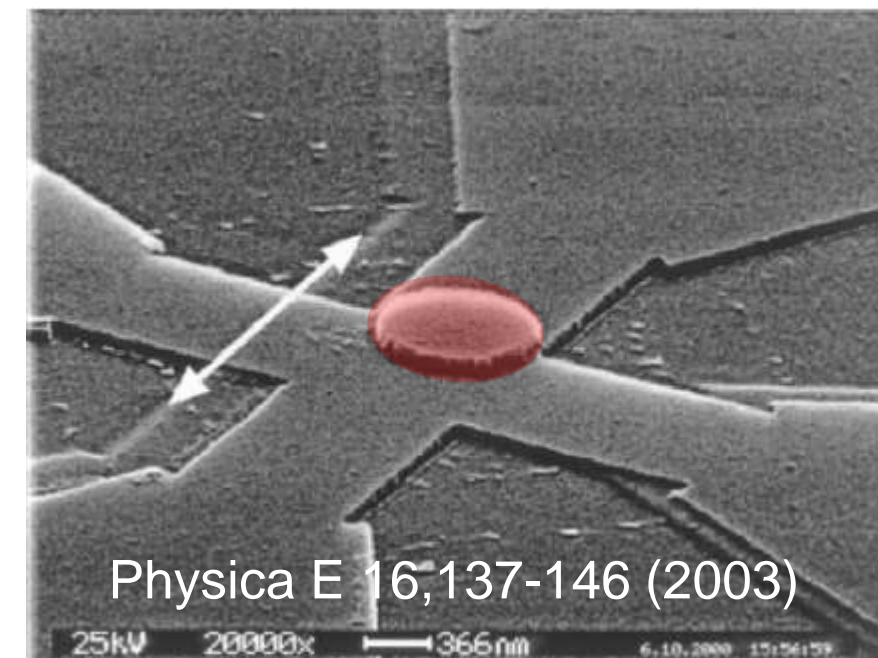
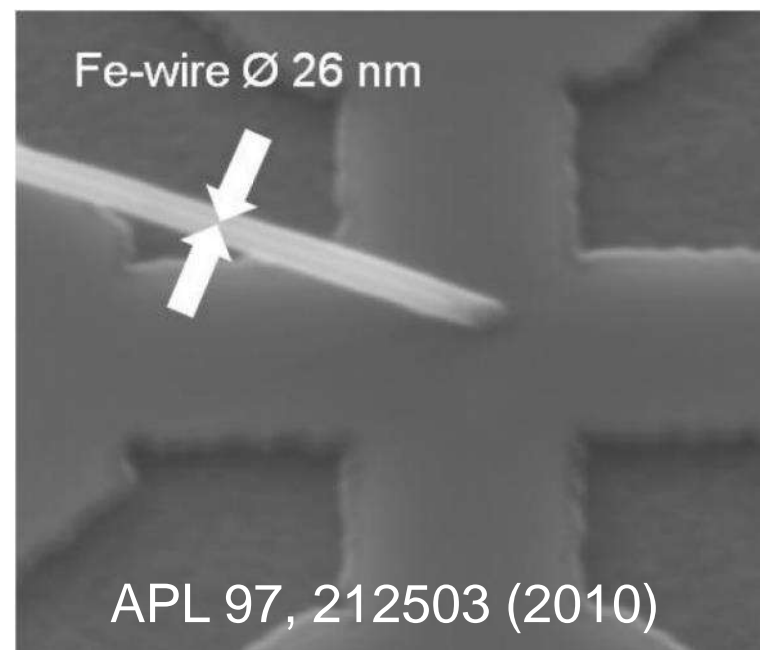
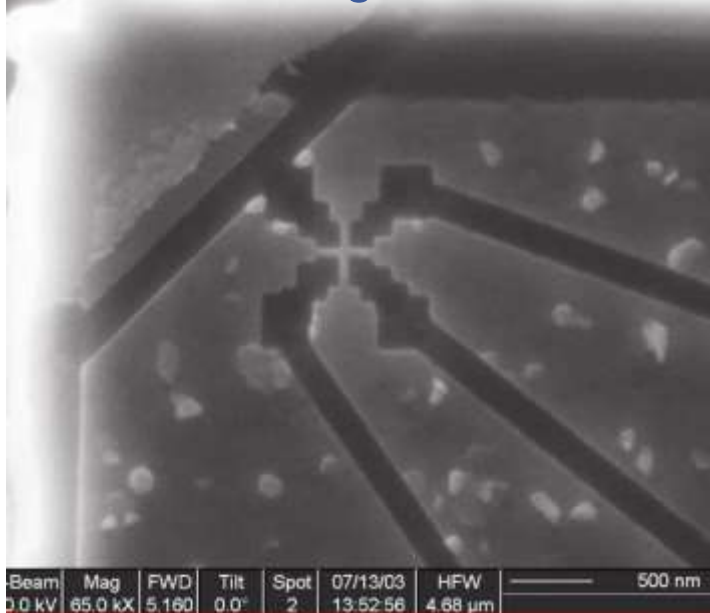
- Typical range from 0.01 mT to 30 T
- Accuracy better than 0.1 %
- DV to 30 kHz

■ Micro Hall probes for characterization of nanomagnetic phenomena

■ Scanning Hall probe microscopy (SHPM)



www.nanomagnetics-inst.com





- **Measurements of magnetization loops (quasi-static)**
 - Vibrating sample magnetometer (VSM)
 - Alternating gradient force magnetometer (AGM)
 - SQUID magnetometer
 - **First order reversal curves (FORC)**
 - BH Looper (inductive)
 - Magneto-optical methods

- **Measurements of magnetization dynamics**
 - Ferromagnetic resonance

- **Methods for determining magnetization are divided into closed-circuit and open circuit measurements**
 - Sample is (or not) a part of a complete magnetic circuit

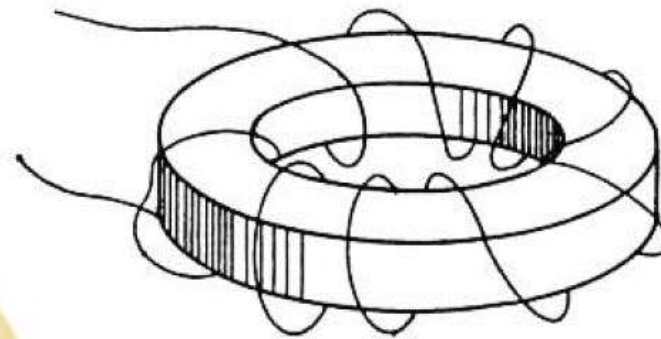
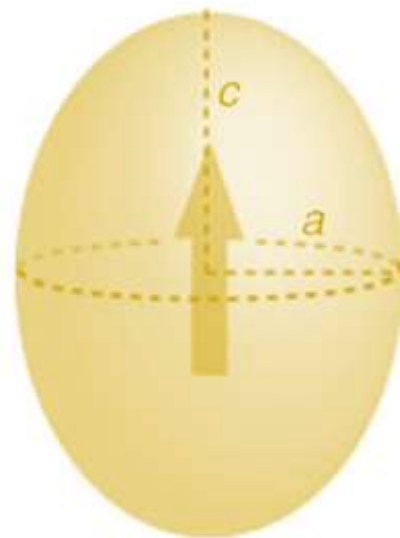
Method	Open/closed circuit	Typical sensitivity
Vibrating sample	Open	10^{-9} Am^2
Alternating gradient force	Open	10^{-10} Am^2
BH-Looper	Open	10^{-9} Am^2
SQUID	Open	10^{-11} Am^2
Magneto-optics	Open	10^{-11} Am^2
Hysteresigraph	Closed	10^{-4} Am^2
Faraday	Open	10^{-6} Am^2

Comparison of methods for measuring magnetization loops of magnetic materials (adapted from M. Coey, Magnetism and Magnetic Materials, Cambridge University Press 2010)

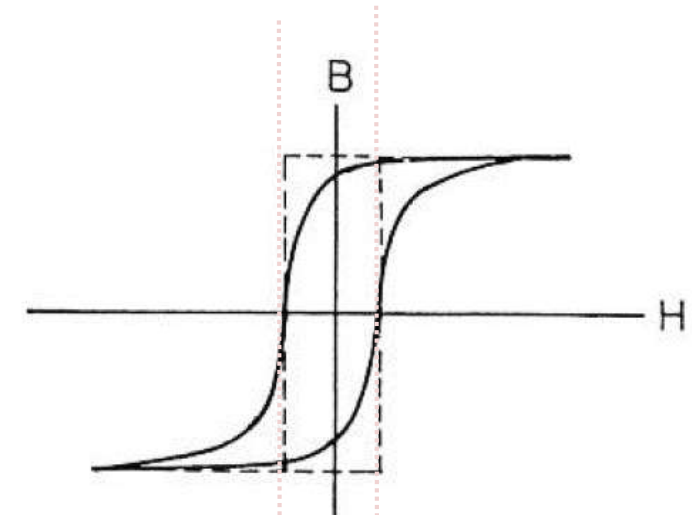
- Magnetic poles induced on the sample surface
- Demagnetization factor N depending on sample shape
- N for ellipsoids exactly defined

$N_a + N_b + N_c = 1$
(a, b, c : ellipsoid axes)

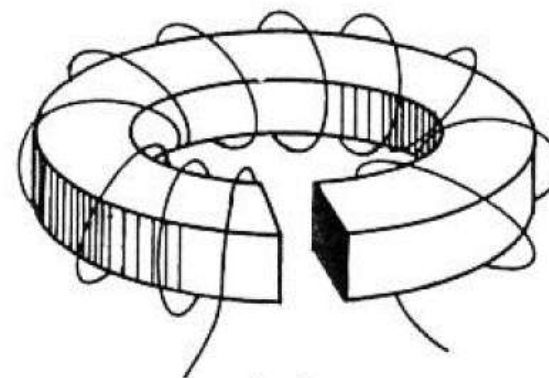
Ellipsoid with dimensions a and c .



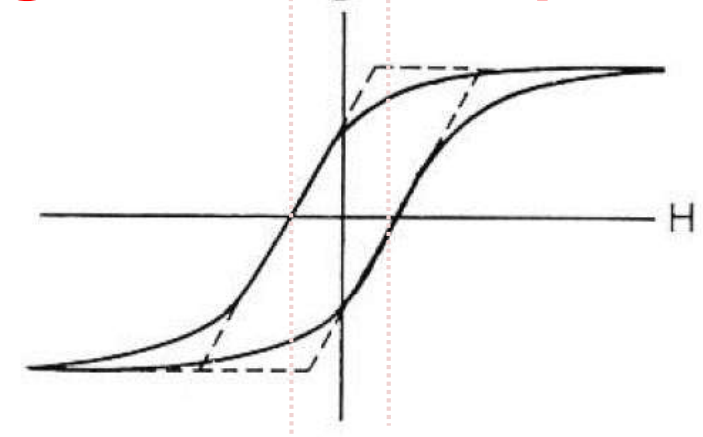
Closed circuit



Sheared magnetization loops



Open circuit ($N \neq 0$)



- „Flat disk“ $N_c \approx 1$; $N_a = N_b \approx 0$
- Sphere $N_a = N_b = N_c = 1/3$
- „Cylinder“ $N_c \approx 0$; $N_a = N_b \approx 1/2$

J. Appl. Phys. **79** (8), 15 April 1996

The vibrating sample magnetometer: Experiences of a volunteer (invited)

S. Foner

Francis Bitter National Magnet Laboratory and Department of Physics, MIT, Cambridge, Massachusetts 02139

- **Scientific inventions can happen at home!**

That summer we were living in a small farm-hand's house about 1 km from the laboratory and just off the runway at Hanscom Field, a Strategic Air Command (SAC) base at that time. While shaving one evening I decided to try ac induction for magnetic measurements. With some Duco cement, a small \$2.00 (in 1955) replacement loudspeaker, a conical paper cup, and a paper straw (the latter components were light and conveniently available at night from the lunch room), the first working model VSM was assembled.

- **Flux detection method!**
- A simple, inexpensive, and versatile instrument!

Basic components of a VSM

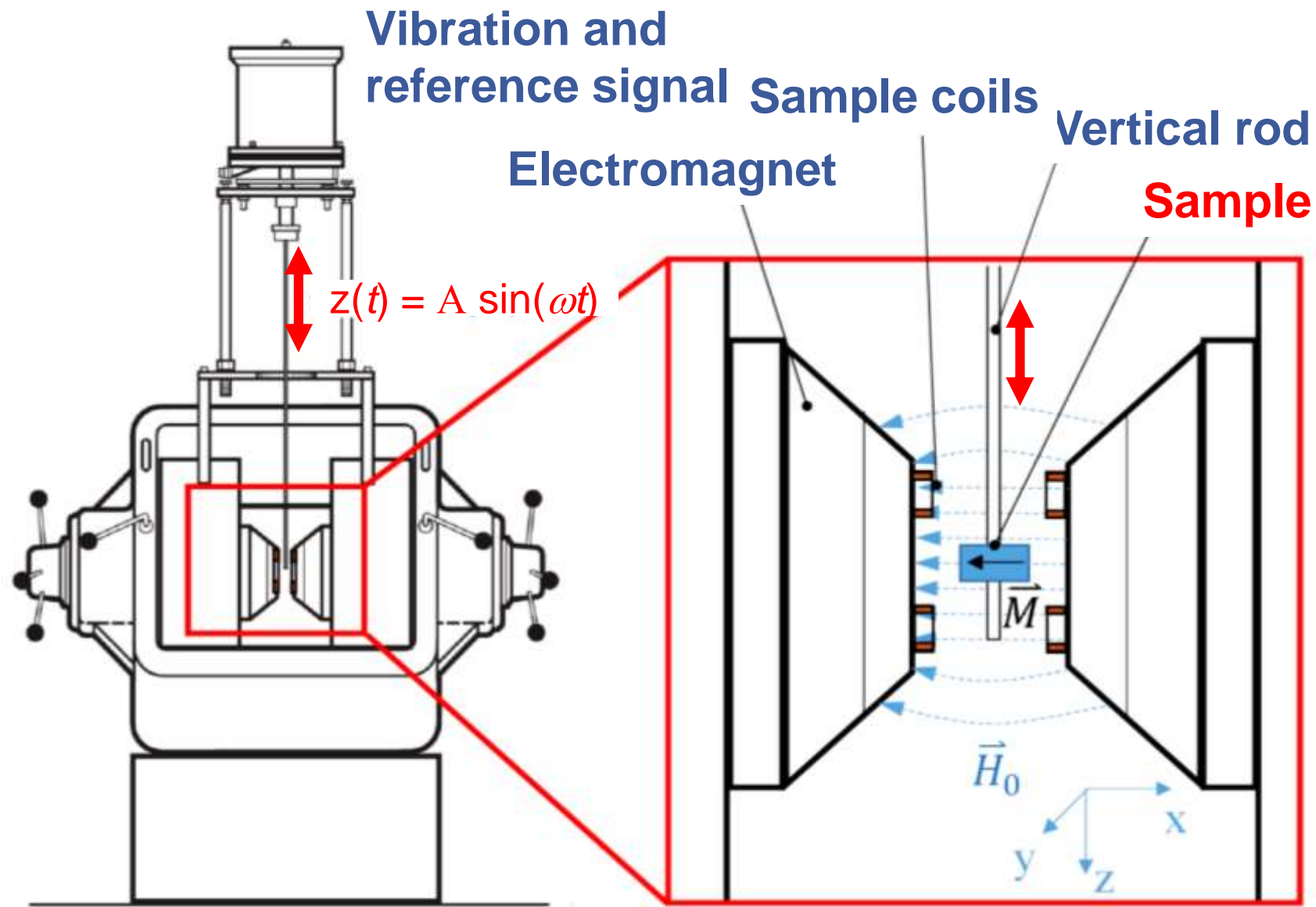


- Measurement magnetic moment (after calibration)
- Measurement of magnetization loops
- Electromagnetic induction
- Lock-in signal detection (10 to 100 Hz)

$$z(t) = A \cdot \sin(\omega \cdot t)$$

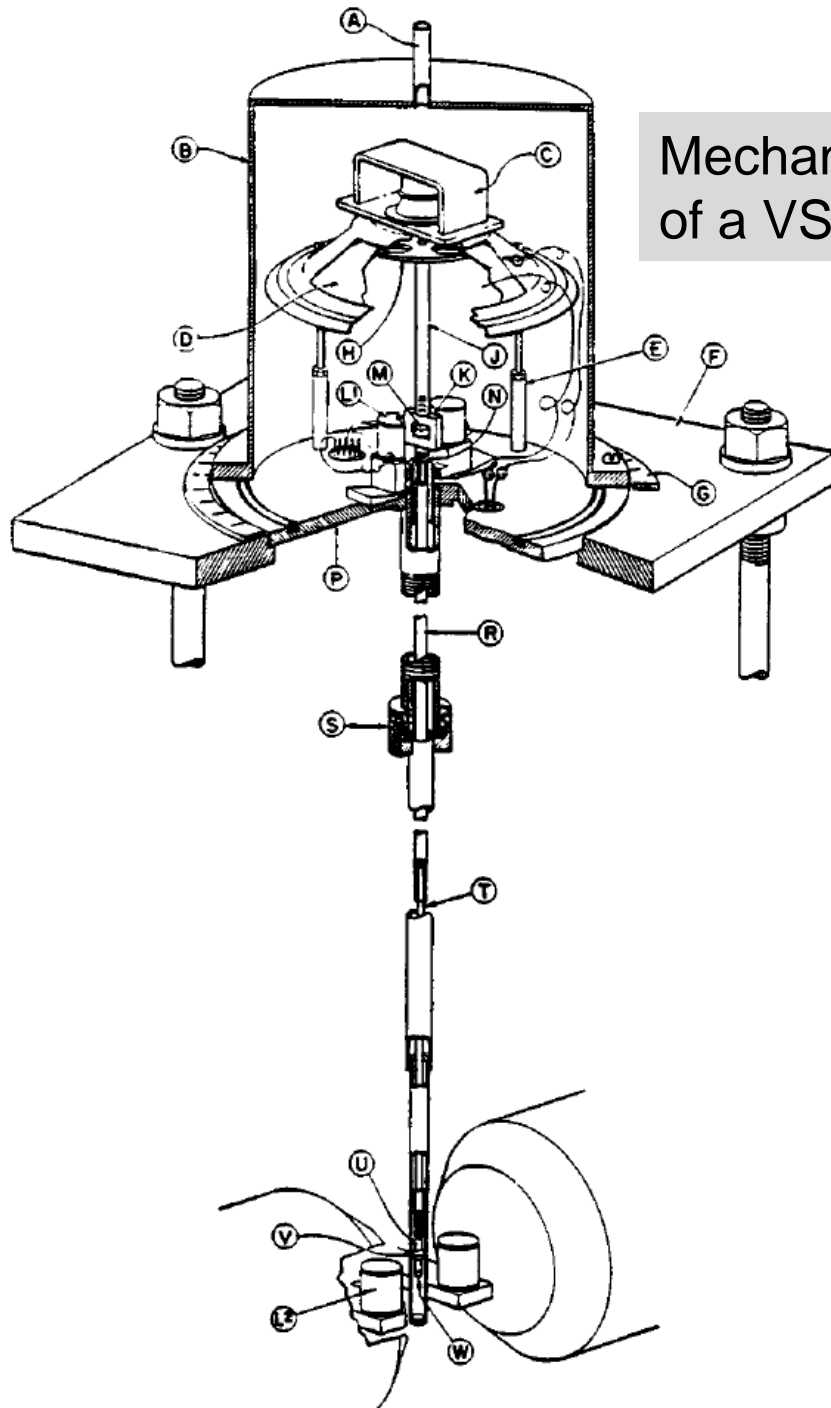
$$\frac{\partial z}{\partial t} = A \cdot \omega \cdot \cos(\omega \cdot t)$$

$$U(t) = -\frac{\partial \Phi}{\partial t} = -\frac{\partial \Phi}{\partial z} \cdot \frac{\partial z}{\partial t} = \underset{\text{sensitivity function}}{\mathbf{G}} \cdot \underset{\text{magnetic moment of sample}}{m} \cdot \frac{\partial z}{\partial t}$$

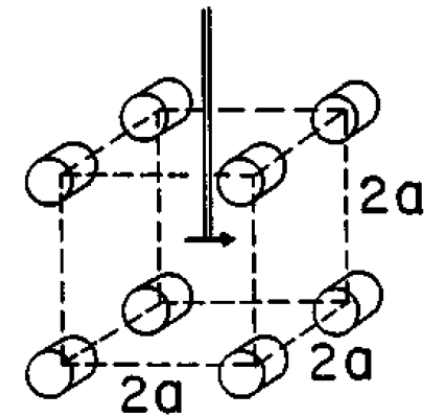
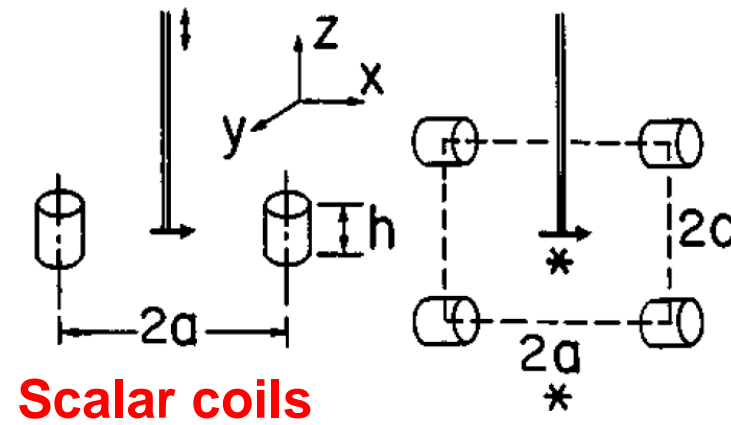


Sketch of a VSM (transverse configuration).

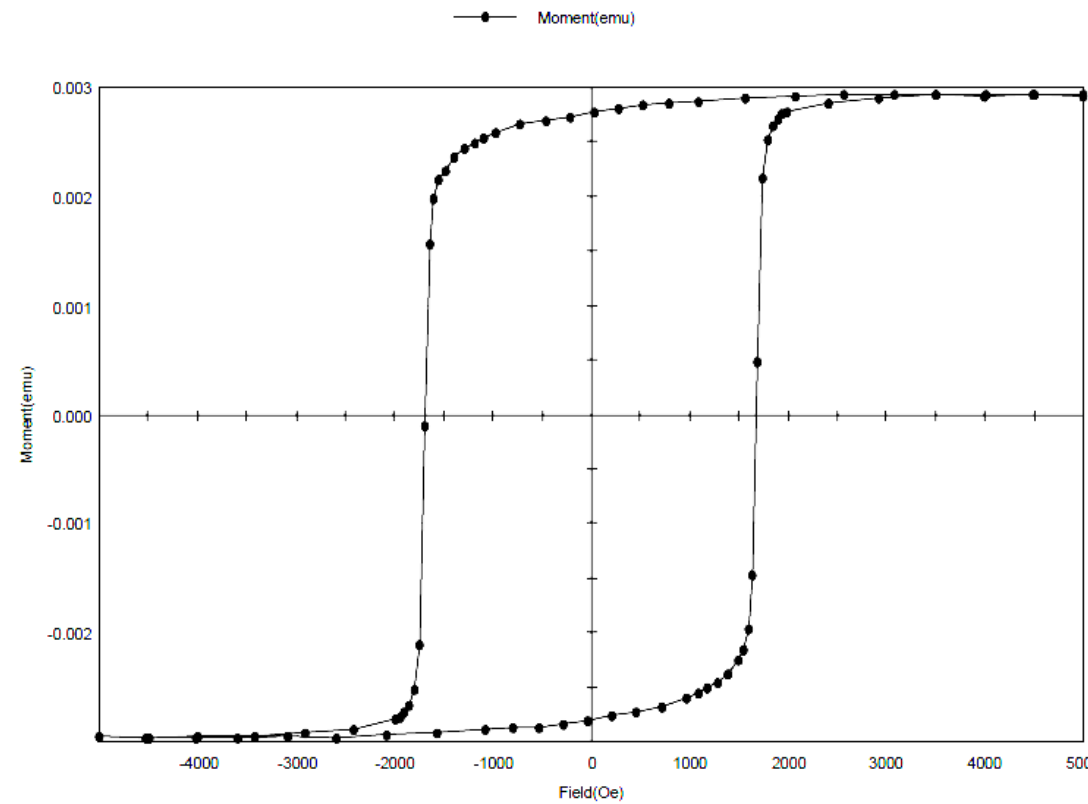
Vibrating sample magnetometer



Mechanical details of a VSM



Examples of VSM coil configurations



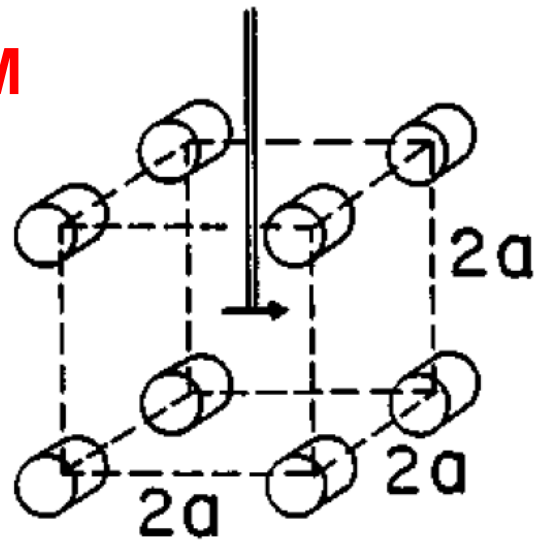
Coercivity(Hc1): 1.69 kiloOe Retentivity(Mr): 0.00279 emu Magnetization: 0.00294 emu
 Switching Field Distribution 2: 0 Squariness Ratio: 0.947 S*: 0.951

Magnetization loop for hard disk CoPt magnetic film deposited on a rigid disk substrate. $M(H)$ loop parameters are indicated in the figure.

Example VSM loops – vector magnetometry

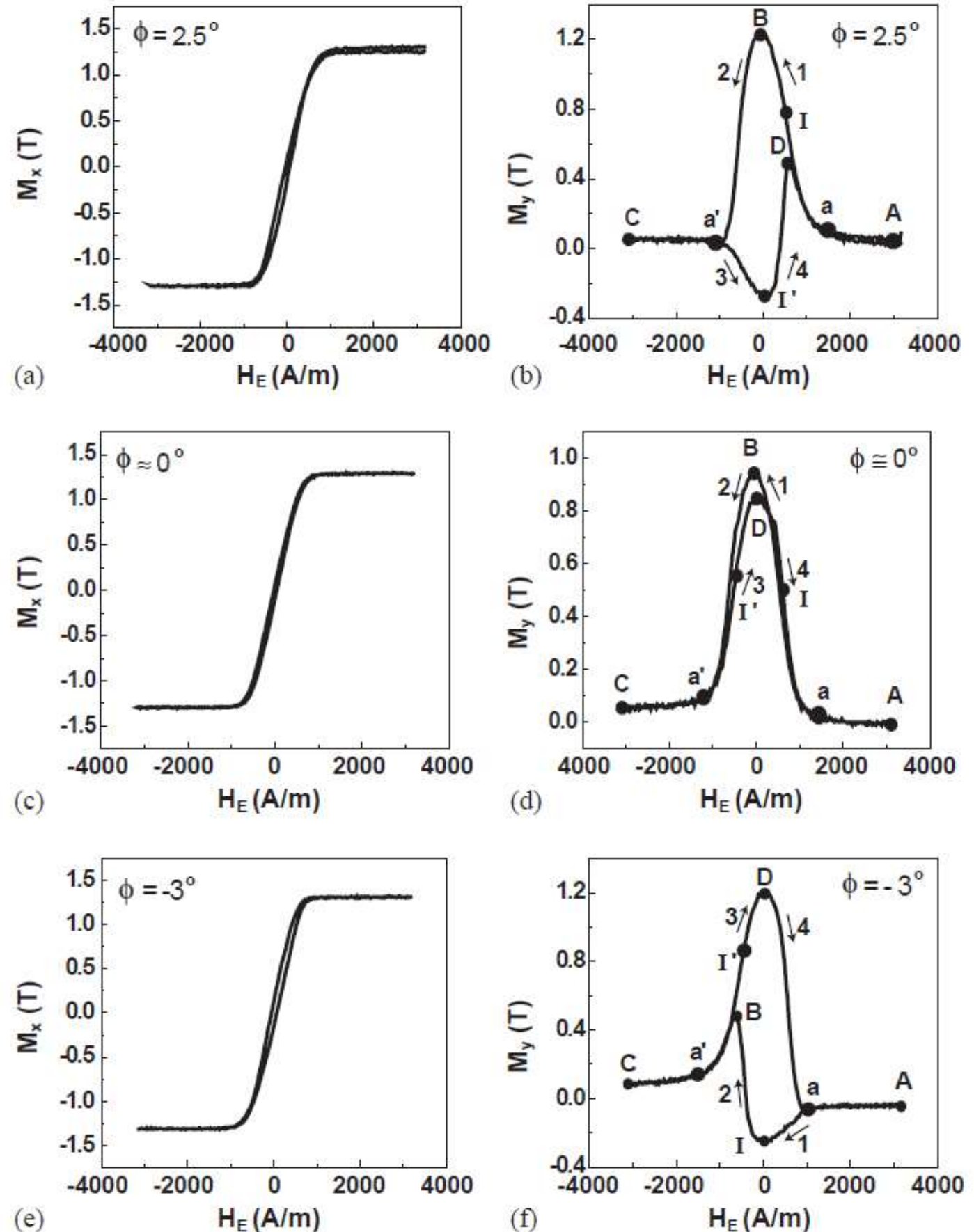


Vector-VSM



- Soft magnetic thin film with anisotropy dispersion
- Also earth field present!

M_x hysteresis and M_y -hysteresis loops of a Permalloy film with slightly varying magnetic field angles applied close to the hard axis of magnetic anisotropy.

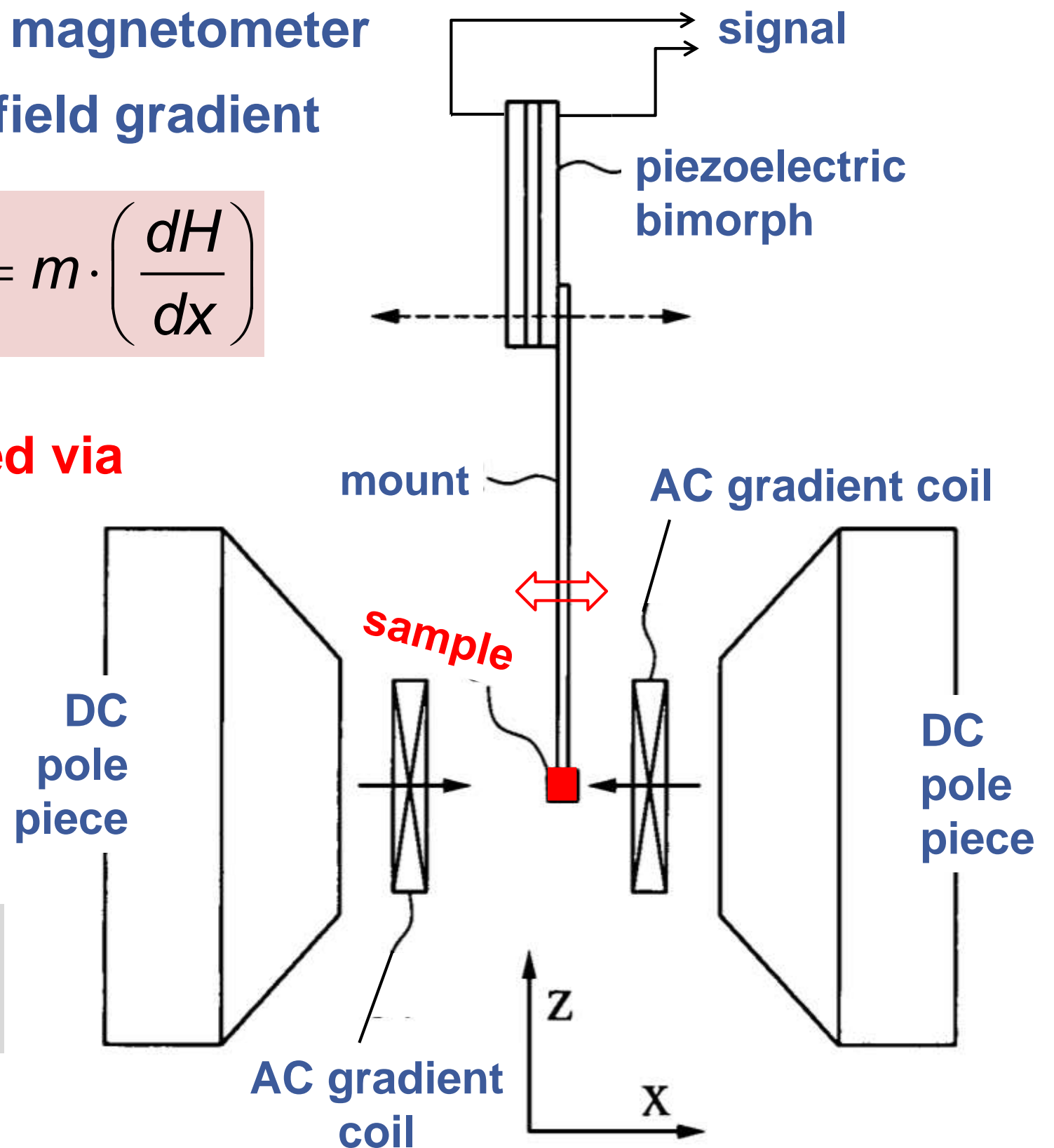


Alternating gradient force magnetometer (AGM)



- Alternating gradient force magnetometer
- DC field with overlaid AC field gradient
- Non uniform field
- Resonance mode
- **Alternating force measured via piezoelectric transducer**
- **Fast!**
- **High sensitivity!**

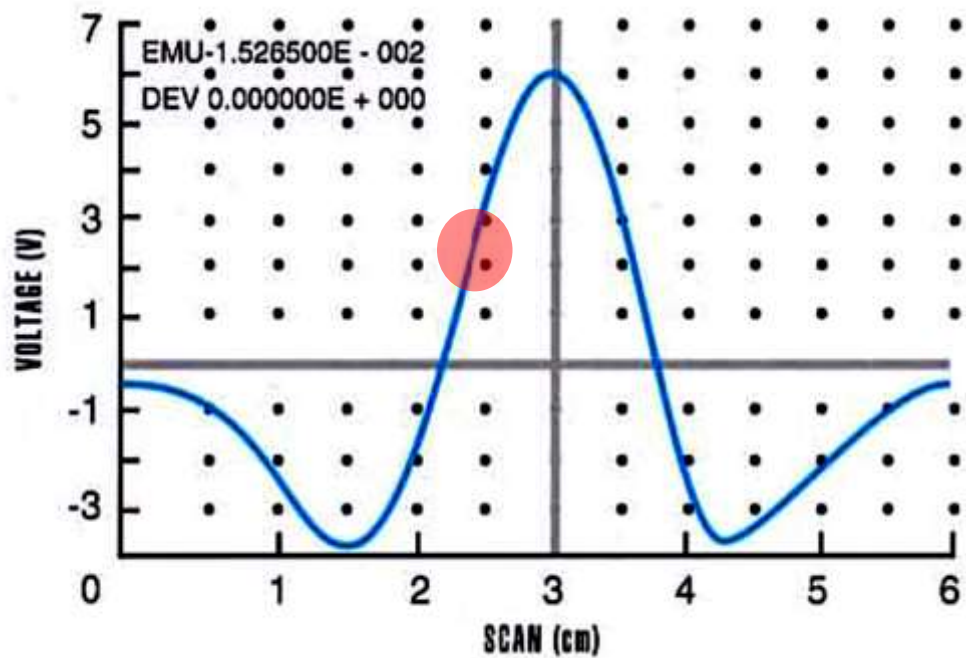
$$F = m \cdot \left(\frac{dH}{dx} \right)$$



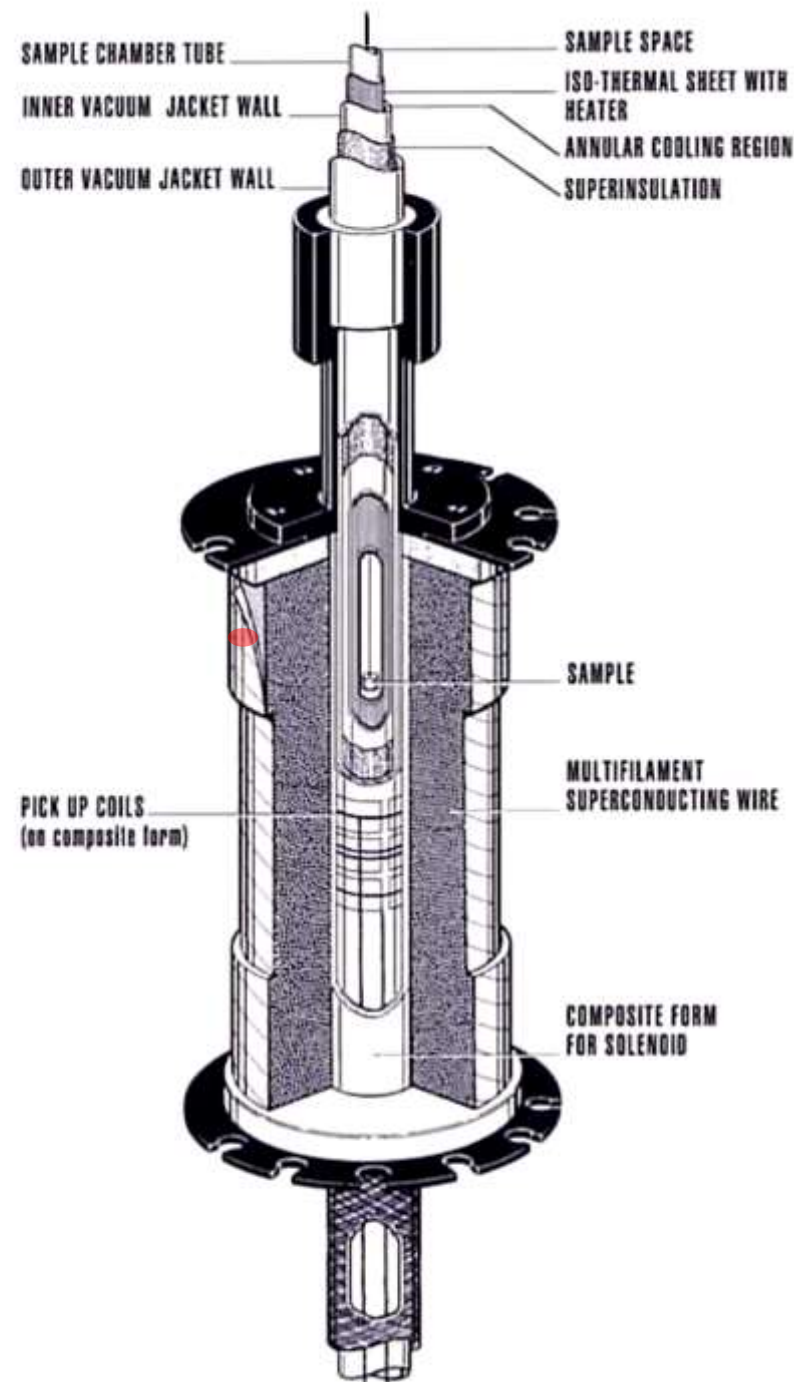
Schematic of an AGM. An alternating gradient field leads to an alternating signal in the piezoelectric bimorph.

Superconducting Quantum Interferences Device

- Based on two parallel Josephson junctions
- Measures magnetic fields changes of the order of a quantum flux

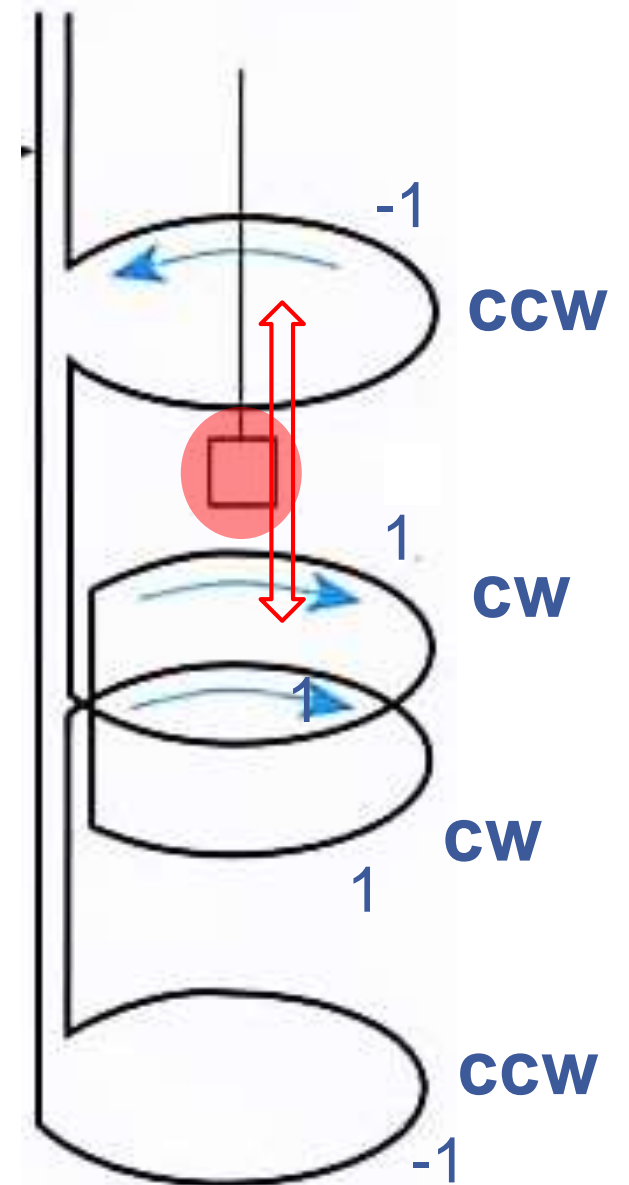


SQUID Response
(voltage vs. sample position)

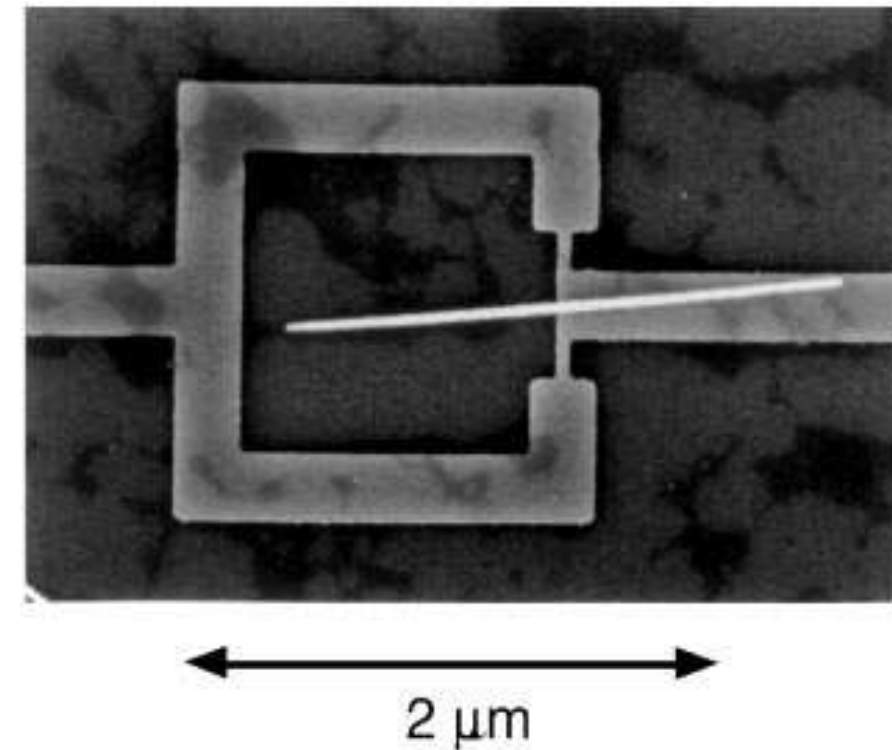
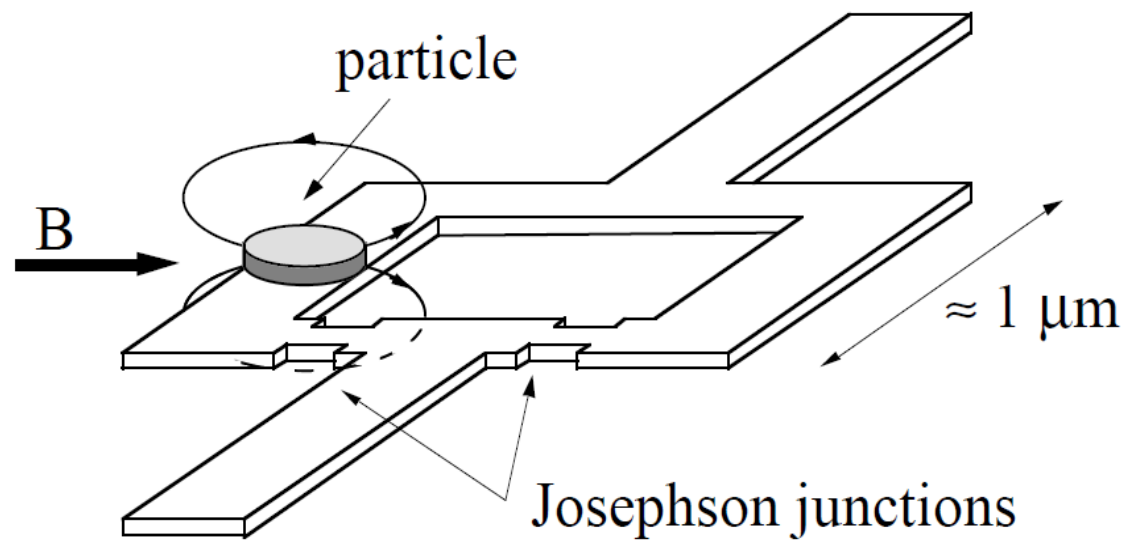


M. McElfresh, Fundamentals of magnetism and magnetic measurement systems (1994)

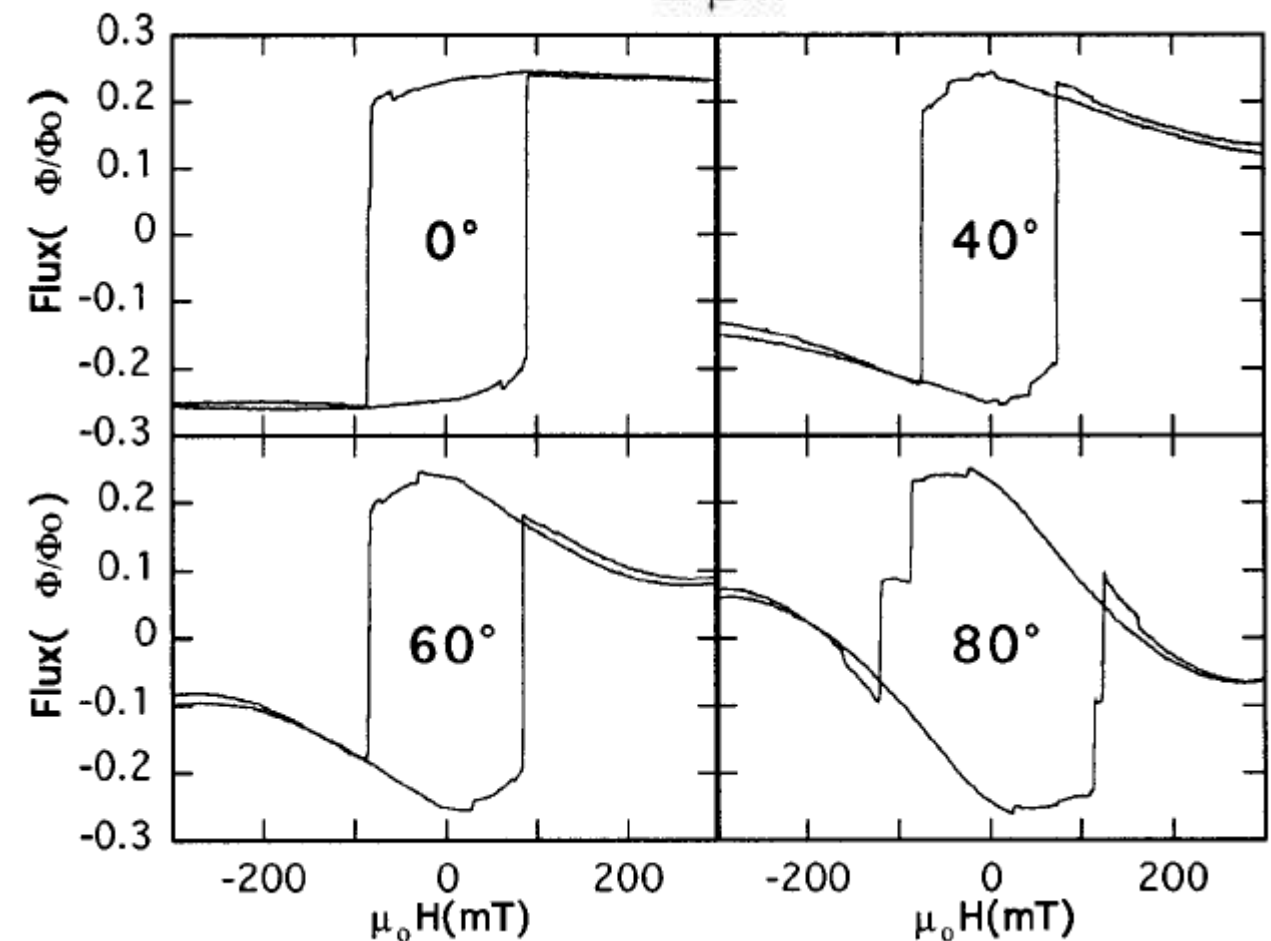
SQUID



2nd order
gradiometer
superconducting
detection coil)



- **Measuring single nano objects**
 - Switching of the magnetization of single Ni wires (diameter 65 nm)



W. Wernsdorfer, Phys. Rev. Lett. 77, 1873 (1996)

Characterizing interactions in fine magnetic particle systems using first order reversal curves

Christopher R. Pike^{a)}

Department of Geology, University of California, Davis, California 95616

Andrew P. Roberts

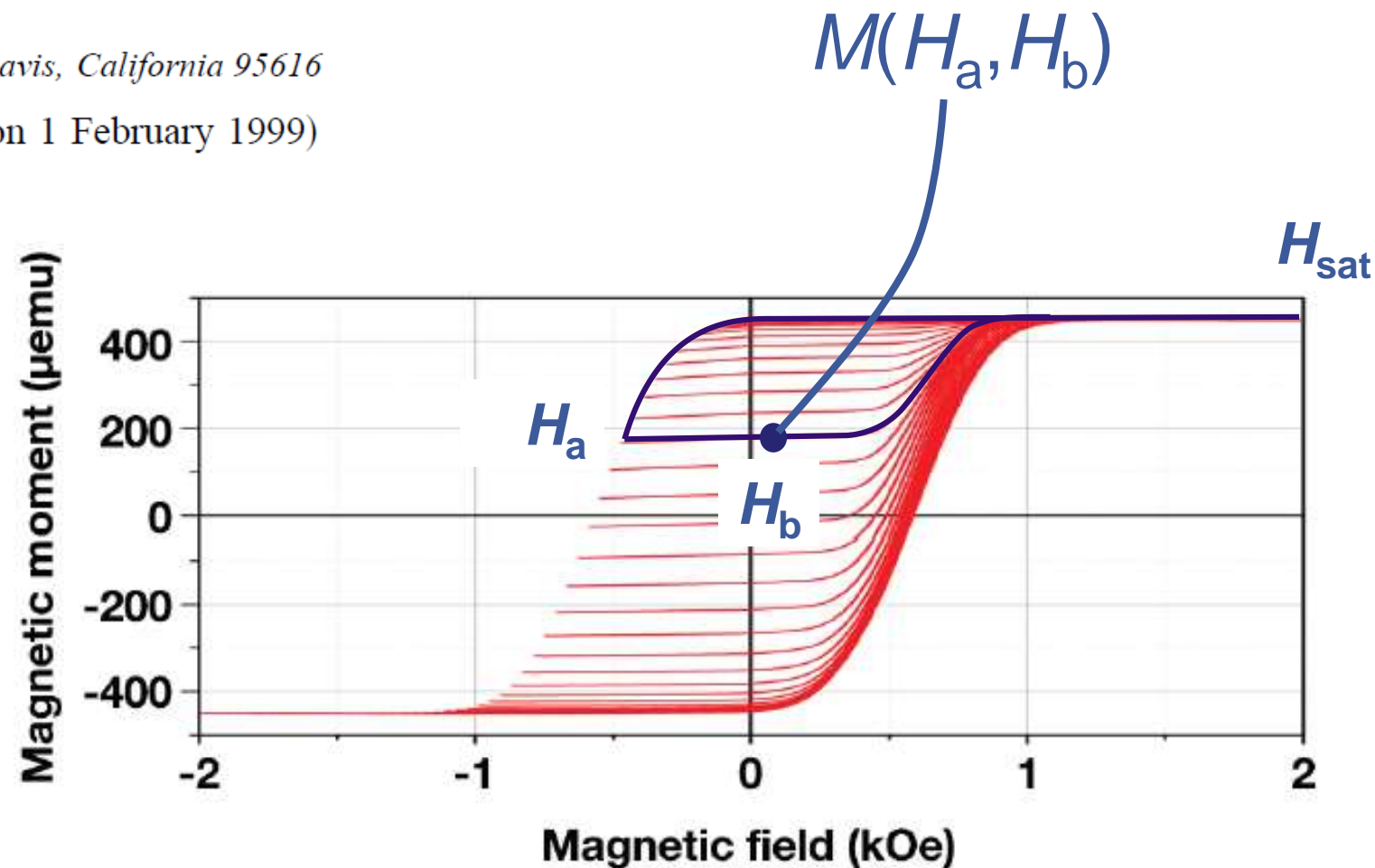
Department of Oceanography, University of Southampton, Southampton Oceanography Centre, European Way, Southampton SO14 3ZH, United Kingdom

Kenneth L. Verosub

Department of Geology, University of California, Davis, California 95616

(Received 1 June 1998; accepted for publication 1 February 1999)

- Minor loop measurements
- Saturation field H_{sat}
- Reversal field H_a
- Field swept back H_a to H_b
- $M(H_a, H_b)$

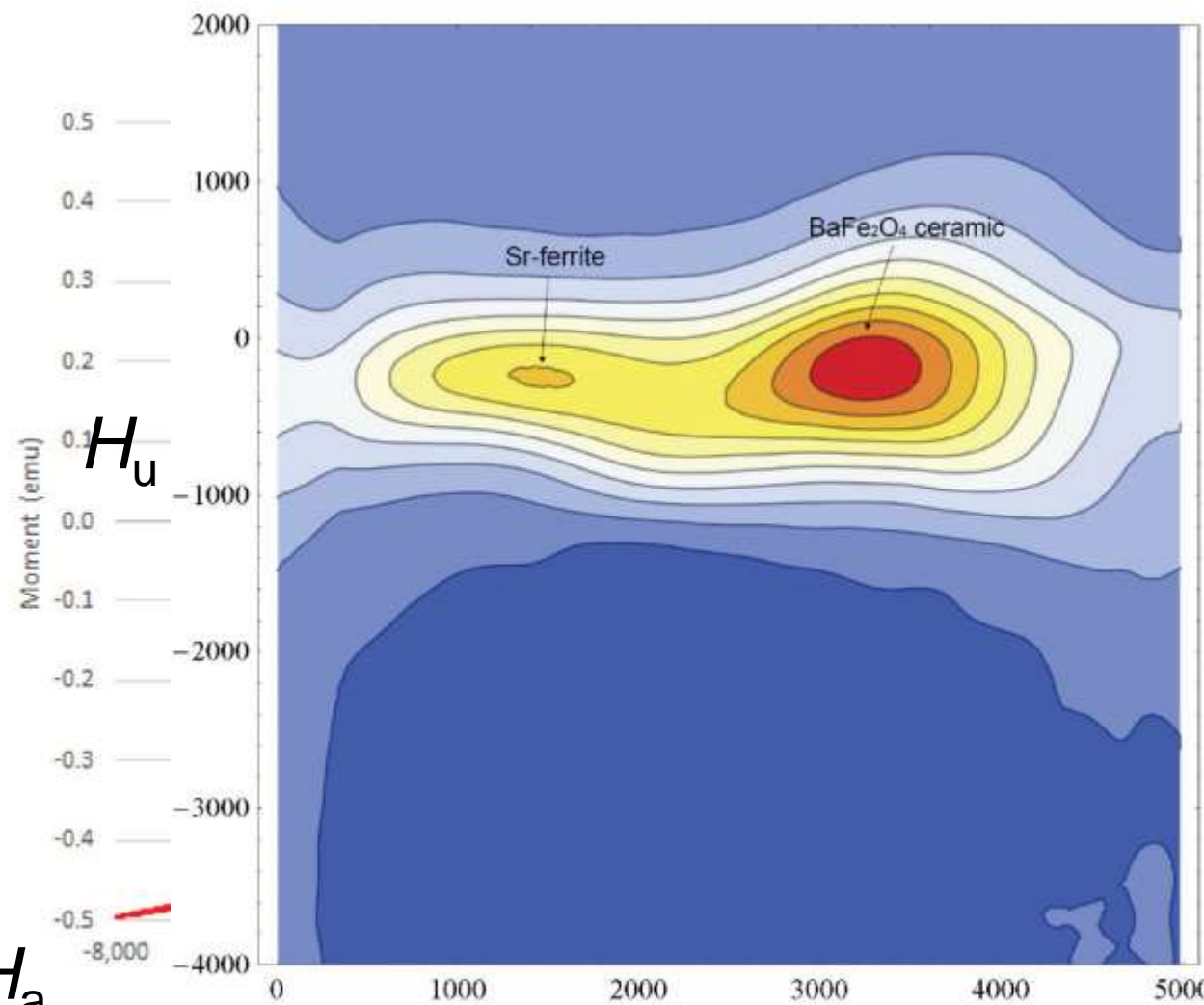


$$M(H_a, H_b) \longrightarrow \rho(H_a, H_b) = -\frac{1}{2} \frac{\partial^2 M(H_a, H_b)}{\partial H_a \partial H_b}$$

One measurement can take days!

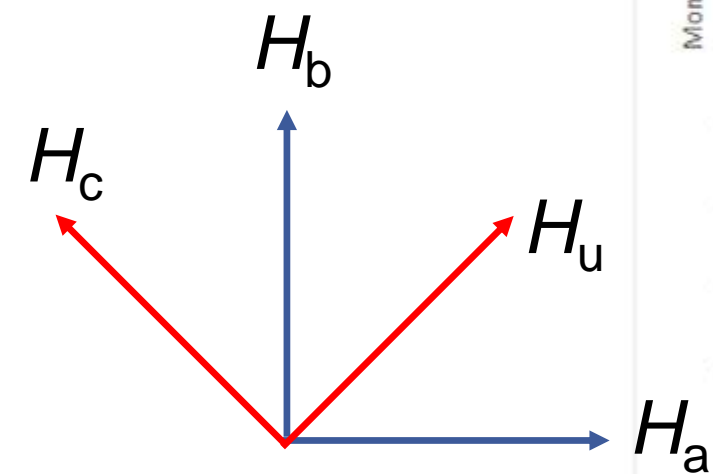
- Transformation (common)

- Distribution coercive fields $H_c = (H_b - H_a)/2$
- Distribution of interaction or reversal fields $H_u = (H_b + H_a)/2$



2D FORC diagram

Sr-ferrite powder and BaFe₂O₄



H_c

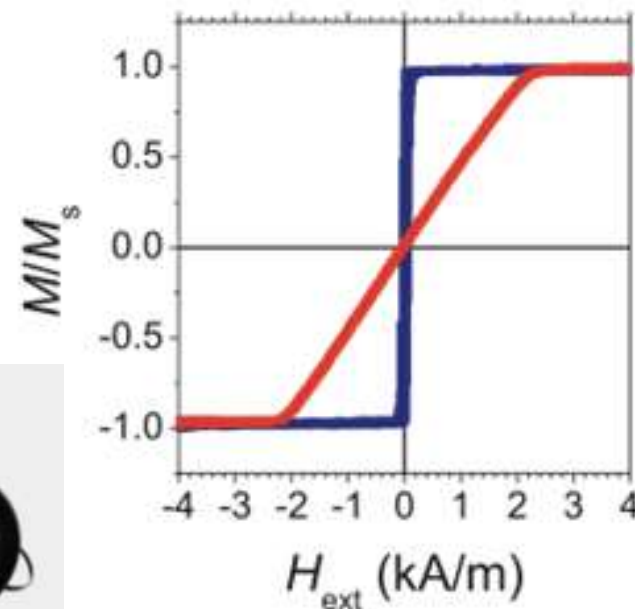
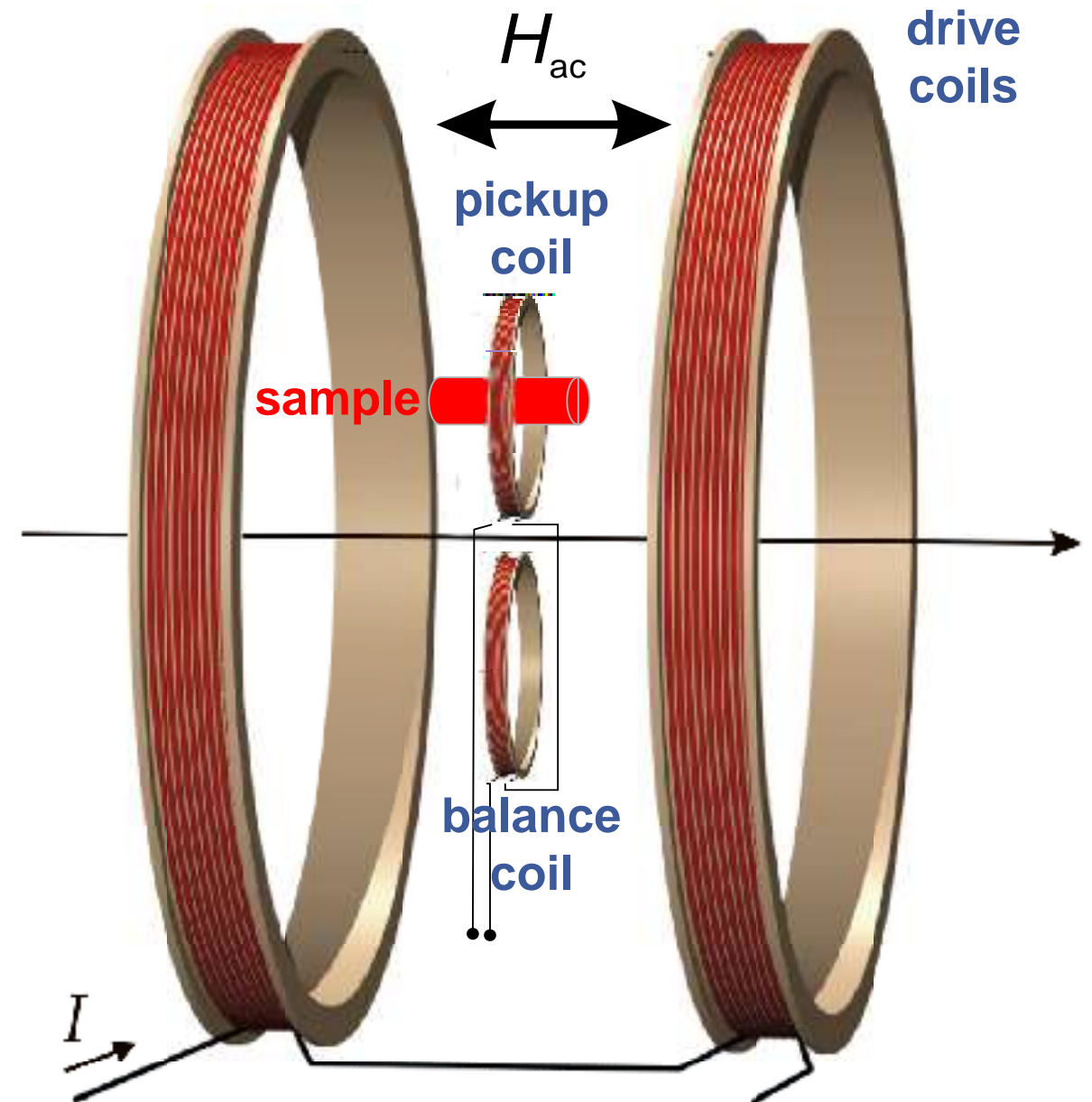
BH-Looper - Hysteresis loop tracer



- Sample in AC field
- Stray field picked up in vicinity of sample
- Balance induction

$$U_{\text{sample}} = U_{\text{sense}} - U_{\text{balance}}$$

- Real time hysteresis measurements (10 Hz)



BH-Looper principle - A pickup coil senses the flux density of a magnetic sample. A balance coil picks up the induction due to the drive field.





- **Mostly based on the magneto-optical Kerr effect (MOKE)**
 - Plane of polarization of light is rotated when light is reflected from a magnetic material surface
 - Other effects exist!
- **Surface sensitive**
 - Depth of information approx. 30 nm
 - Very high sensitivity for magnetic thin films

Also used for magnetic domain imaging!

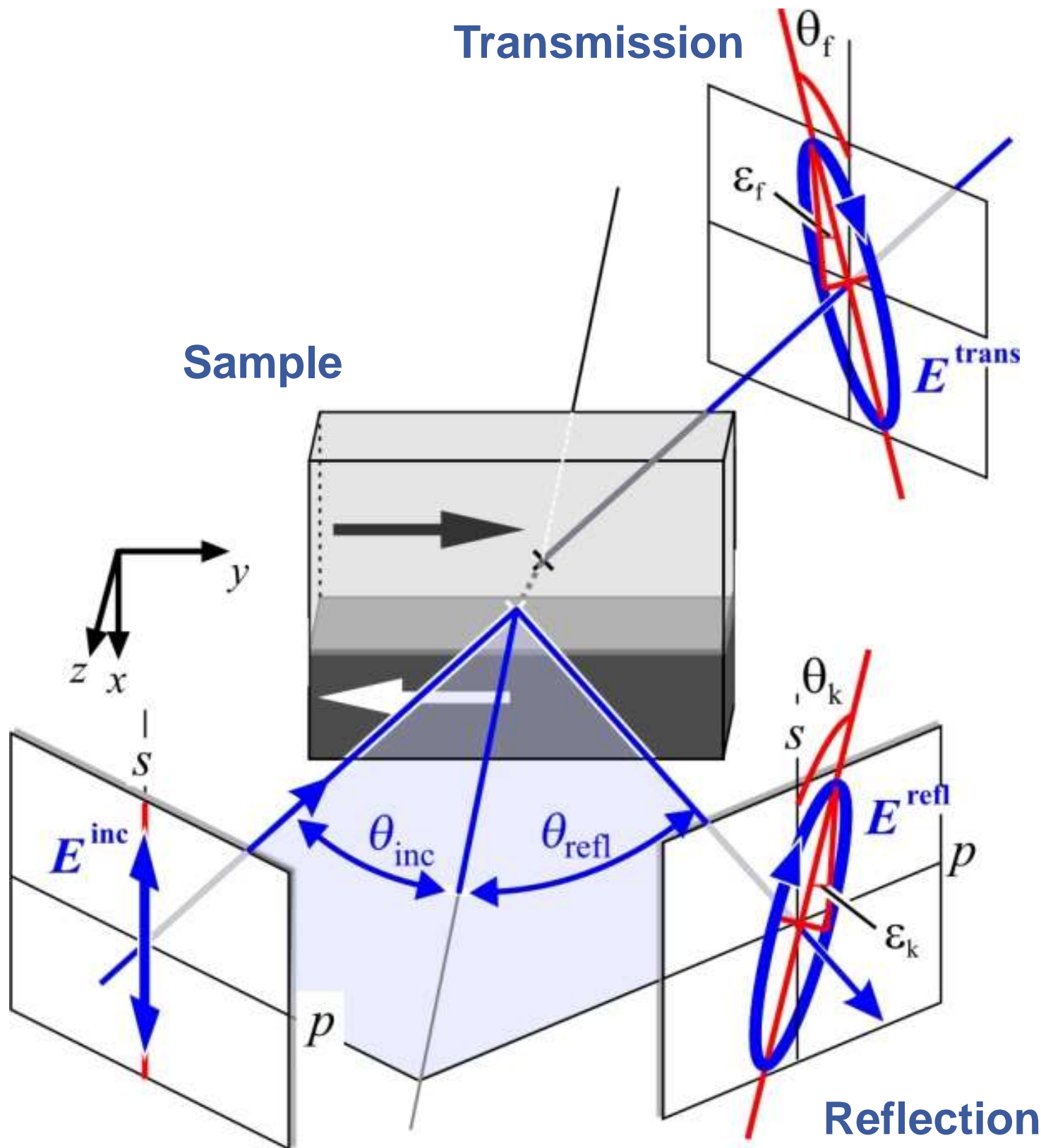
Geometry	Physical phenomena	Dep. with M
$M \parallel k$	Magnetic circular birefringence (<u>MO</u> <u>F</u> araday <u>E</u> ffect and <u>MO</u> <u>K</u> err <u>E</u> ffect)	linear
$M \parallel k$	Magnetic circular dichroism	linear
$M \perp k$	Magnetic linear birefringence (<u>MO</u> <u>V</u> oigt <u>E</u> ffect)	quadratic
$M \perp k$	Magnetic linear dichroism	quadratic
$\partial M \perp k$	Gradient contrast (<u>MO</u> <u>G</u> radient <u>E</u> ffect)	differential

“Circular birefringence” $\sim M$ “Linear birefringence” $\sim M^2$

$$D = \varepsilon_{total} E$$

$$\varepsilon_{total} = \varepsilon \underbrace{\begin{pmatrix} 1 & -iQm_3 & iQm_2 \\ iQm_3 & 1 & -iQm_1 \\ -iQm_2 & iQm_1 & 1 \end{pmatrix}}_{\text{Faraday or Kerr effect}} + \underbrace{\begin{pmatrix} B_1 m_1^2 & B_2 m_1 m_2 & B_2 m_1 m_3 \\ B_2 m_1 m_2 & B_1 m_2^2 & B_2 m_2 m_3 \\ B_2 m_1 m_3 & B_2 m_2 m_3 & B_1 m_3^2 \end{pmatrix}}_{\text{Voigt effect}}$$

- Electric vector of light wave E
- Dielectric tensor ε
- Dielectric displacement vector D
- Magnetization vector components m
- **Complex Voigt constant Q** **Faraday and Kerr effect**
- **Complex material constants B_1, B_2** **Voigt effect**



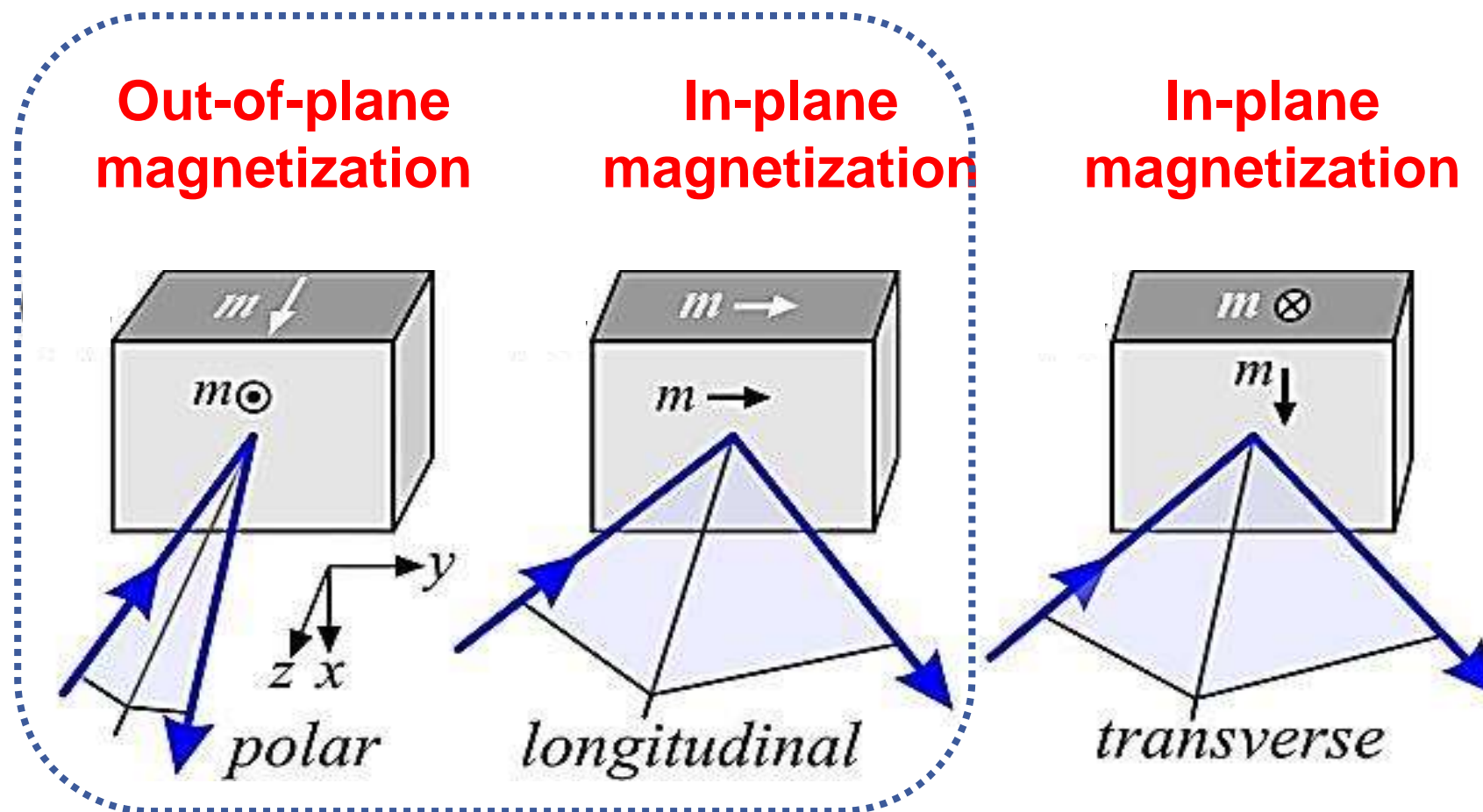
Faraday effect (MOFE)

Longitudinal Faraday and Kerr effect under an angle of incidence θ_{inc} relative to the surface normal. The case of s-polarization is sketched. By the MO interaction with the magnetic medium the linearly polarized incoming light (E^{inc}) is transformed to an elliptically polarized light E^{trans} and E^{refl} . The resulting Faraday rotation θ_f and ellipticity e_f , respectively, Kerr rotation θ_k and ellipticity e_k are shown. θ_{refl} is the angle of reflection of light.

Kerr effect (MOKE)

J.McCord, Journal of Physics D: Applied Physics 48, 333001 (2015)

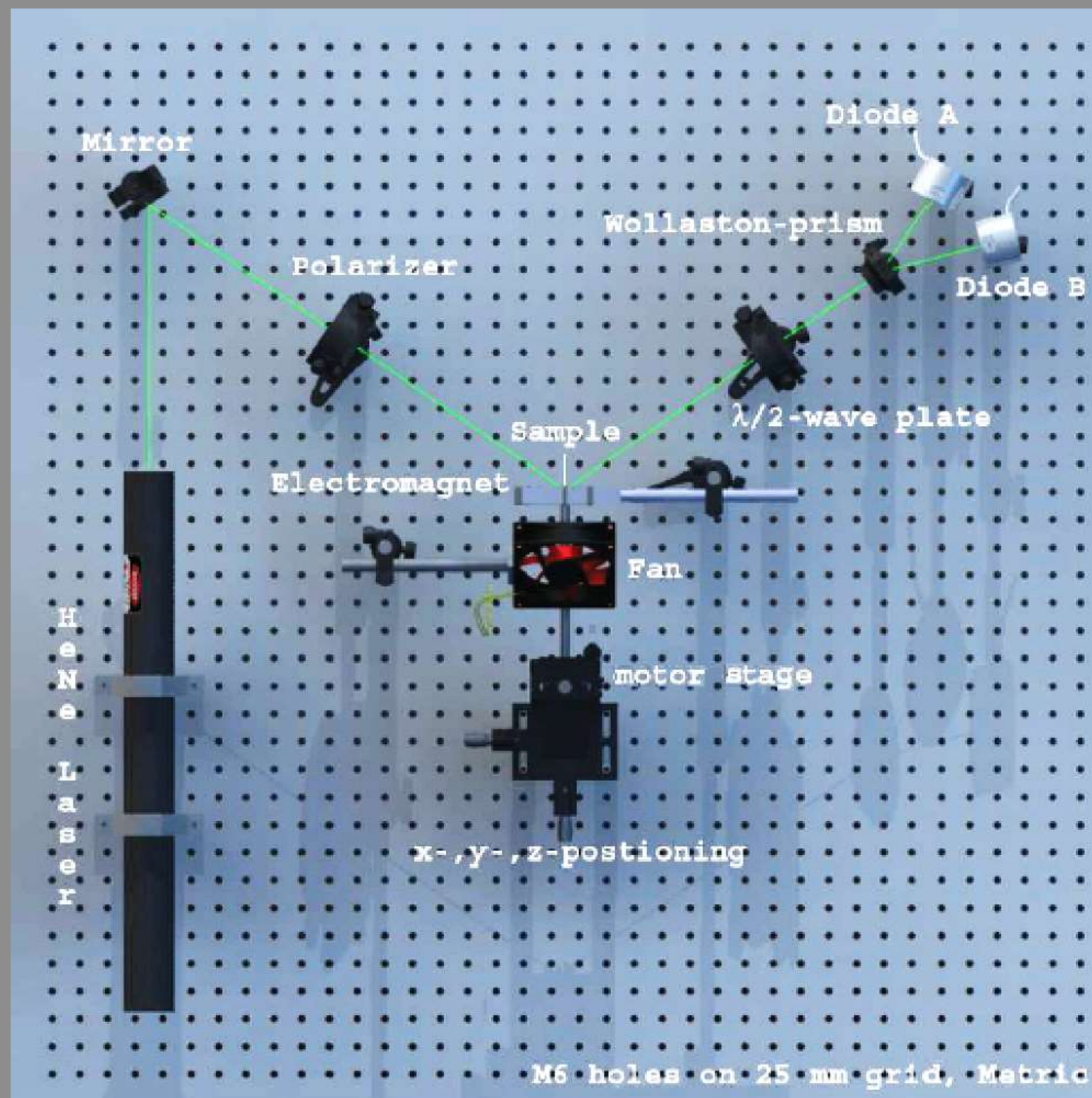
The effects might come together!



The three basic configurations of the (a) polar, (b) longitudinal, and (c) transverse magneto-optical Kerr effect. The unit vector of magnetization m is lying along the corresponding sensitivity axes (as indicated).

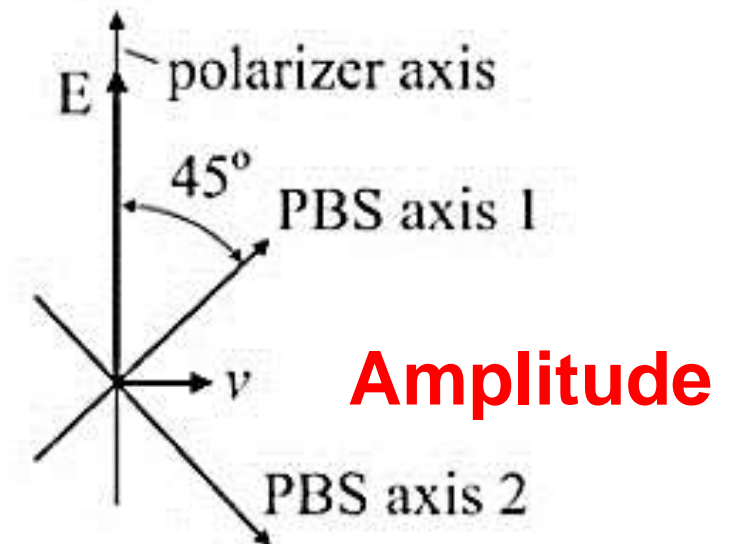
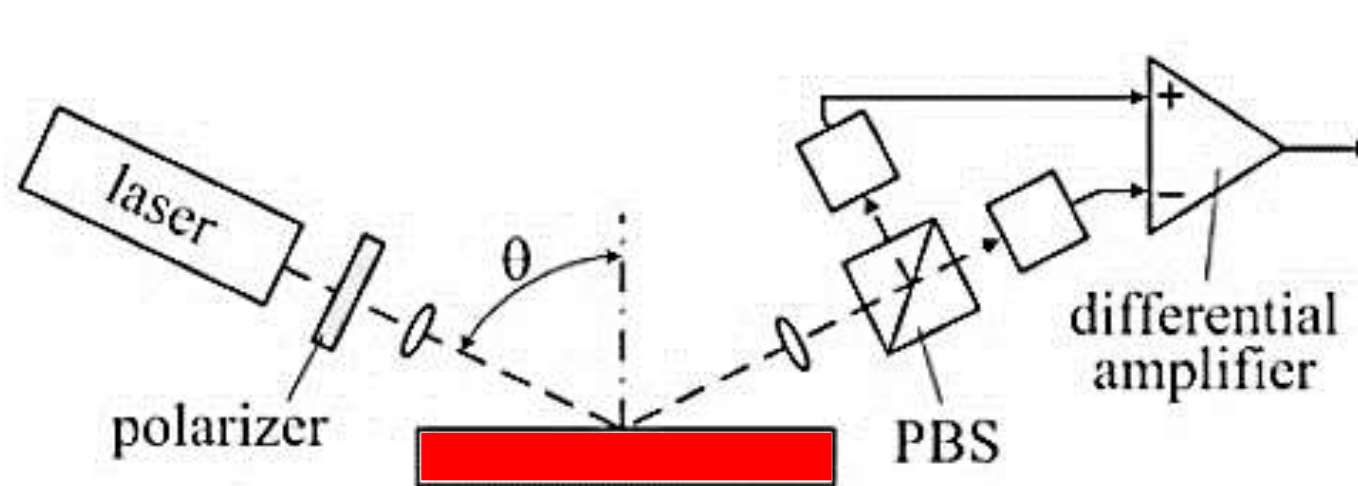
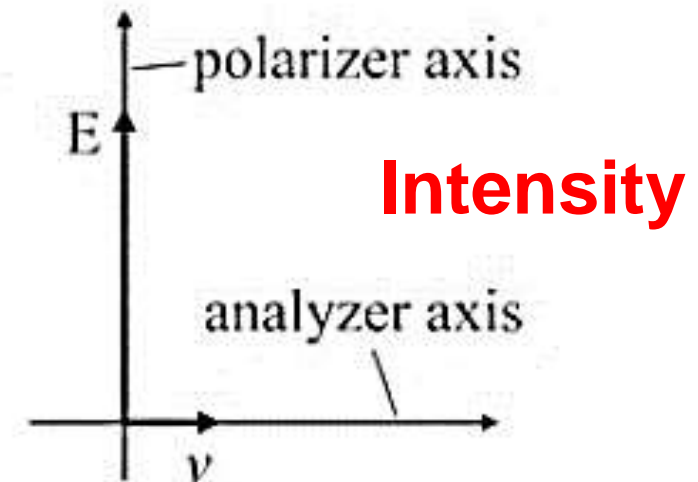
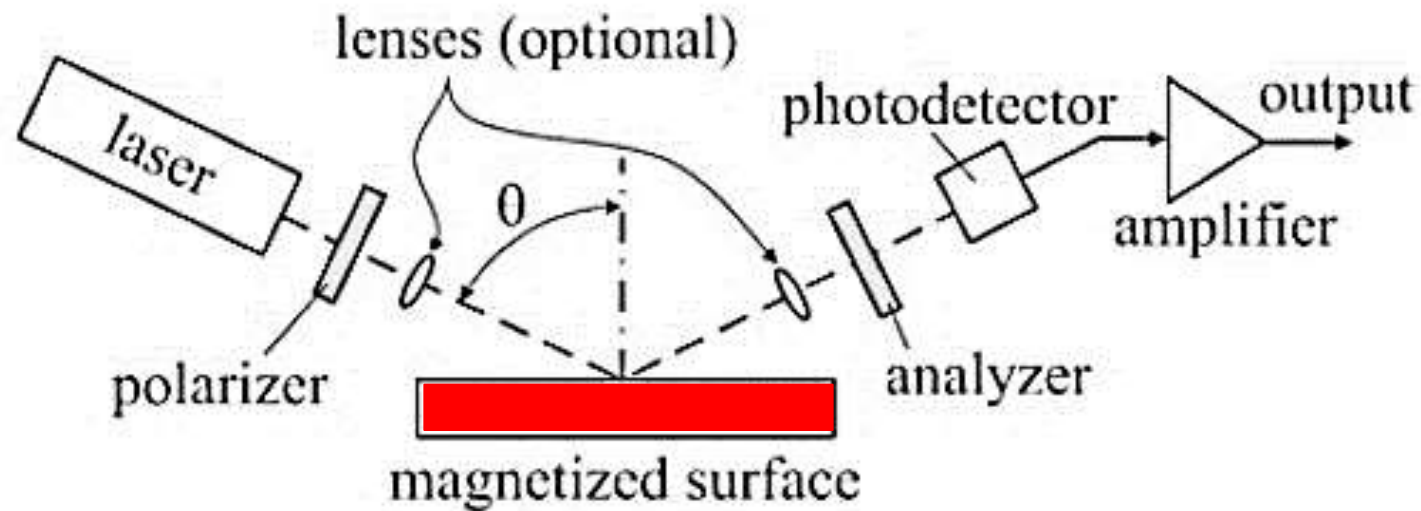
J.McCord, Journal of Physics D: Applied Physics 48, 333001 (2015)

Typical simple MOKE magnetometry setup



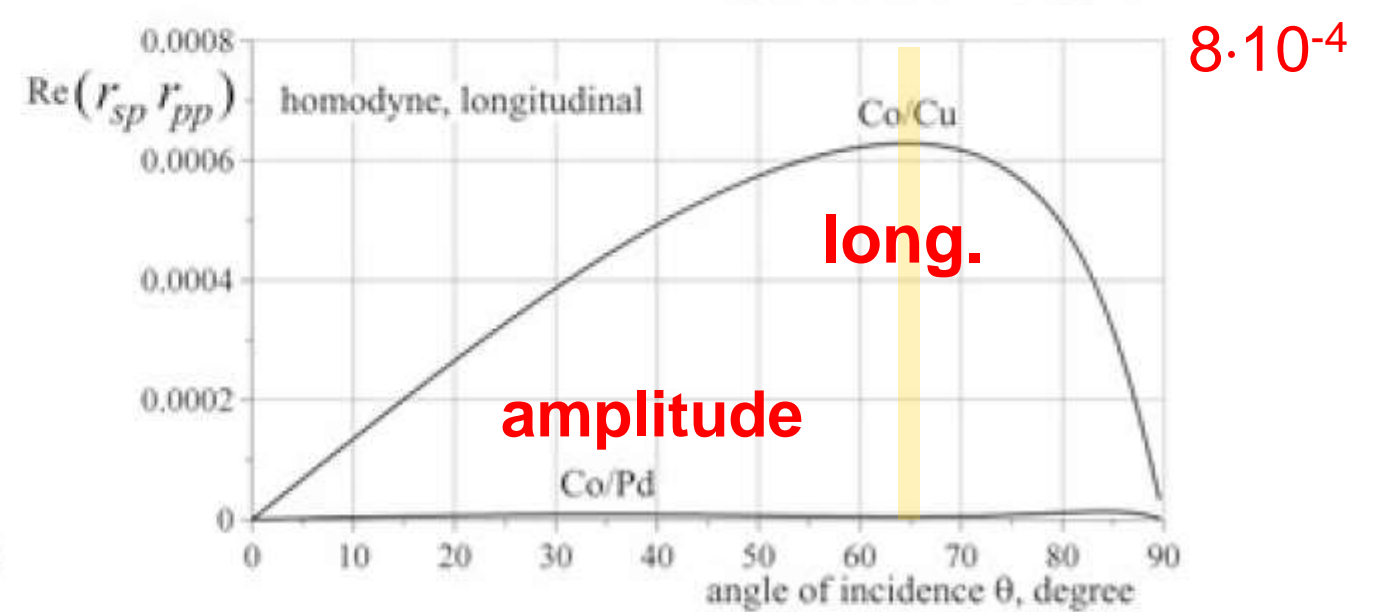
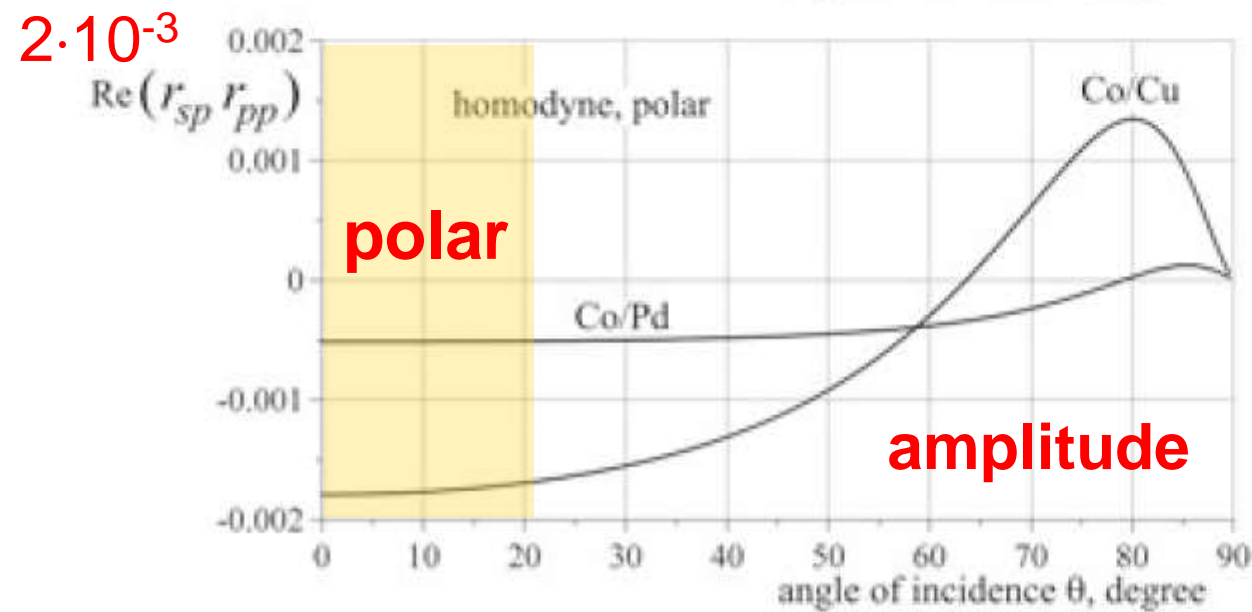
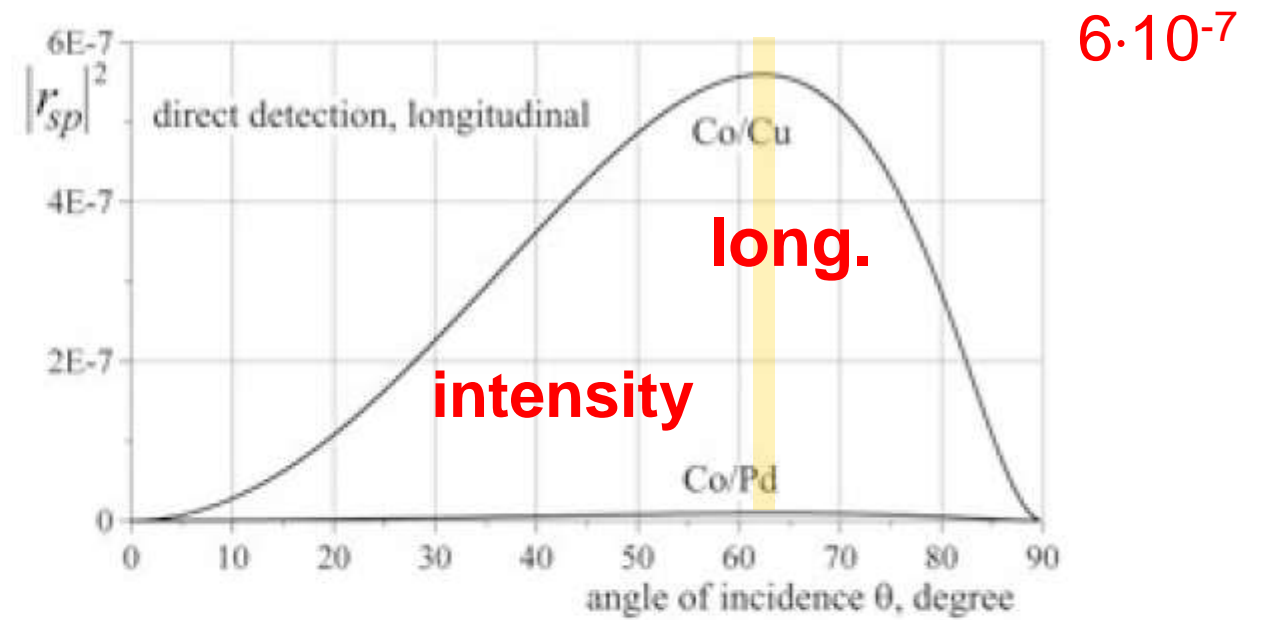
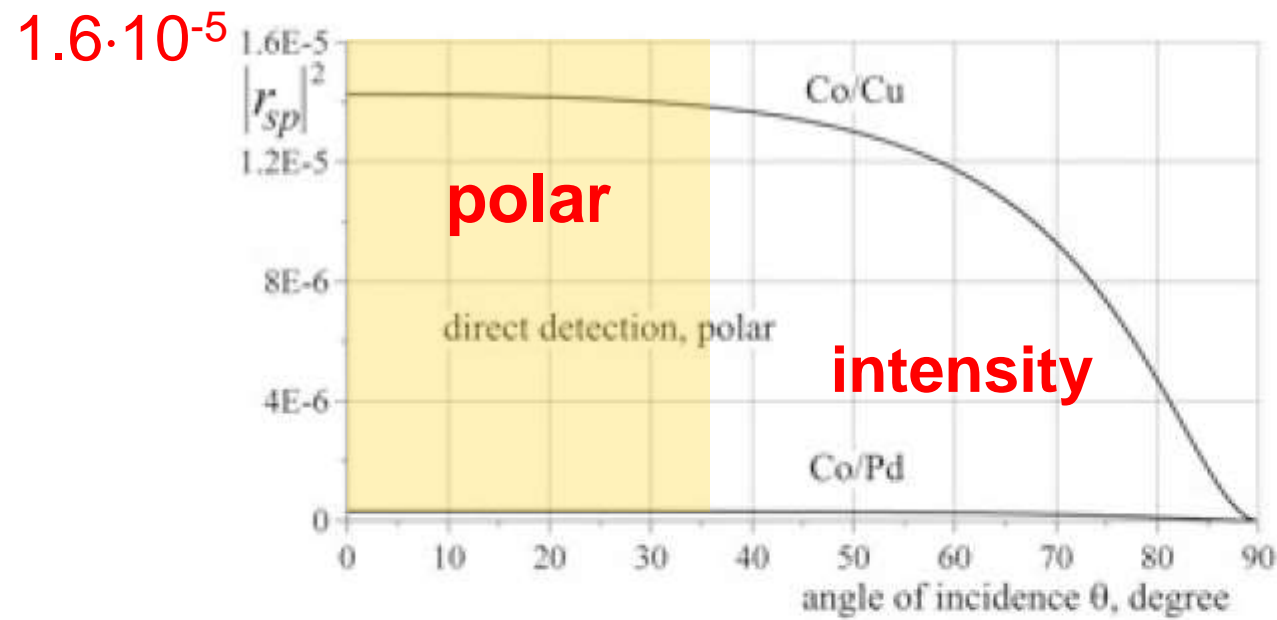
J. M. Teixeira et al.
Review of Scientific
Instruments 82, 043902
(2011)

Typical detection schemes



Direct detection (upper) and bi-channel homodyne (lower) schemes use low-noise lasers (PBS: polarizing beam-splitting cube).

Polar and longitudinal MOKE – angle of incidence



Practical opto-electronics, Springer (2014)
V.V. Protopopov, Magneto-optics

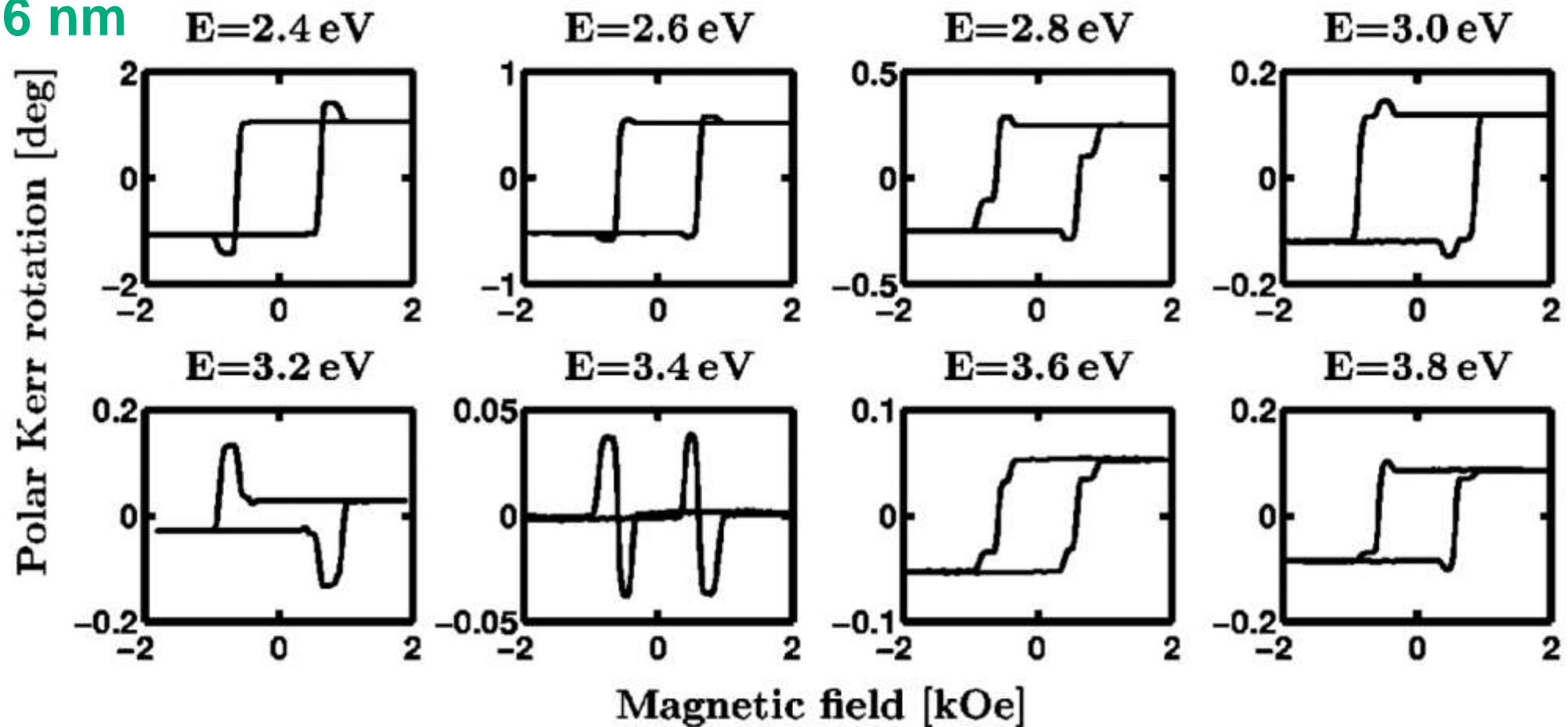
Angular dependence of MO signals for direct and bi-channel detection schemes.

Layer sensitive MOKE magnetometry



J. Hamrle et al., Phys. Rev. B **66**, 224423

516 nm

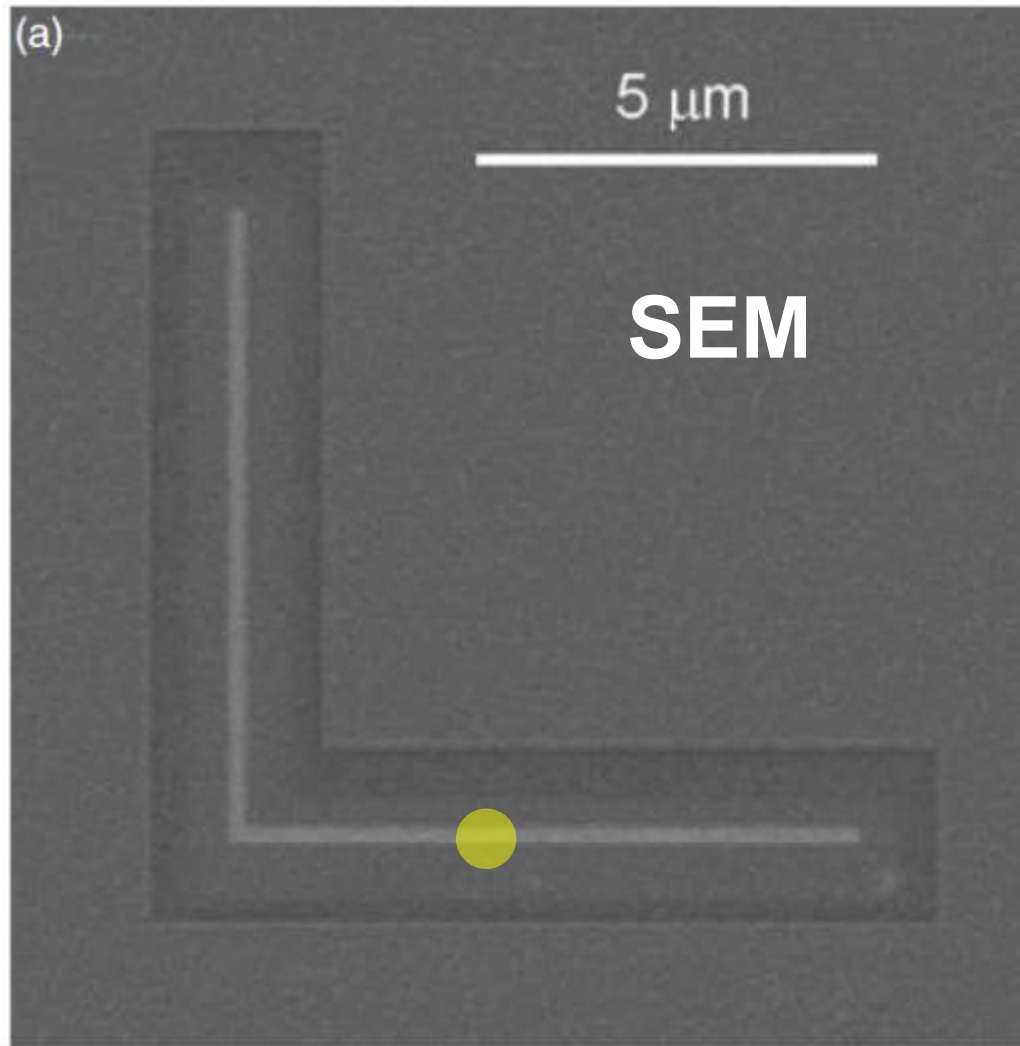


326 nm

Example of polar Kerr rotation hysteresis loops measured at several photon energies E on the $(\text{TbFe}/\text{Si}_3\text{N}_4)_4$ sample. Each step in the hysteresis loop corresponds to a MOKE signal coming from a given TbFe stack.

4 × {	Si_3N_4	67 nm
	$[\text{Tb}(0.8 \text{ nm})/\text{Fe}(1.1 \text{ nm})]_{10}$	19 nm
	Si_3N_4	10.5 nm
	glass	

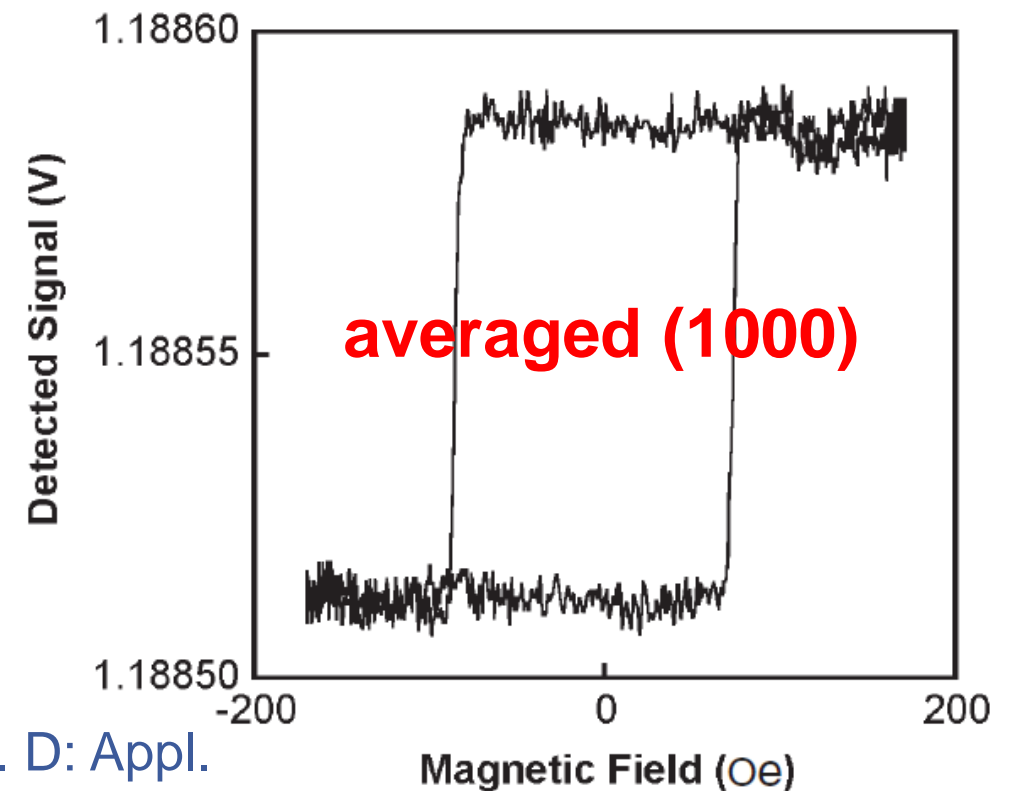
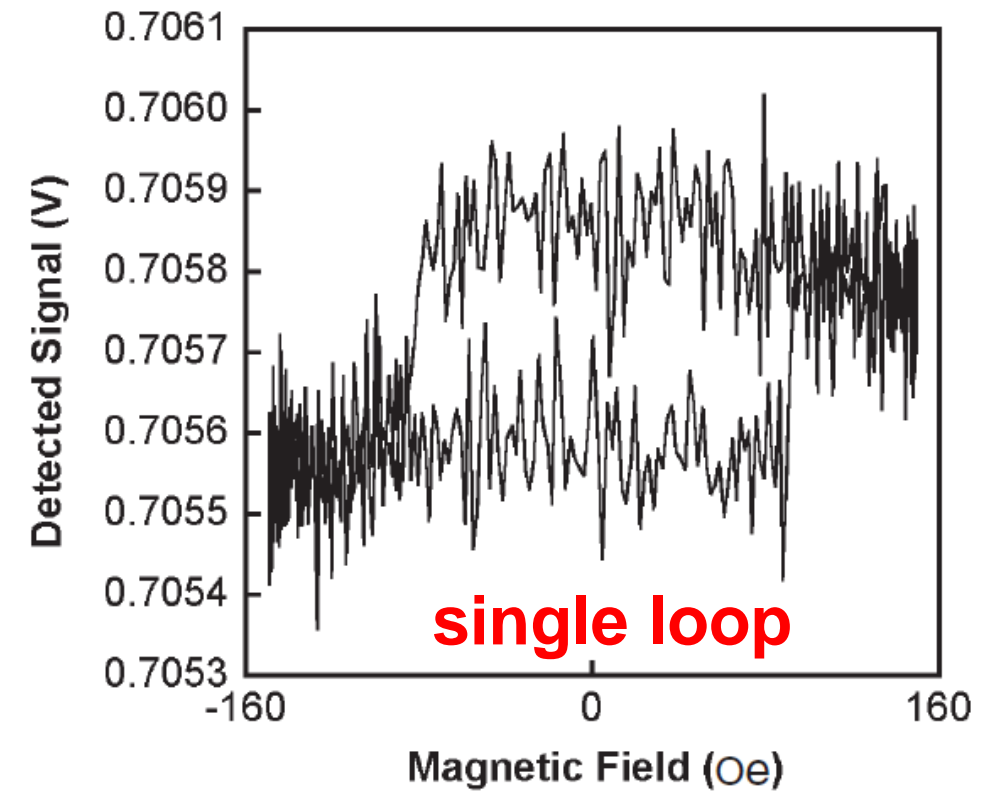
High resolution MOKE magnetometry



FIB-milled Permalloy L-shaped nanowire.

■ Permalloy

- thickness $t = 5$ nm
- width $w = 200$



D.A. Allwood et al., J. Phys. D: Appl. Phys. **36** (2003) 2175–2182

- Described by Landau-Lifschitz-Gilbert equation of magnetization dynamics

$$\frac{d}{dt} \vec{M} = \underbrace{-\gamma \vec{M} \times H_{\text{eff}}}_{\text{Precession}} + \underbrace{\frac{\alpha}{M_s} \left(\vec{M} \times \frac{d}{dt} \vec{M} \right)}_{\text{Relaxation}}$$

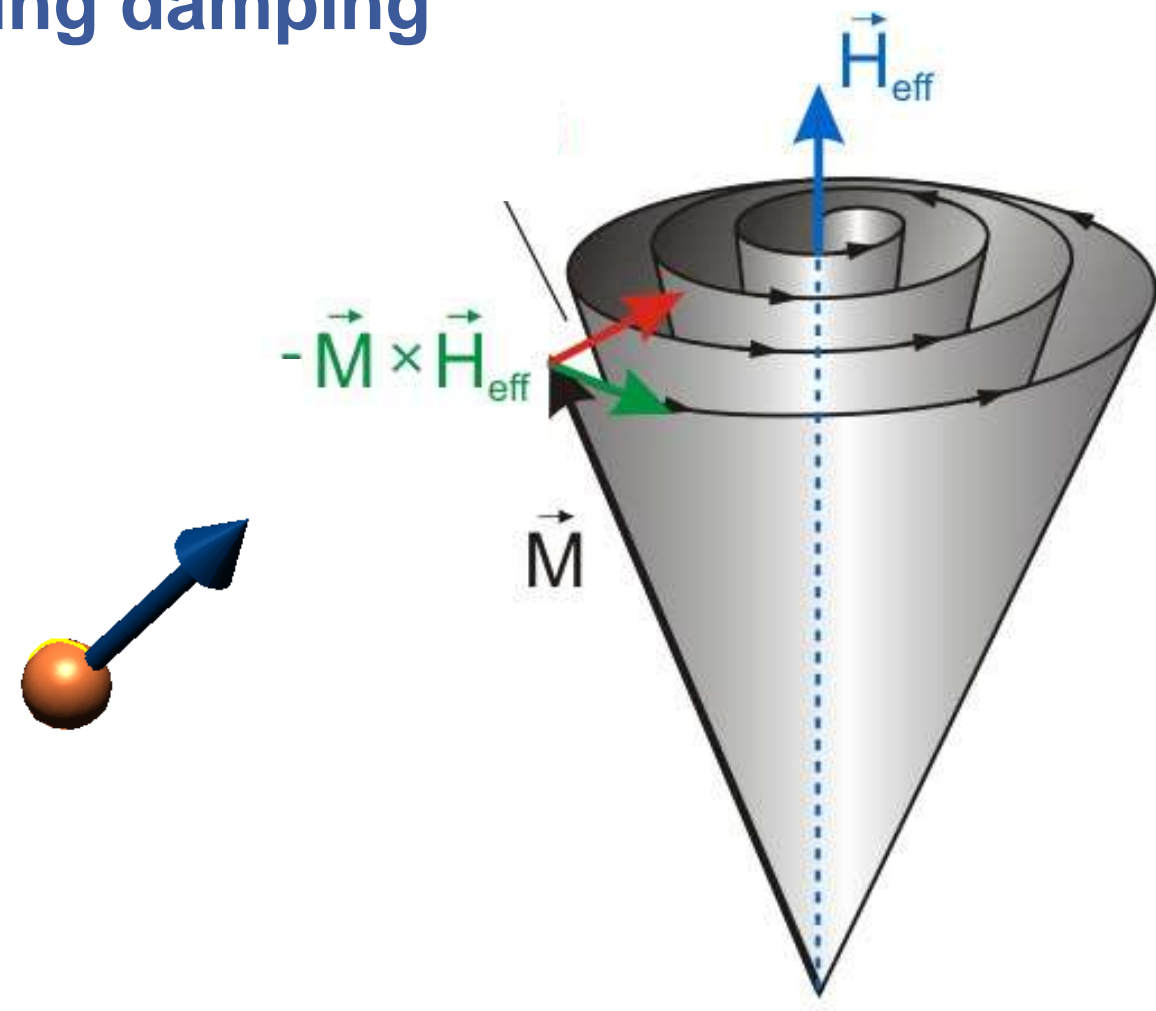
- Precession of magnetization including damping

$$f_{\text{res}} = \frac{\gamma \mu_0}{2\pi} \sqrt{M_s H_{\text{eff}}} \sim \sqrt{H_{\text{eff}}}$$

Precessional frequency f_{res}

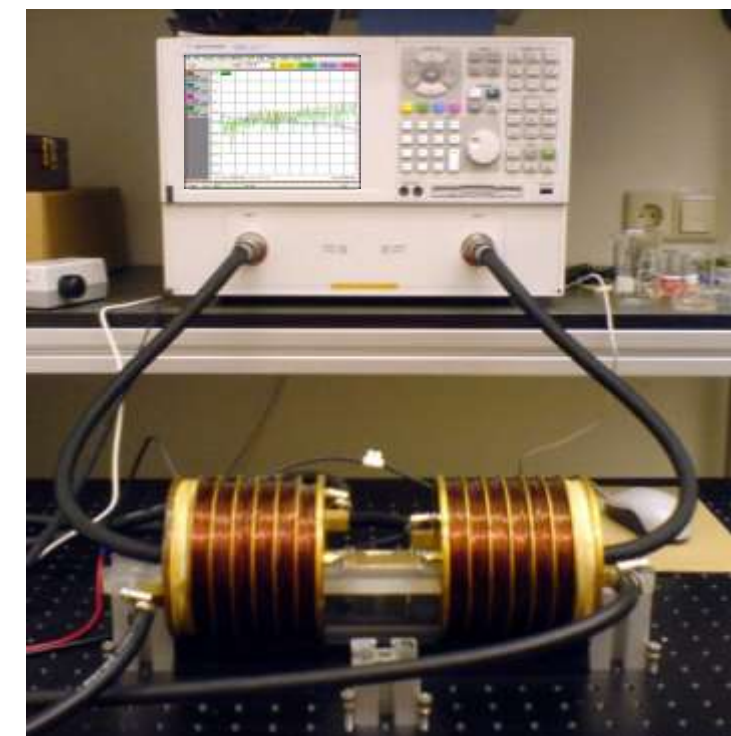
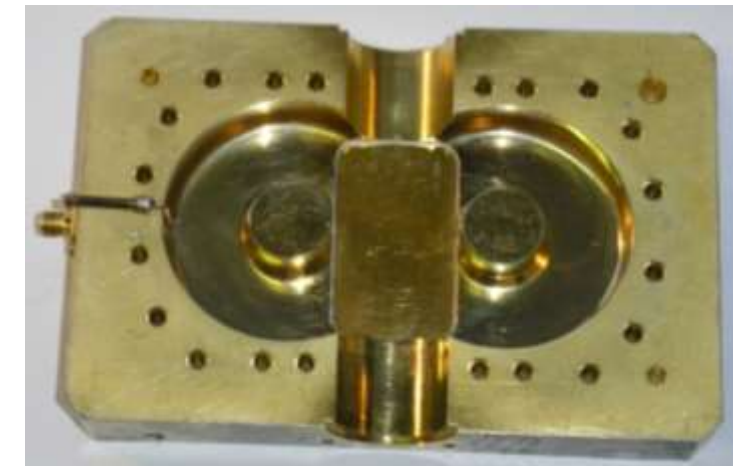
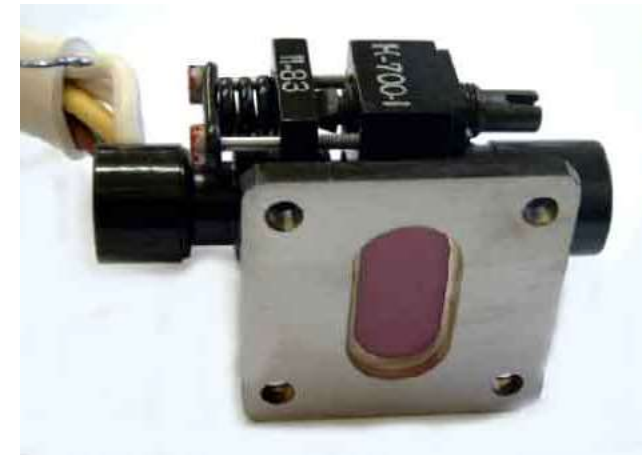
$$\alpha_{\text{eff}} = \frac{2}{\tau \gamma \mu_0 M_s} \sim \frac{1}{\tau}$$

Damping parameter α (small fields)



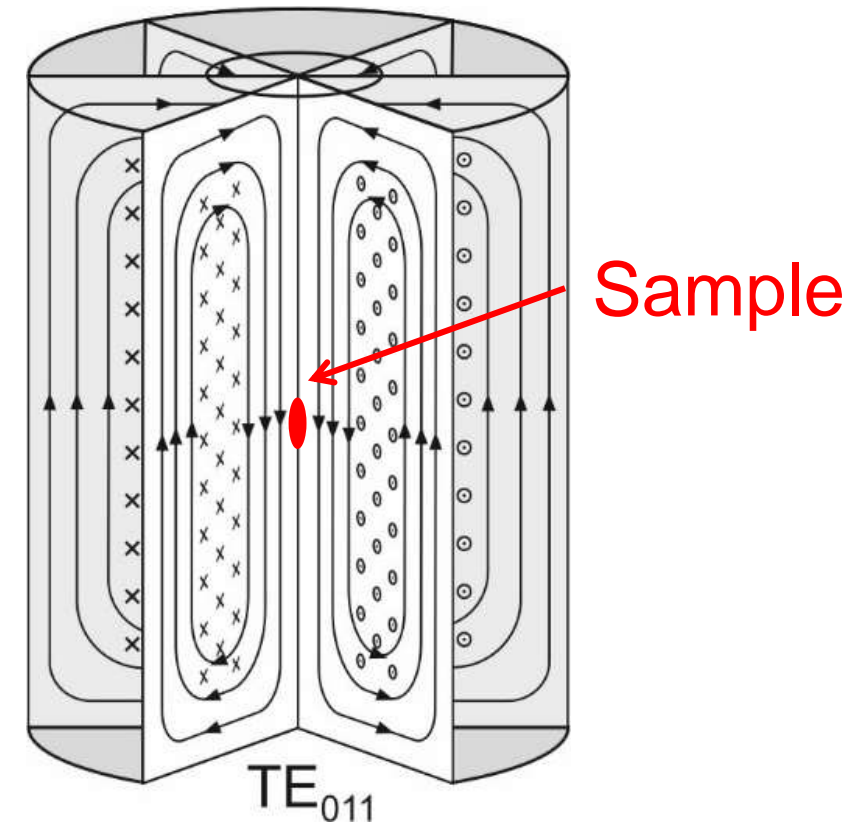
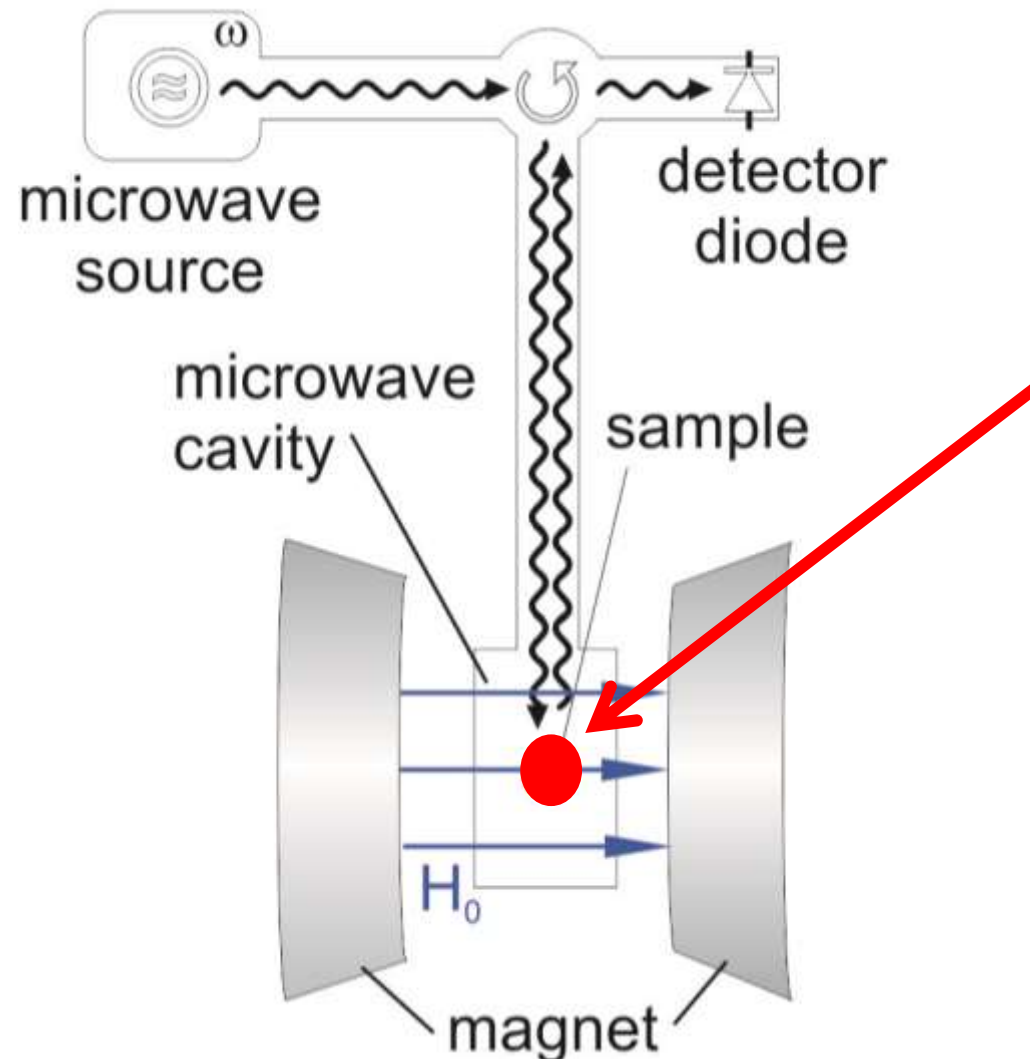
FMR measurement modes

- **Magnetic field sweep with constant frequency**
 - Standard FMR technique
 - High sensitivity through resonant cavity (resonator)
- **Frequency sweep with constant magnetic field**
 - Broadband sources needed
 - Allows for zero field measurements



Material from K. Lenz, HZDR,

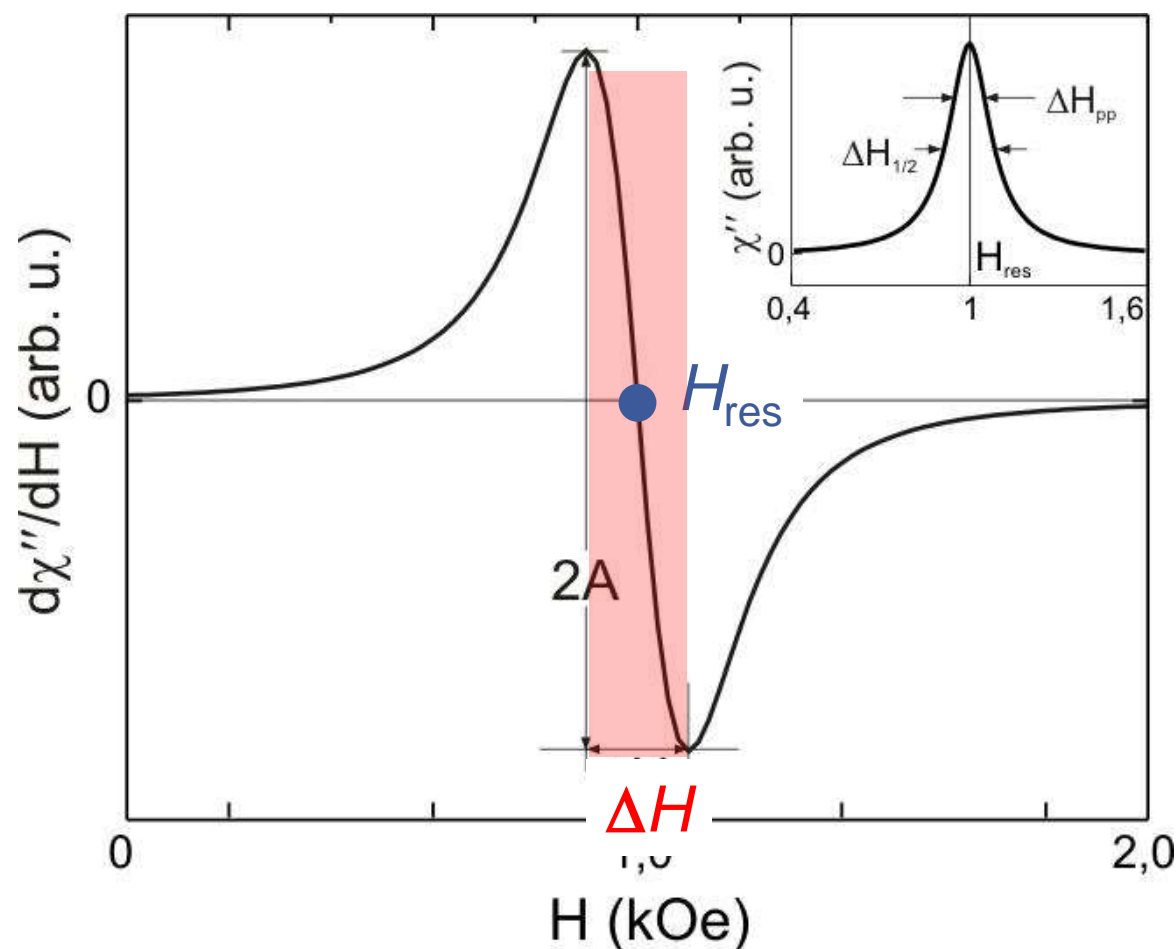
- Resonator with microwave bridge
 - Sensitivity: $\sim 10^{10}$ spins
 - x-band FMR @ 9 GHz
 - Up to 500 GHz



Material from K. Lenz, HZDR, Germany

- Microwave absorption ~ susceptibility
- rf-susceptibility (imaginary part)

$$\chi(\omega) = \frac{\gamma M_s}{\gamma H_{\text{eff}} + i\alpha\omega} \left(1 + \frac{\omega^2}{(\gamma M_s + \gamma H_{\text{eff}} + i\alpha\omega)(\gamma H_{\text{eff}} + i\alpha\omega) - \omega^2} \right)$$



Measurement signal is a Lorentz curve

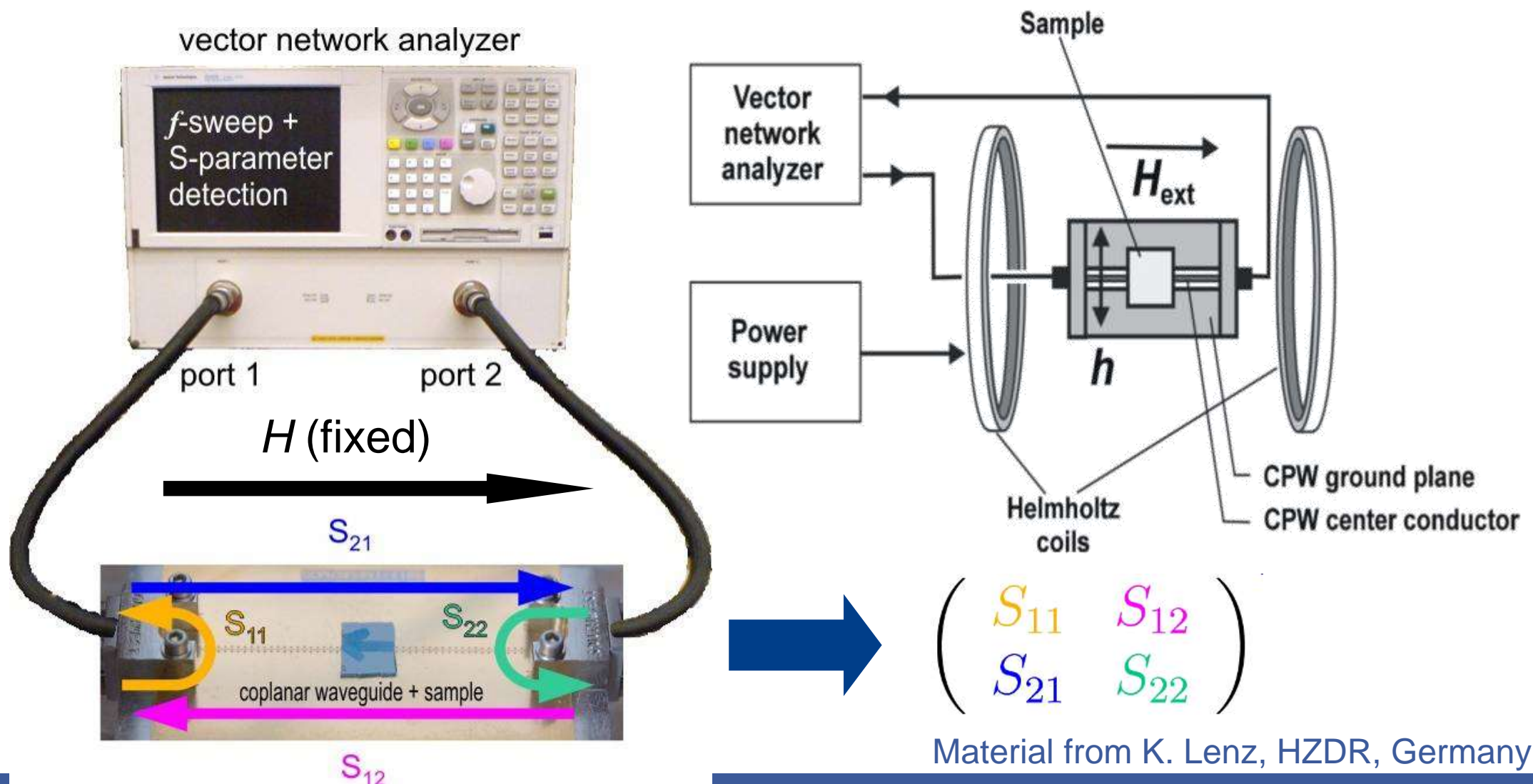
- Resonance field H_{res}
- Line width ΔH
- Amplitude A

H_{res} → anisotropy

ΔH → damping parameter

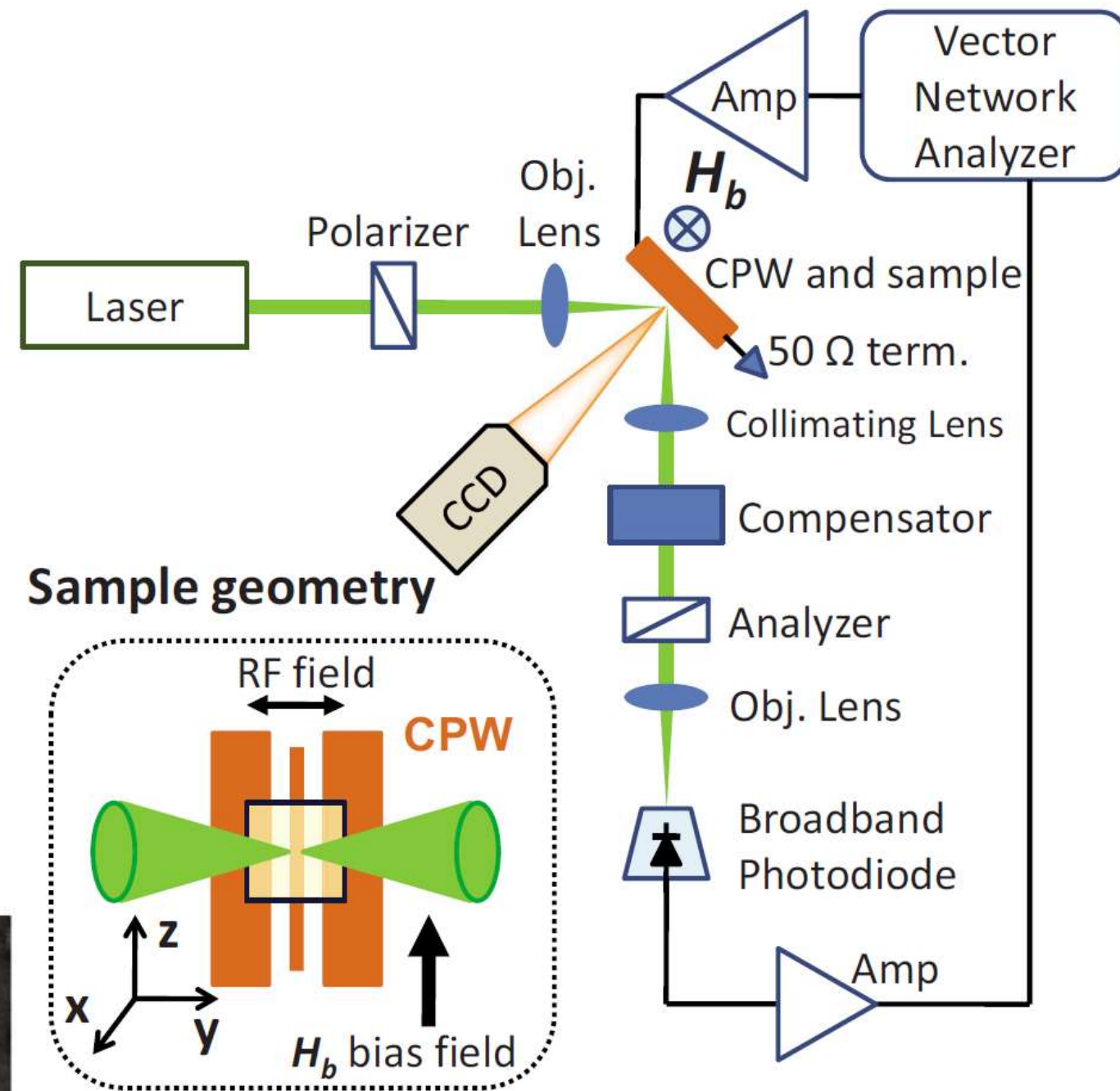
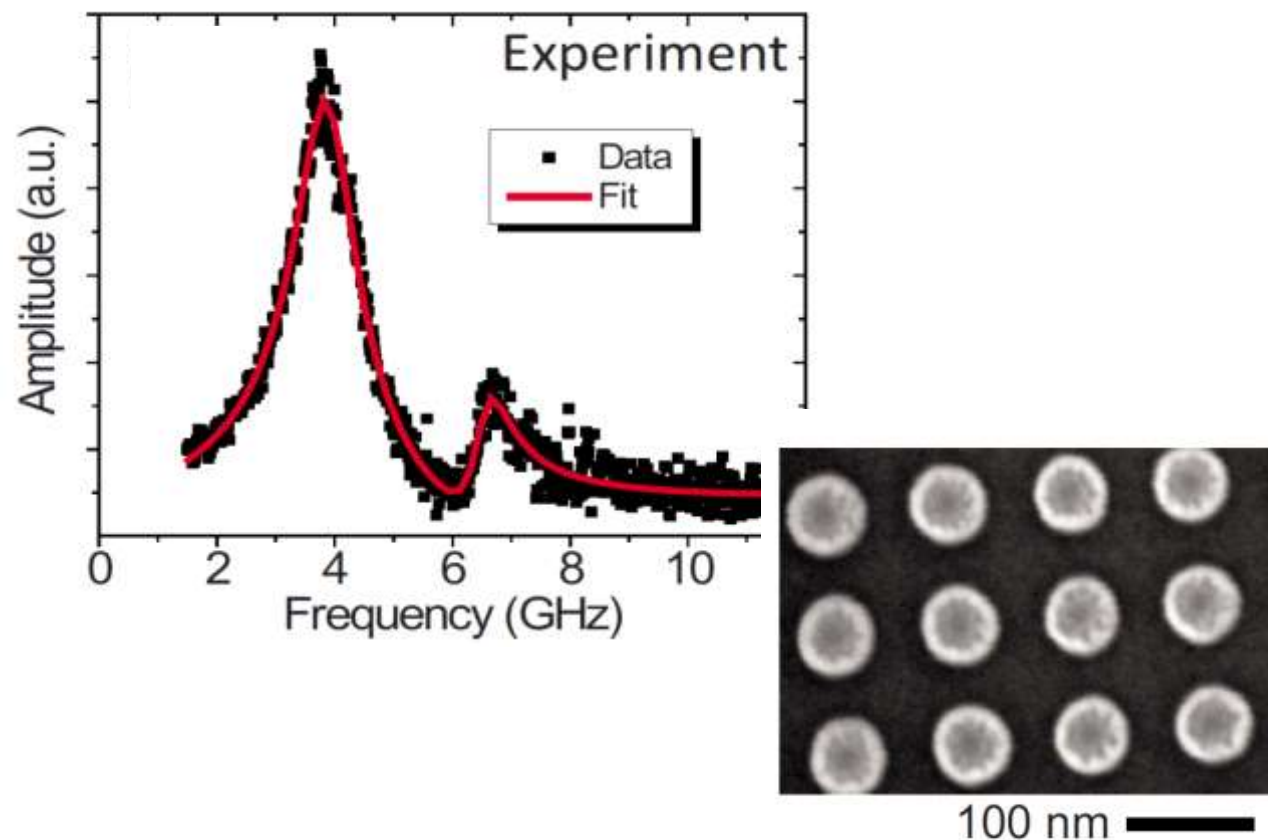
Broadband FMR

- Tunable microwave source (Vector Network Analyzer (VNA))
- Excitation through wave guide (antenna)
- Measuring of transmission and reflection coefficients
 - Transmission S_{ij} ($i \neq j$) and reflection coeff. S_{ii} ($i = j$)



Magneto-optical FMR (FR-MOKE)

- Sample on top of wave-guide
 - rf-field excitation
 - Detection of $M_x(t)$ by fast PD
 - Spatially resolved FMR



J.M. Shaw et al. Phys. Rev. B 79, 184404 (2009)

... definitely not a complete list ...

Method	Remarks	Typical sensitivity
Vibrating sample	Slow	10^{-9} Am^2
Alternating gradient force	Fast	10^{-10} Am^2
BH-Looper	Even faster	10^{-9} Am^2
SQUID	Highest sensitivity	10^{-12} Am^2
Magneto-optics	Fast and high surface sensitivity	10^{-15} Am^2
FMR	Dynamic properties	10^{-16} Am^2



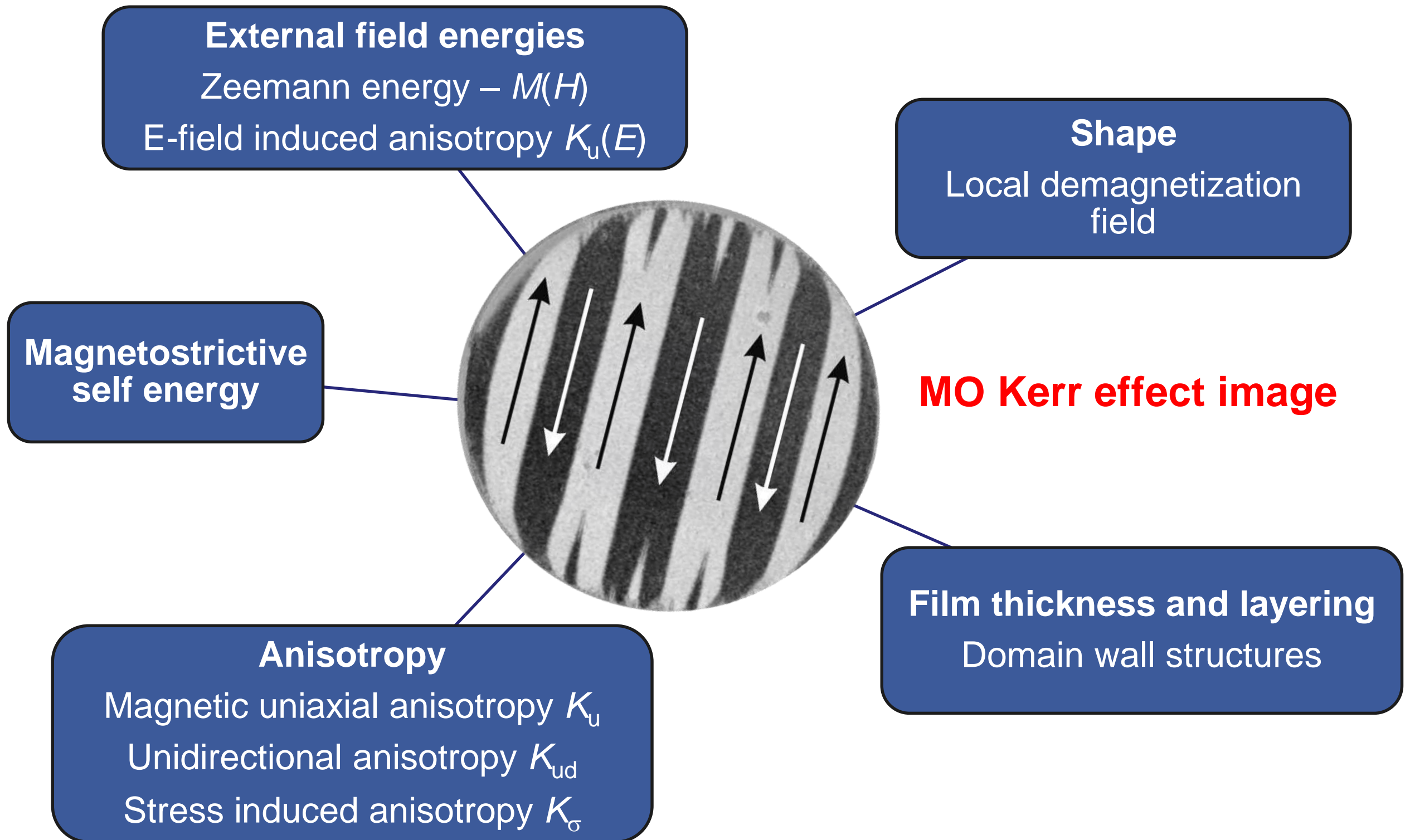
... papers, papers, and papers ...

- Review of Scientific Instruments (AIP Publishing)
- Web-presence of vendors
- Coey, John MD. *Magnetism and magnetic materials*. Cambridge University Press, 2010.
- Cullity, Bernard Dennis, and Chad D. Graham. *Introduction to magnetic materials*. John Wiley & Sons, 2011.



- Magnetic fields
- Quasi-static measurements
- Dynamic measurements
- **Quasi-static magnetic domain imaging**
- **Imaging of magnetization dynamics**

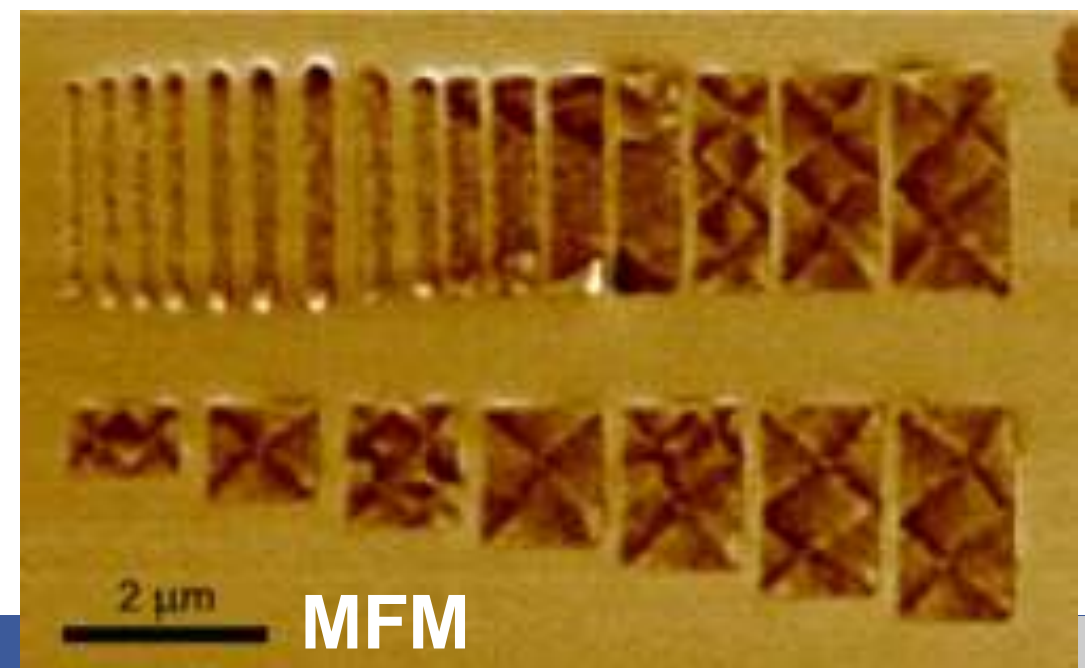
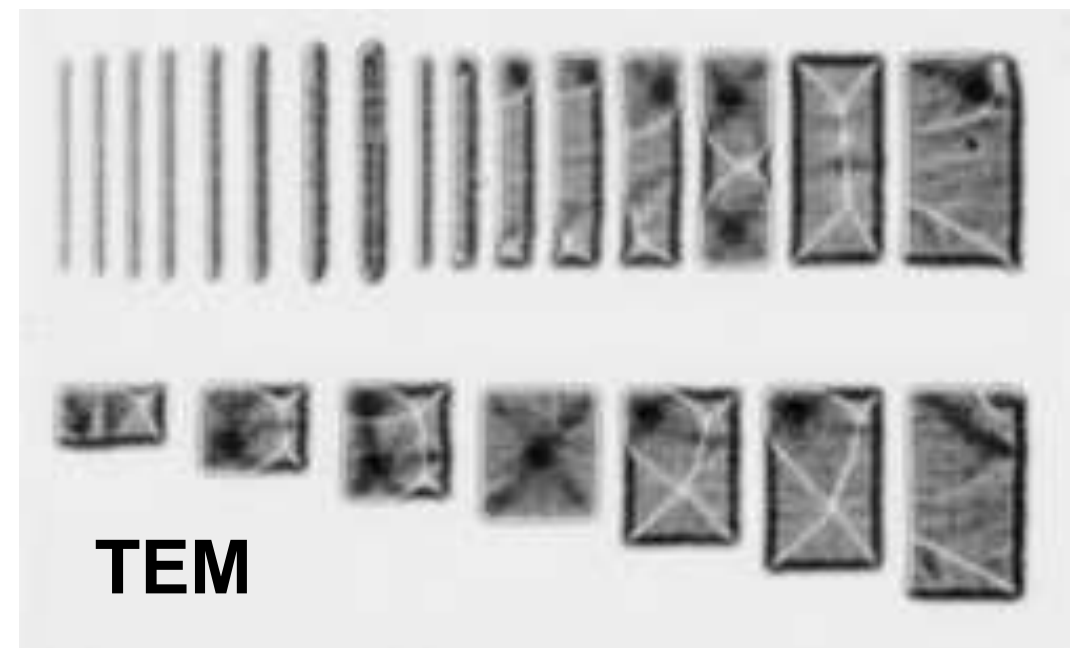
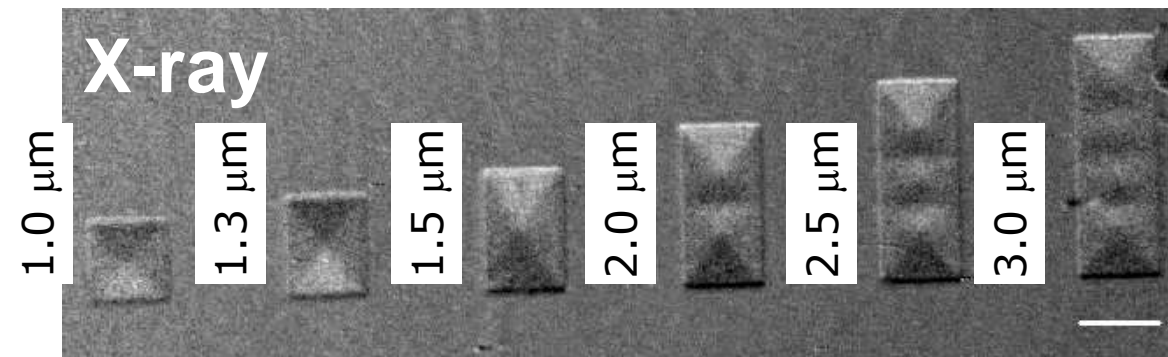
Again, far from being complete!

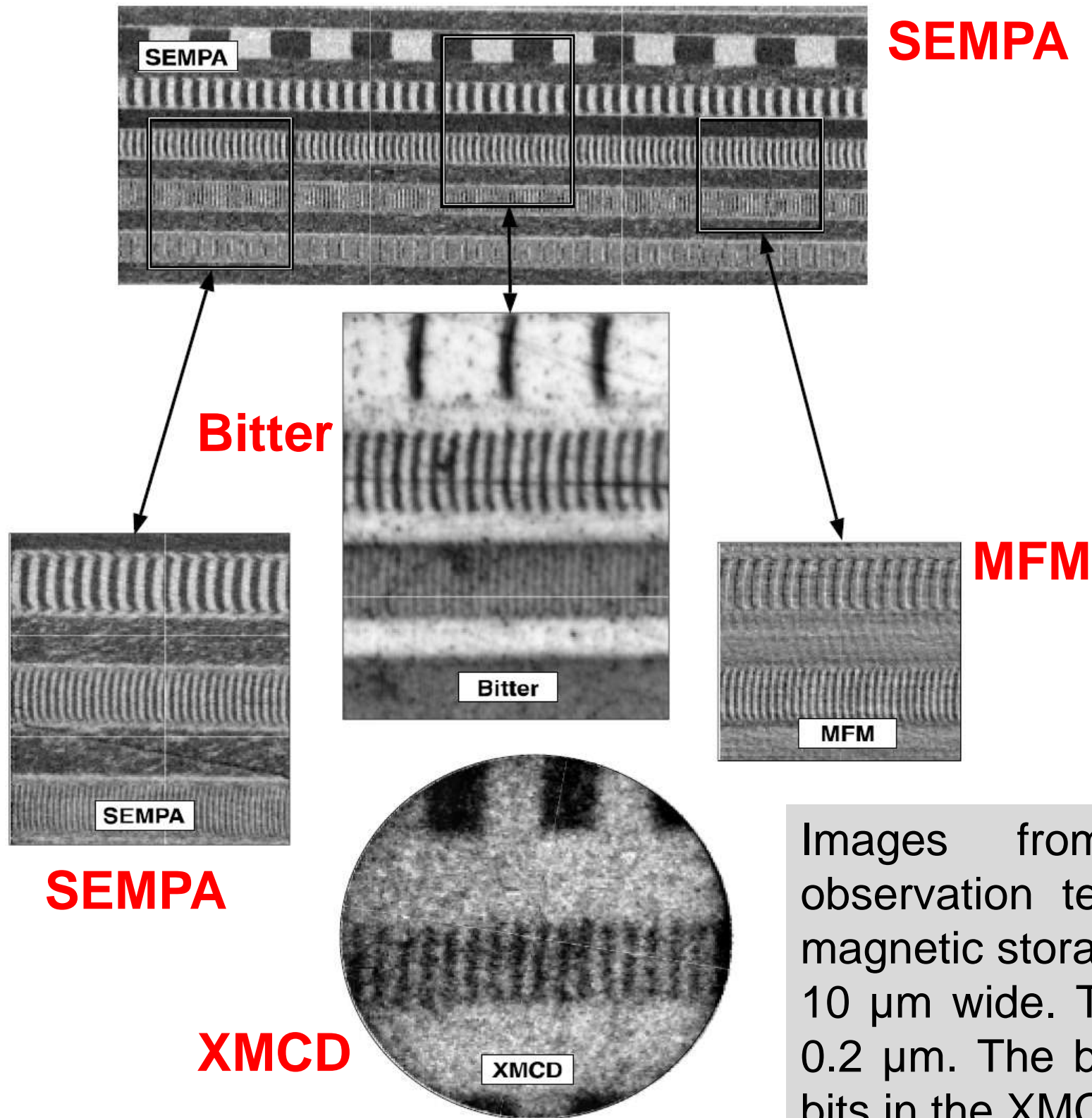


Parameters may vary laterally!

- **Magnetic material property measurements**
- **Magnetic imaging**
 - Quasi-static and dynamic imaging methods
- **Vary by ...**
 - ... contrast mechanism (M , dM/dx , ...)
 - ... spatial resolution
 - ... temporal resolution

... it is all about magnetic domains ...

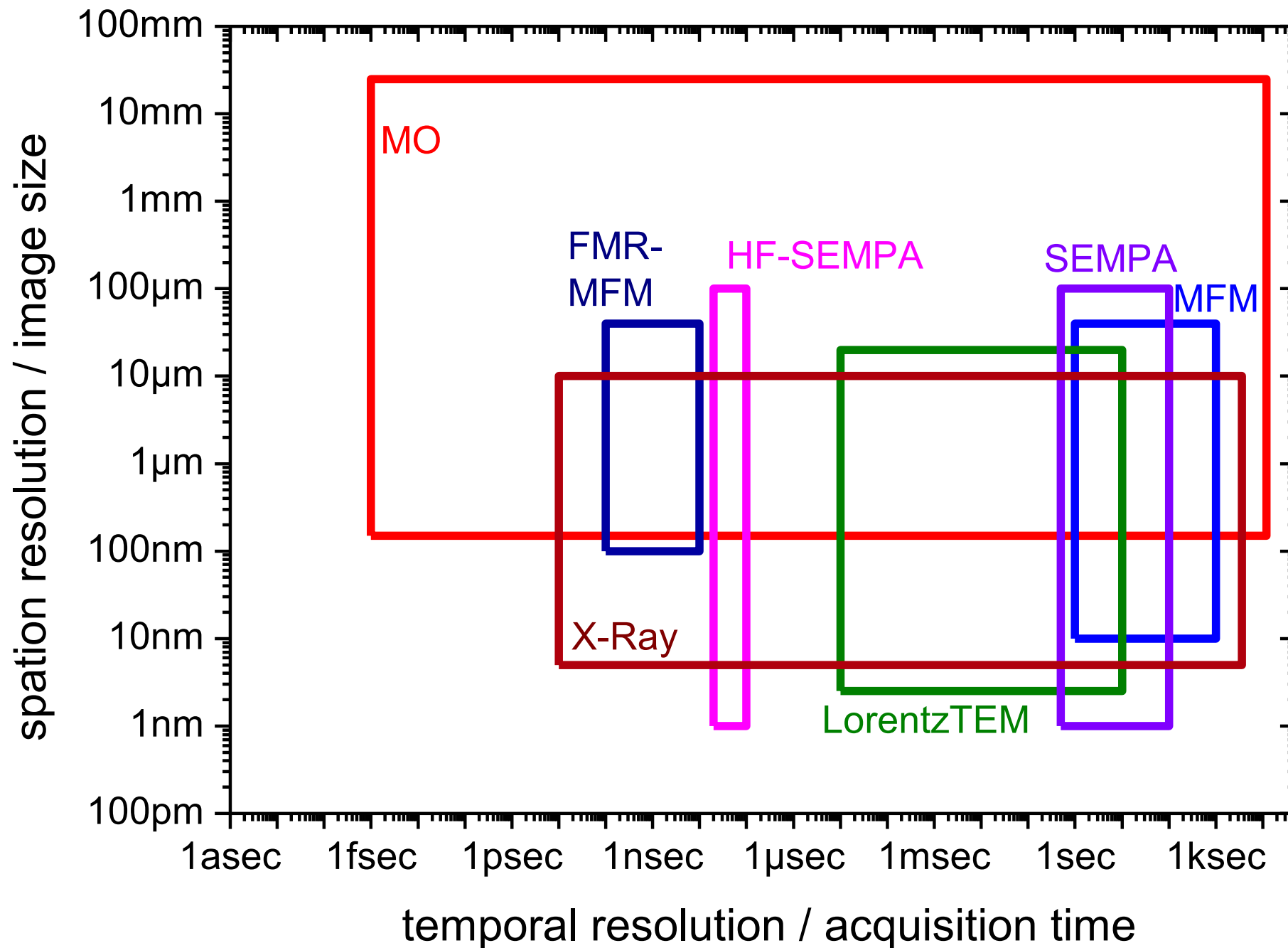




R. Celotta et al., Techniques to Measure Magnetic Domain Structures. Characterization of Materials. 1–15. Wiley (2012)

Images from several magnetic domain observation techniques from bits written on a magnetic storage media. The track width is about 10 μm wide. The bit length ranges from 10.0 to 0.2 μm . The bit length and spacing of the large bits in the XMCD electron yield image is 10 μm .

Magnetic domain imaging techniques



Magnetic force microscopy (MFM)

X-Ray microscopy

Scanning electron microscopy (SEMPA)

Transmission electron microscopy (TEM)

Imaging methods



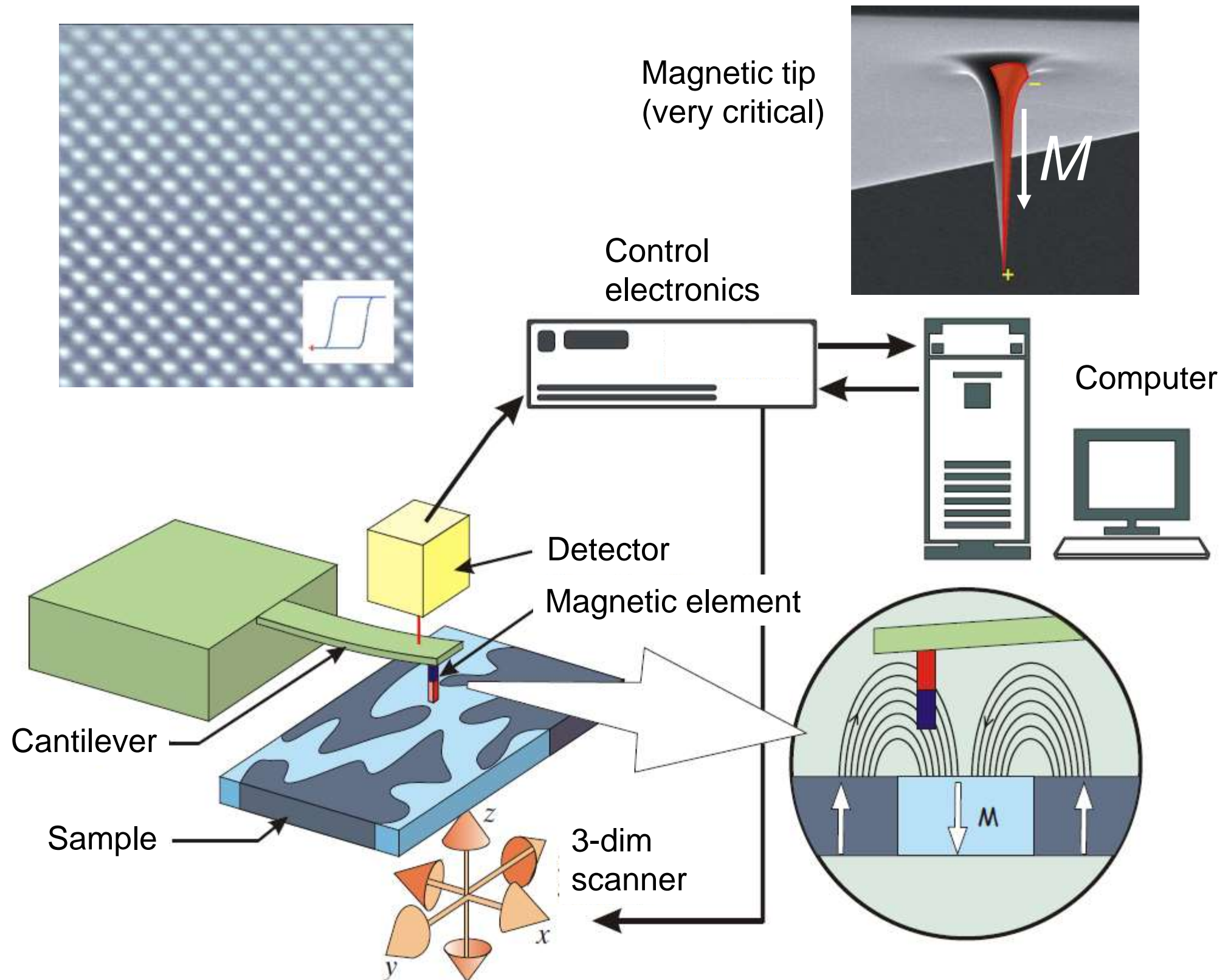
	Bitter pattern	MFM	SEM-I Secondary	TEM Fresnel and Foucault	TEM DPC	TEM Holography	SEM-II Back-scattered	SEMPA	SPLEEM	MOKE (Kerr microscopy)	XPEEM	STXM ^(a)
Contrast mechanism	∇B_{ext}	∇B_{ext}	∇B_{ext}	B	B	B, Φ_B	B	M	M	M	M	M
Evaluation of the magnetization, $M(r)$	Indirect	Indirect	Q	Indirect	Q	Q	Q	Q	Q	Q	Q	Q
Spatial resolution (nm) Typical / Limit	$\frac{300}{80}$	$\frac{60}{20}$	$\frac{1000}{800}$	$\frac{50}{\sim 10}$	$\frac{10}{2}$	$\frac{20}{5}$	$\frac{2000}{1000}$	$\frac{150}{20}$	$\frac{40}{20}$	$\frac{800}{250}$	$\frac{300}{50}$	$\frac{30}{15}$
Depth of information (nm)	500–1000	20–500	10–50 nm	Thickness integrated <150 nm	Thickness integrated <100 nm	Thickness integrated <100 nm	10,000	1–2	<1	<20 (metals)	<5 nm	Thickness integrated <100 nm
Time for image acquisition	30 msec	5–20 mins	10–60 sec	50 msec–60 sec	5–60 secs	50 msec–10 sec	10–60 sec	1–100 min	~1sec	1 msec–5 sec	~1sec	~1sec
Limits on applied magnetic fields	None	<500 kA/m	Not advised	~100–500 kA/m	~100–500 kA/m	50 kA/m	Not advised	Not advised	Not advised	None	Not advised	None
Imaging conditions	None	In air	HV	HV	HV	HV	HV	UHV	UHV	In air	UHV	None
Max thickness	None	None	None	<150 nm	<100 nm	<100 nm	None	None	None	None		60–100 nm
Sample smoothness	R	R	NR	Preferred	Preferred	Preferred	NR	NR	R	R	NR	NR
Sample clean surface	NR	NR		Preferred	Preferred	Preferred	NR	R	R	NR	Preferred	NR

K. Krishnan, Fundamentals and applications of magnetic materials, OXFORD University Press (2016)

Elements of magnetic force microscopy



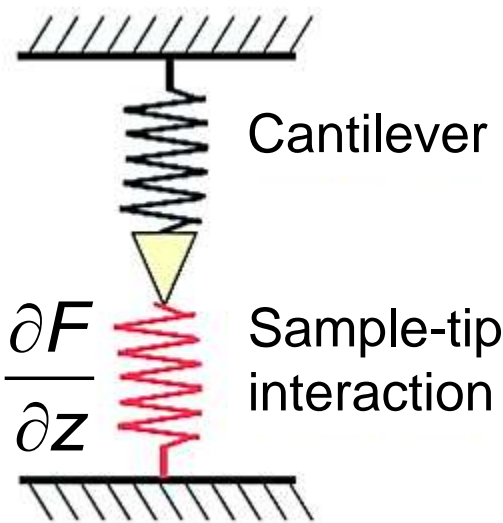
	MFM
Contrast mechanism	∇B_{ext}
Evaluation of the magnetization, $M(r)$	Indirect
Spatial resolution (nm)	$\frac{60}{20}$ Typical Limit
Depth of information (nm)	20–500
Time for image acquisition	5–20 mins
Limits on applied magnetic fields	<500 kA/m
Imaging conditions	In air
Max thickness	None
Sample smoothness	R
Sample clean surface	NR



Material from L. Abelmann, Univ. Twente, Netherlands & KIST Europe, Germany

■ Harmonic oscillator

$$f_0 = \frac{1}{2\pi} \sqrt{\frac{c_L}{m}}$$

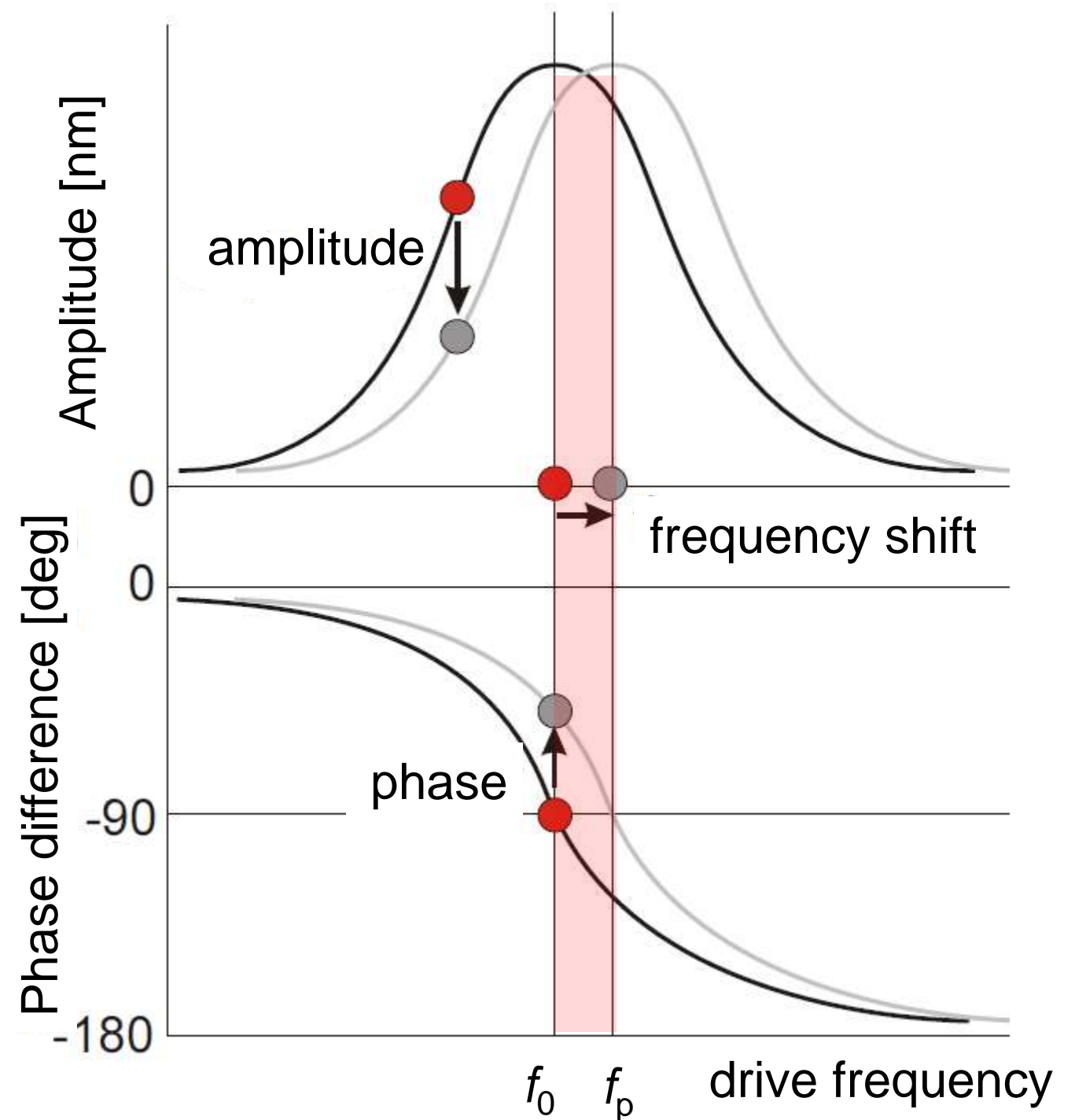


$$f_p = \frac{1}{2\pi} \sqrt{\frac{1}{m} \left(c_L - \frac{\partial F}{\partial z} \right)}$$

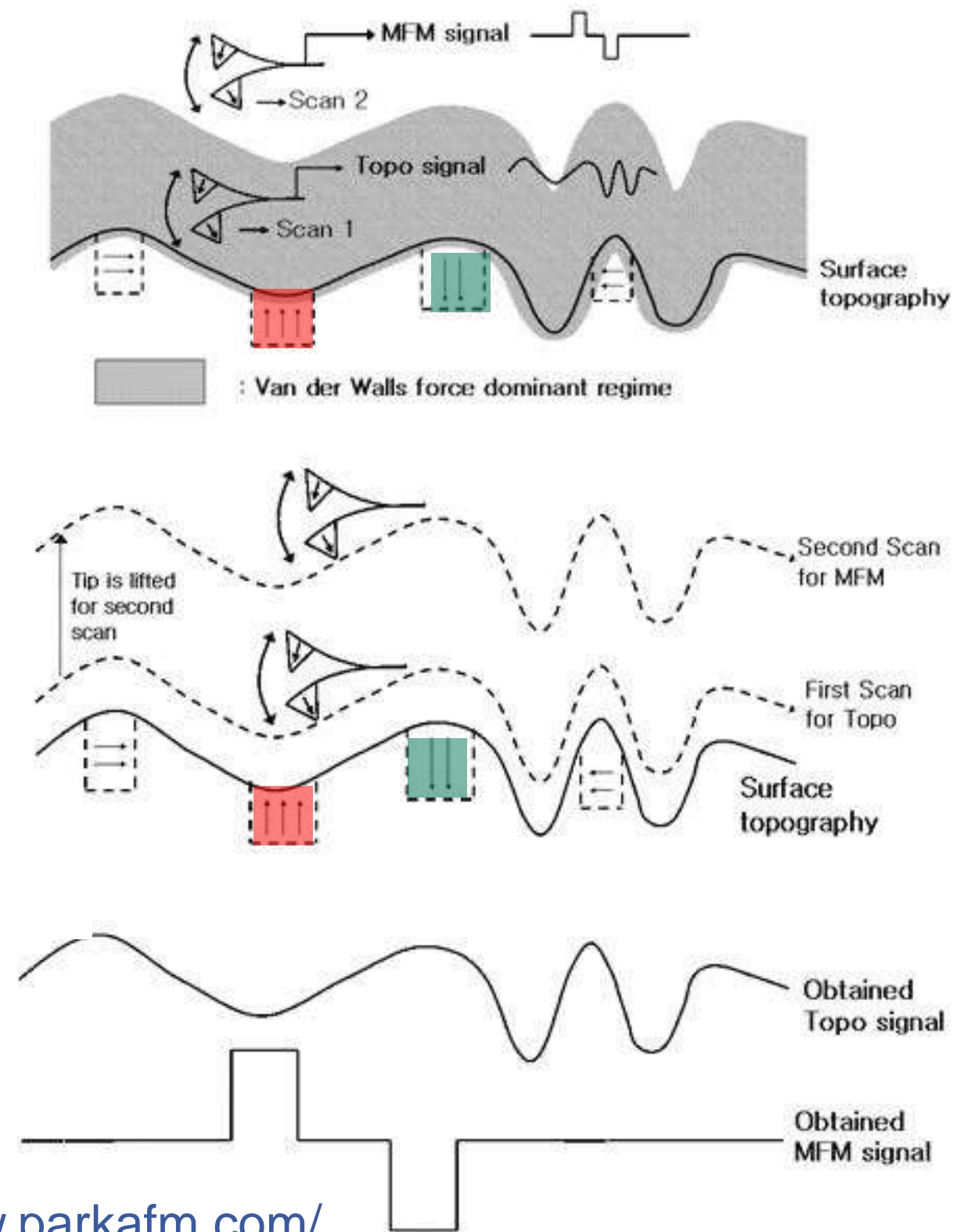
Interaction force gradient $\frac{\partial F}{\partial z}$

$$\delta f = f_0 - f_p = -\frac{f_0}{2c_L} \frac{\partial F}{\partial z}$$

Probing of magnetic interaction



- Stray field interaction between film and magnetic tip
- Small forces on the order of 10^{-10} N detected with cantilever
 - Dynamic force sensing: Cantilever is oscillated at a frequency close to its resonance frequency – detection of frequency shift
- Lift mode (non contact mode)
 - Tapping mode (AFM mode)
 - Subsequent MFM trace



<http://www.parkafm.com/>

Transitions in perpendicular recording media



- 51 kfc
- 203 kfc
- 305 kfc
- 406 kfc
- 508 kfc
- 610 kfc
- 711 kfc
- 813 kfc
- 914 kfc
- 1016 kfc

A. Moser et al., JMMM 287 (2005) 298–302

kfc (kilo flux changes per inch)

Electrical switching of a vortex core seen by MFM

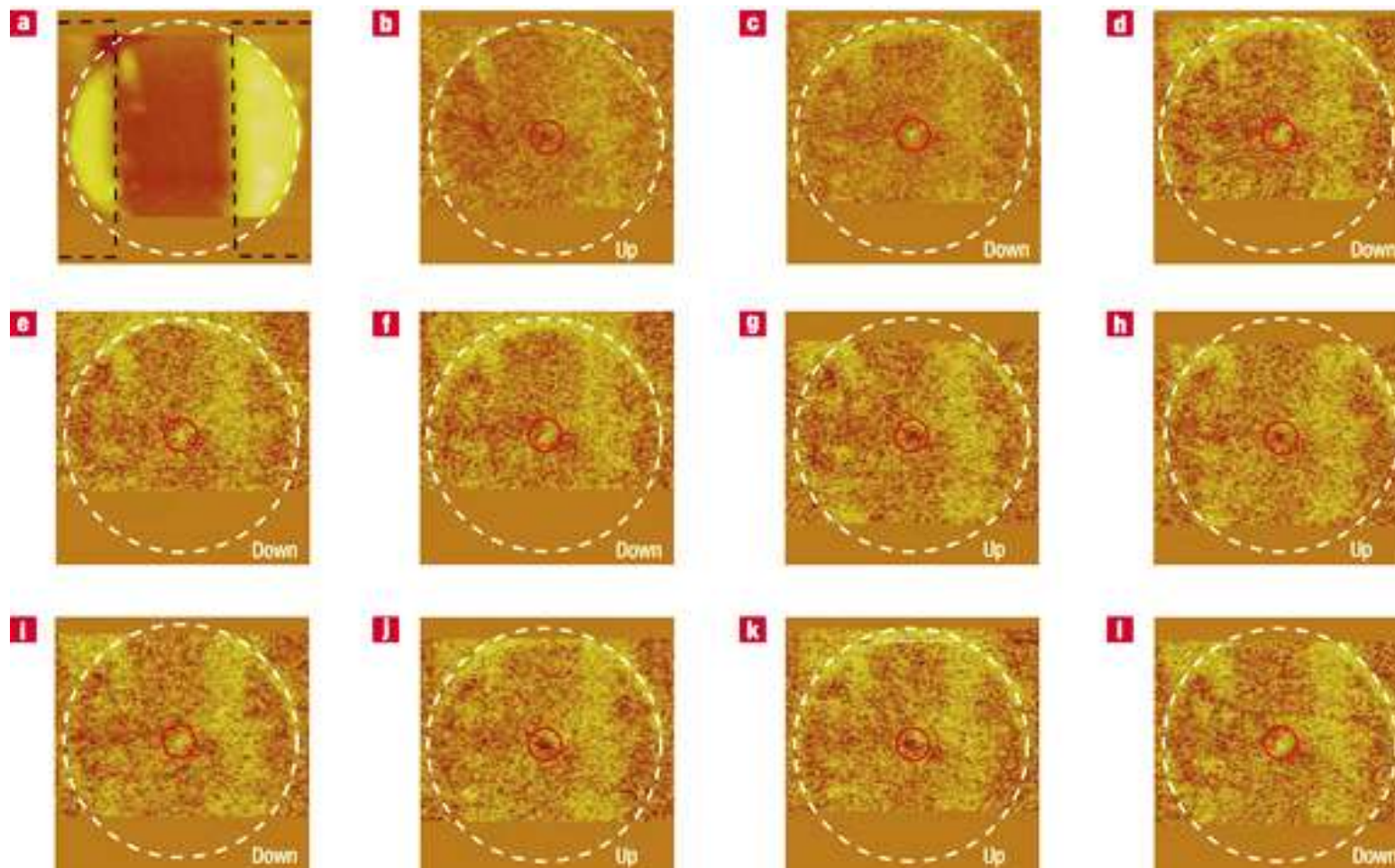
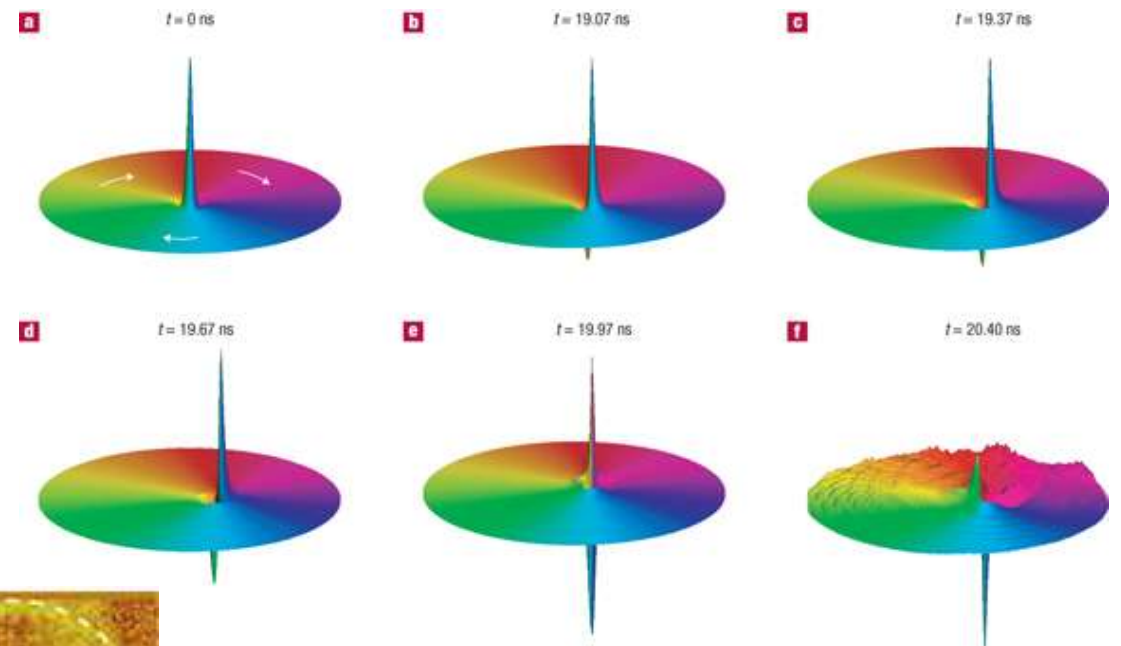


$\text{Ni}_{81}\text{Fe}_{19}$

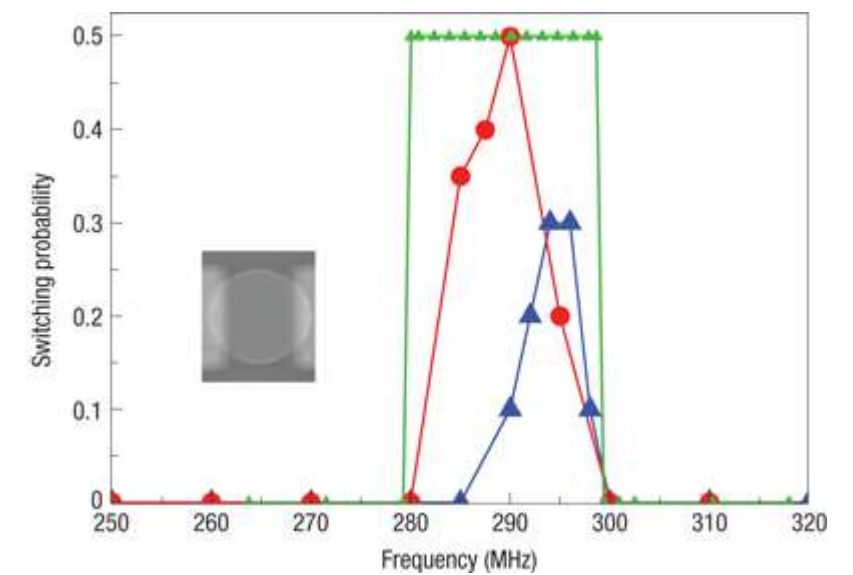
Diameter 500 nm, thickness 50 nm

$f = 290 \text{ MHz}$

$j = 3.5 \cdot 10^{11} \text{ Am}^{-2}$



K Yamada et al., Nature Materials 6, 270 - 273 (2007)





- Maps the derivative of the magnetic stray field
- Spatial resolution down to 10 nm (vacuum)
- Non-destructive
- Mostly sensitive to the z-component of stray field (depending on tip)

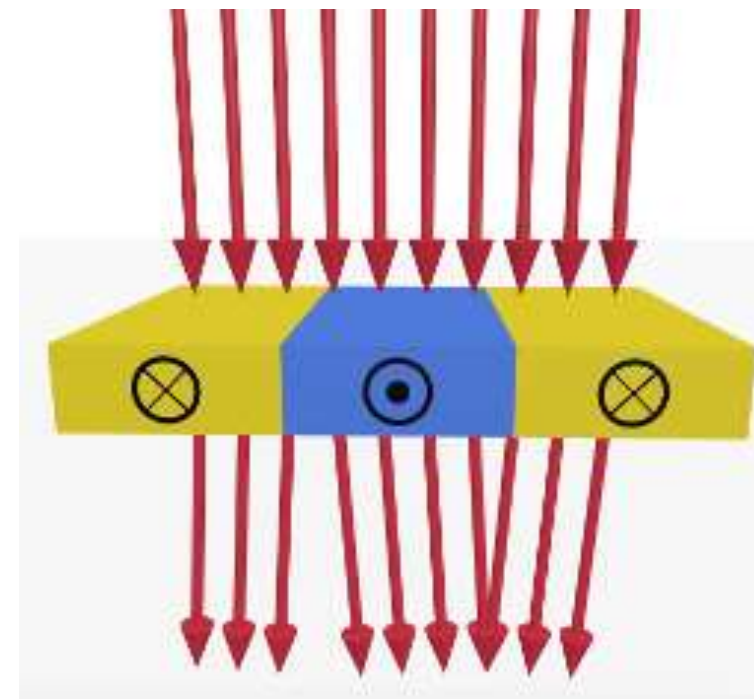
- No sample preparation needed
- Surface should be relatively flat

- **Tip quality is critical**
- Tip-sample interaction: induced change of magnetic state
- Limitations to measure magnetically soft samples

	TEM Fresnel and Foucault	TEM DPC
Contrast mechanism	B	B
Evaluation of the magnetization, $\mathbf{M}(\mathbf{r})$	Indirect	Q
Spatial resolution (nm) $\frac{\text{Typical}}{\text{Limit}}$	$\frac{50}{\sim 10}$	$\frac{10}{2}$
Depth of information (nm)	Thickness integrated <150 nm	Thickness integrated <100 nm
Time for image acquisition	50 msec–60 sec	5–60 secs
Limits on applied magnetic fields	~ 100 –500 kA/m	~ 100 –500 kA/m
Imaging conditions	HV	HV
Max thickness	<150 nm	<100 nm
Sample smoothness	Preferred	Preferred
Sample clean surface	Preferred	Preferred

$$F = |e|(\mathbf{v} \times \mathbf{B})$$

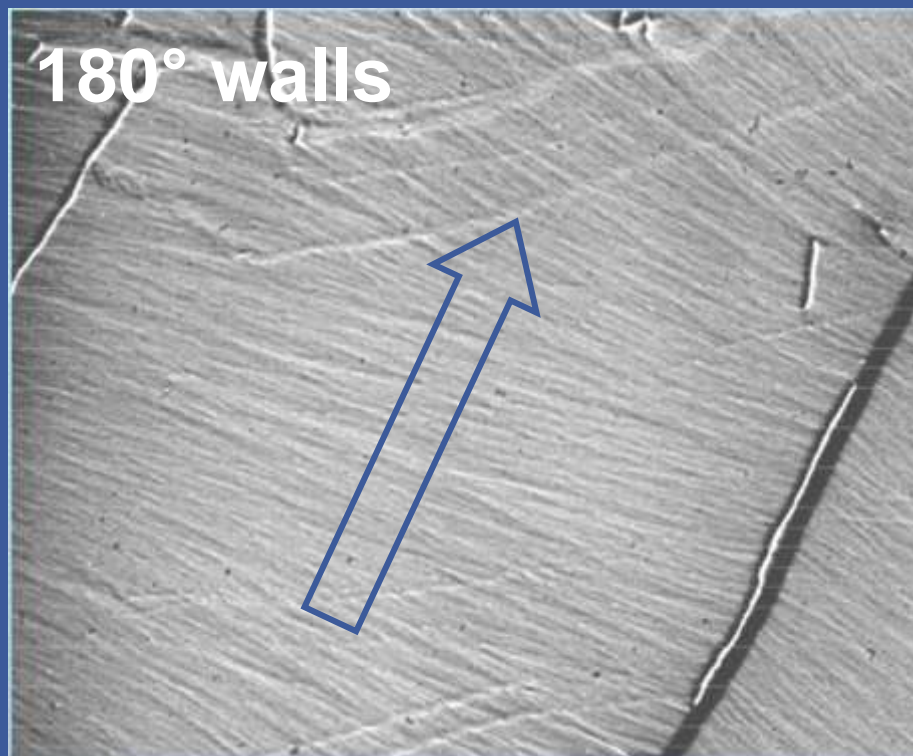
Lorentz force



$$\beta_L = \frac{e\lambda(\mathbf{B} \times \mathbf{n})}{h} t \approx 100 \mu\text{rad}$$

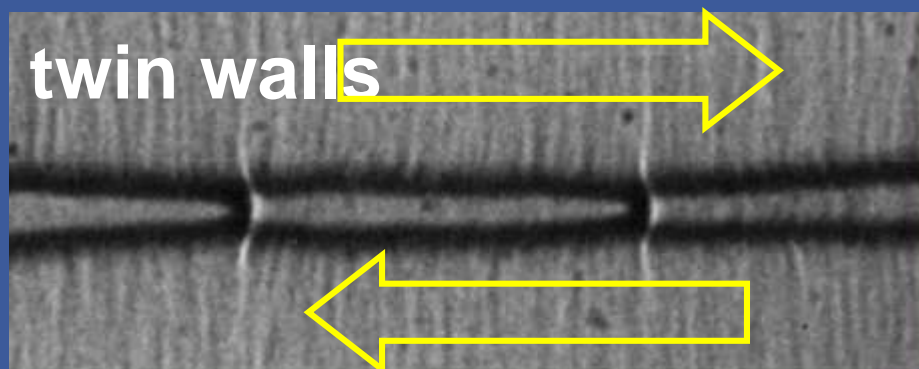
Lorentz deflection angle

Domain walls in thin films (Fresnel mode)



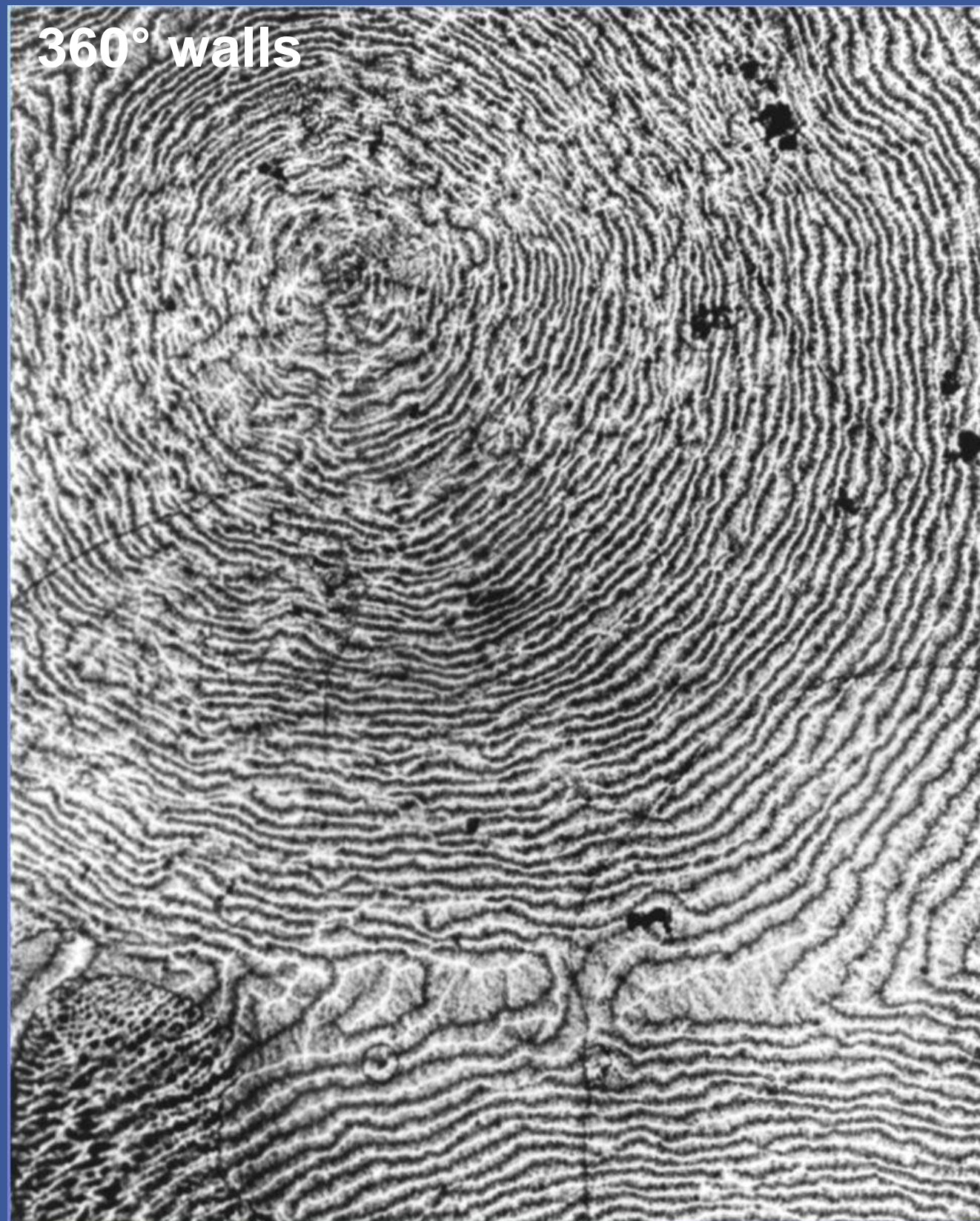
180° walls

10 μm



twin walls

10 μm



360° walls

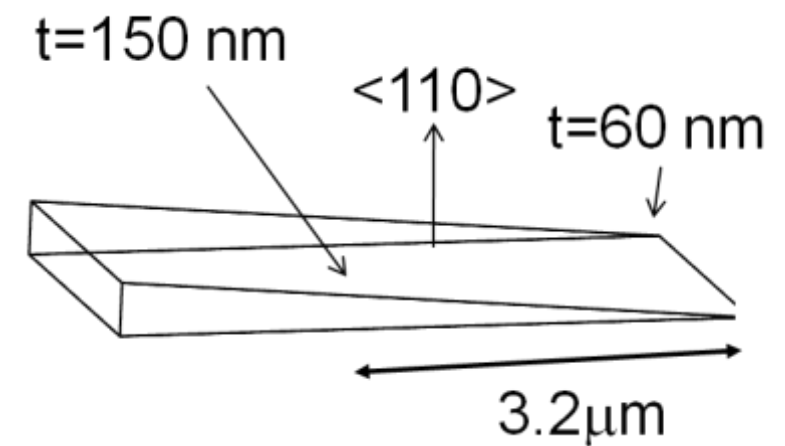
10 μm

Material from L. Heyderman, ETH Zürich, Switzerland



$T = 250\text{K}$

$\sim 130\text{ Oe (remanance)}$



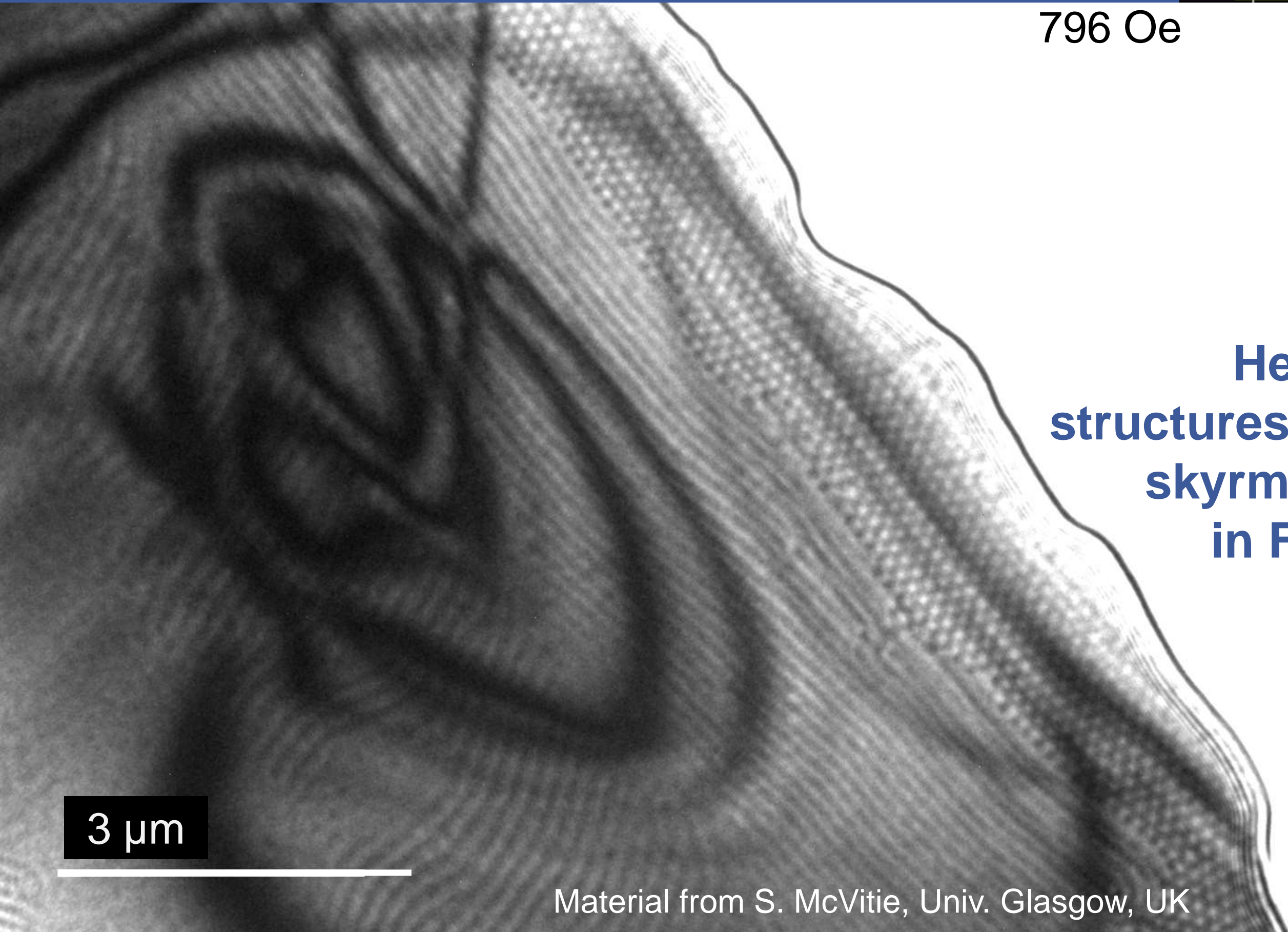
**Helical
structures
in FeGe**

3 μm

Material from S. McVitie, Univ. Glasgow, UK



796 Oe



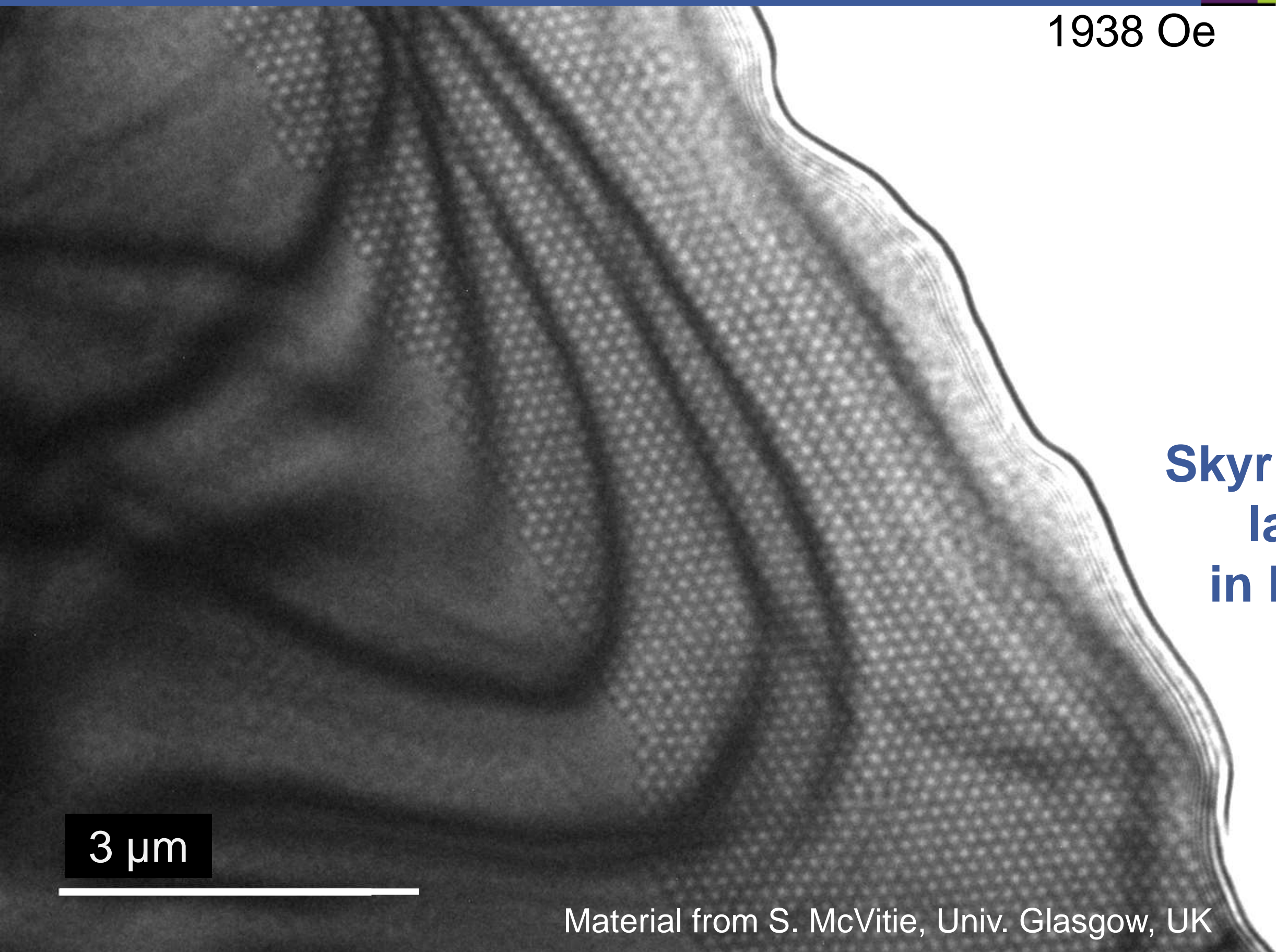
**Helical
structures and
skyrmions
in FeGe**

3 μm

Material from S. McVitie, Univ. Glasgow, UK



1938 Oe



**Skymion
lattice
in FeGe**

3 μm

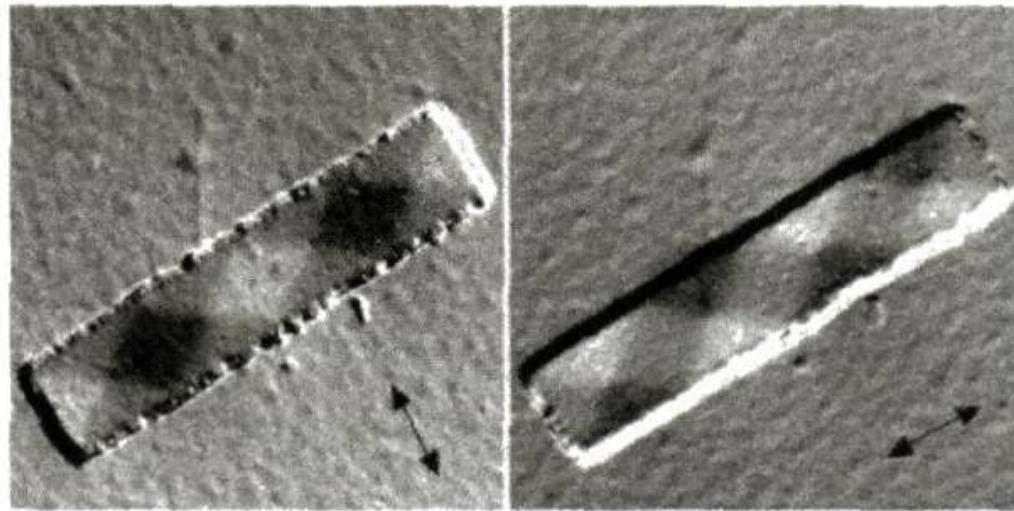
Material from S. McVitie, Univ. Glasgow, UK

Differential Phase Contrast

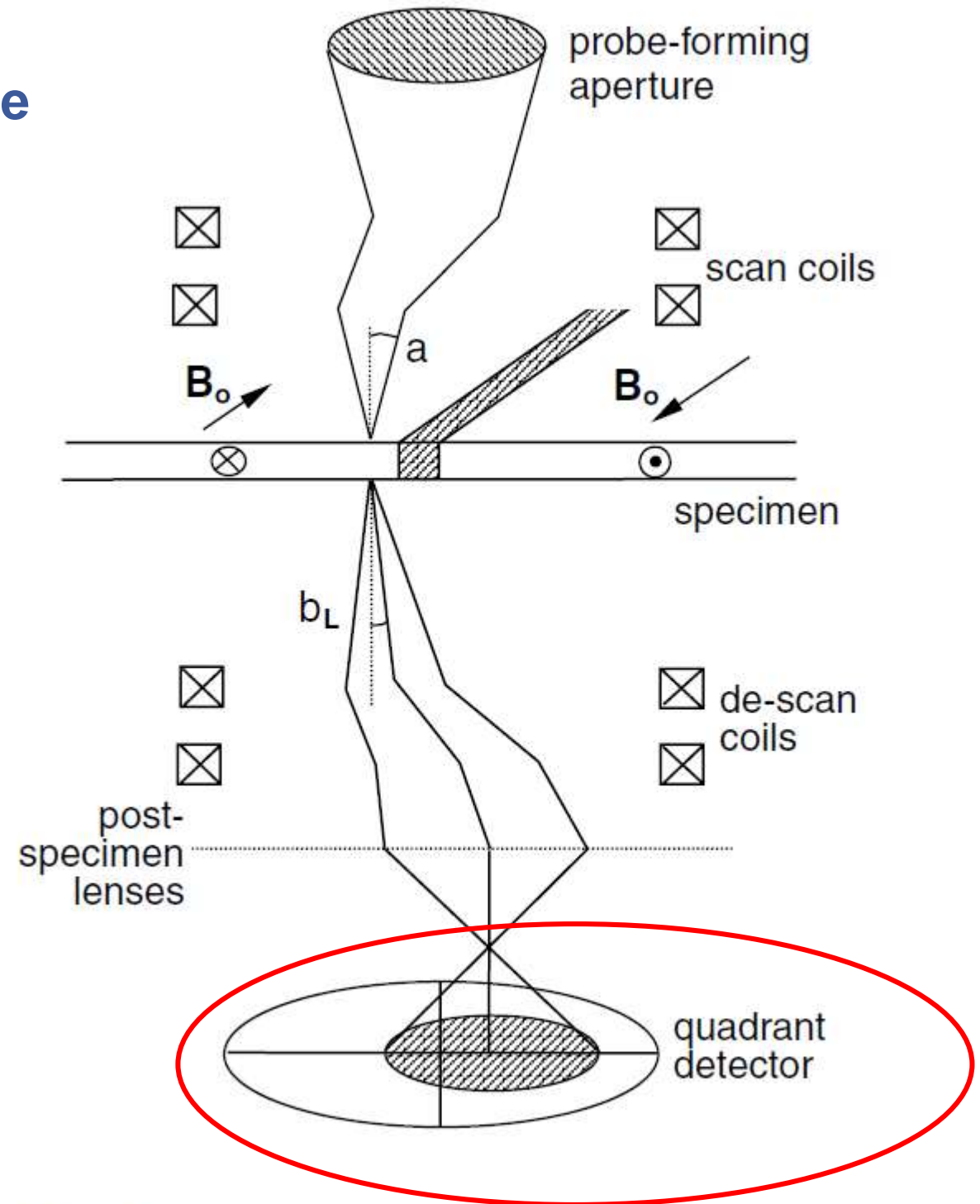
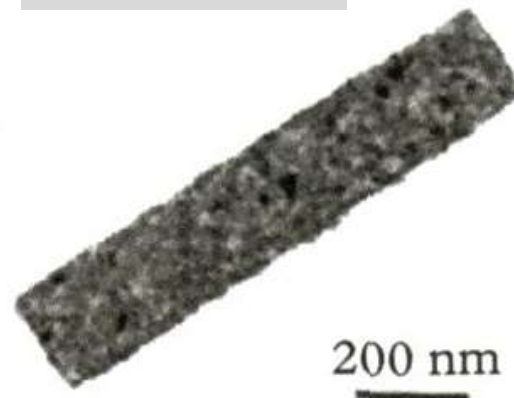
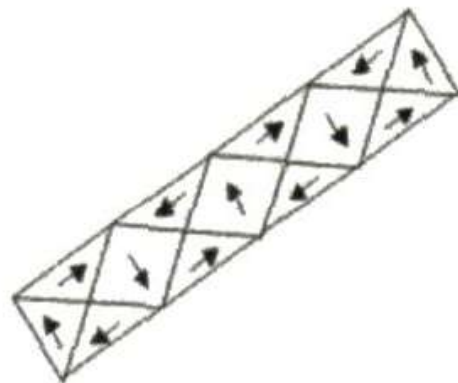


$$\beta_L = \frac{e\lambda(\mathbf{B} \times \mathbf{n})}{h} t$$

Lorentz deflection angle



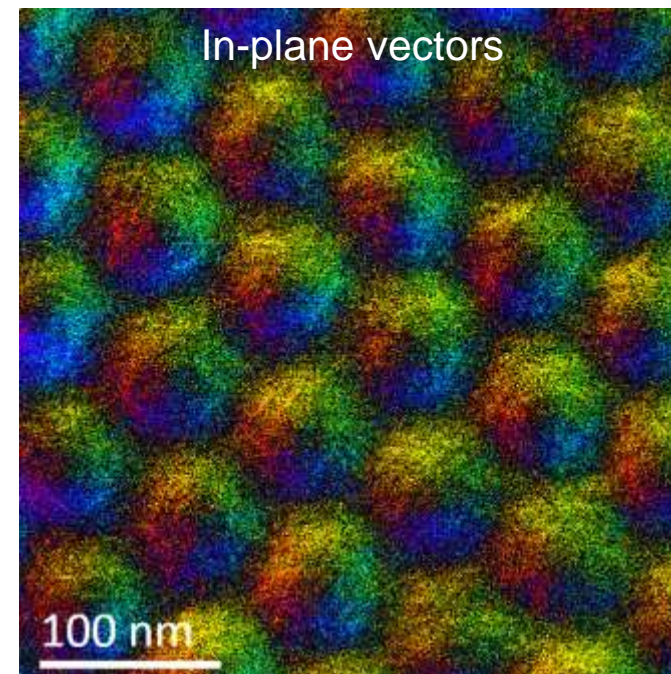
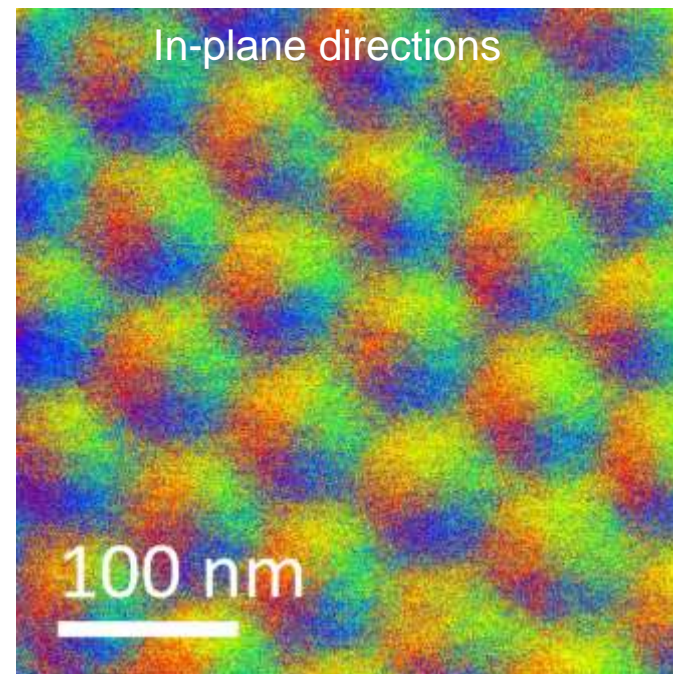
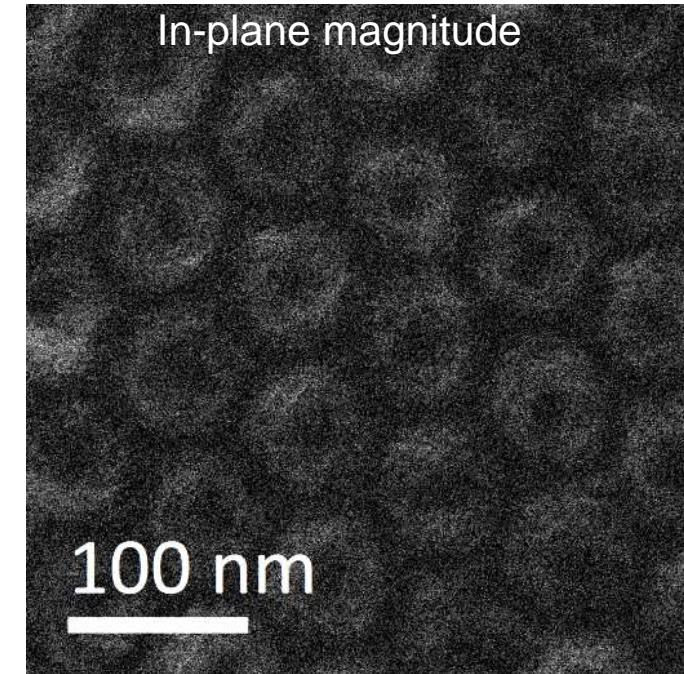
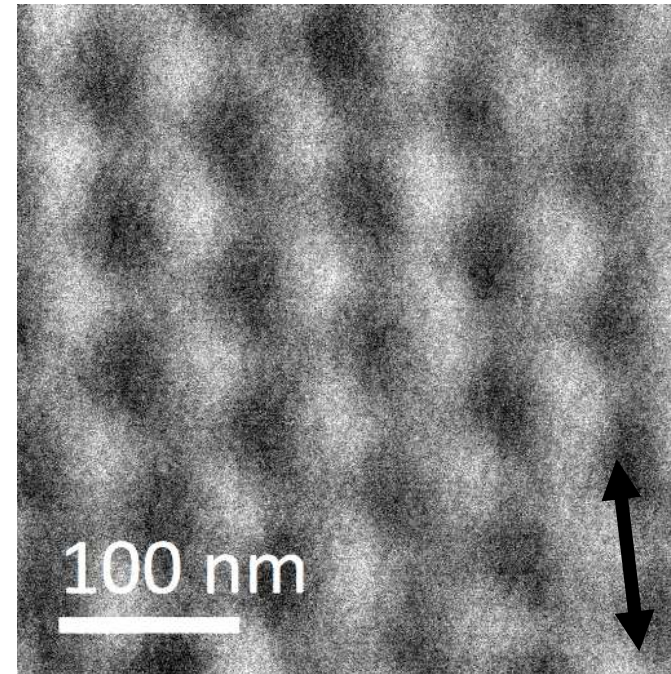
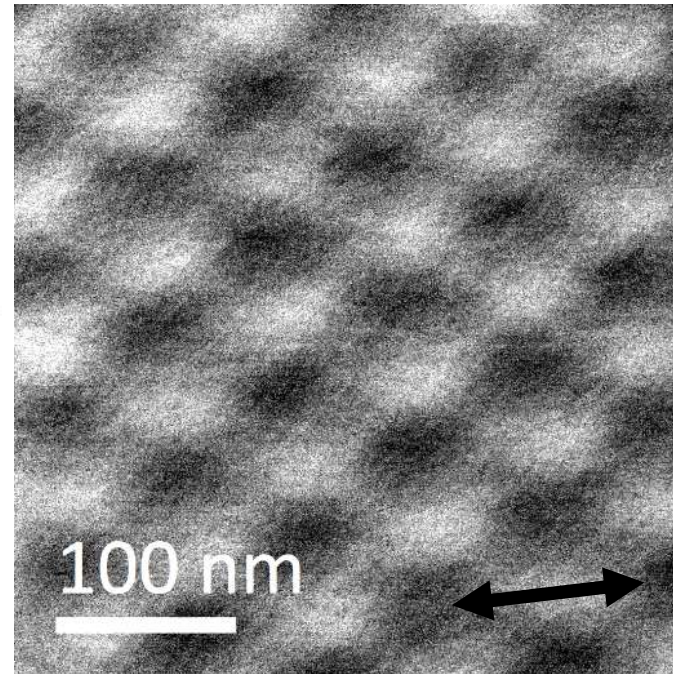
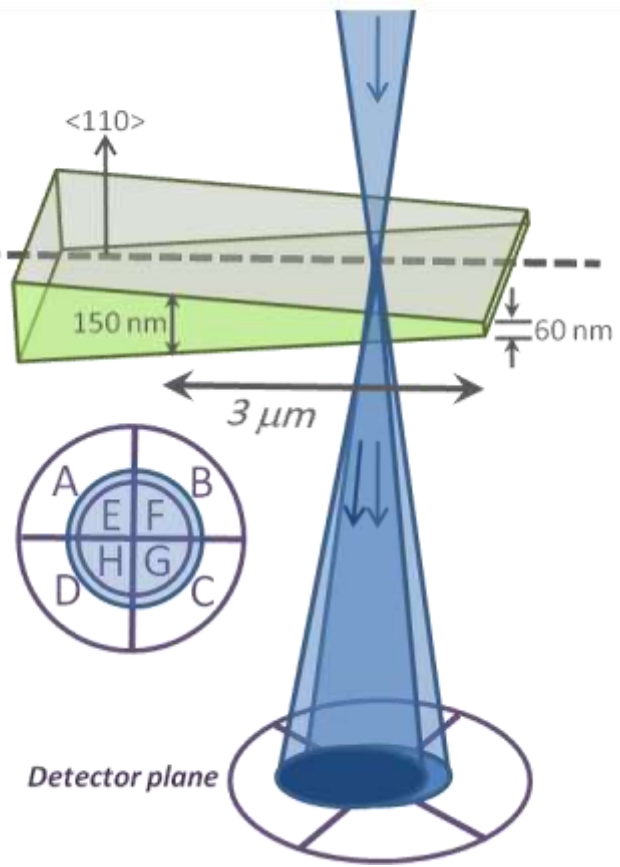
Co element



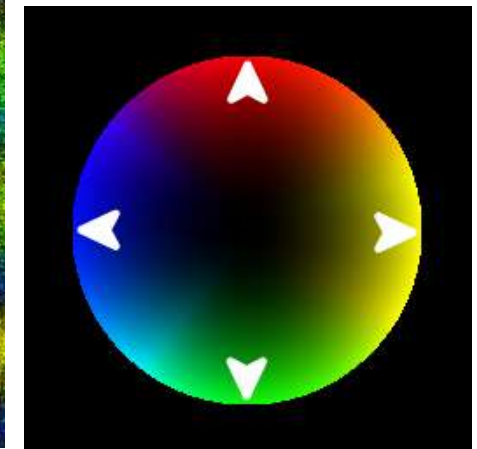
Schematic of the DPC imaging technique

A.K. Petford-Long & J.N. Chapman, Lorentz microscopy, in Magnetic Microscopy of Nanostructures, Springer (2005)

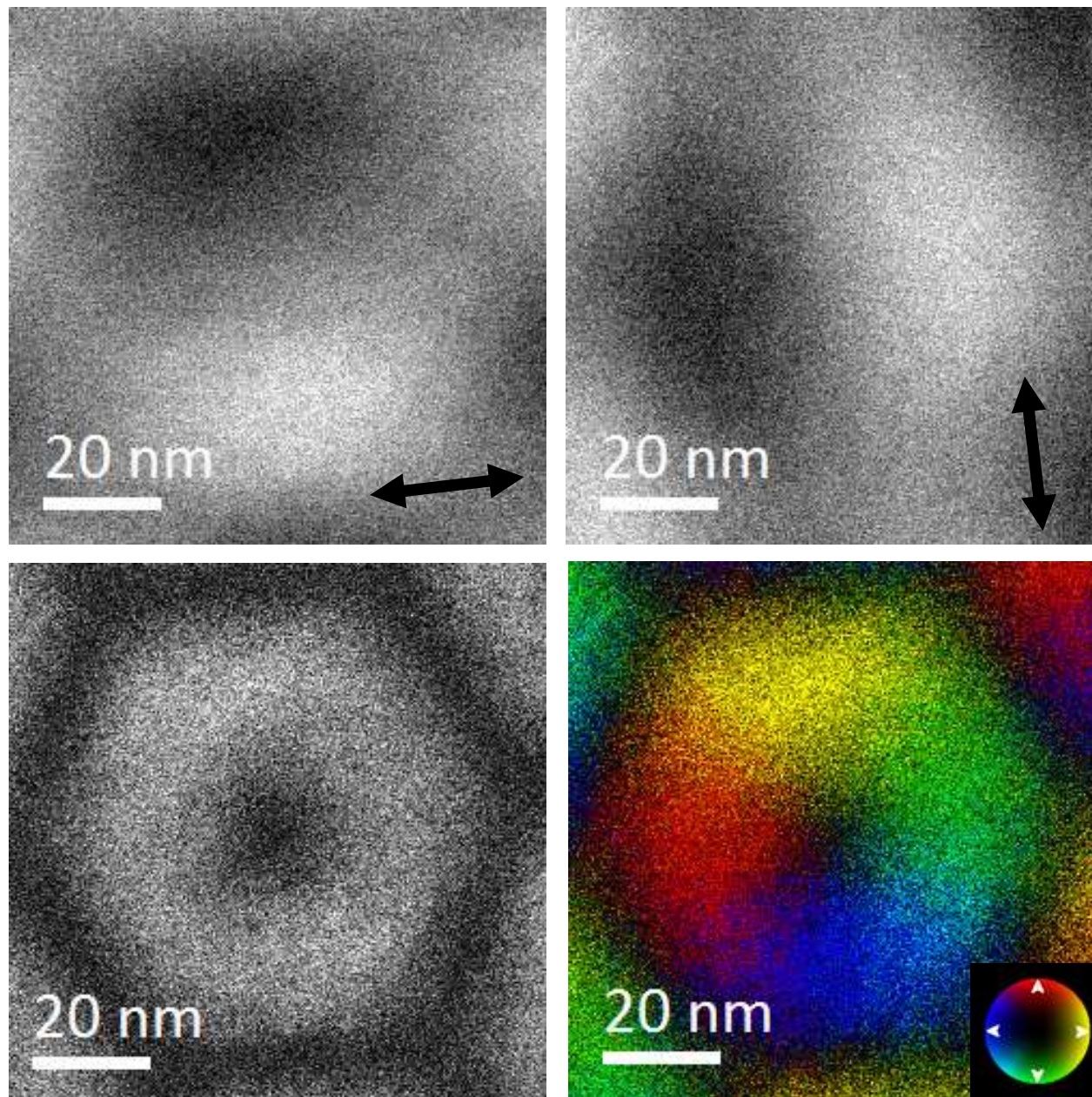
Skyrmion lattice



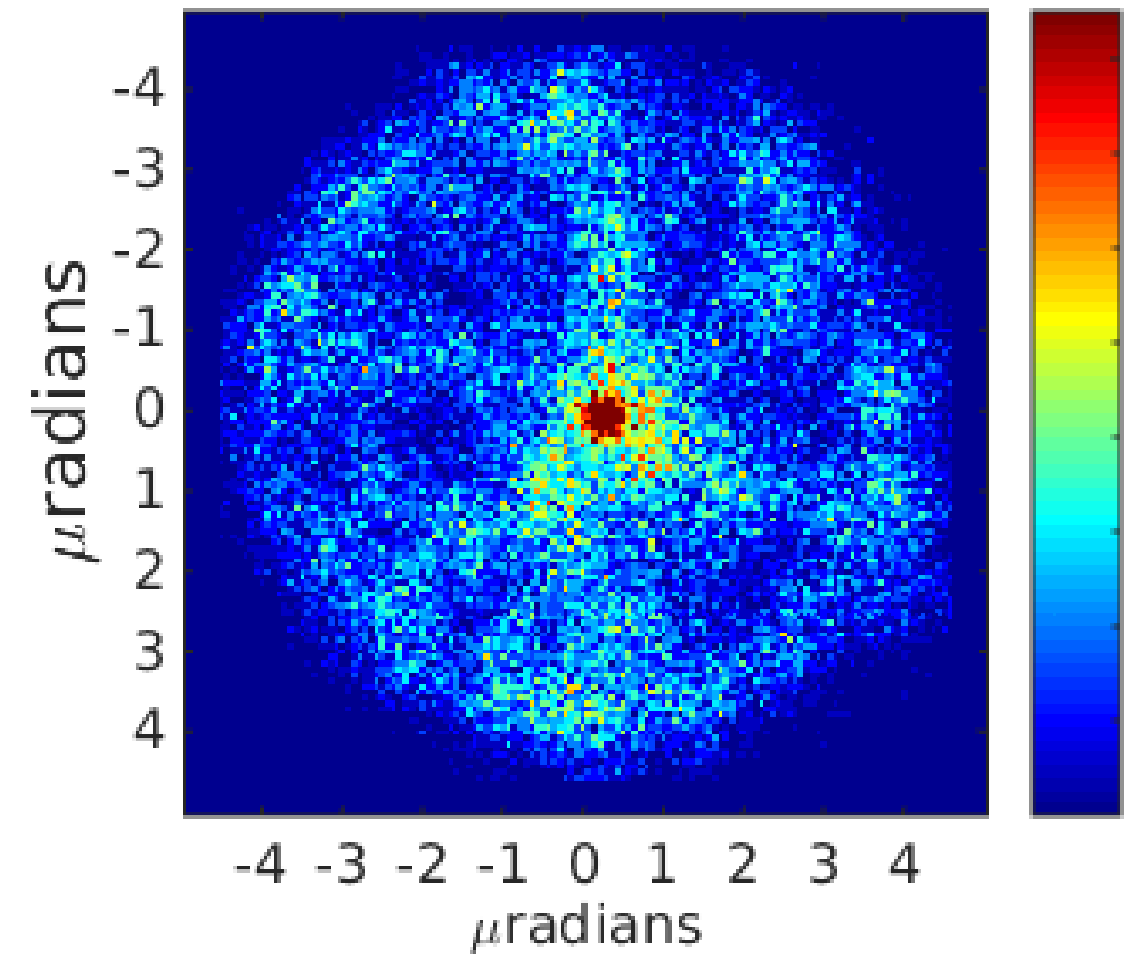
$H = 796 \text{ Oe}$



Material from S. McVitie, Univ. Glasgow, UK



3D histogram analysis



- Lorentz deflection angle $\pm 4 \mu\text{radians}$ – equiv. to $B_S \sim 0.2$ Tesla
- Six-fold symmetry

Material from S. McVitie, Univ. Glasgow, UK

- High spatial resolution (better than 5 nm possible)
- Information on domain and domain wall structures
- Thin films

- Sensitive to induction (sample magnetization & stray fields)
- Quantitative information
- Real time studies (magnetic field & temperature)
- Complementary structural information

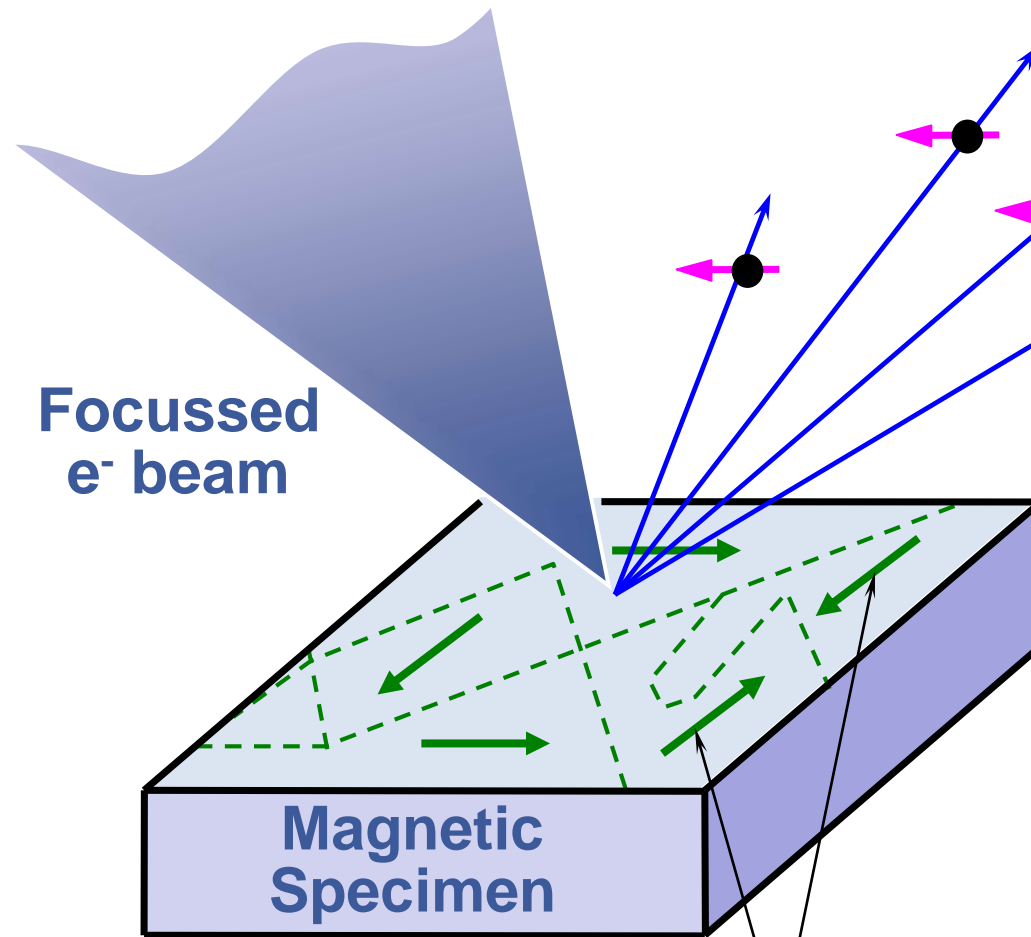
- Limited to thin samples
- Magnetization components parallel to the electron beam invisible
- **Sample preparation is critical!**

SEM with polarization analysis



SEMPA	
Contrast mechanism	M
Evaluation of the magnetization, $M(\mathbf{r})$	Q
Spatial resolution (nm)	$\frac{150}{20}$ Typical Limit
Depth of information (nm)	1-2
Time for image acquisition	1-100 min
Limits on applied magnetic fields	Not advised
Imaging conditions	UHV
Max thickness	None
Sample smoothness	NR
Sample clean surface	R

Incident Electrons From Scanning Electron Microscope (unpolarized)

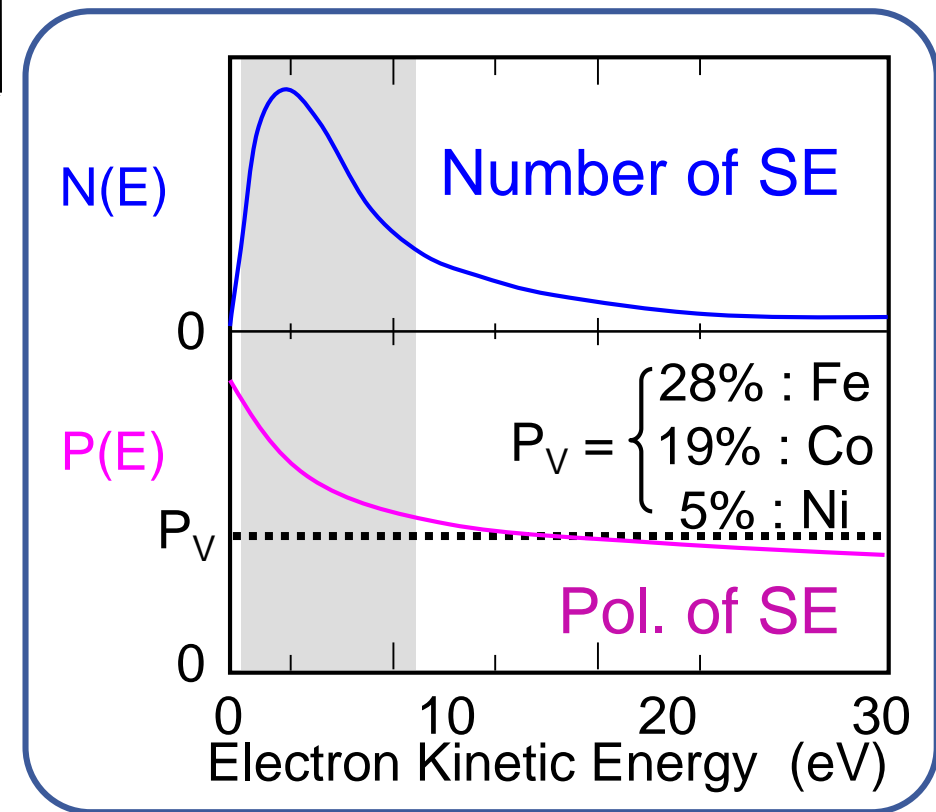


Spin-Polarization Analyzer

$$P = \frac{N_{\uparrow} - N_{\downarrow}}{N_{\uparrow} + N_{\downarrow}}$$

Polarization along z

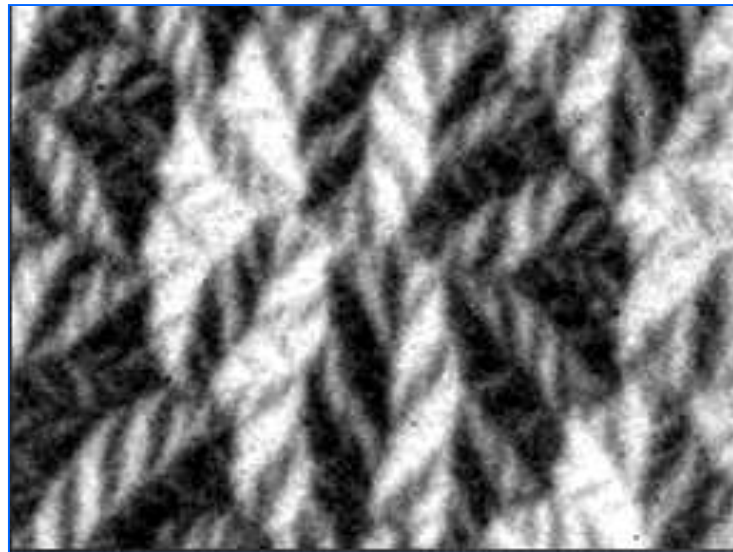
Spin-Polarized Secondary Electrons



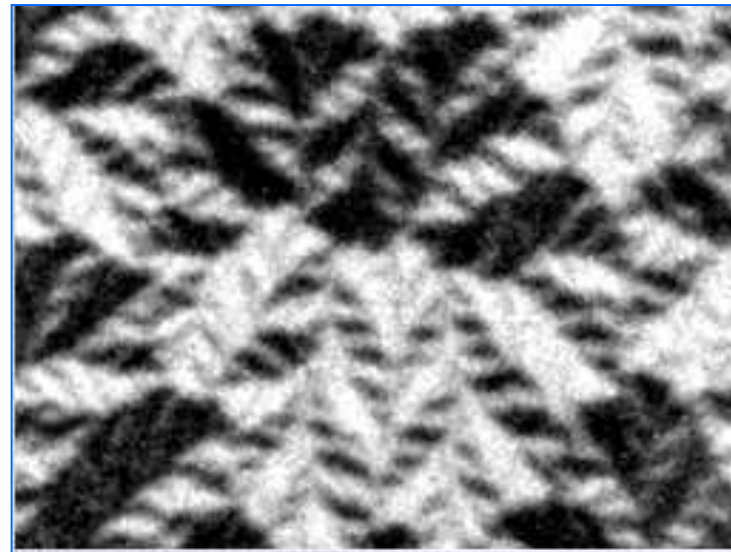
Material from J. Unguris, NIST, USA



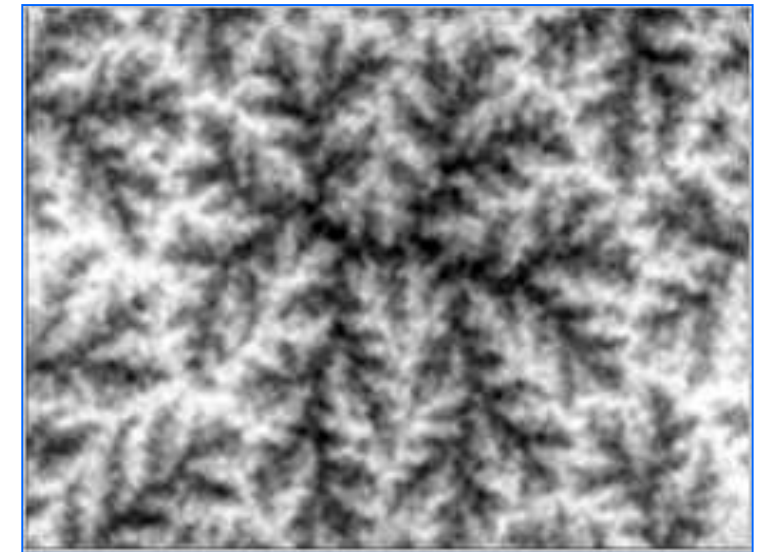
SEMPA images all three components of magnetization vector and intensity



M_x \longleftrightarrow

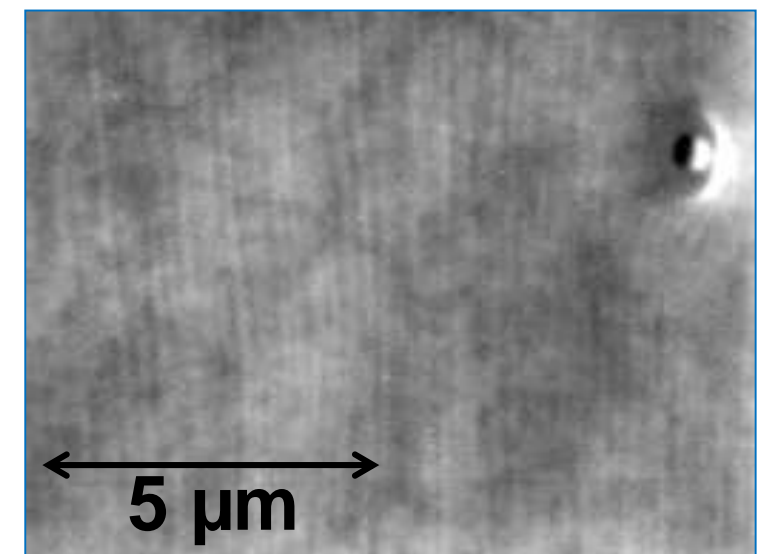
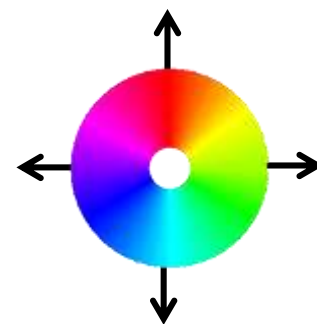
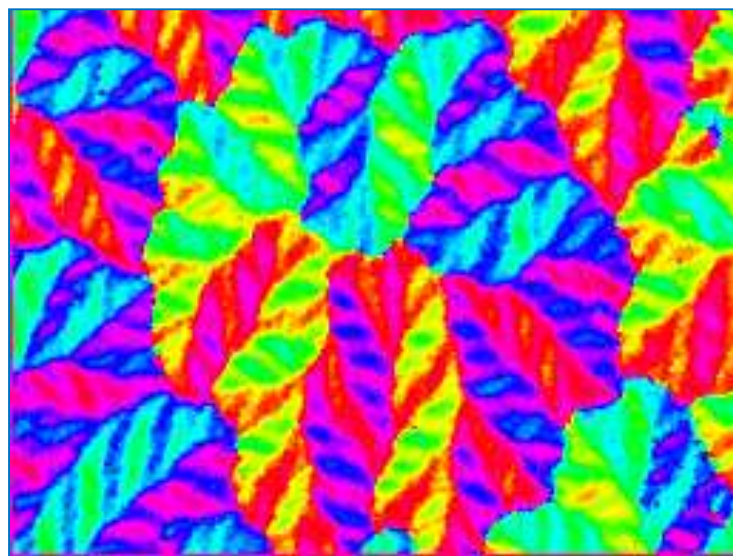


M_y \updownarrow



M_z \odot

Derive In-plane magnetization direction



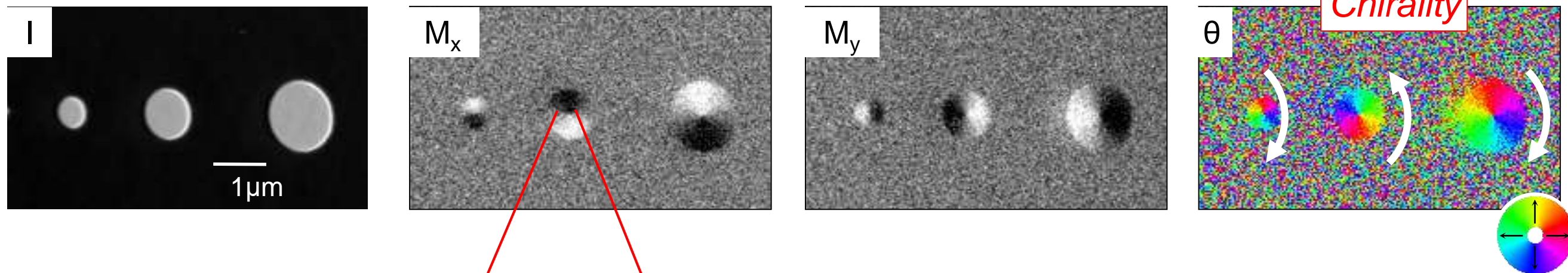
5 μm

Intensity

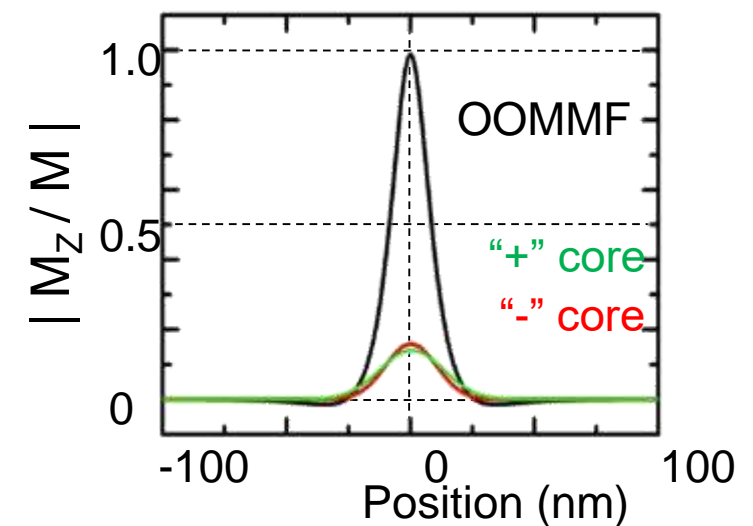
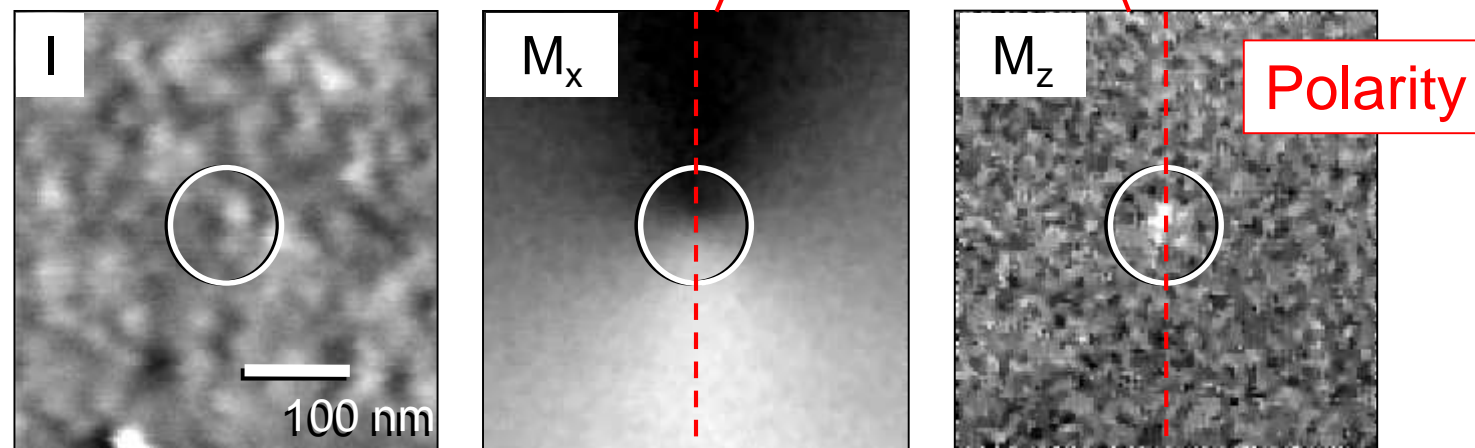
Material from J. Unguris, NIST, USA



In-plane spin analyzers measure chirality:



Out-of-plane analyzers measure vortex core polarity



Chung et al, Ultramicroscopy 110, 177-181 (2010).

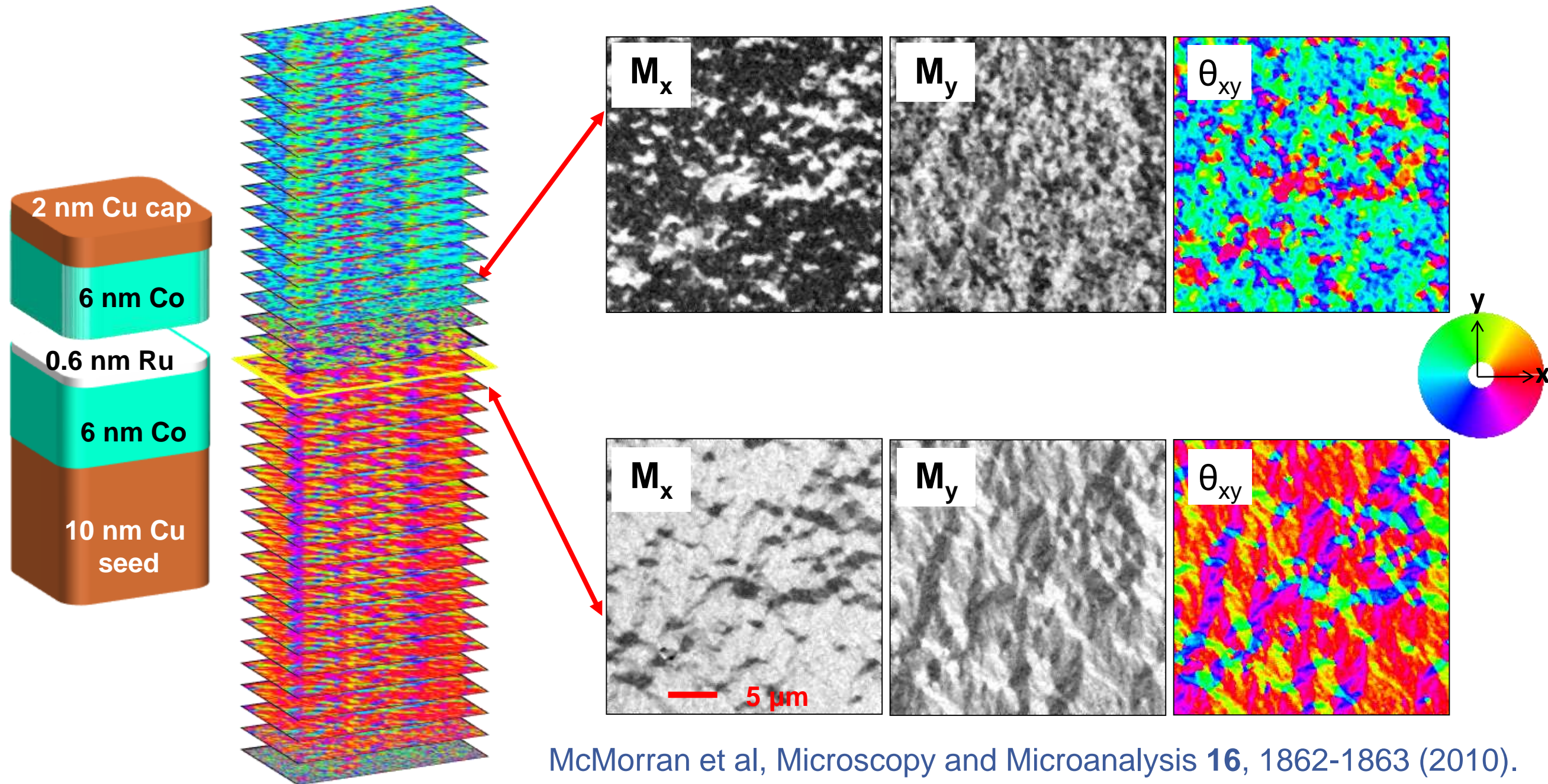
Contrast is reduced by non-local secondary electrons generated by backscattered electrons.

Material from J. Unguris, NIST, USA

Depth profiling magnetization in Co/Ru/Co



Ion mill with Ar ions



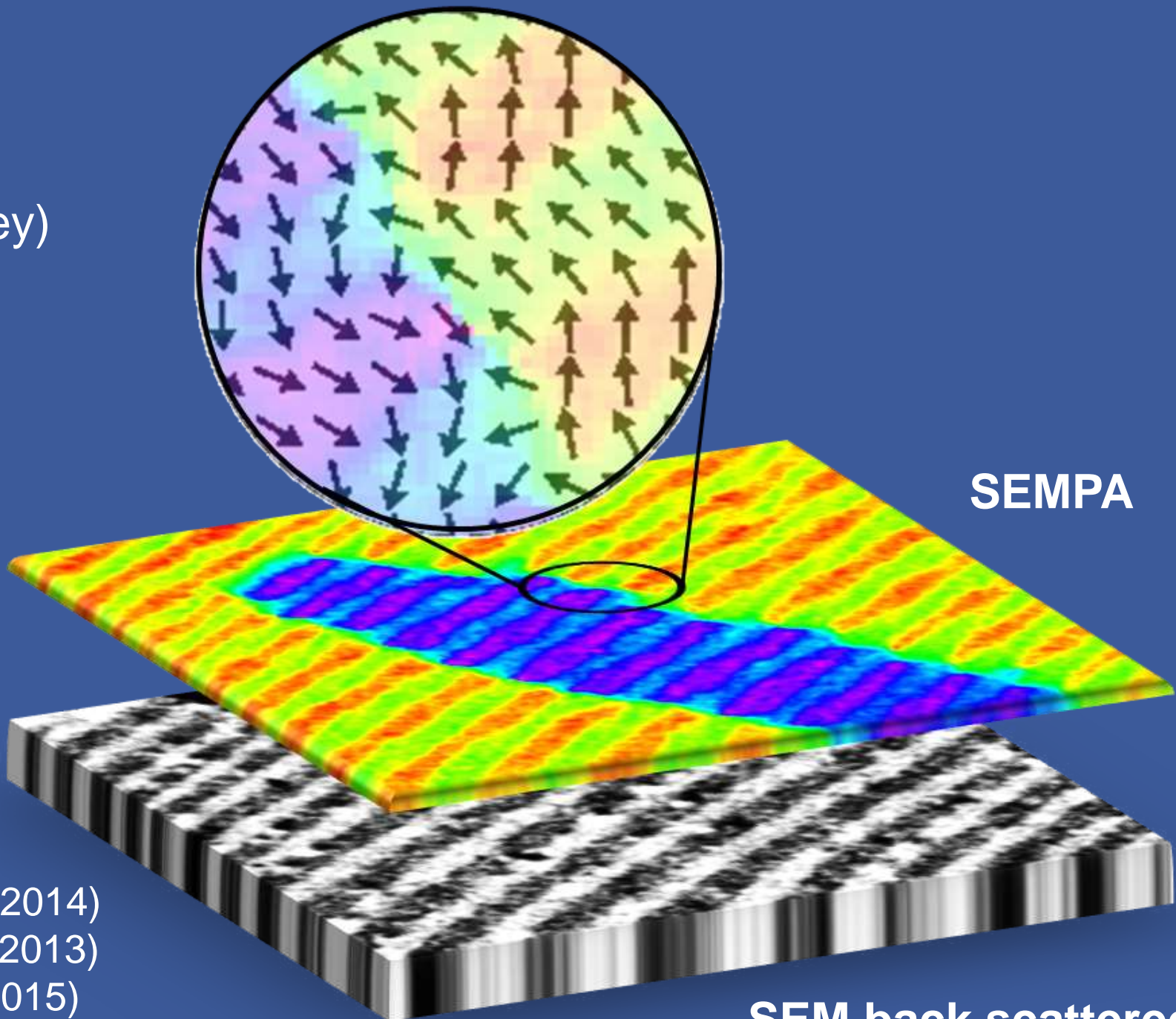
McMorran et al, Microscopy and Microanalysis **16**, 1862-1863 (2010).

Material from J. Unguris, NIST, USA

Ferromagnetic & ferroelectric structure in multiferroics



CoFe/BiFeO₃
(R. Ramesh, Berkeley)



SEMPA

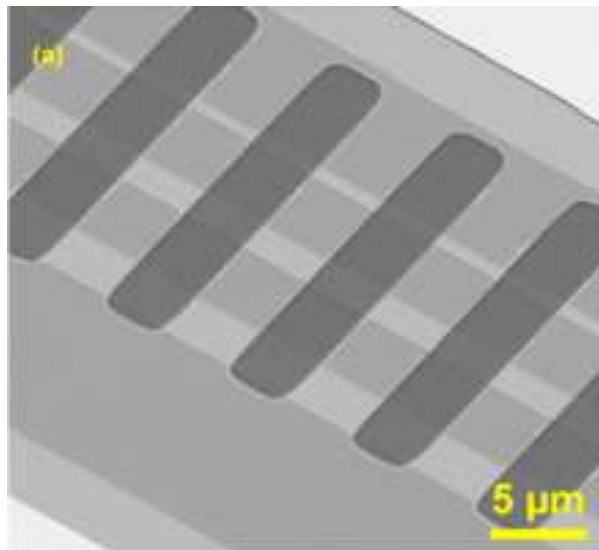
SEM back scattered
electron signal

Unguris et al, APL Materials 2 (2014)
Trassin et al, Phys. Rev. B 87 (2013)
Zhou et al, Nature Comm. 6 (2015)

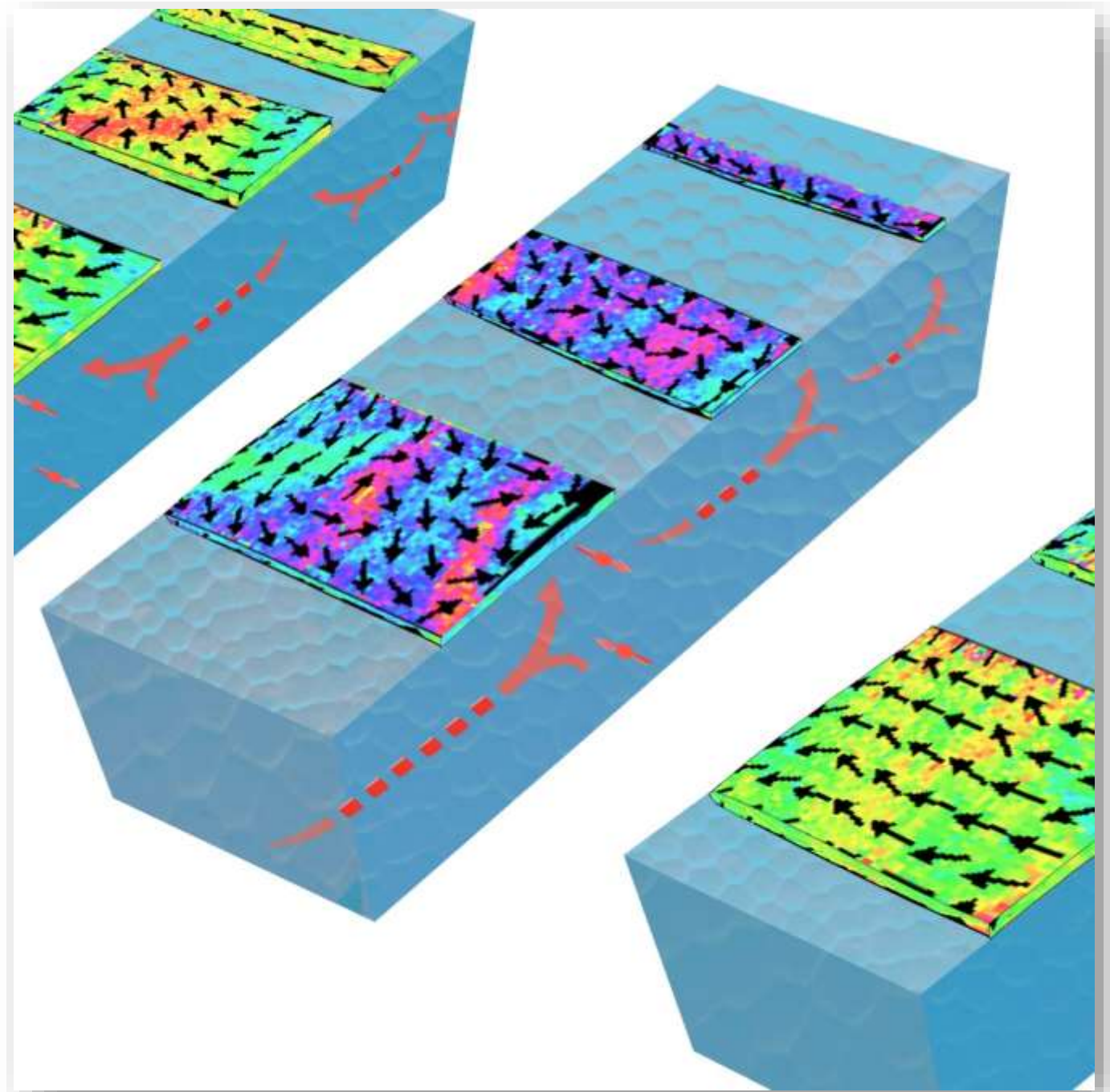
Material from J. Unguris, NIST, USA

Patterned CoFeB (2 nm) on Ta wires

- **Direct visualization of Spin Hall effect induced switching**
- Pt and Ta have opposite spin Hall effects and therefore show opposite switching



I. Gilbert *et al.*, *Phys. Rev. B* 94, 094429 (2016).



Material from J. Unguris, NIST, USA



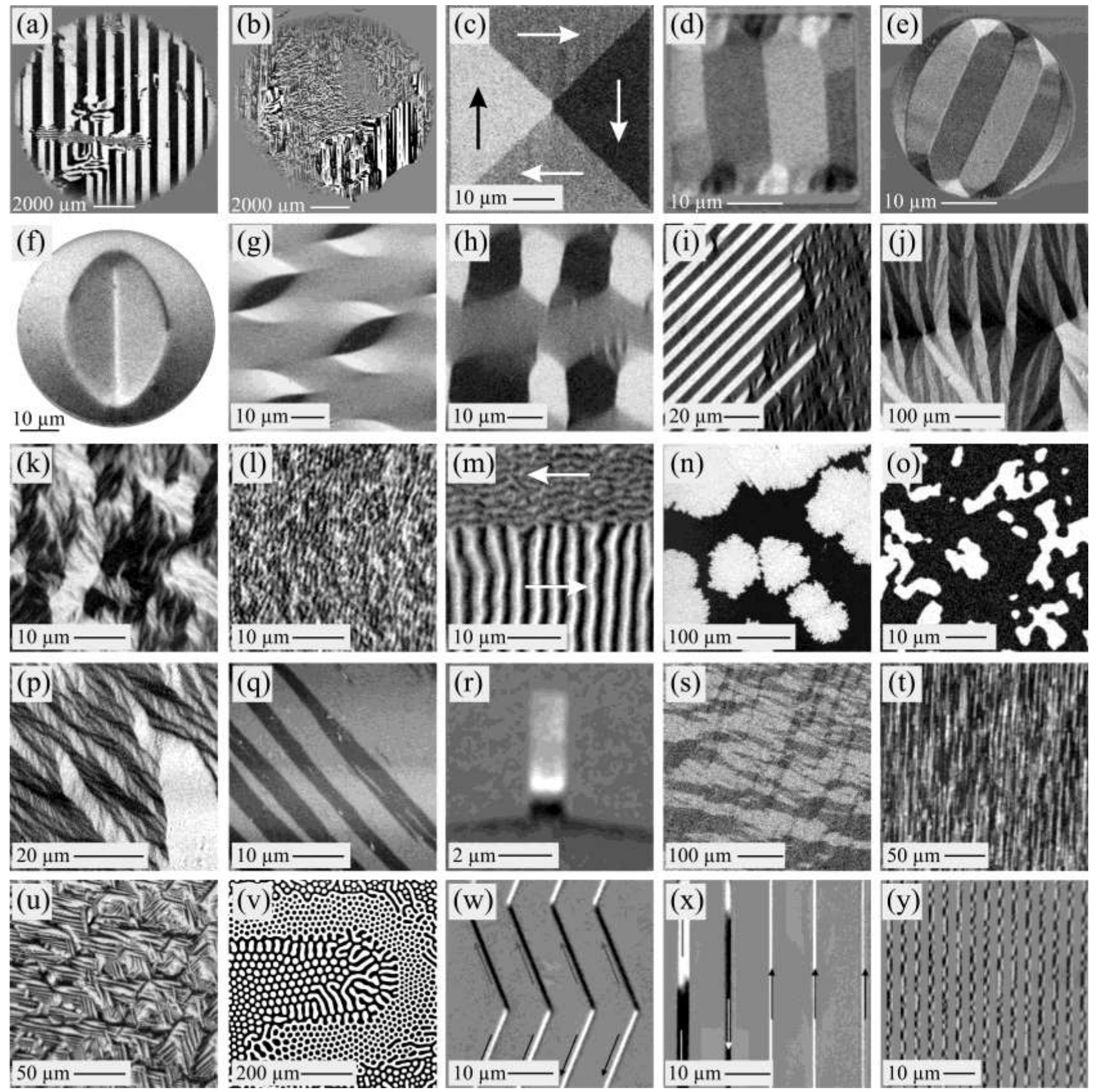
- High spatial resolution (better than 5 nm possible)
- Information on domain and domain wall structures
- Sensitive to induction surface magnetization
- **Quantitative information**
- Complementary structural information
- **Limited to clean surfaces in ultra high vacuum**

Magneto-optical microscopy

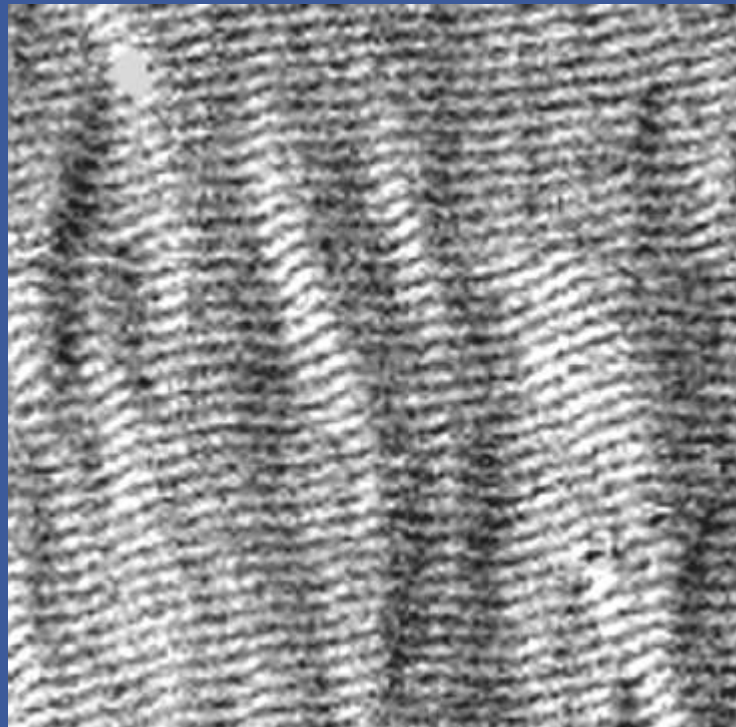


	MOKE (Kerr microscopy)
Contrast mechanism	M
Evaluation of the magnetization, $M(\mathbf{r})$	Q
Spatial resolution (nm) $\frac{\text{Typical}}{\text{Limit}}$	$\frac{800}{250}$
Depth of information (nm)	<20 (metals)
Time for image acquisition	1 msec–5 sec
Limits on applied magnetic fields	None
Imaging conditions	In air
Max thickness	None
Sample smoothness	R
Sample clean surface	NR

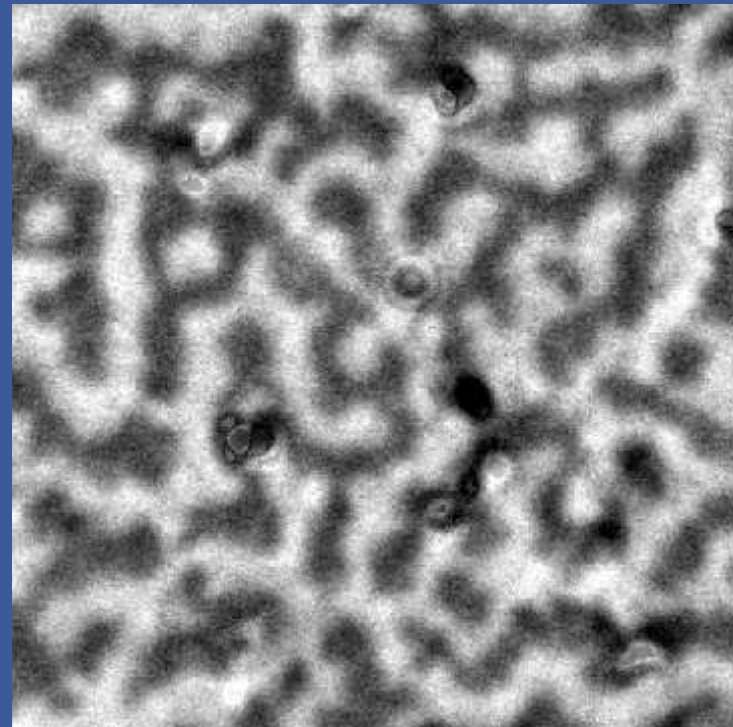
Topical Review
J. McCord,
J. Phys. D: Appl.
Phys. 48,
333001 (2015)



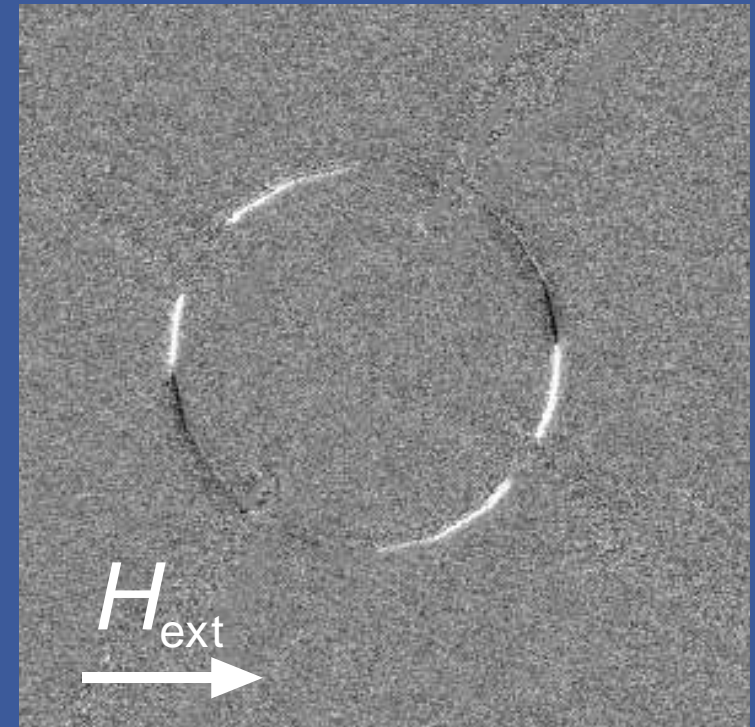
Spatial resolution of MO imaging



— 5 μm



— 2 μm



— 10 μm

**Stripe domains in
 $\text{Ni}_{81}\text{Fe}_{19}$**

Domain width 250 nm

**Interaction domains
in $\text{Nd}_2\text{Fe}_{14}\text{B}$**

Domain width 400 nm

(sample O. Gutfleisch,
TU Darmstadt)

**Magnetic domains in
a angle sensor**

Stripe width 300 nm

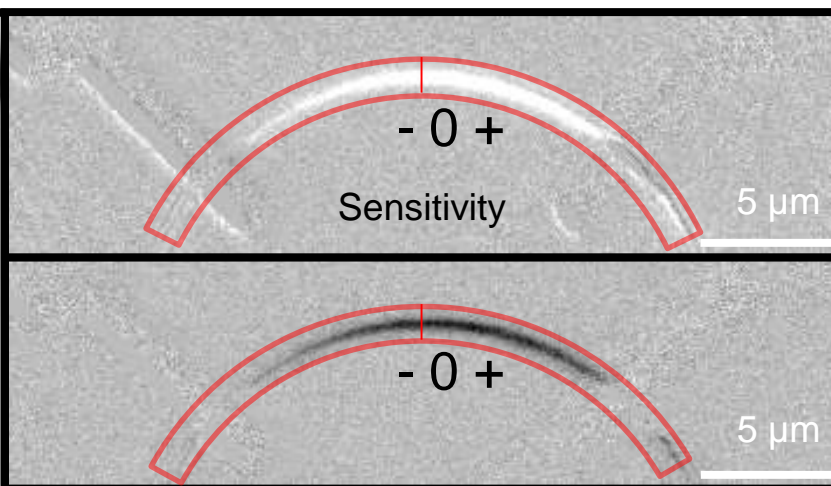
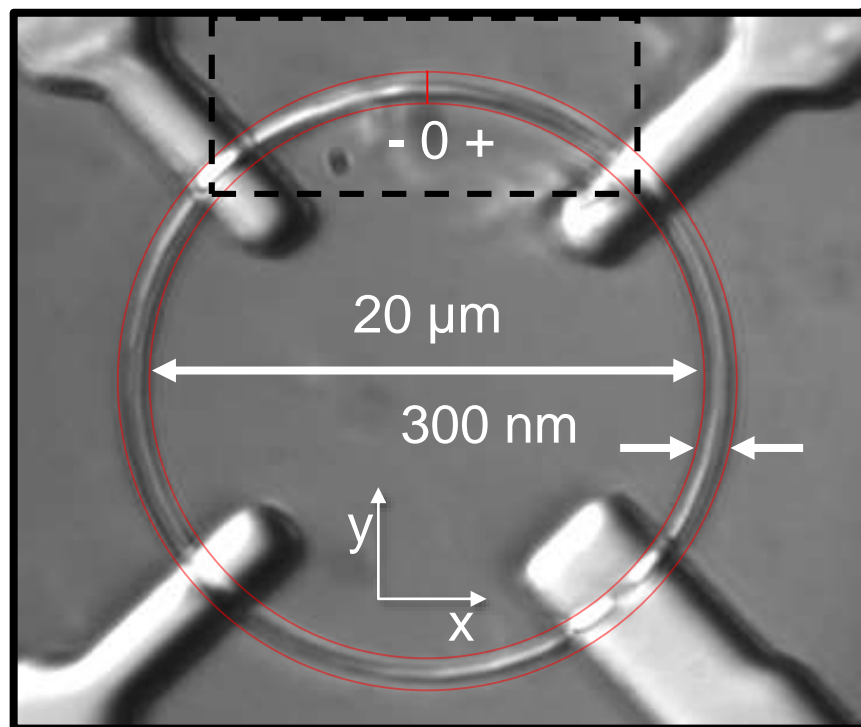
Localization accuracy
10 nm

(sample R. Mattheis,
IPHT Jena)

**200 nm
resolution**

J. McCord, J. Phys. D: Appl. Phys. 48, 333001 (2015)

Stochastic domain wall propagation in field sensors

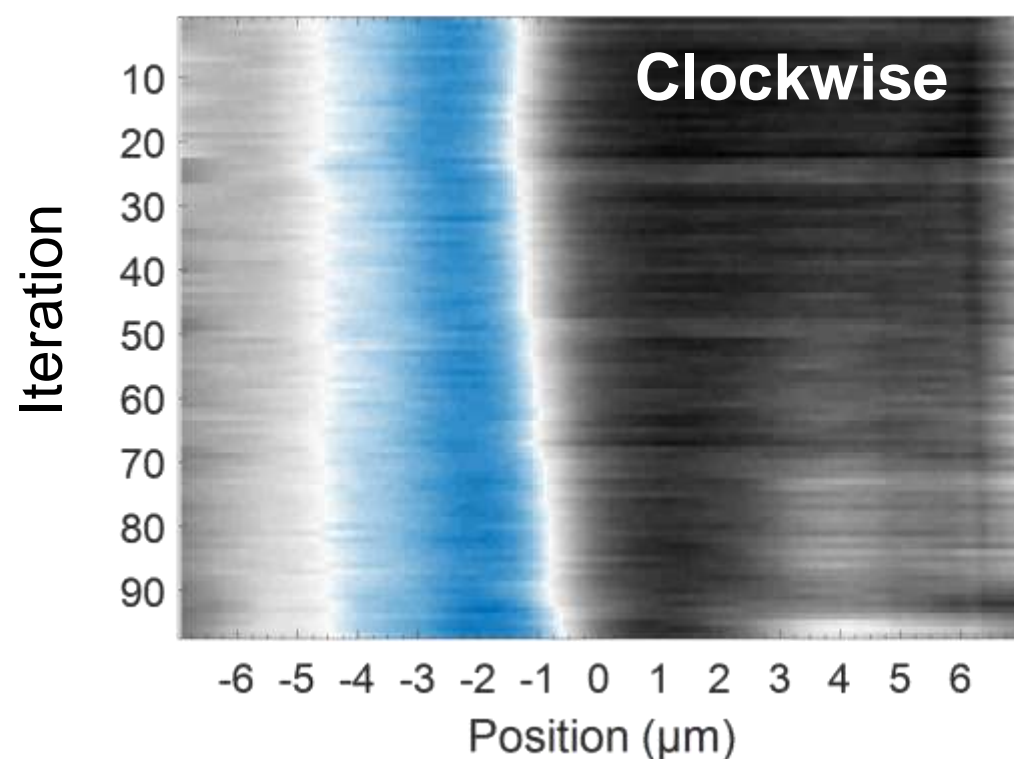


Fully switched L to R

Fully switched R to L

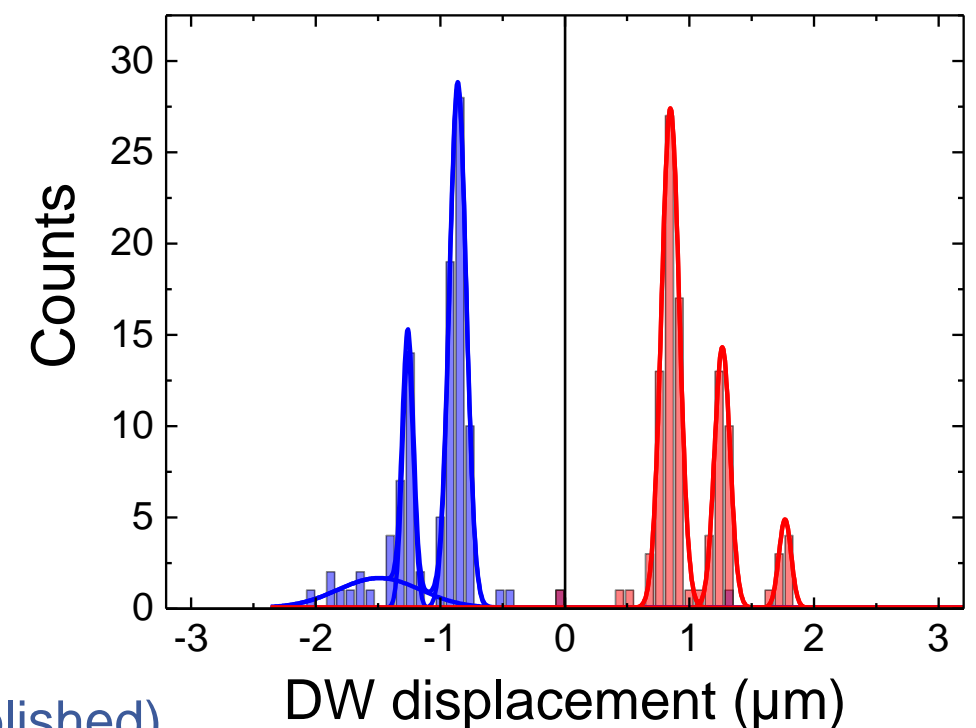
Imaging at the resolution limit!

Extracting domain wall position after CW and CCW rotation

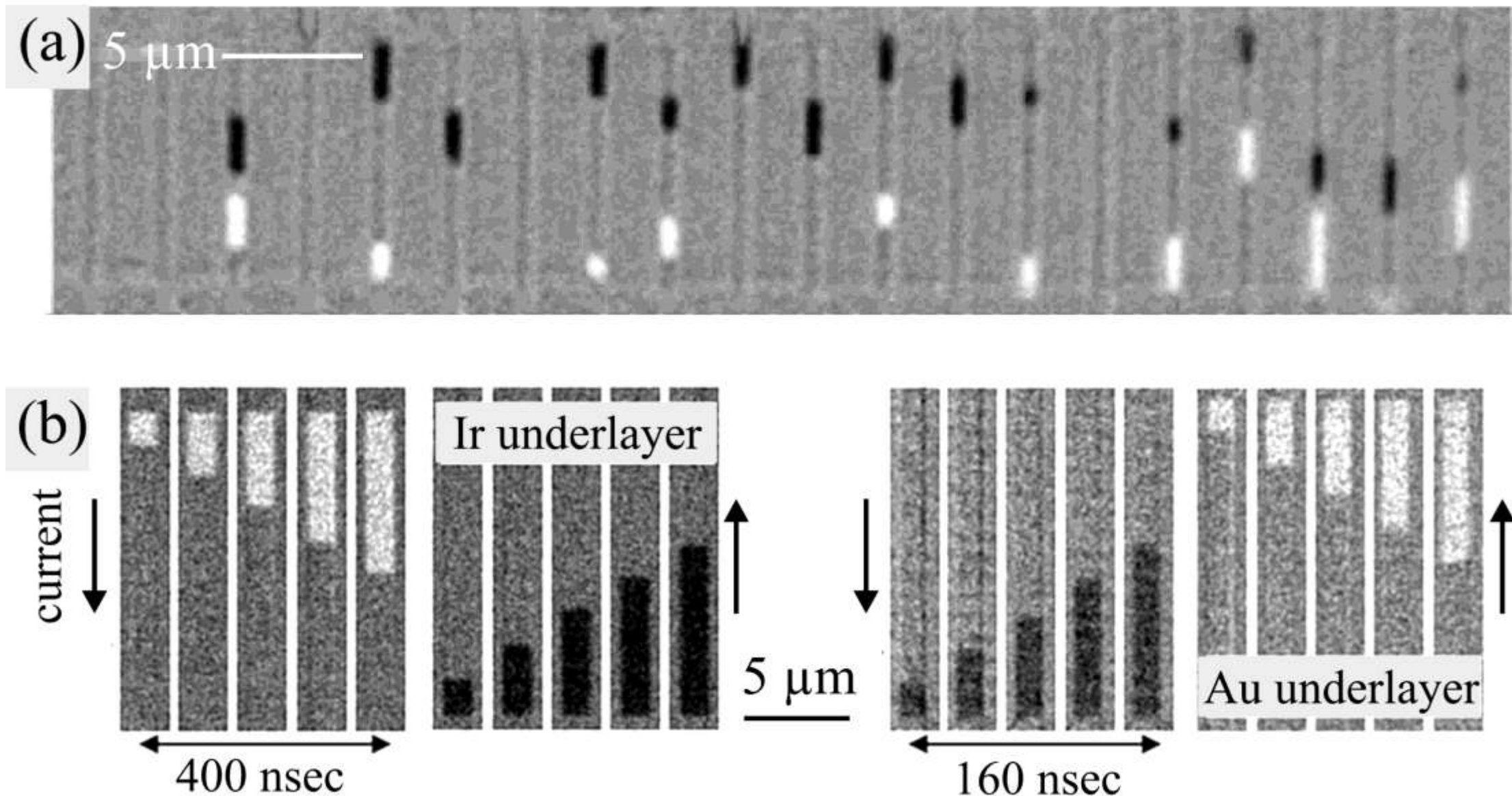


**30 kA/m
5° rotation**

E. Lage et al. (unpublished)

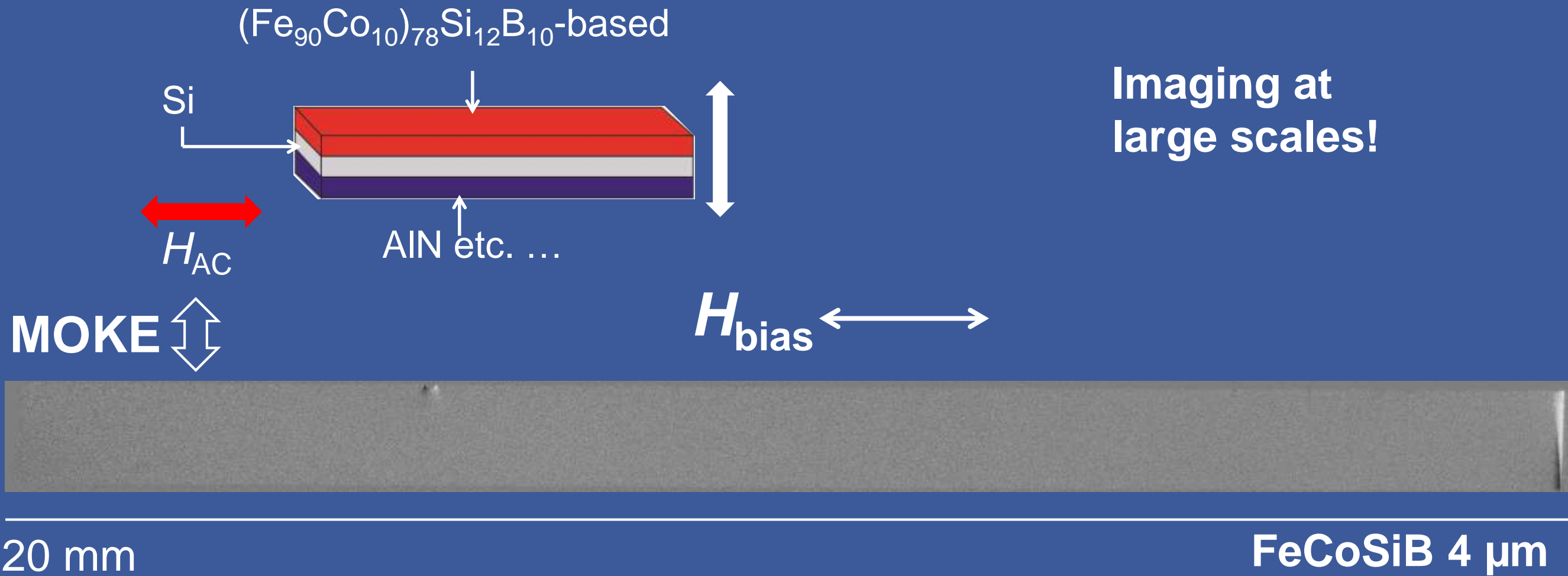


J. McCord, J. Phys. D: Appl. Phys. 48, 333001 (2015)



Current induced magnetic domain wall displacements (a) MOKE images displaying domain wall displacements in Pt/Co/Al₂O₃ magnetic nanowires induced by nanosecond current pulses. (b) Current induced domain motion versus total current pulse length for Ir/Co/Ni/Co and Au/Co/Ni/Co stacks.

LARGE view MOKE microscopy



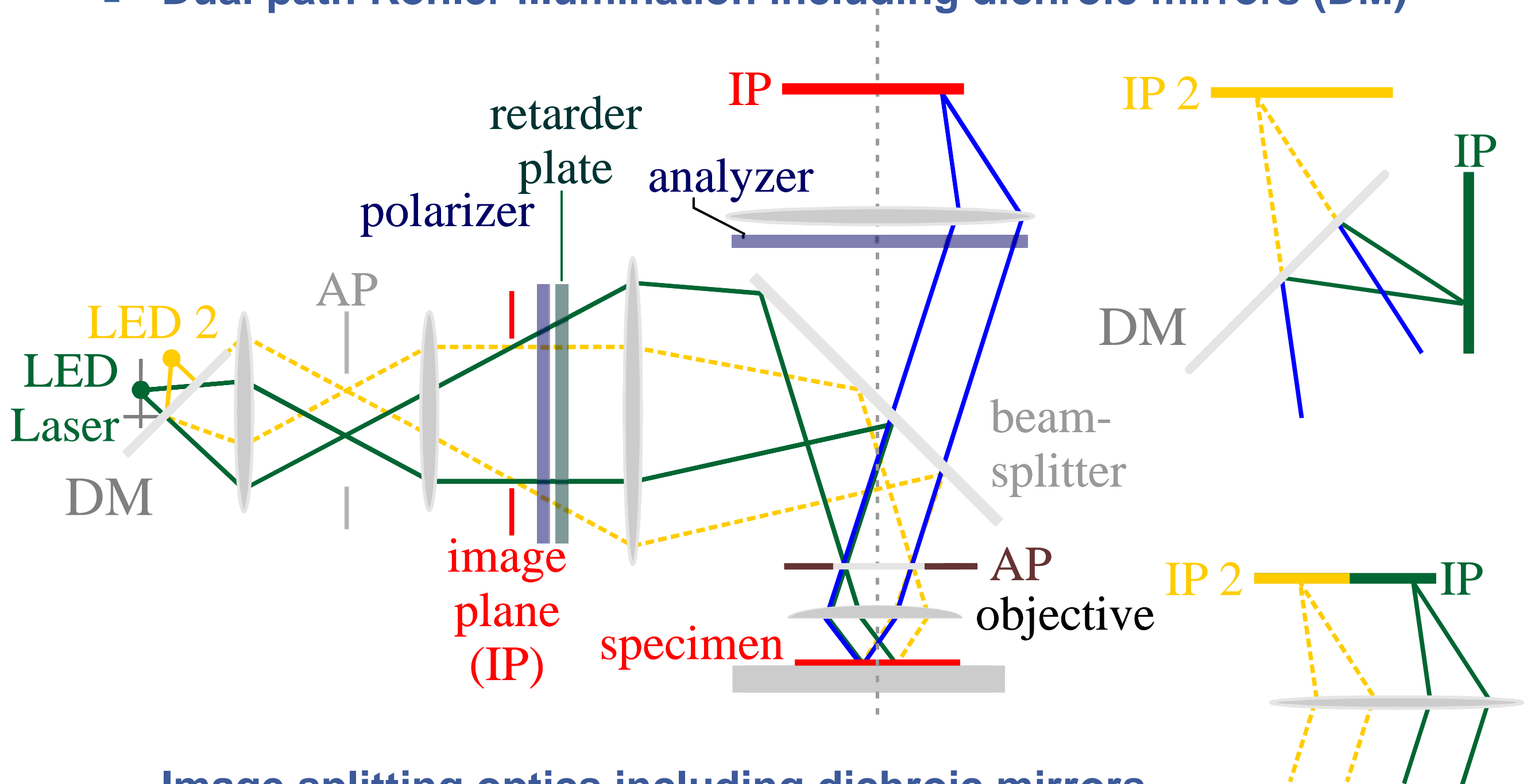
- Noise mechanism in FM/FE composite magneto-electric sensors

J. McCord, J. Phys. D: Appl. Phys. 48, 333001 (2015)

Multi-effect MO imaging (advanced)



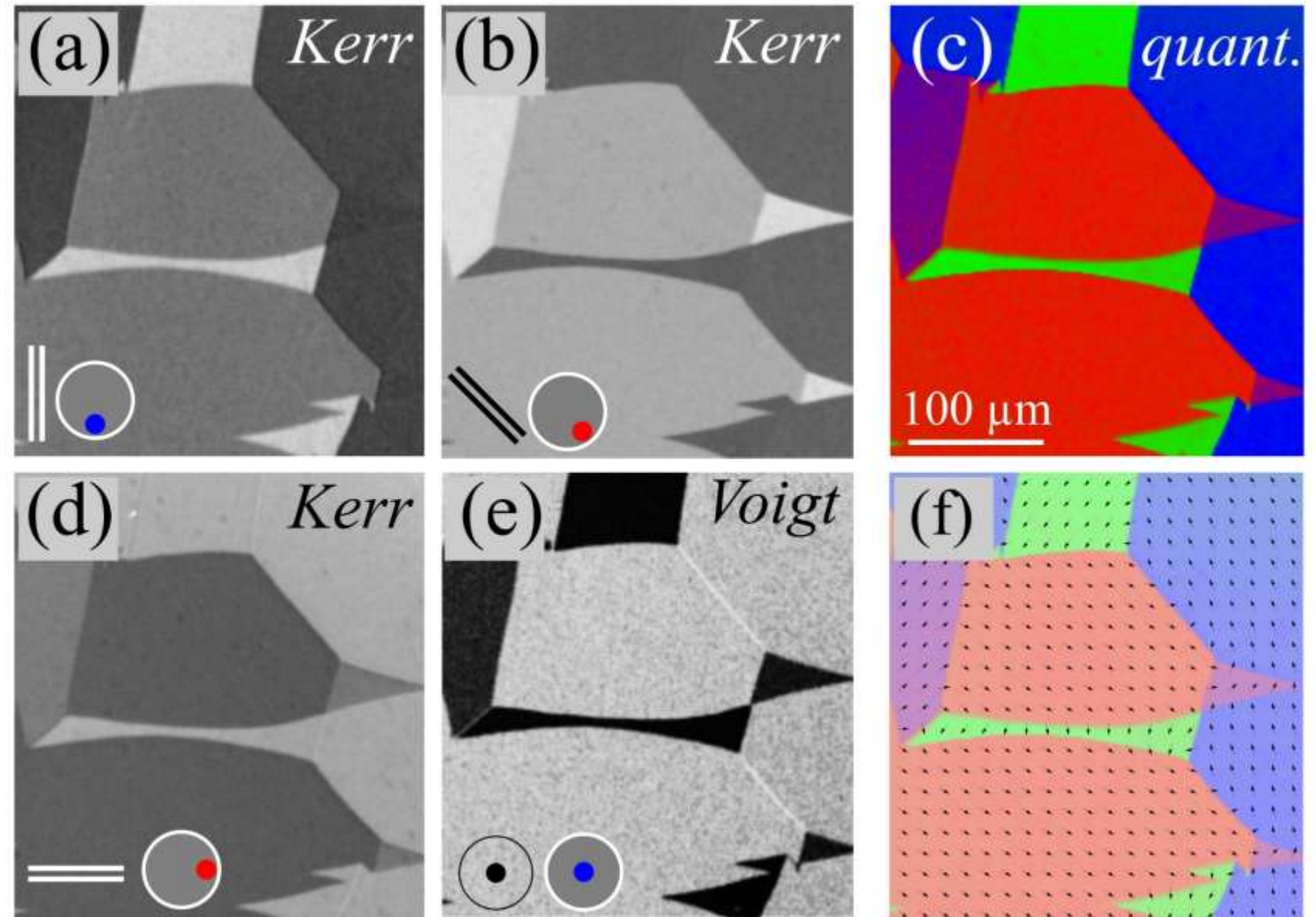
- Dual path Köhler illumination including dichroic mirrors (DM)



- Image splitting optics including dichroic mirrors

N. Urs et al., APL 103, 142410 (2013)
J. McCord, J. Phys. D: Appl. Phys. 48, 333001 (2015)
N. Urs et al., AIP Advances 6, 055605 (2016)

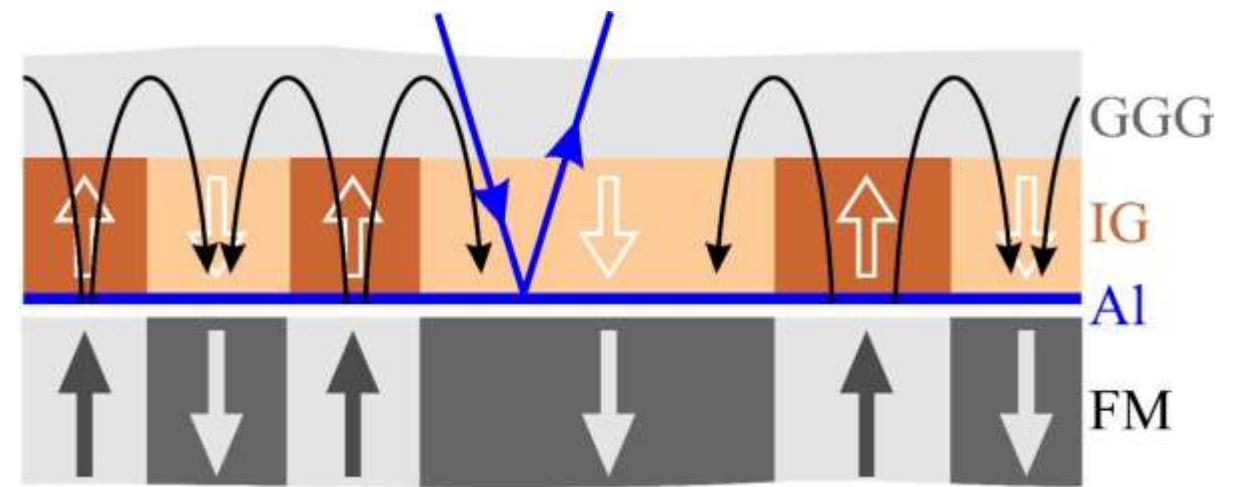
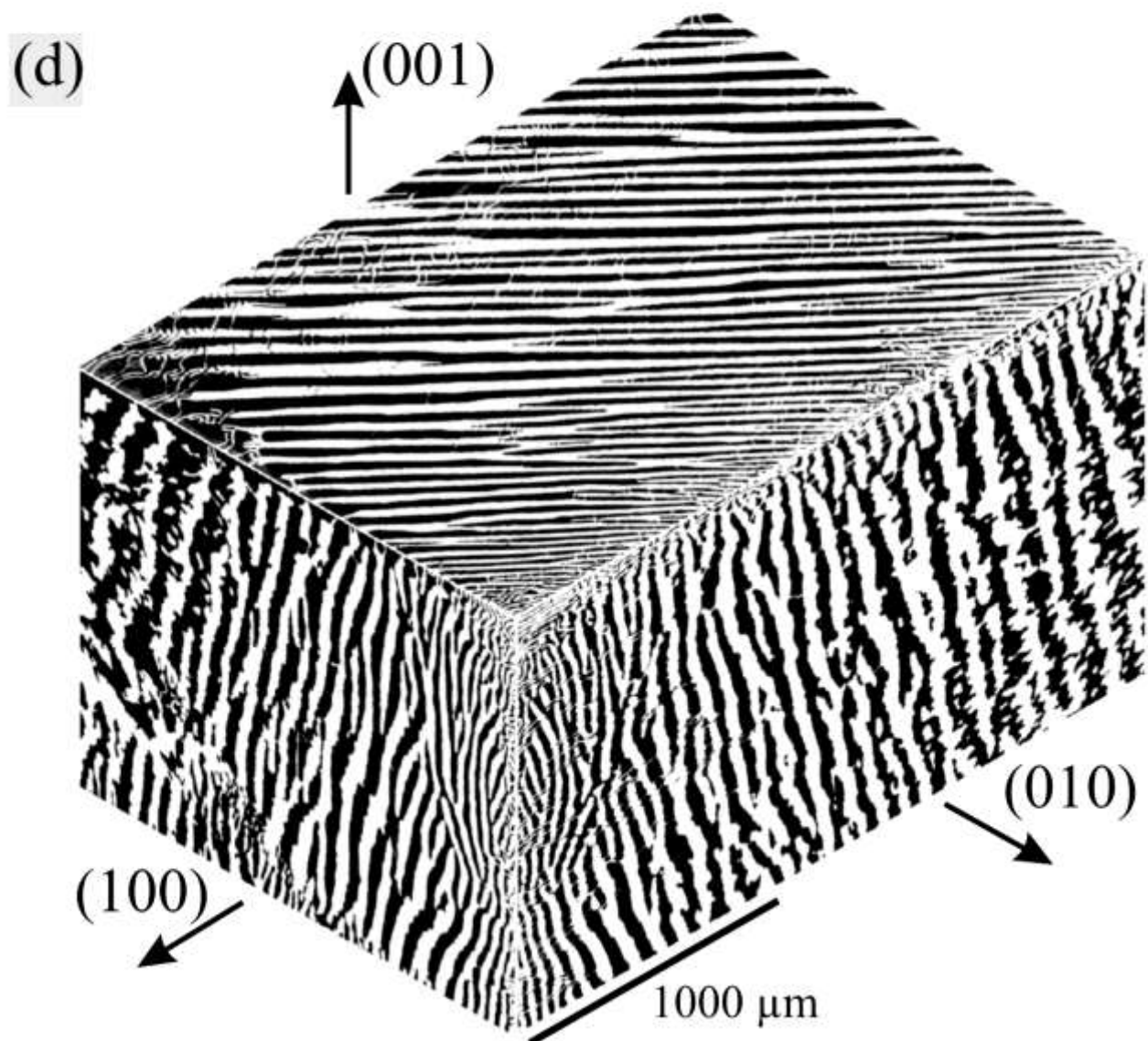
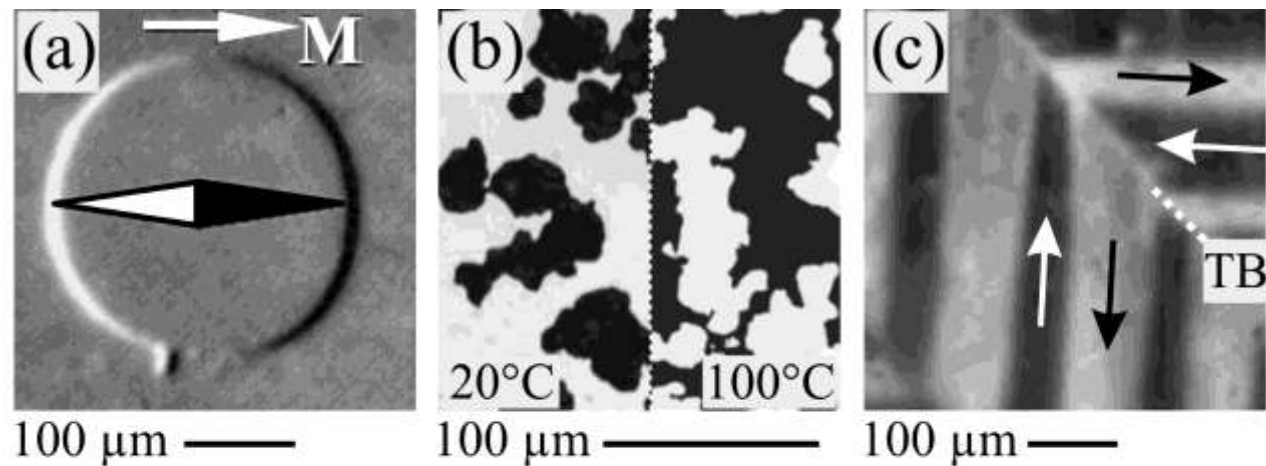
- **Multicomponent & multiple effect imaging**



(a), (b) Concurrently obtained Kerr images of a single crystal iron film with orthogonal sensitivity directions, and (c) obtained quantitative domain image. Concurrently obtained (d) diagonally aligned Kerr and (e) Voigt image. (f) Vector representation of magnetic domain pattern.

J. McCord, J. Phys. D: Appl. Phys. 48, 333001 (2015)

Imaging with magneto-optical detector films



Scheme of imaging magnetic domains of a ferromagnetic sample (FM) with a magneto-optical indicator film (MOIF).

(a) MOIF image of a region of an exchange spring sample with an opening. (b) Inversion of magnetization of a GdCoCu single crystal below and above the compensation temperature. (c) Domain structure from a Ni_2MnGa crystal across a twin boundary (TB).

J. McCord, J. Phys. D: Appl. Phys. 48, 333001 (2015)



- **Flat and smooth surface required**
- **Spatial resolution approx. 200 nm**

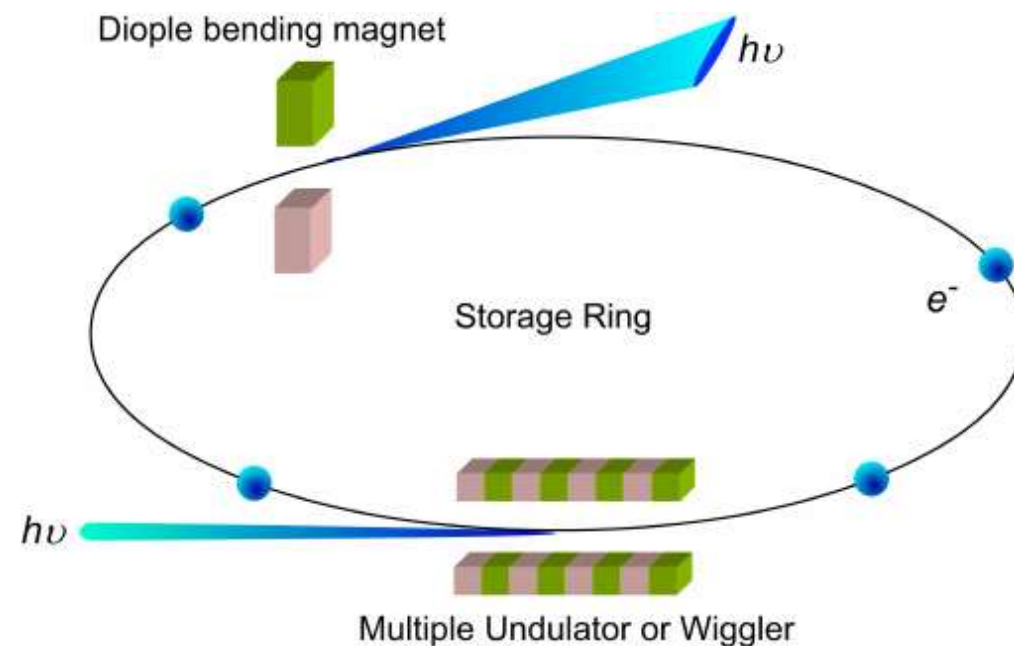
- **Magnetization can be observed directly**
- **Quantitative measurements possible**
- **Almost no influence on magnetization (but light induced heat)**

- **Straightforward sample manipulation (fields, temperature, stress)**
- **Surface sensitive (approx. 30 nm)**

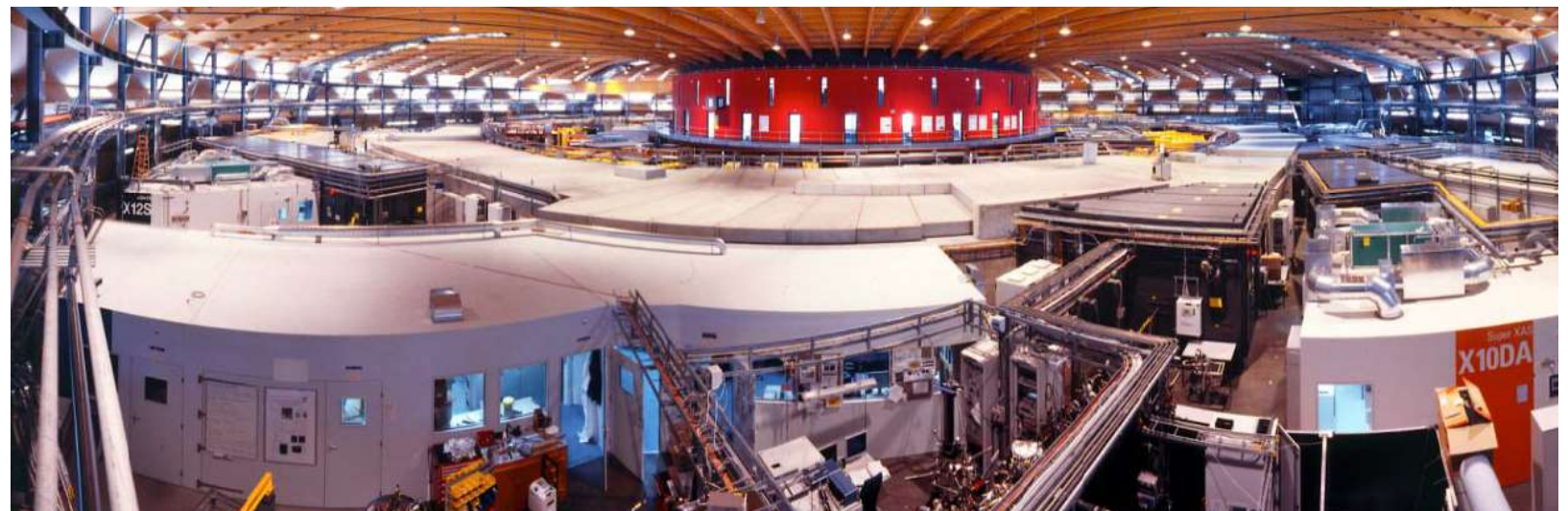
	XPEEM	STXM ^(a)
Contrast mechanism	M	M
Evaluation of the magnetization, $M(\mathbf{r})$	Q	Q
Spatial resolution (nm) Typical Limit	300 50	30 15
Depth of information (nm)	<5 nm	Thickness integrated <100 nm
Time for image acquisition	~1sec	~1sec
Limits on applied magnetic fields	Not advised	None
Imaging conditions	UHV	None
Max thickness		60–100 nm
Sample smoothness	NR	NR
Sample clean surface	Preferred	NR

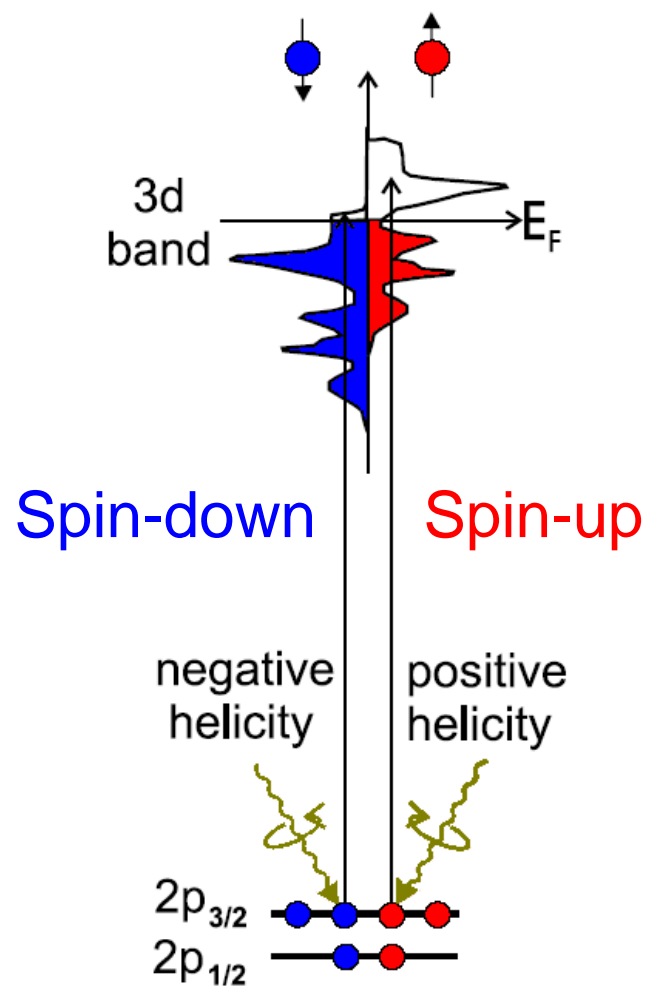
Synchrotron based

- Undulators and bending magnets cause electrons emit light

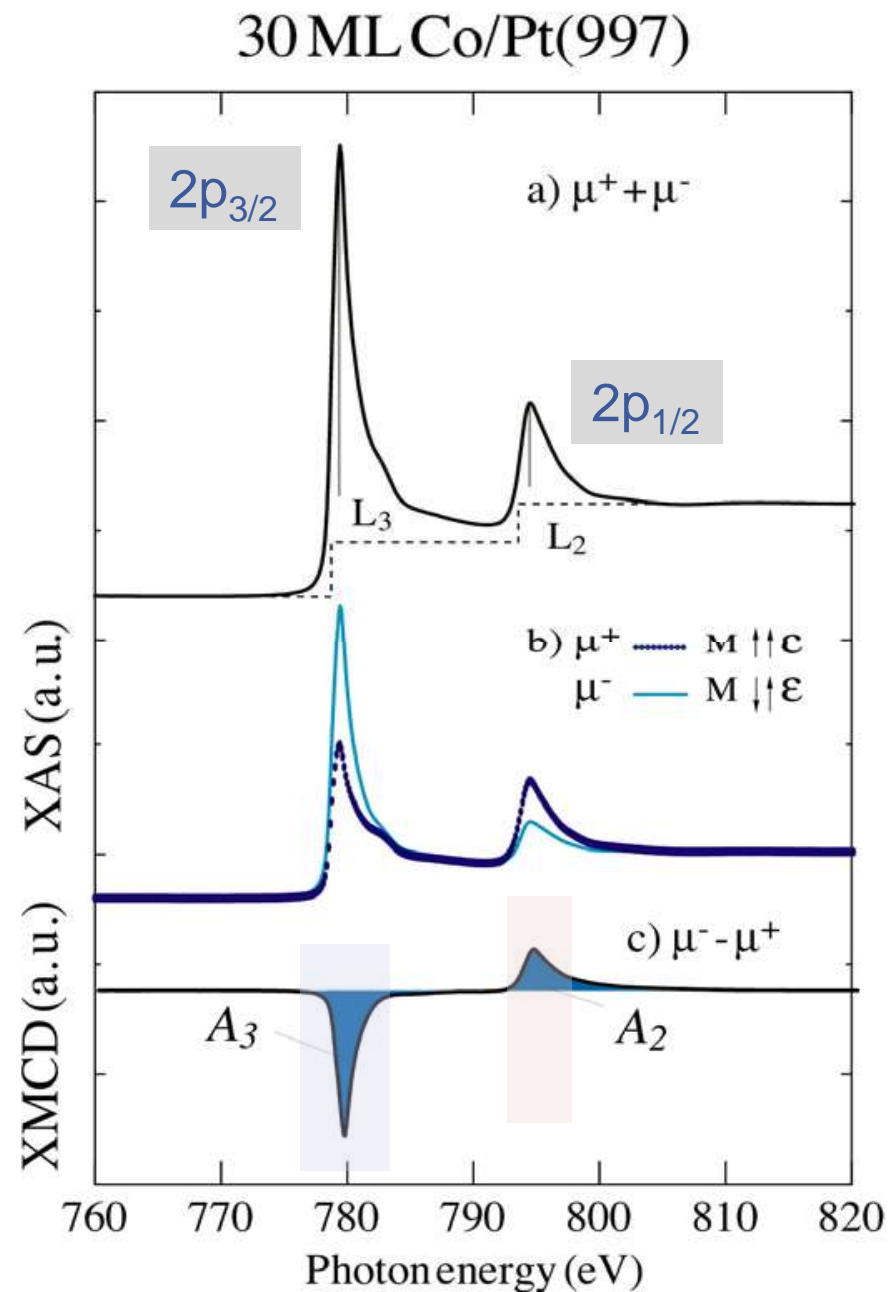


- **Big illuminator!**





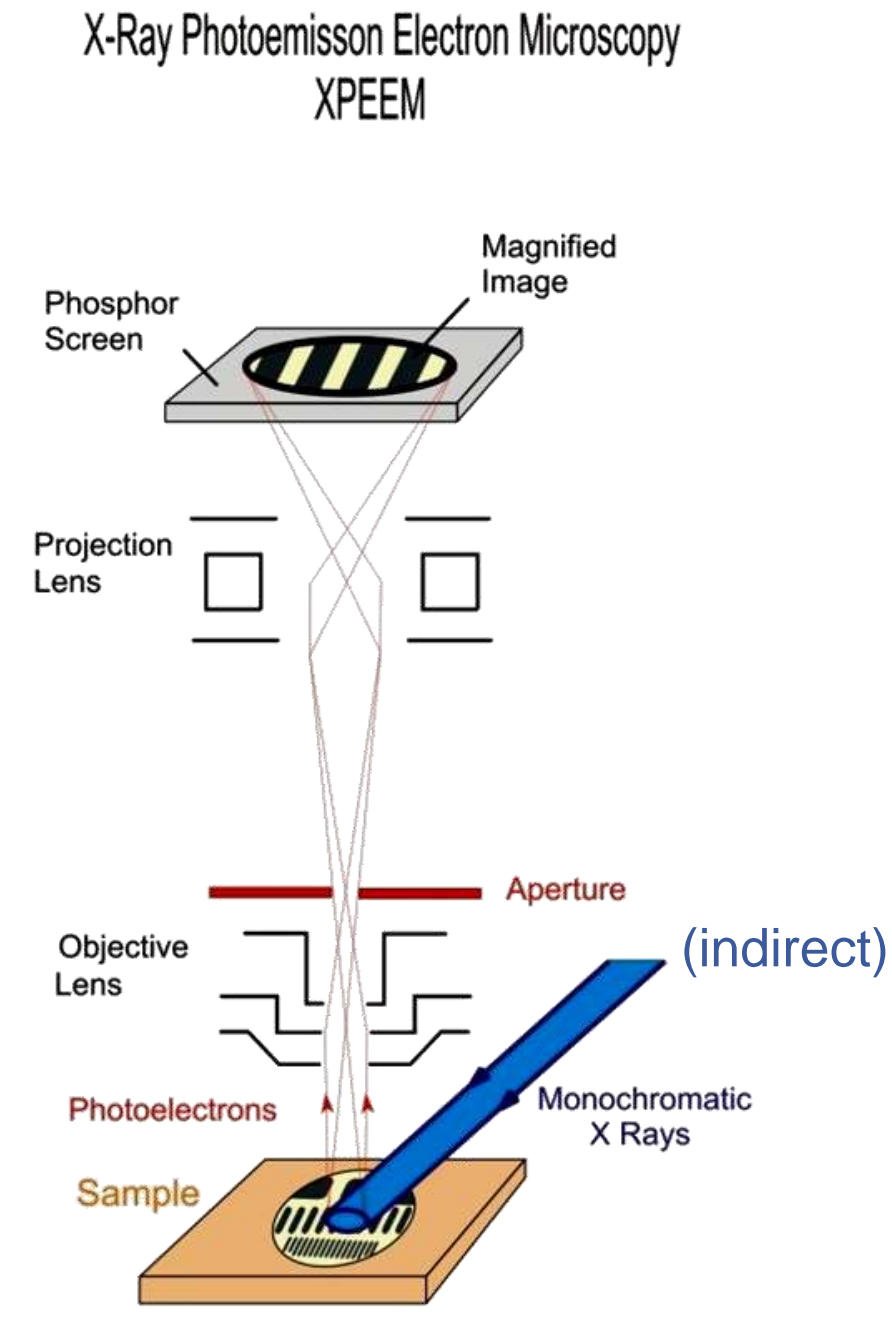
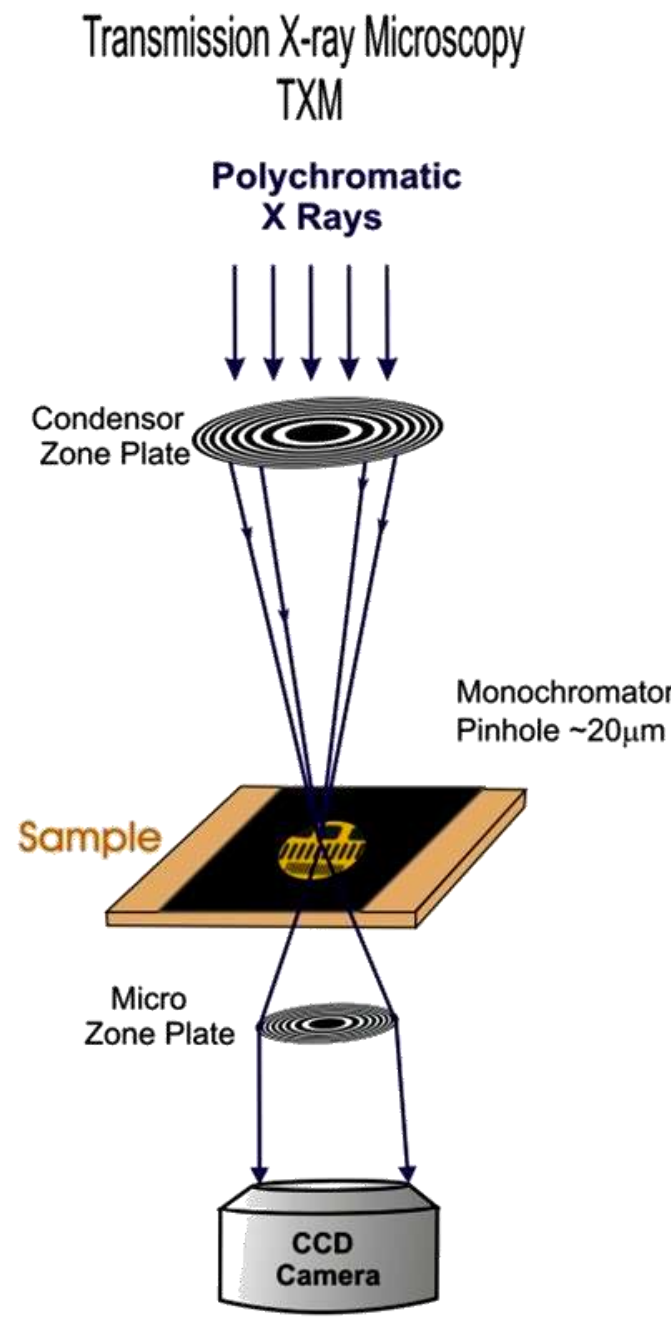
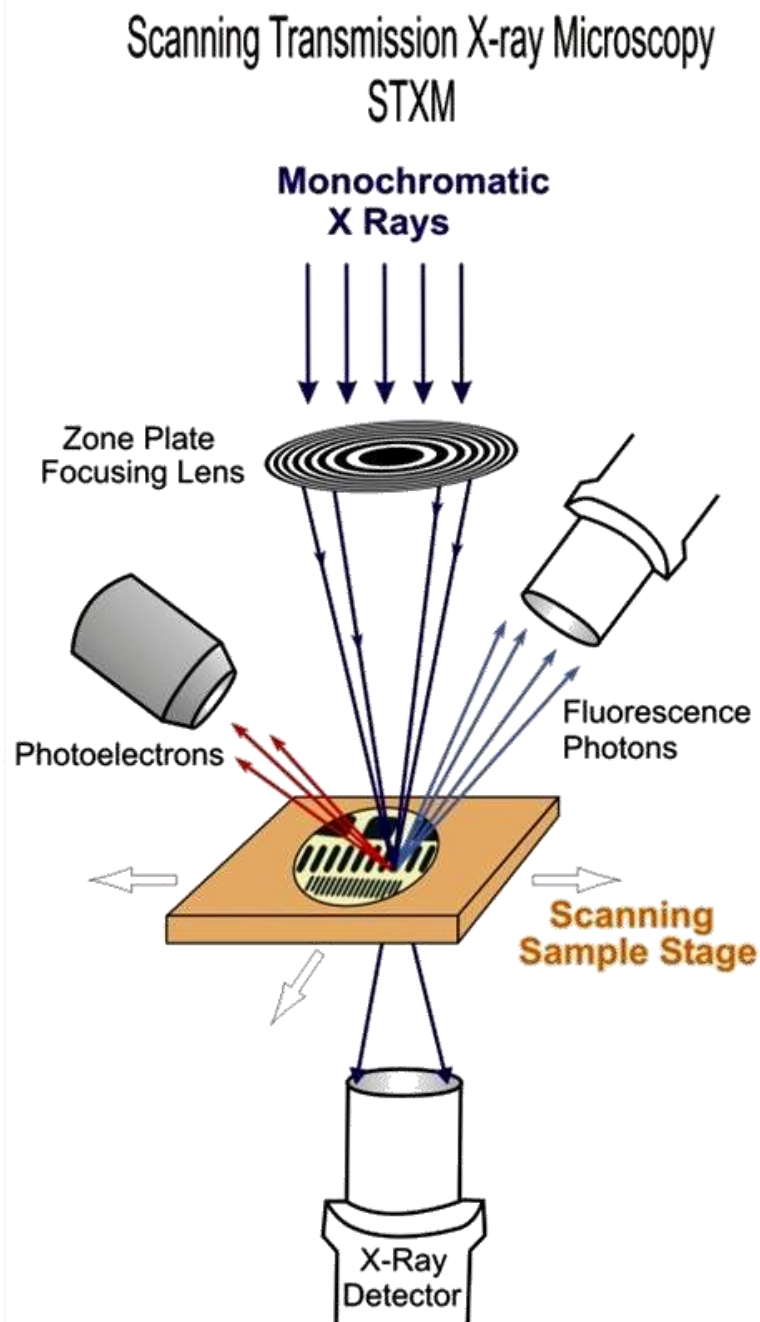
Transition of electrons following dipole selection rules from 2p-3d levels in L-edge x-ray absorption



X-ray absorption spectra

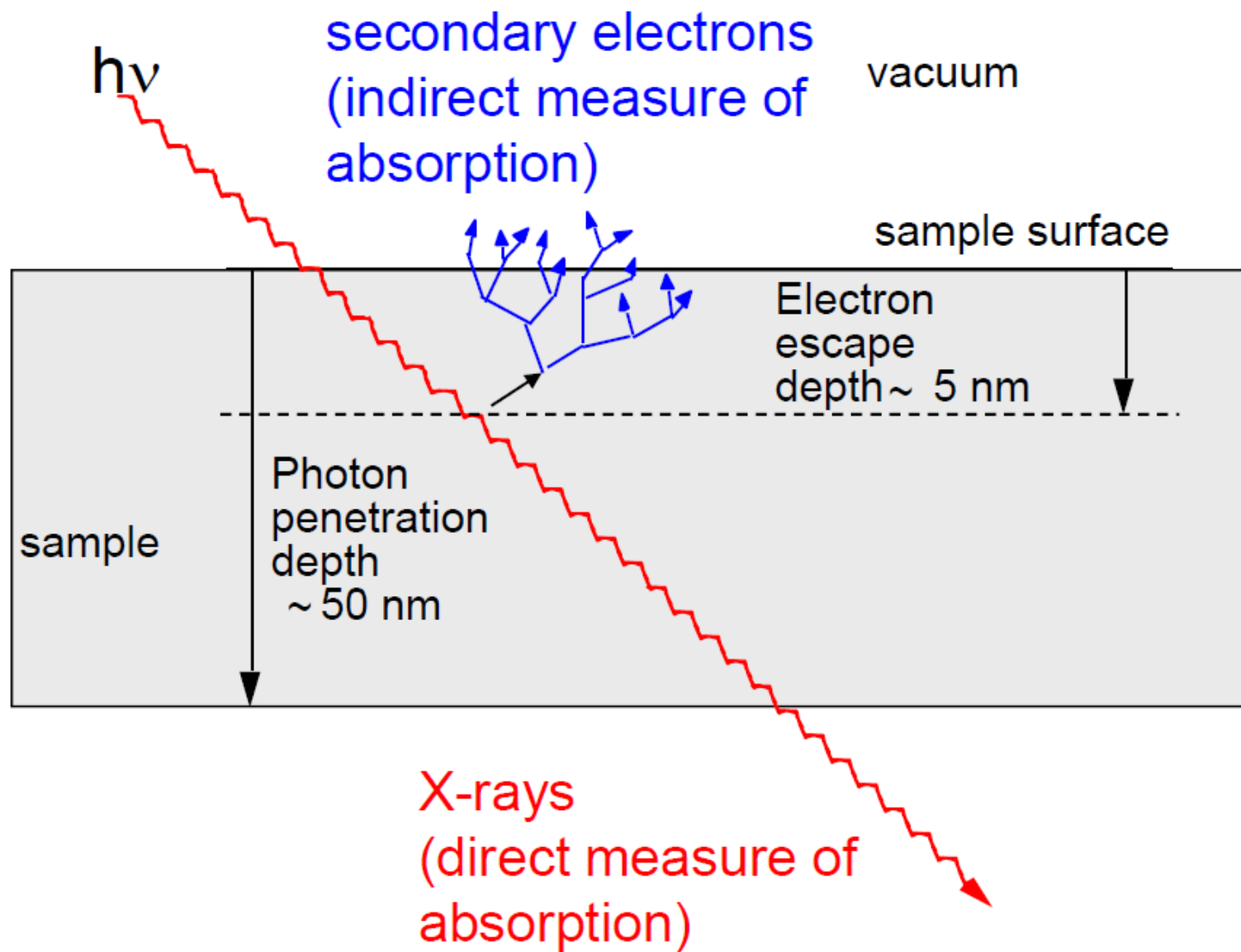
X-ray Magnetic Circular Dichroism (XMCD)

Magnetic soft x-ray spectro microscopies



Real-space!

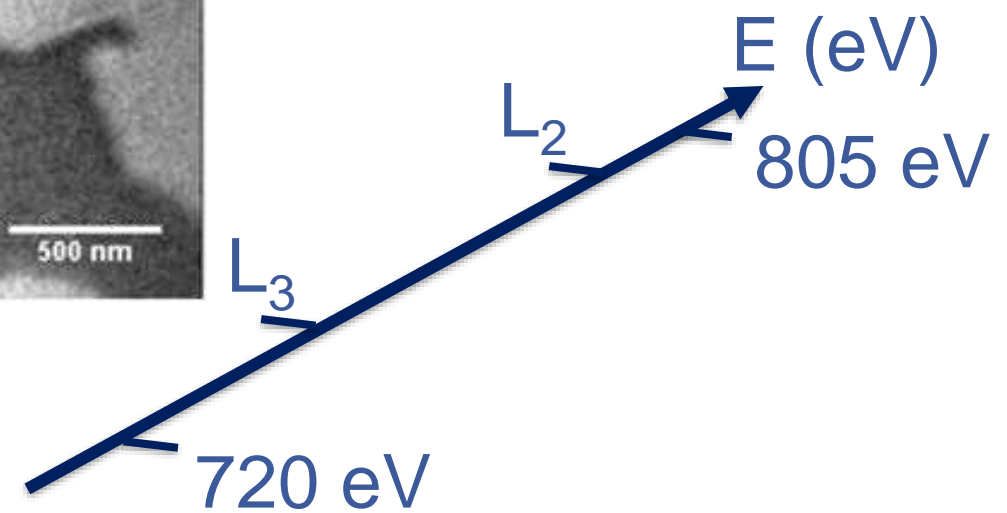
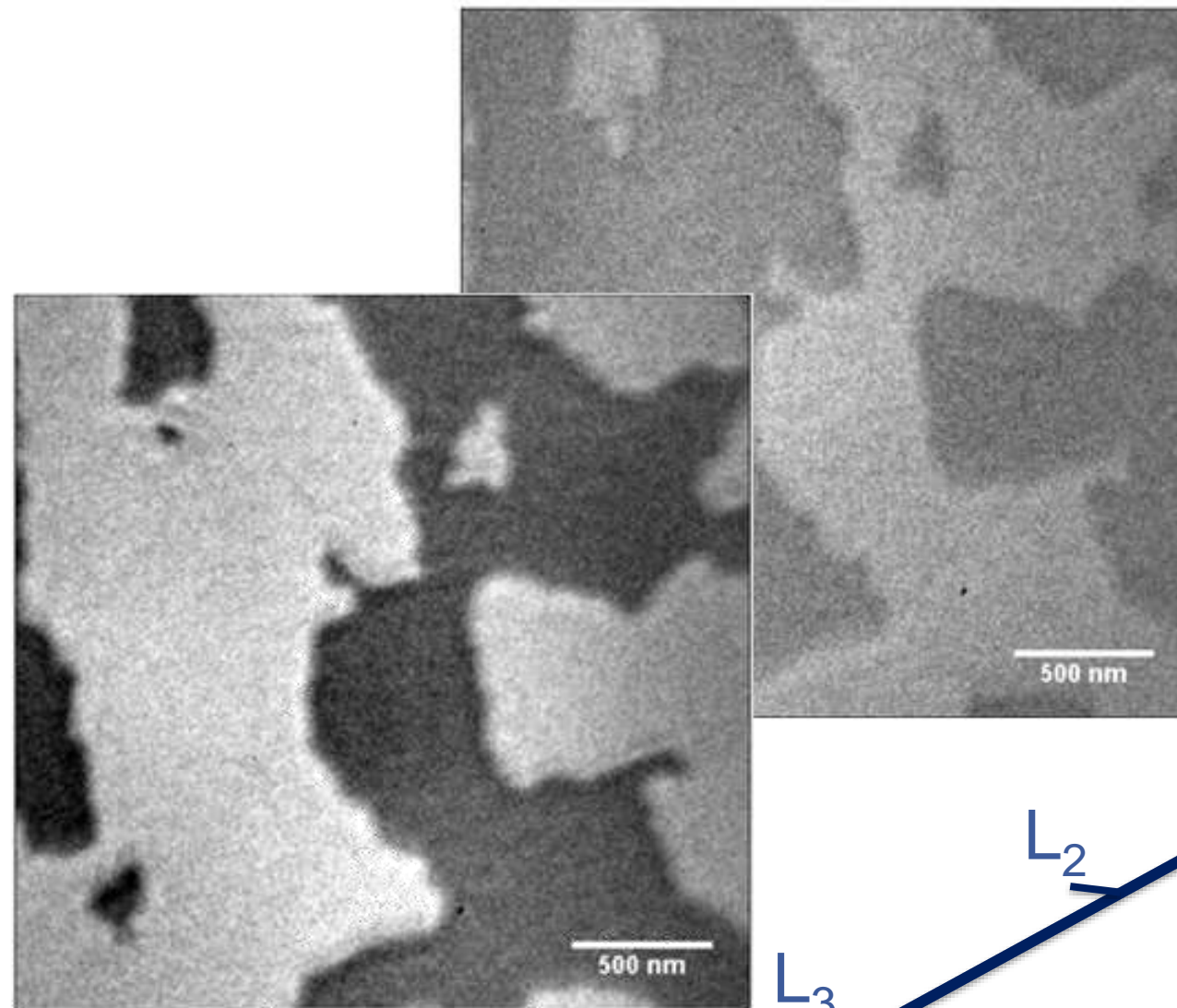
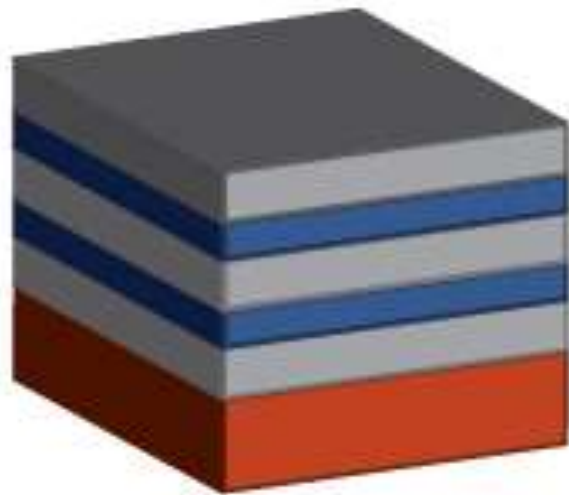
Material from P. Fischer, Lawrence Berkeley Natl. Lab, USA



**Photoemission
Electron
Microscopy
(PEEM) to probe
surface / interfaces**

**Transmission
X-ray Microscopy
(TXM)**

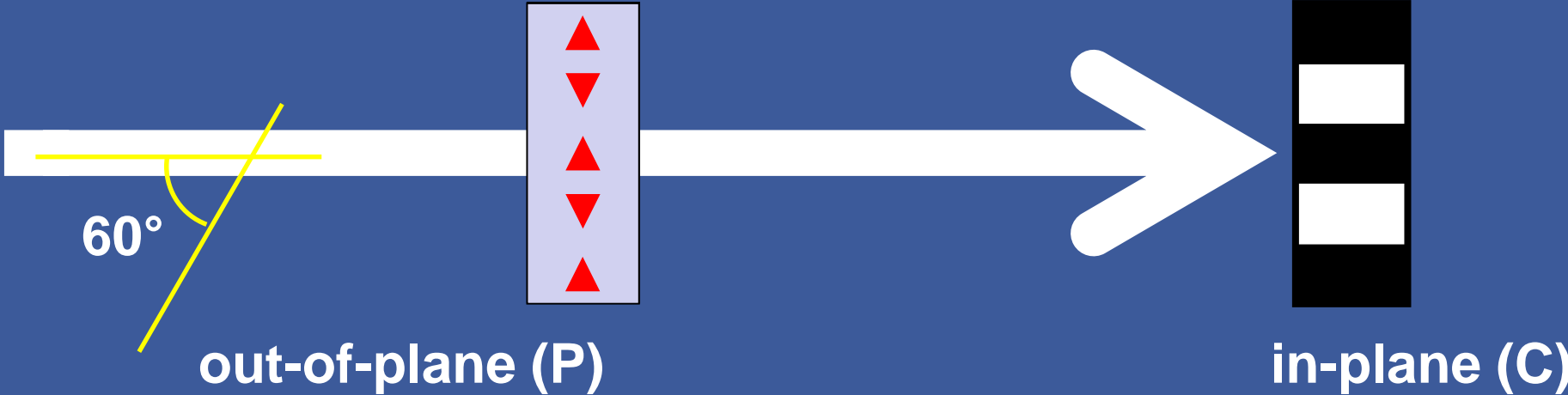
(Co 0.3nm/Pt 0.5nm)x30



Spectroscopic series of magnetic TXM images across Co L_3 and L_2 edges

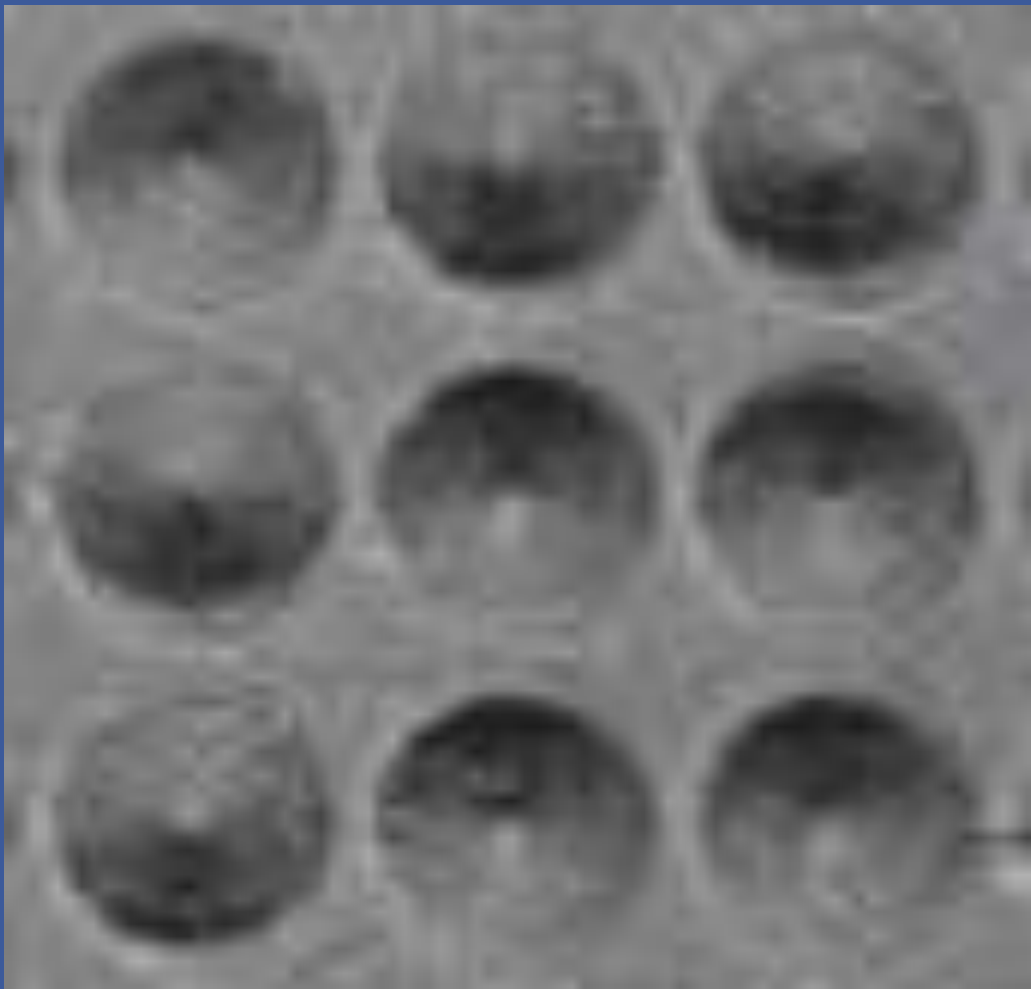
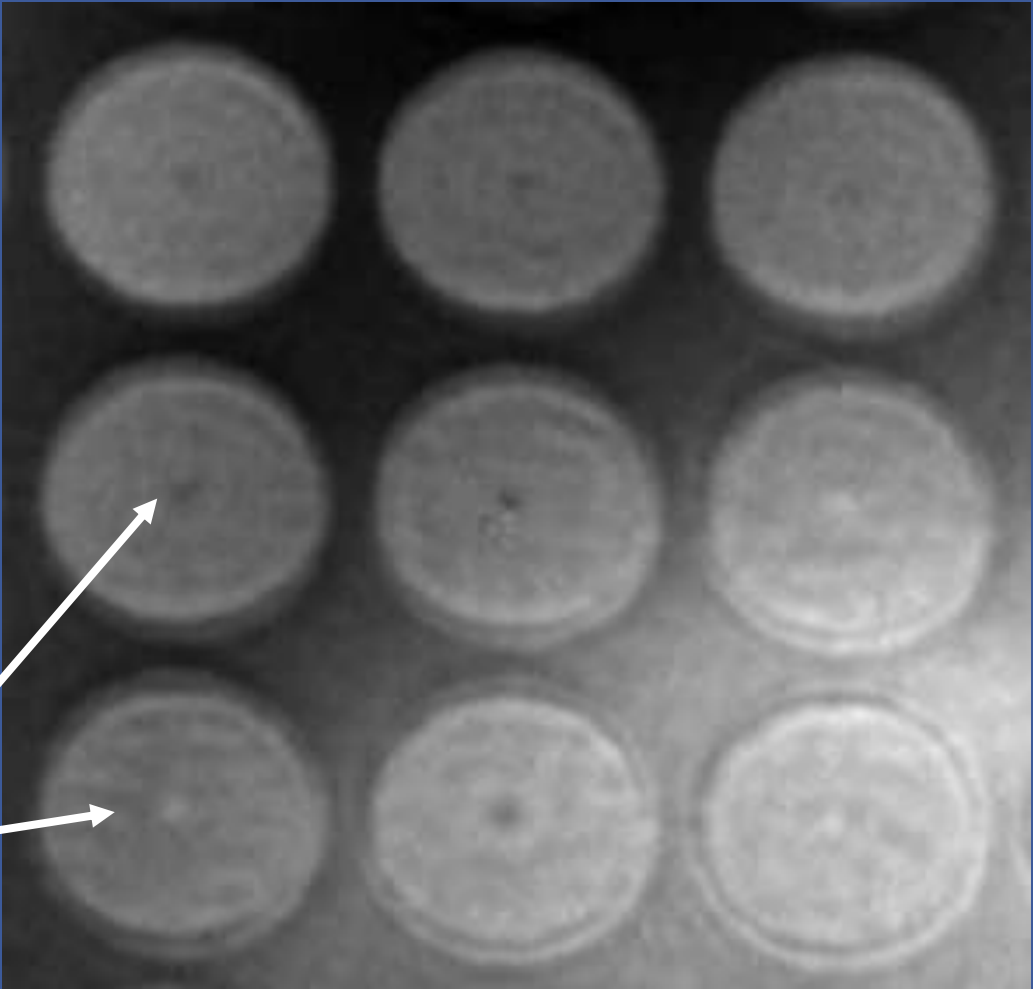
Material from P. Fischer, Lawrence Berkeley Natl. Lab, USA

X-ray imaging of vortex states



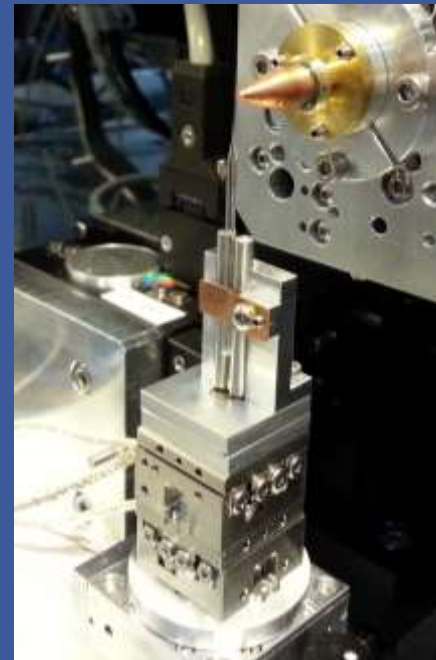
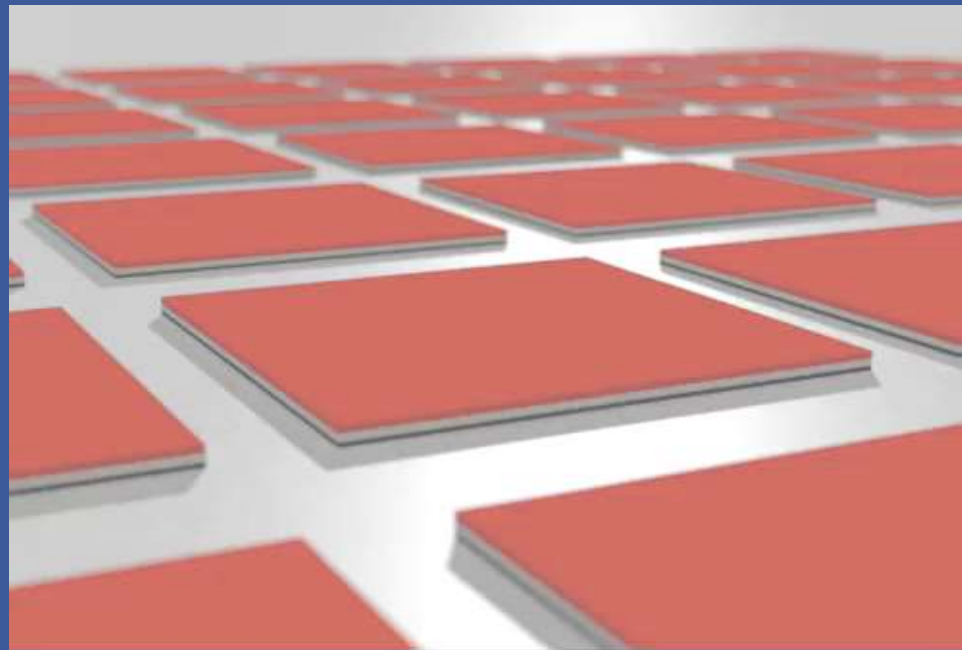
$\text{Ni}_{80}\text{Fe}_{20}$
 $h = 100 \text{ nm}$
 $r = 400 \text{ nm}$

Vortex
core



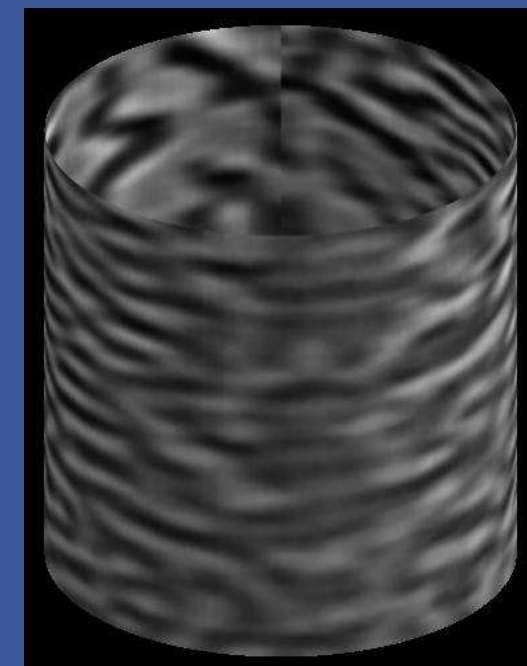
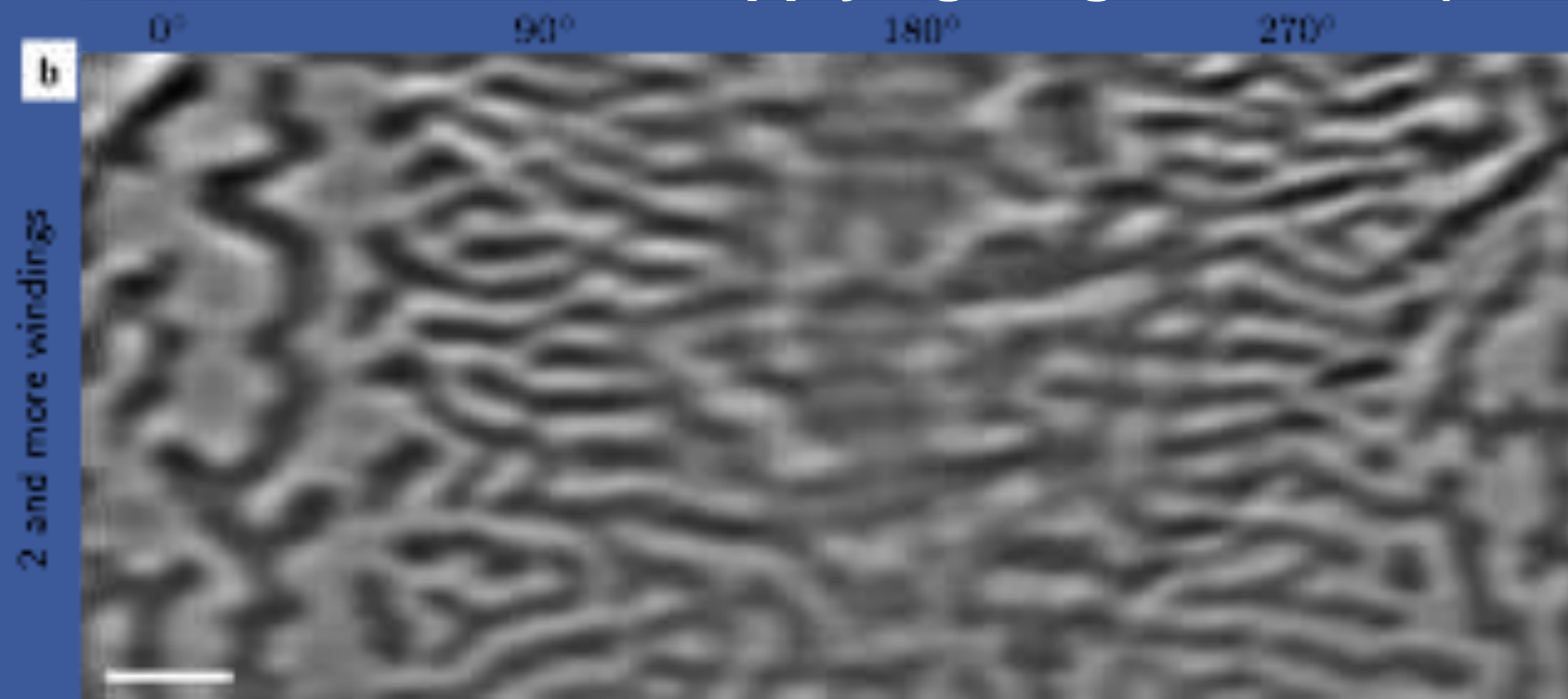
Material from P. Fischer, Lawrence Berkeley Natl. Lab, USA

Magnetic soft x-ray Tomography - 3D imaging



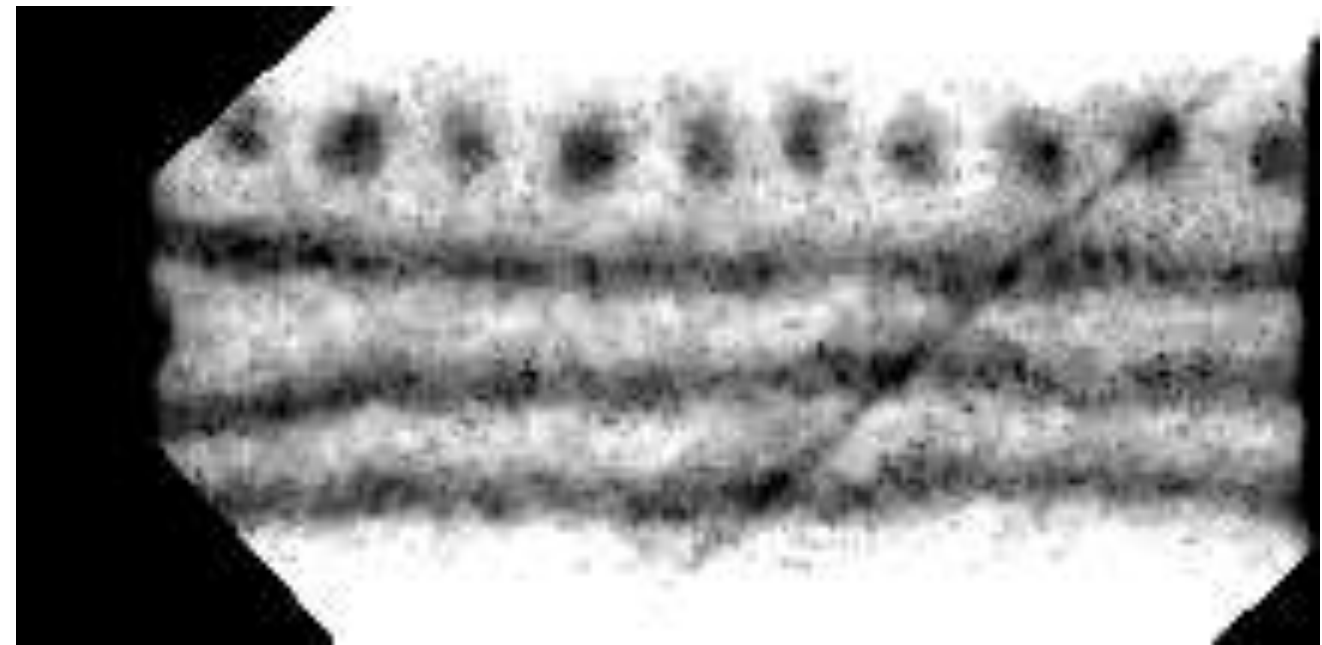
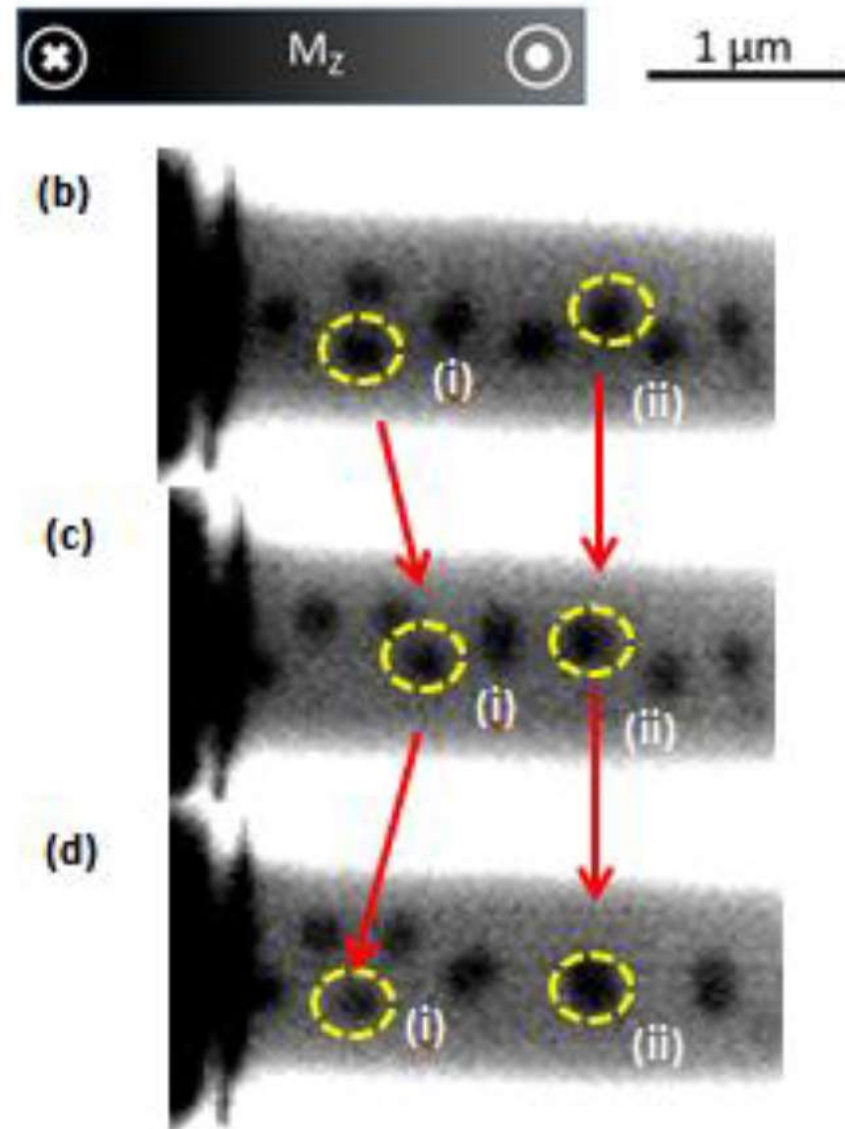
R. Streubel, F. Kronast, P. Fischer, D. Parkinson, O.G. Schmidt, D. Makarov, Nature Communication 6 7612 (2015)

Remanent state after applying magnetic field (200 kA/m) along 180°



3D view

Material from P. Fischer, Lawrence Berkeley Natl. Lab, USA

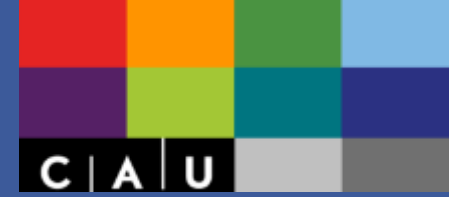


- Current pulses of $\pm 3.9 \cdot 10^{11} \text{ Am}^{-2}$.
- Forward and backward motion of skyrmion bubbles (**static images**)

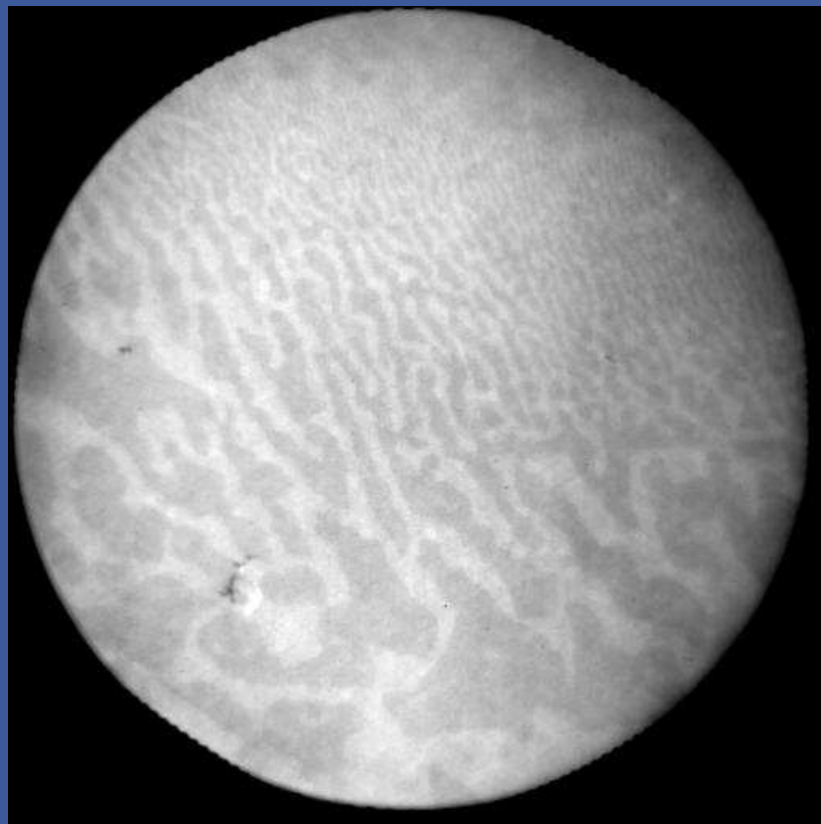
$[\text{W}(5 \text{ nm})/\text{CoFeB}(0.8 \text{ nm})/\text{MgO}(2 \text{ nm})]_{10}/\text{Ta}(5 \text{ nm})$

Material from M. Kläui, Johannes Gutenberg-University Mainz, Germany

XMCD-PEEM - magnetic and topographic information



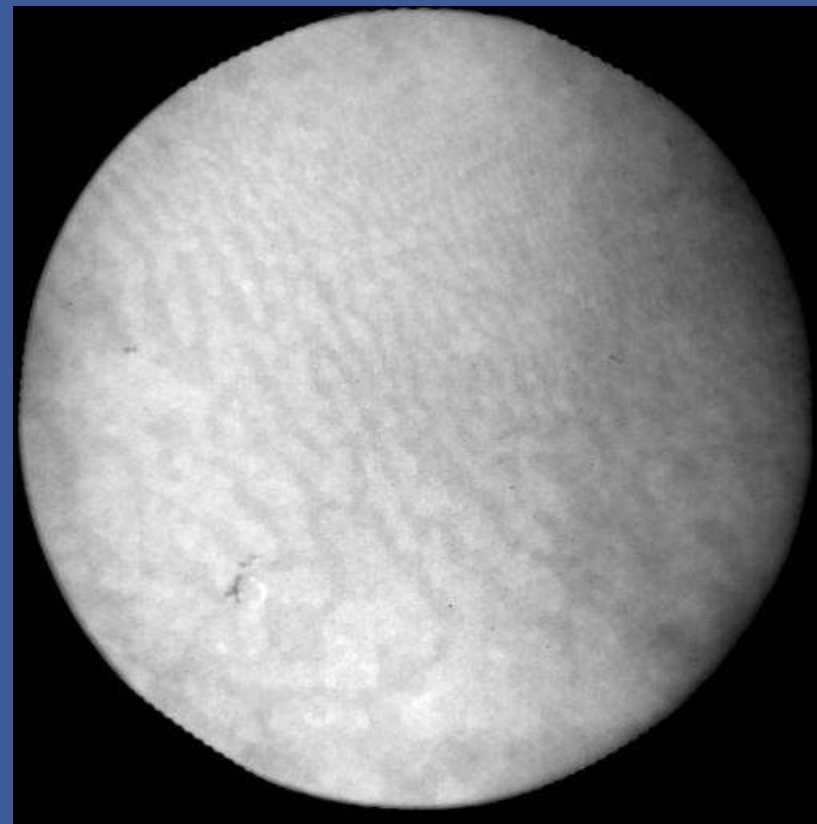
Positive helicity



$$I(\sigma^+)$$

W. Kuch, K. Fukumoto,
J. Wang, MPI-MSP,
C. Quitmann, F. Nolting,
T. Ramsvik, PSI-SLS,
unpublished.

Negative helicity



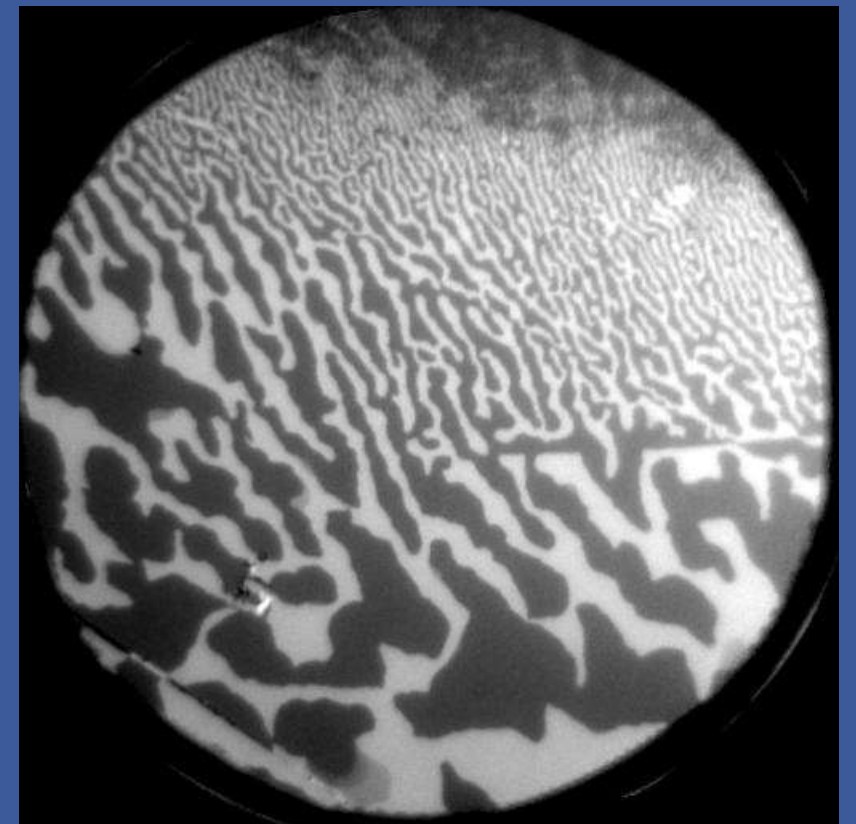
$$I(\sigma^-)$$

20 μm

Co/Ni/Cu(001)

Ni L3 edge

Normalized difference signal



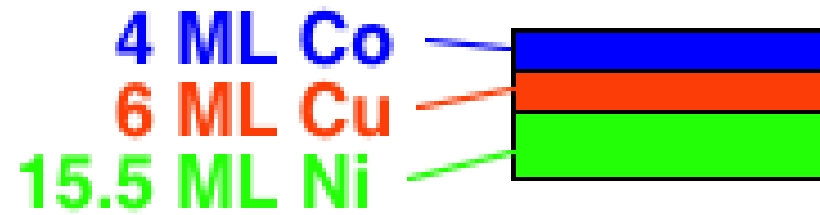
$$\frac{I(\sigma^+) - I(\sigma^-)}{I(\sigma^+) + I(\sigma^-)}$$

Material from W. Kuch, FU Berlin, Germany

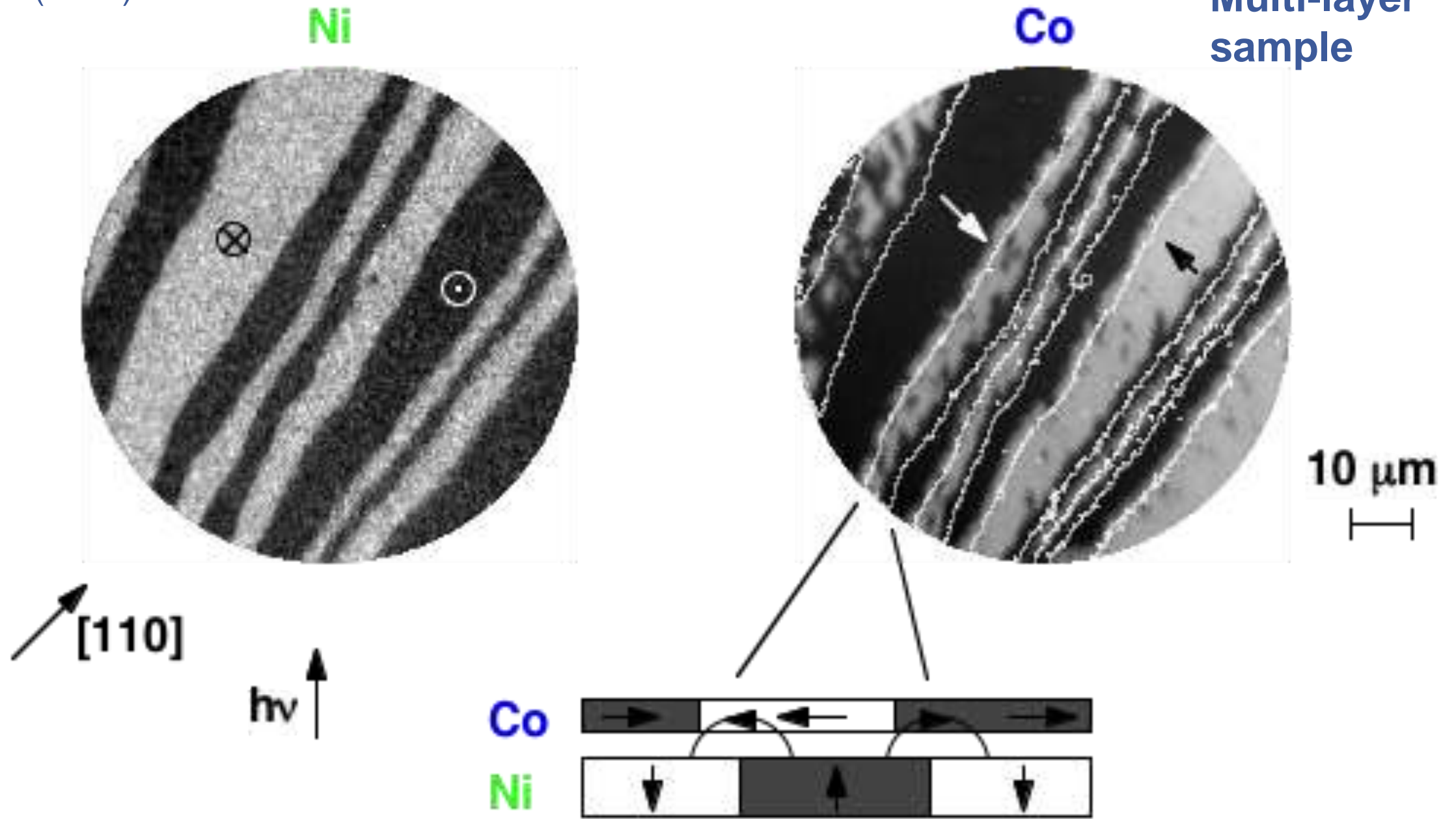
Element selectivity - local magnetic coupling



W. Kuch et al., Phys. Rev. B
67, 214403 (2003)



Multi-layer
sample

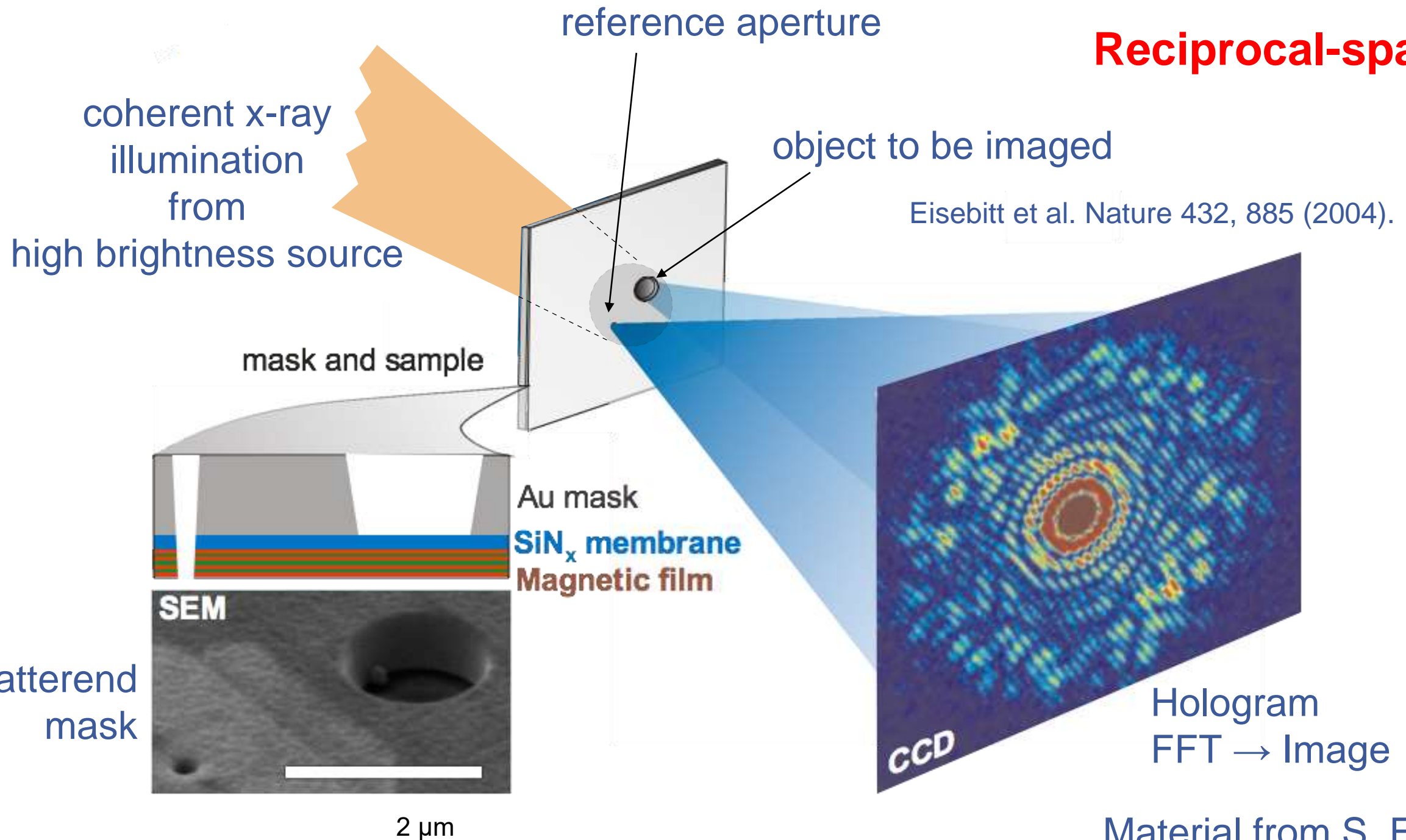


Material from W. Kuch, FU Berlin, Germany



- **Element selectivity (multilayers)**
- Sample can be in air or vacuum
- Spatial resolution below 15 nm
- Sensitivity to out-of-plane magnetization (transmission, but tilting possible)
- Imaging with applied magnetic fields
- X-ray damage
- Sample must allow transmission of x-rays

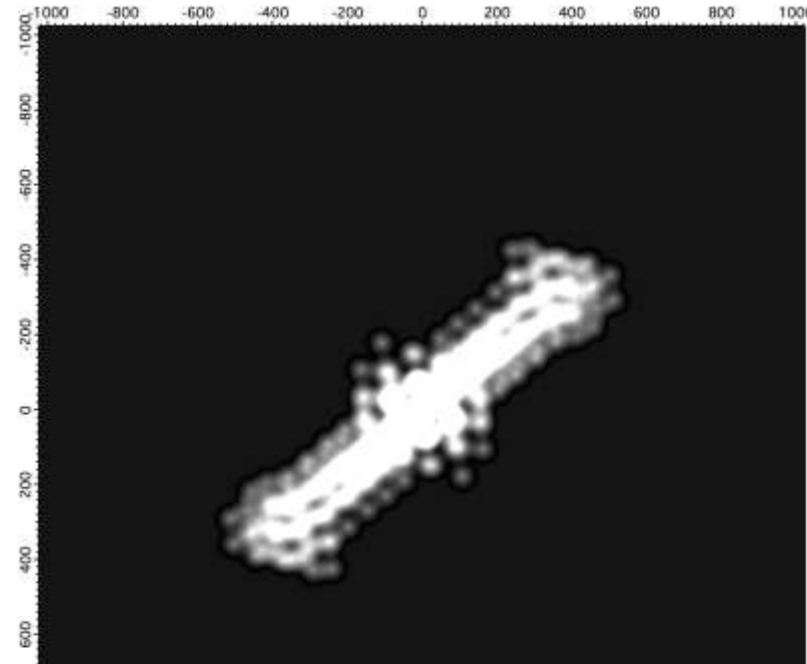
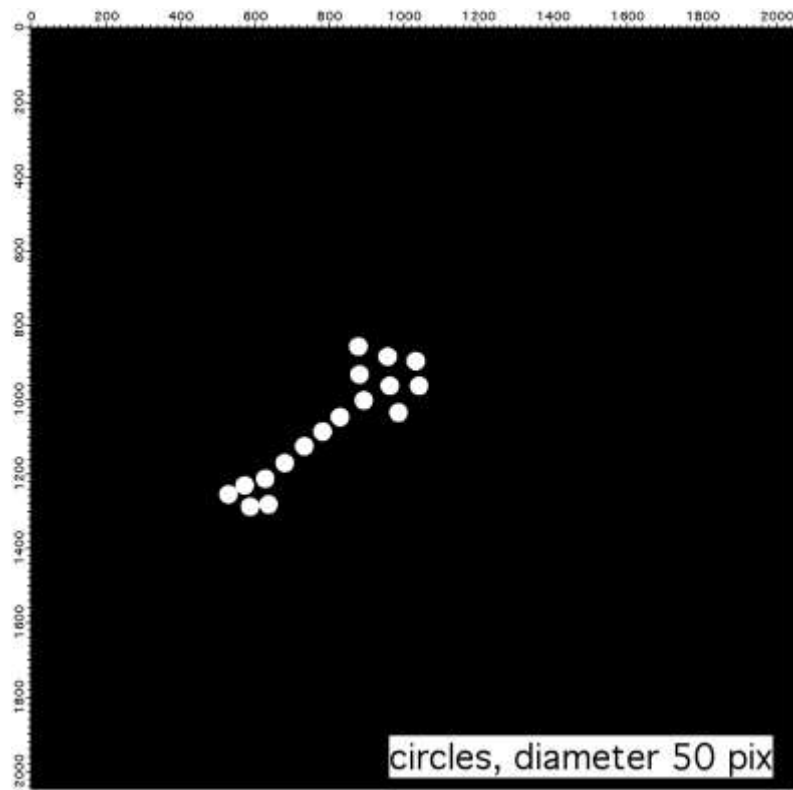
Reciprocal-space!



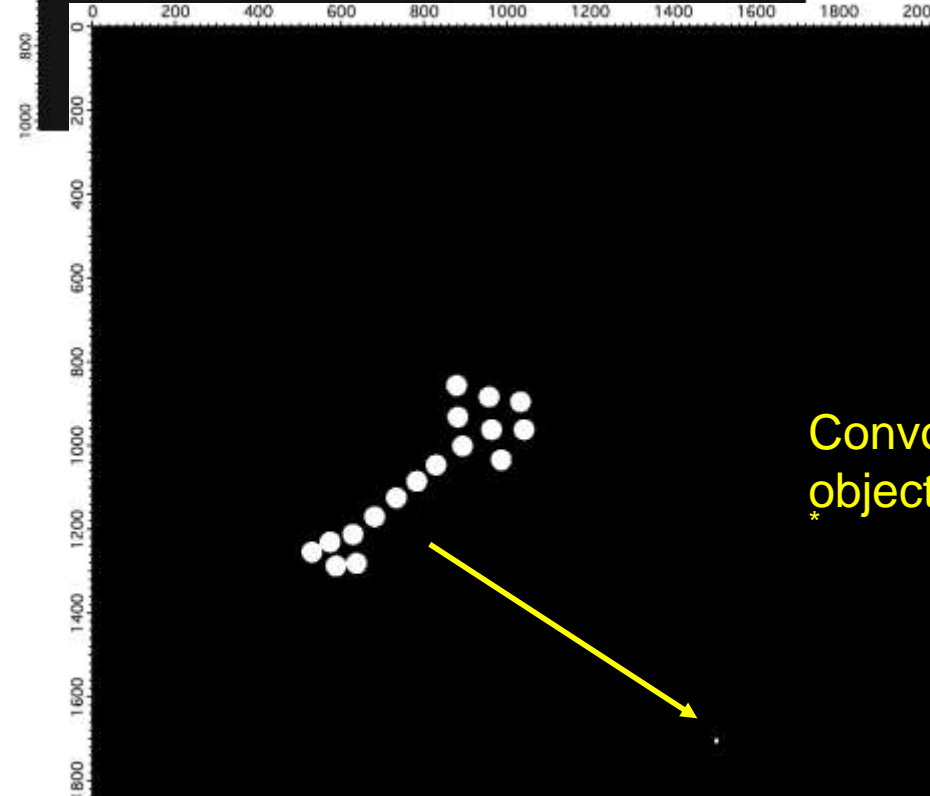
- **Coherent X-rays**
- **Object and reference locked (high stability to detect small signals)**

Material from S. Eisebitt,
Max-Born-Institut,
Germany

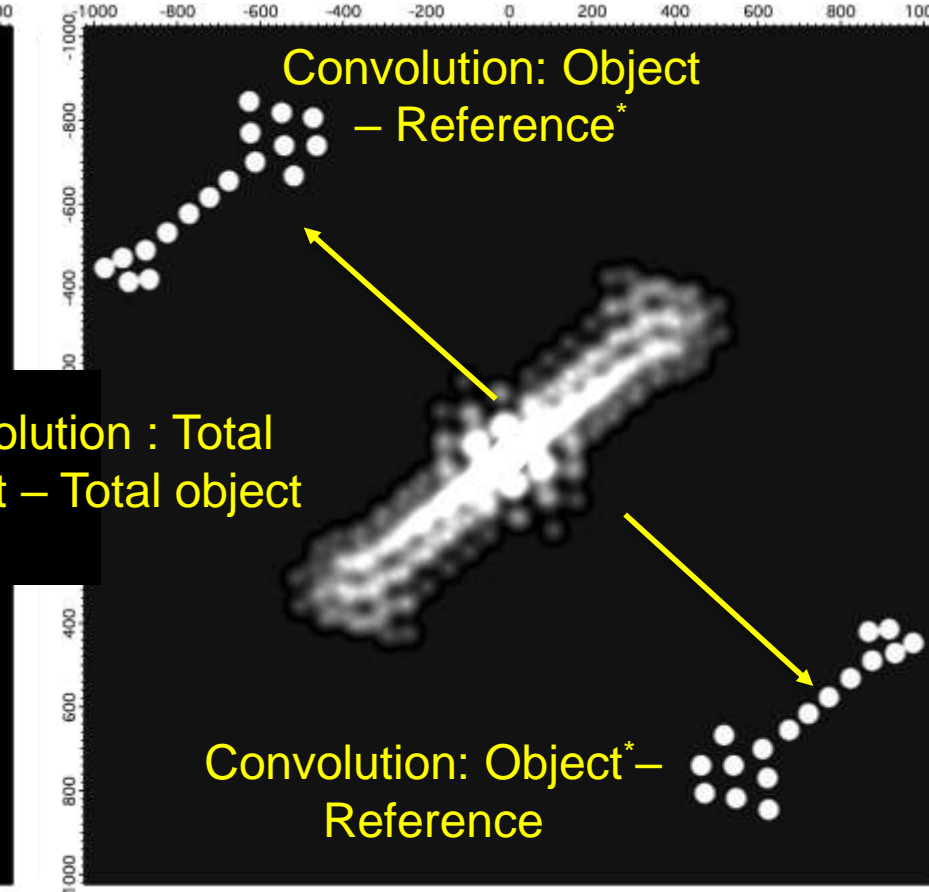
Image formation



Material from S. Eisebitt,
Max-Born-Institut,
Germany



A small additional point in the object acts as a source for a reference beam



Reference aperture makes the image easily interpretable.

One directly obtains an image of the object!

Convolution : Total object - Total object*

Convolution: Object - Reference*

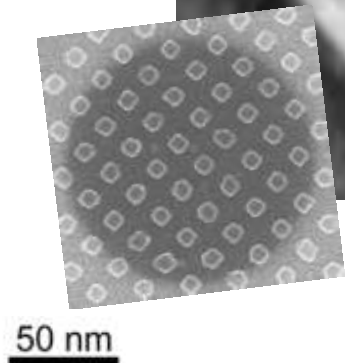
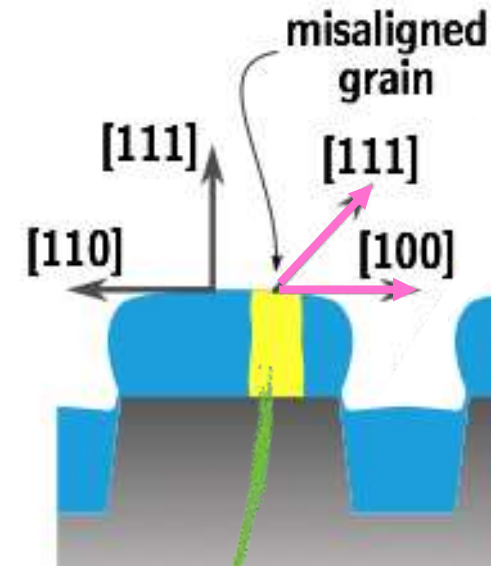
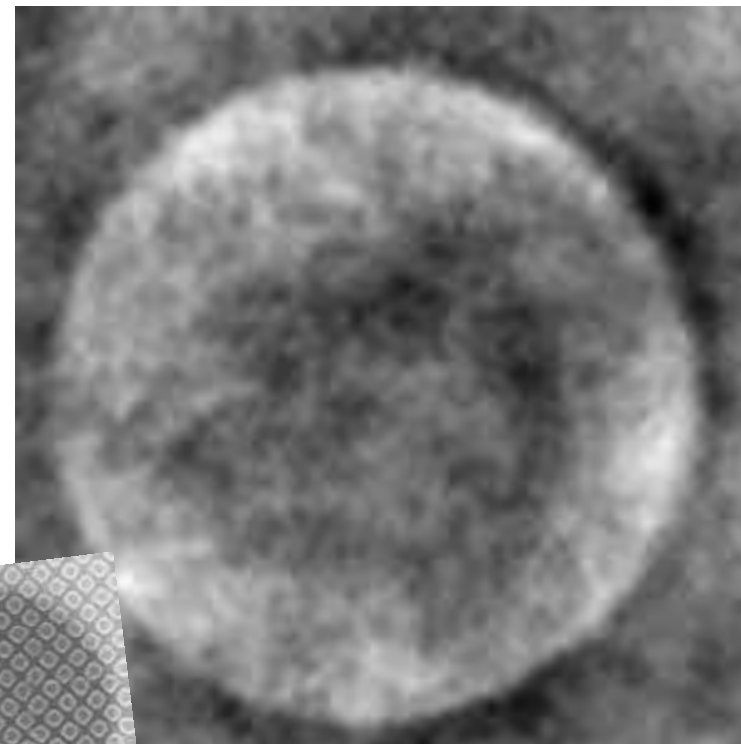
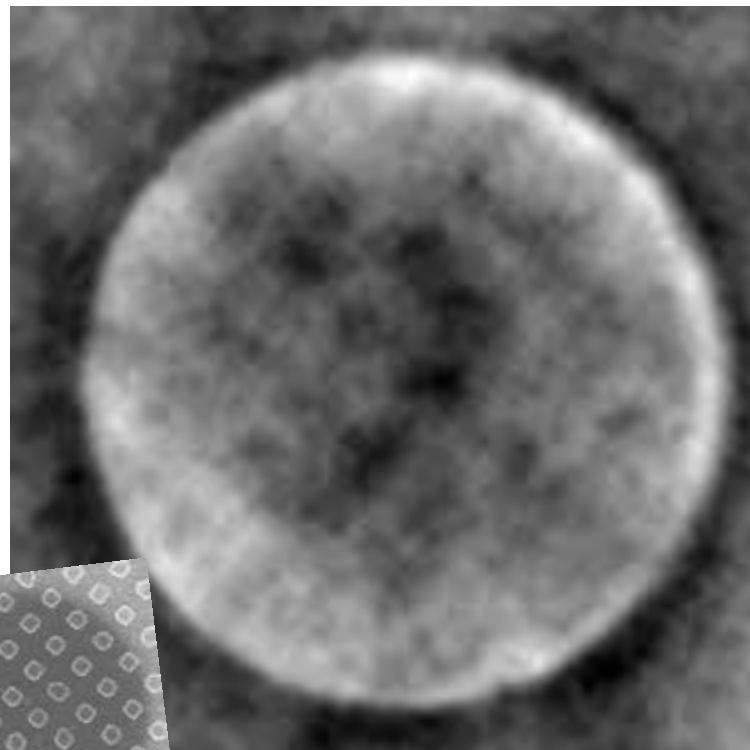
Convolution: Object* - Reference

Functionality of magnetic nanomaterials



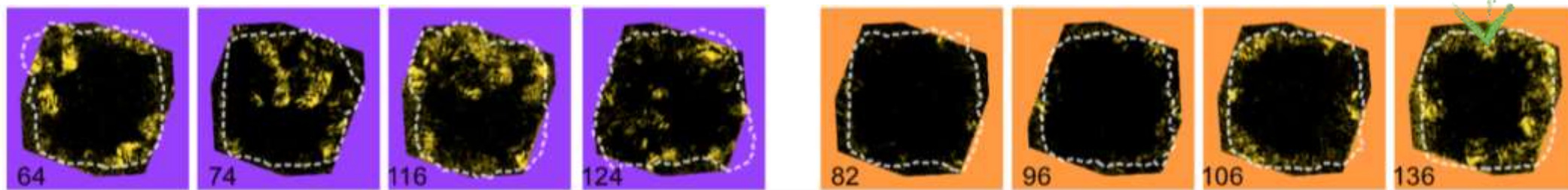
Prototype hard drive data storage media (Hitachi GST)
Magnetic contrast via XMCD (Co L₃)

Magnetization switching in external B-field



easy switchers

hard switchers



Presence and position of misaligned grains in a 80x80 nm bit-square (yellow) determine switching properties

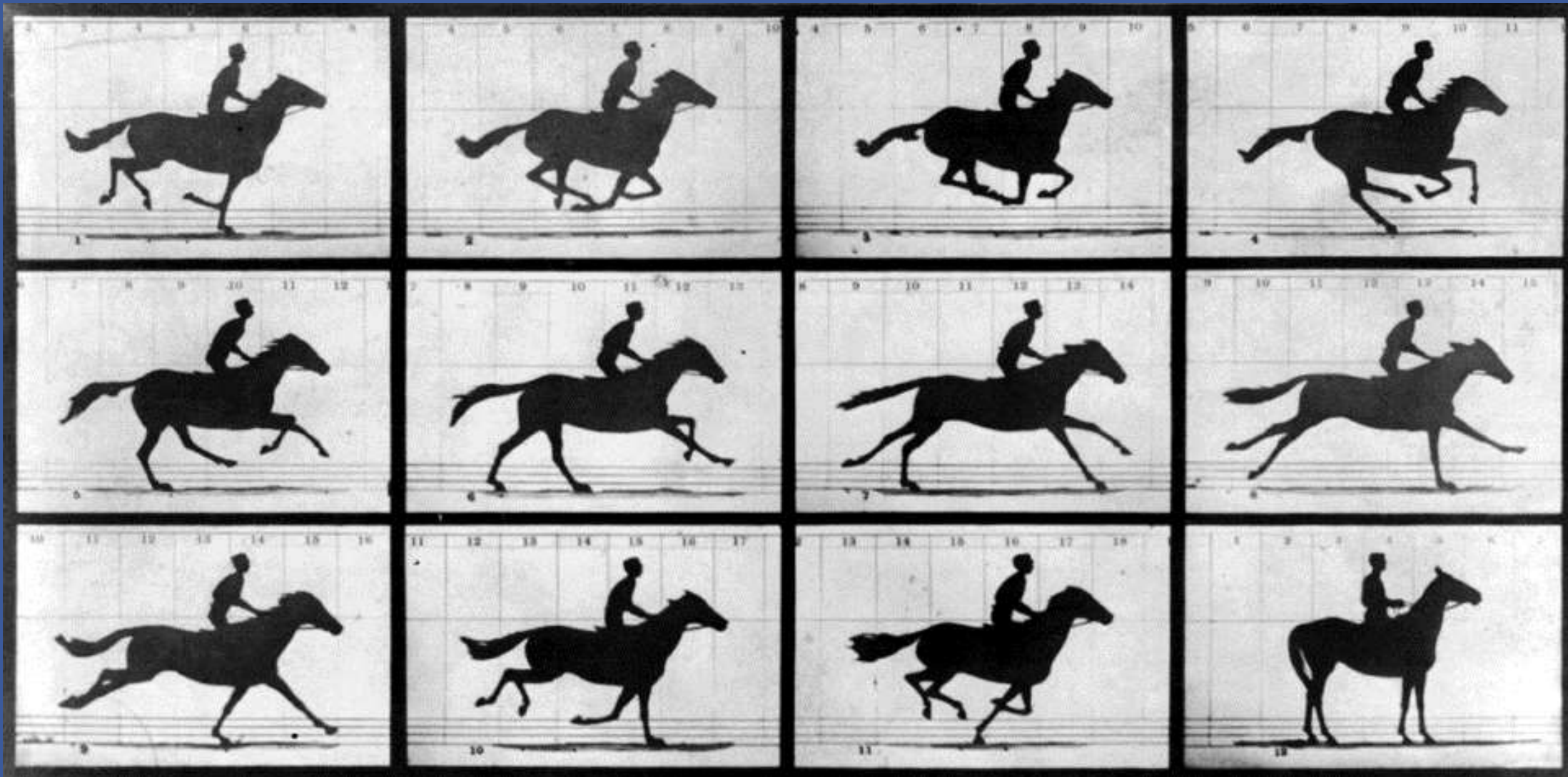
B. Pfau et al, APL **99**, 062502 (2011) & APL **105**, 132407 (2014)

Material from S. Eisebitt, Max-Born-Institut, Germany



- **Current spatial resolution 20 nm (best) – 50 nm (every day)**
- **Atomic, chemical, magnetic sensitivity via resonant scattering**
- **Extreme stability to track small effects**
- **Requires coherent x-ray illumination**

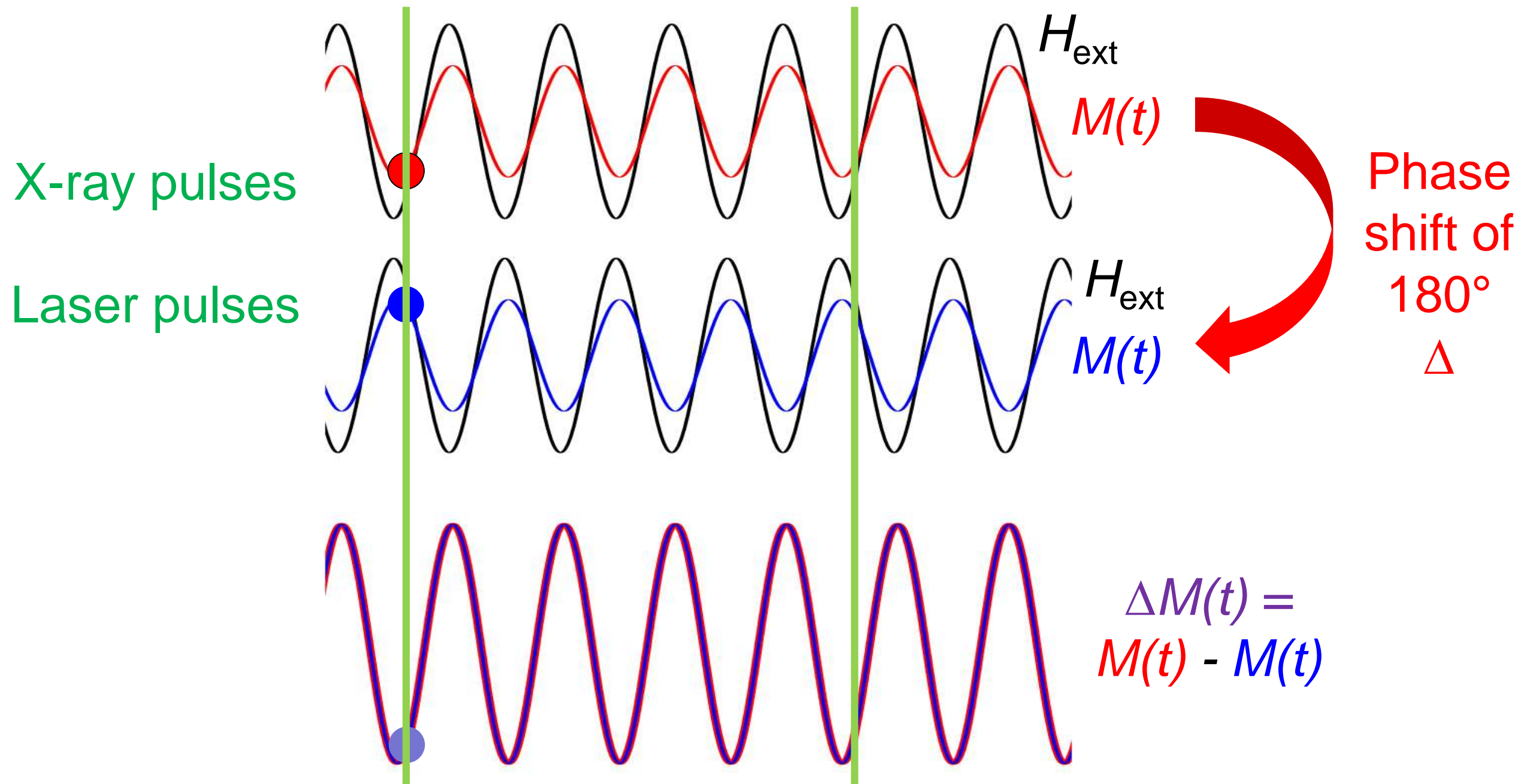
Mostly stroboscopic imaging



Magneto-optical methods capable of dynamic imaging

- X-ray based methods
- MOKE microscopy

Stroboscopic imaging (differential mode)

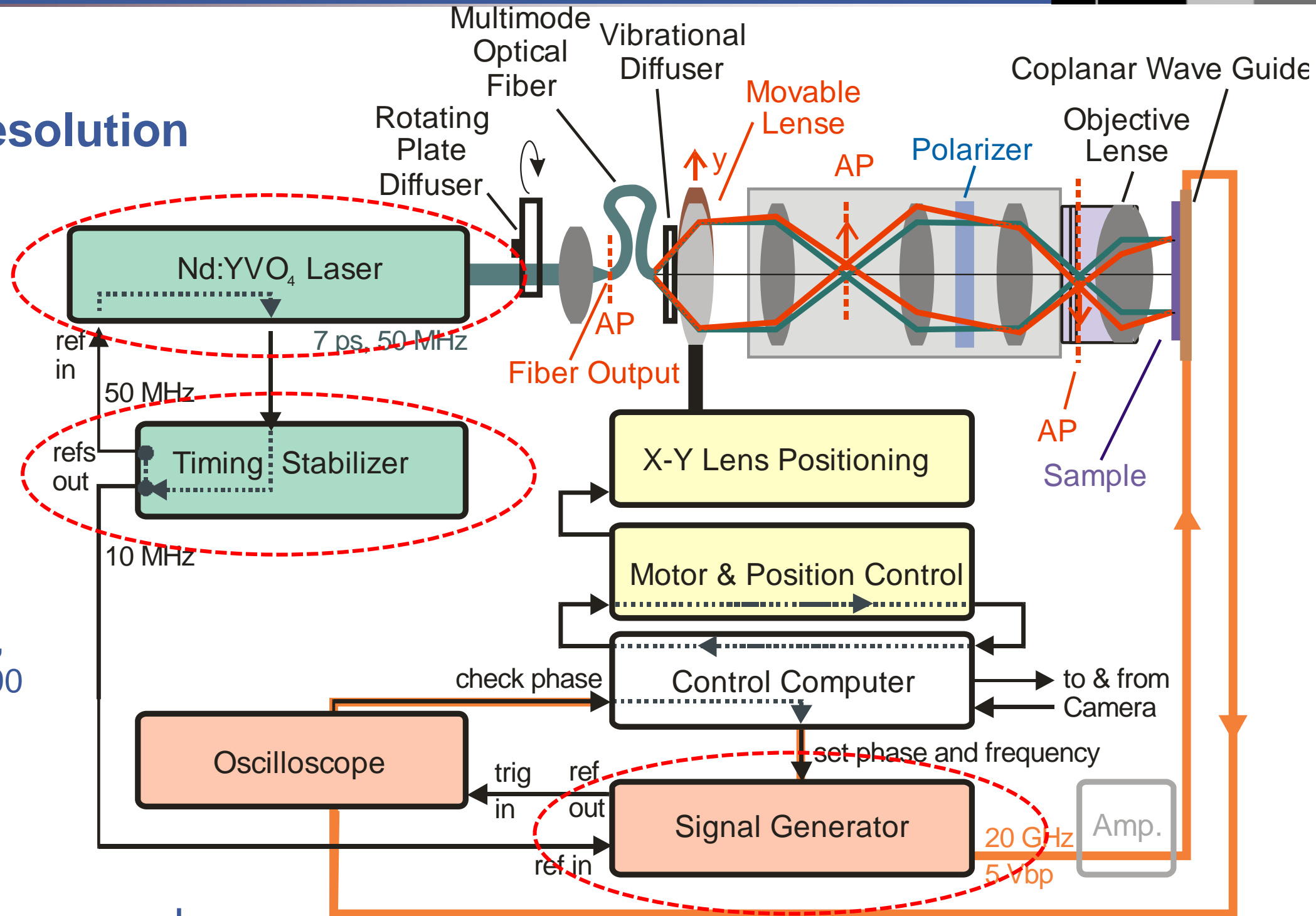


Accumulation of many repeatable events!

Time-resolved magneto-optical microscopy



- 10 ps time resolution



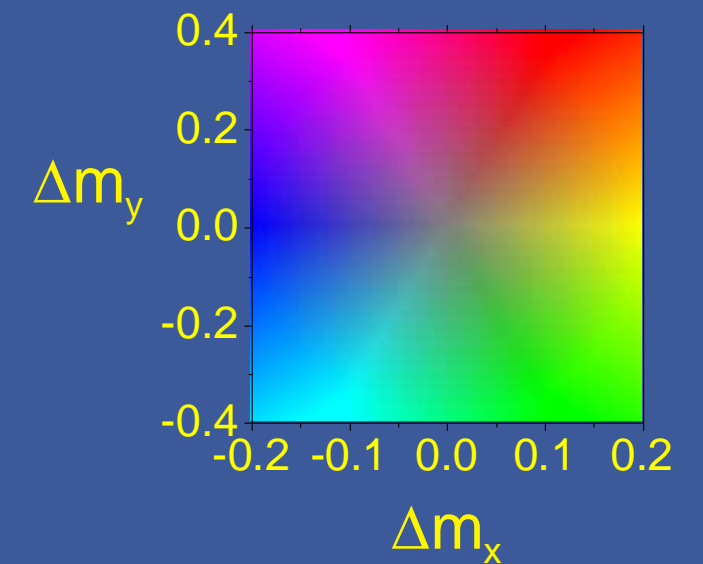
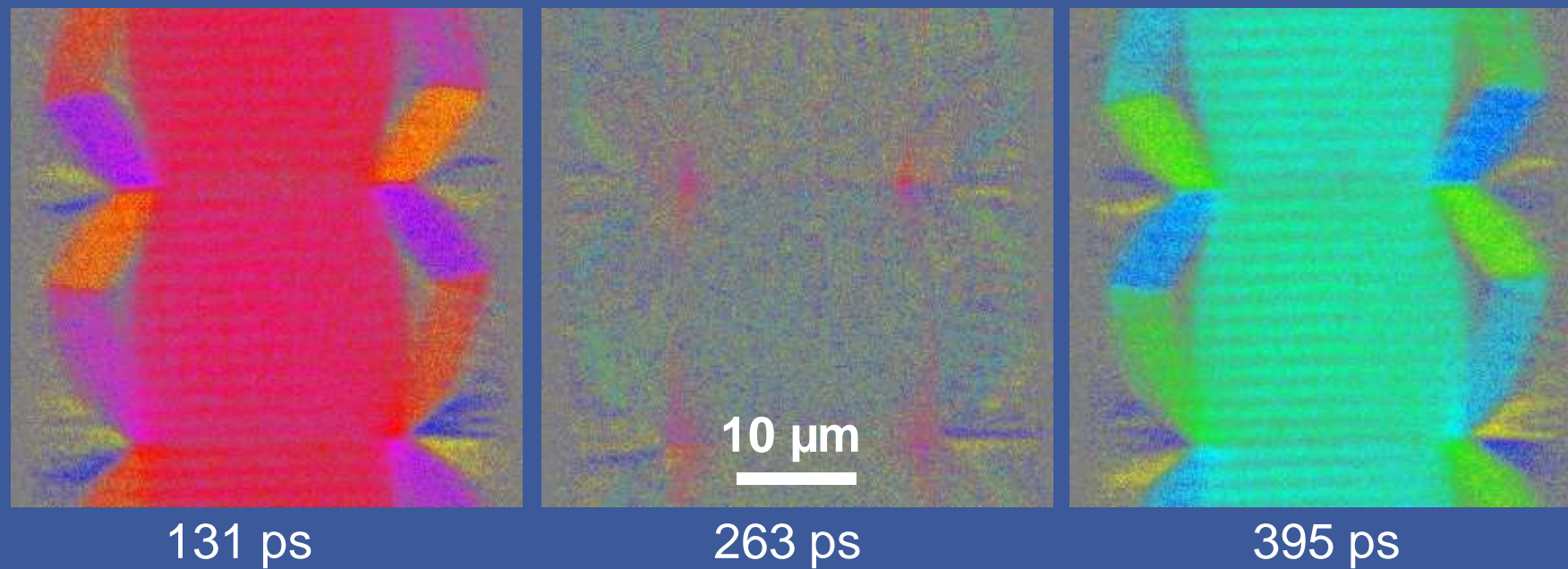
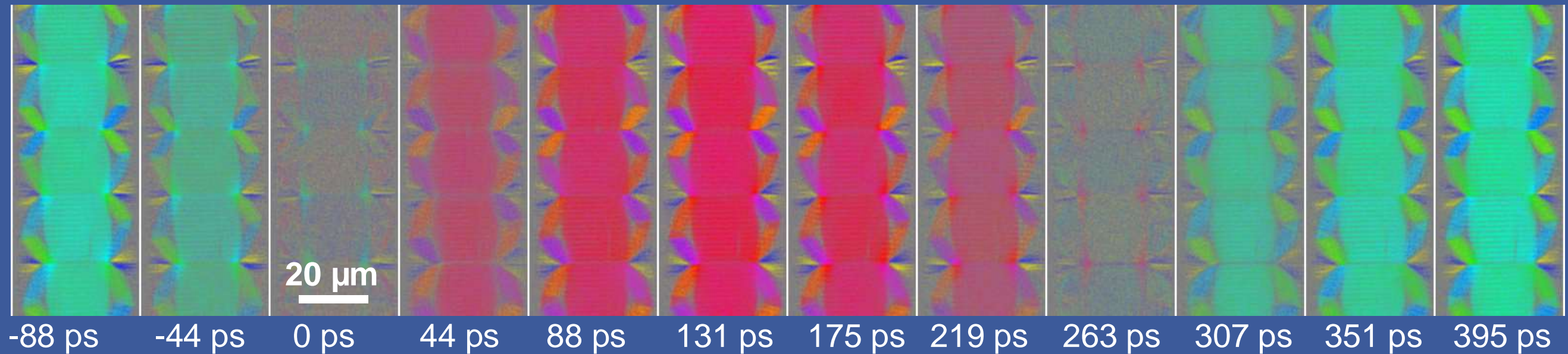
R. Holländer et al.,
JMMM 432, 283–290
(2017)

- Stroboscopic pump-probe
- 10⁷ pump-probe events/image
- Only fully repeatable dynamics

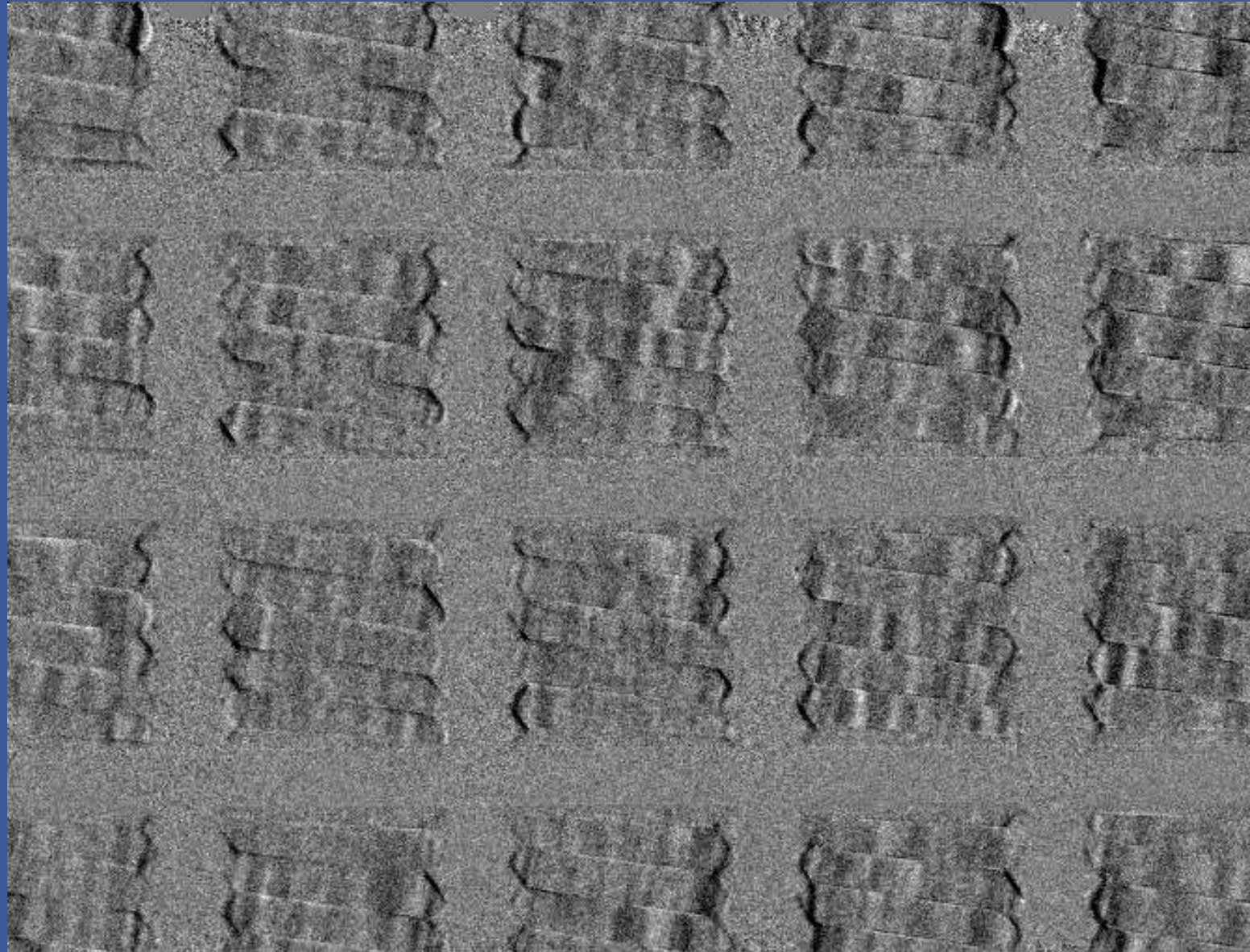
Time-resolved quantitative MO imaging @ 2 GHz



R. Holländer et al., JMMM 432, 283–290 (2017)



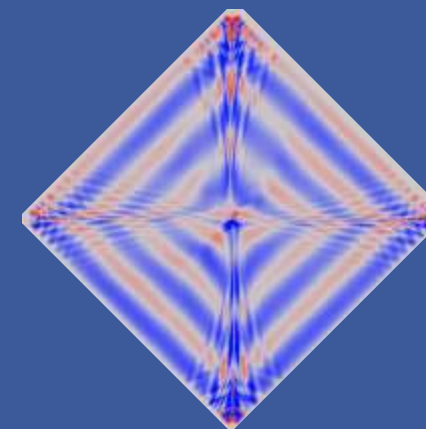
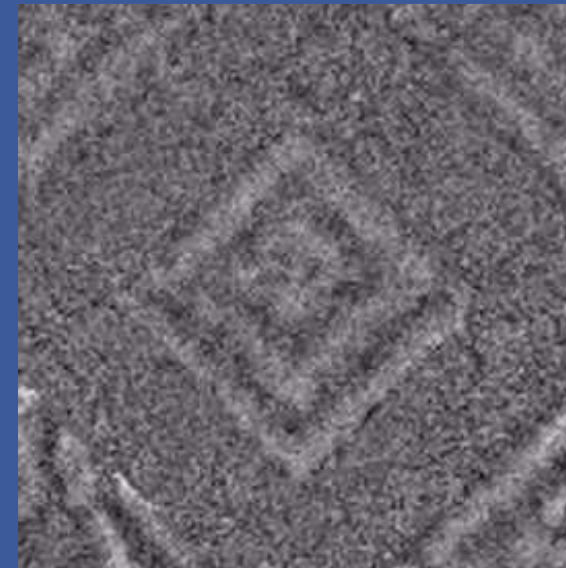
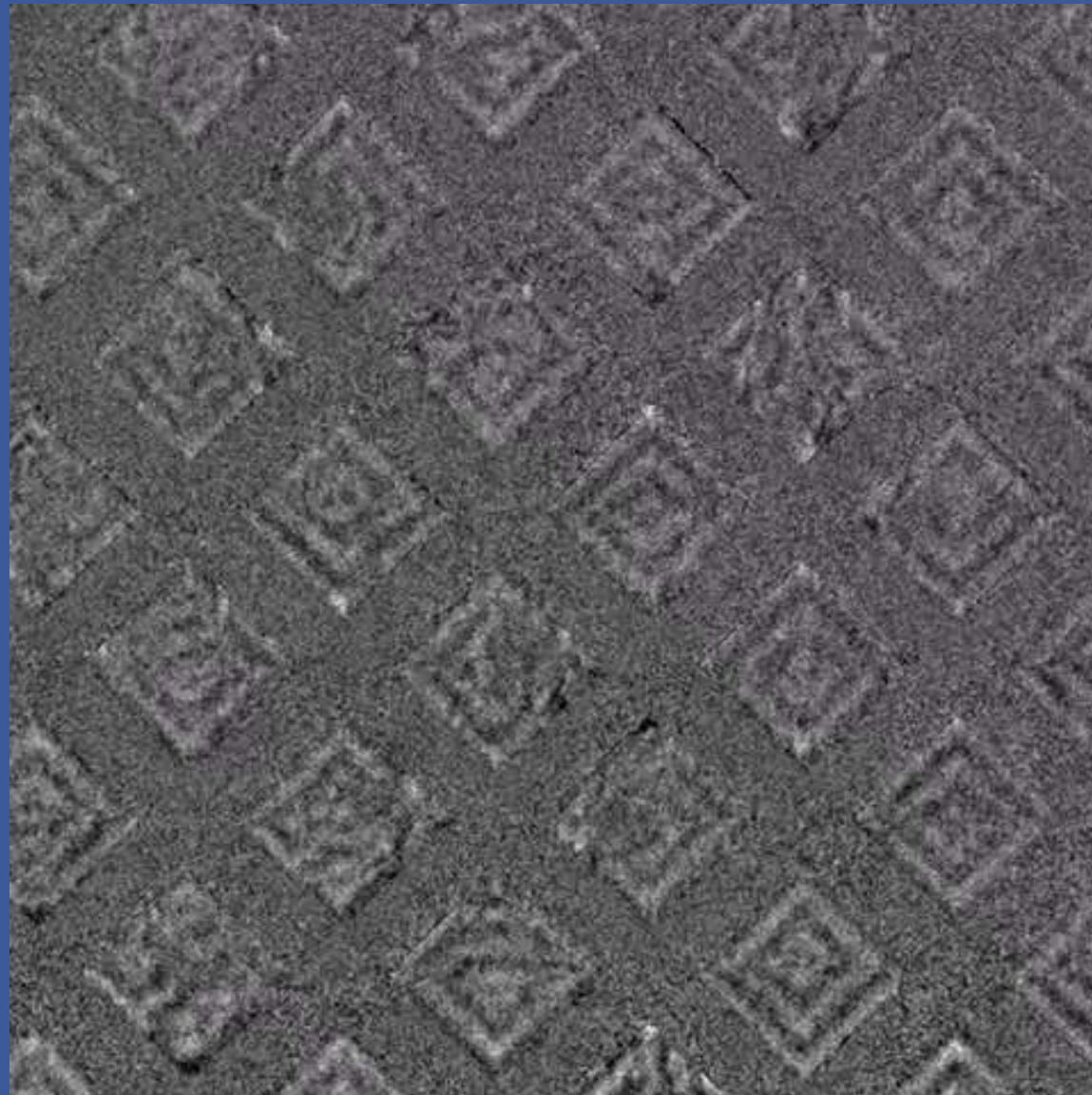
Dynamic response of Landau structure



- **Domain wall induced generation of spin waves from local edge resonances**

B. Mozooni, J. McCord, APL 107, 042402 (2015)

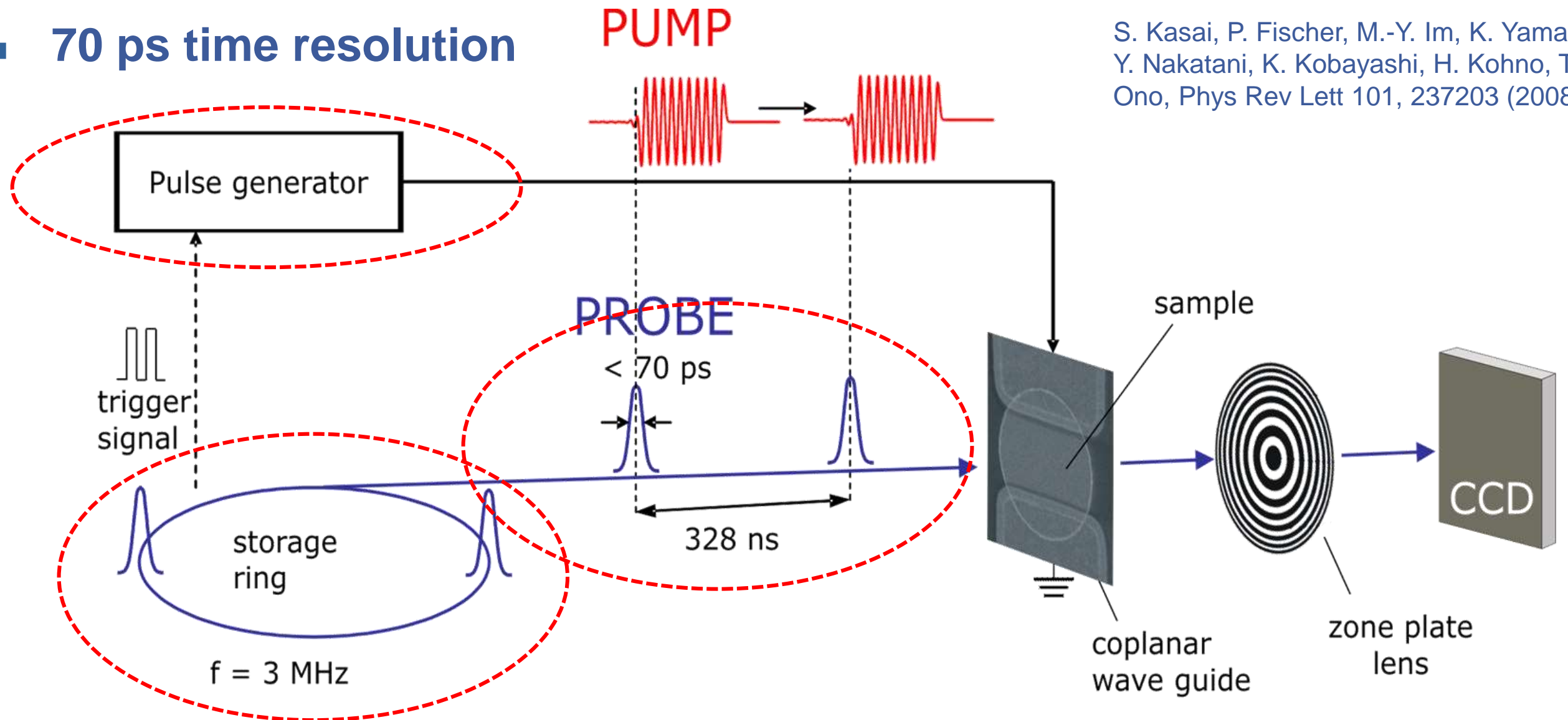
Excitations of spin waves in $\text{Ni}_{81}\text{Fe}_{20}$ @ 4 GHz



- **Antennaless generation of spin waves from local edge resonances**

M. Lohmann et al., accepted for JMMM (2017)

70 ps time resolution



S. Kasai, P. Fischer, M.-Y. Im, K. Yamada, Y. Nakatani, K. Kobayashi, H. Kohno, T. Ono, Phys Rev Lett 101, 237203 (2008)

- Stroboscopic pump-probe
- 10^8 pump-probe events/image
- Only fully repeatable dynamics

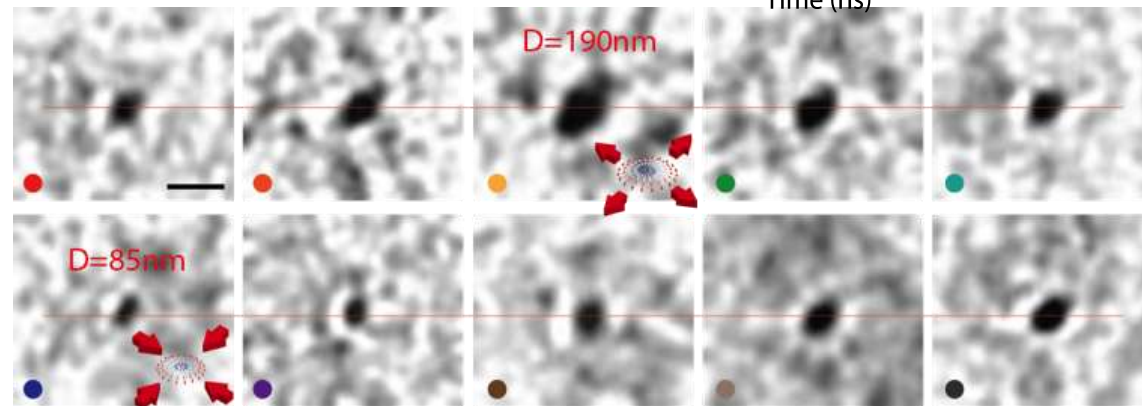
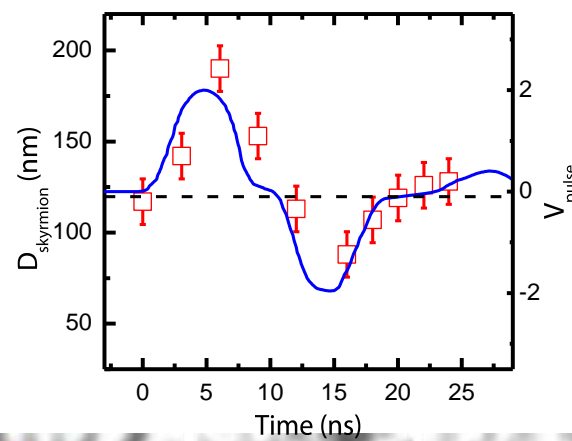
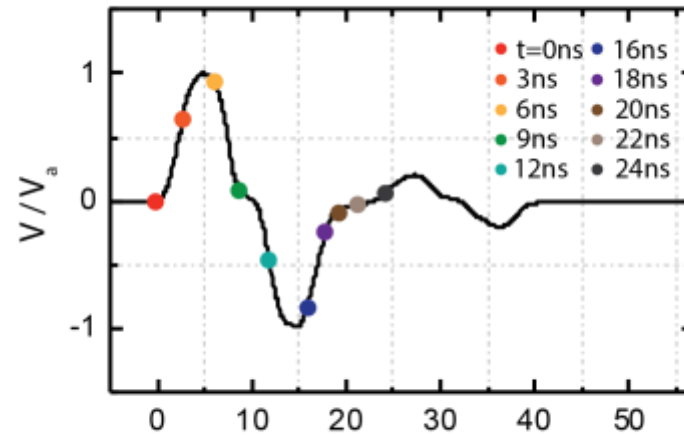
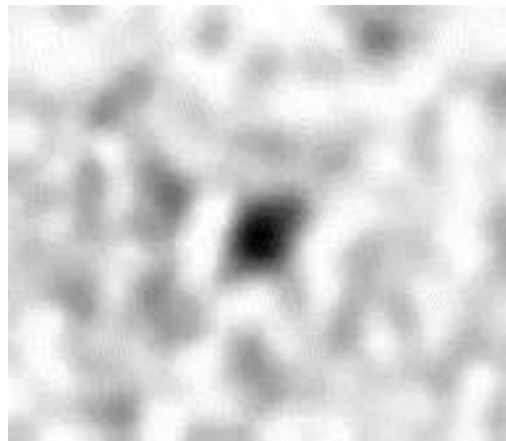
Material from P. Fischer, Lawrence Berkeley Natl. Lab, USA

Spin-orbit torque driven skyrmion dynamics



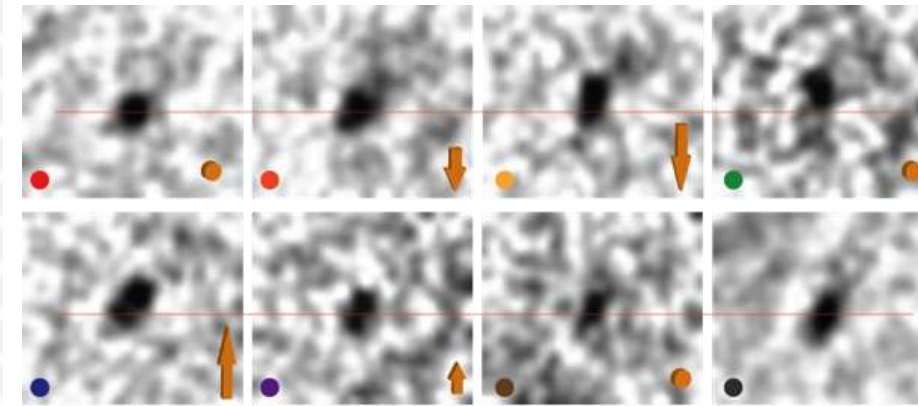
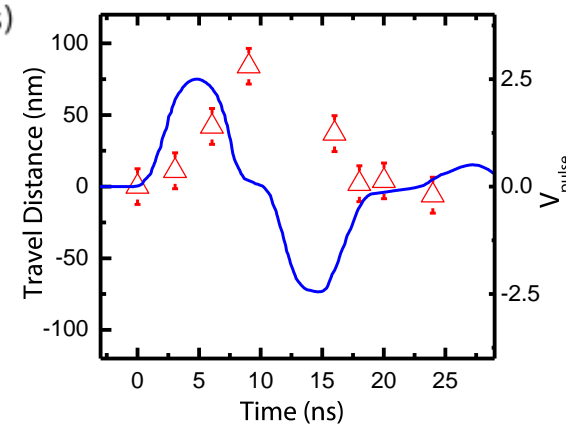
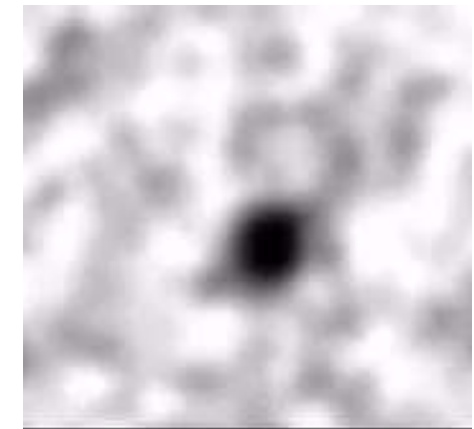
S. Woo et al. Nature Comm. (2017) accepted

2A



breathing mode

2.5A

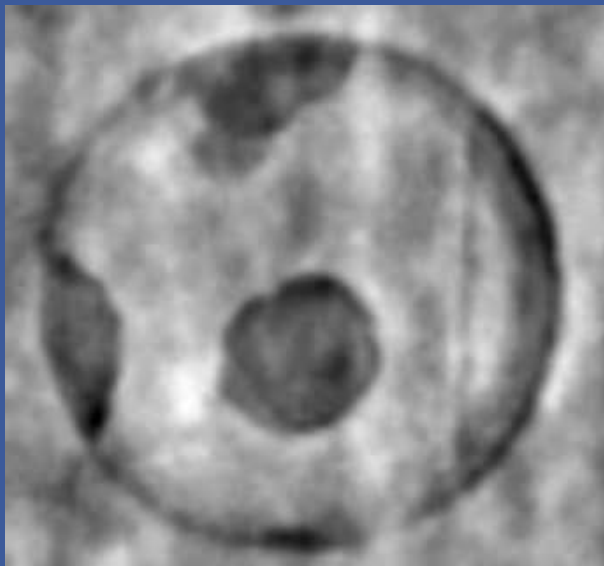


current induced translation

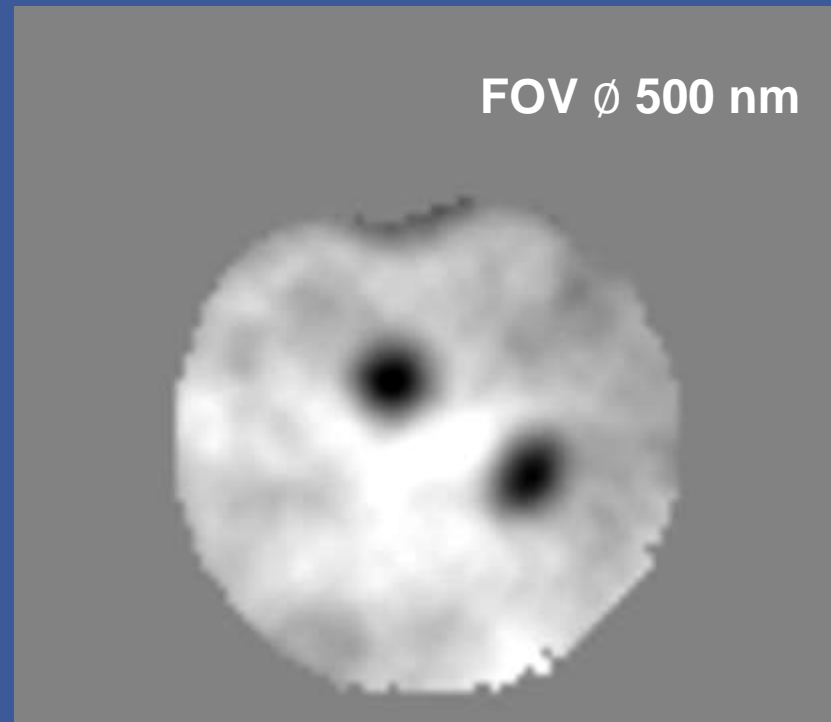
Material from P. Fischer, Lawrence Berkeley Natl. Lab, USA

Skyrmions as information carriers

Skyrmion fine structure



FOV \varnothing 1 μm
resolution < 20 nm

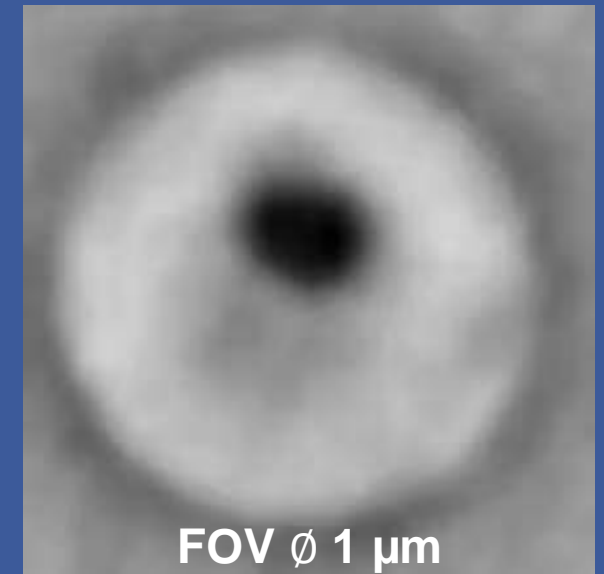


FOV \varnothing 500 nm

Skyrmion intrinsic GHz dynamics

F. Büttner et al., Nature Physics 11, 225 (2015).

Skyrmion motion

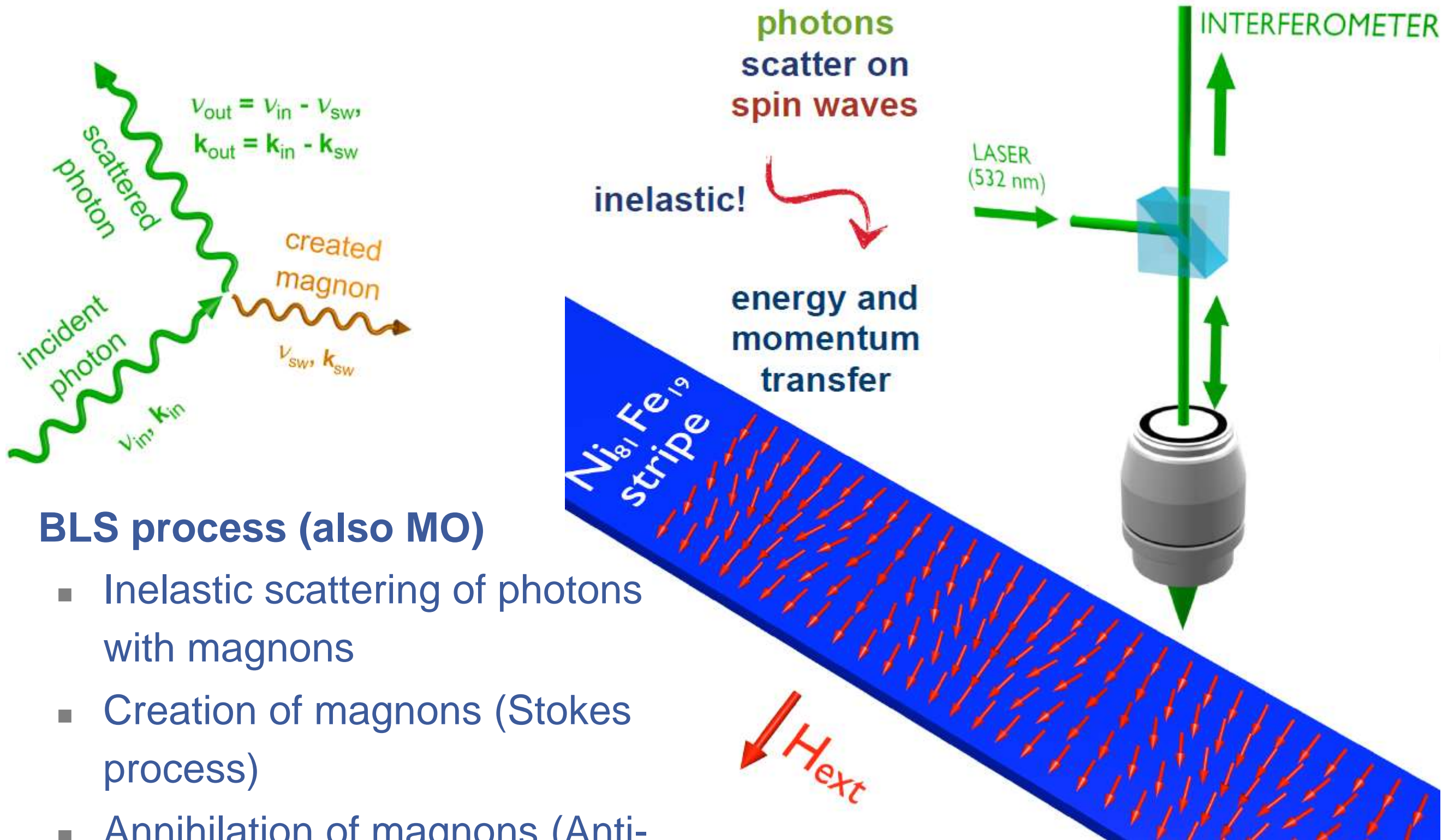


FOV \varnothing 1 μm

F. Büttner et al. (submitted,
arXiv 1705.01927)

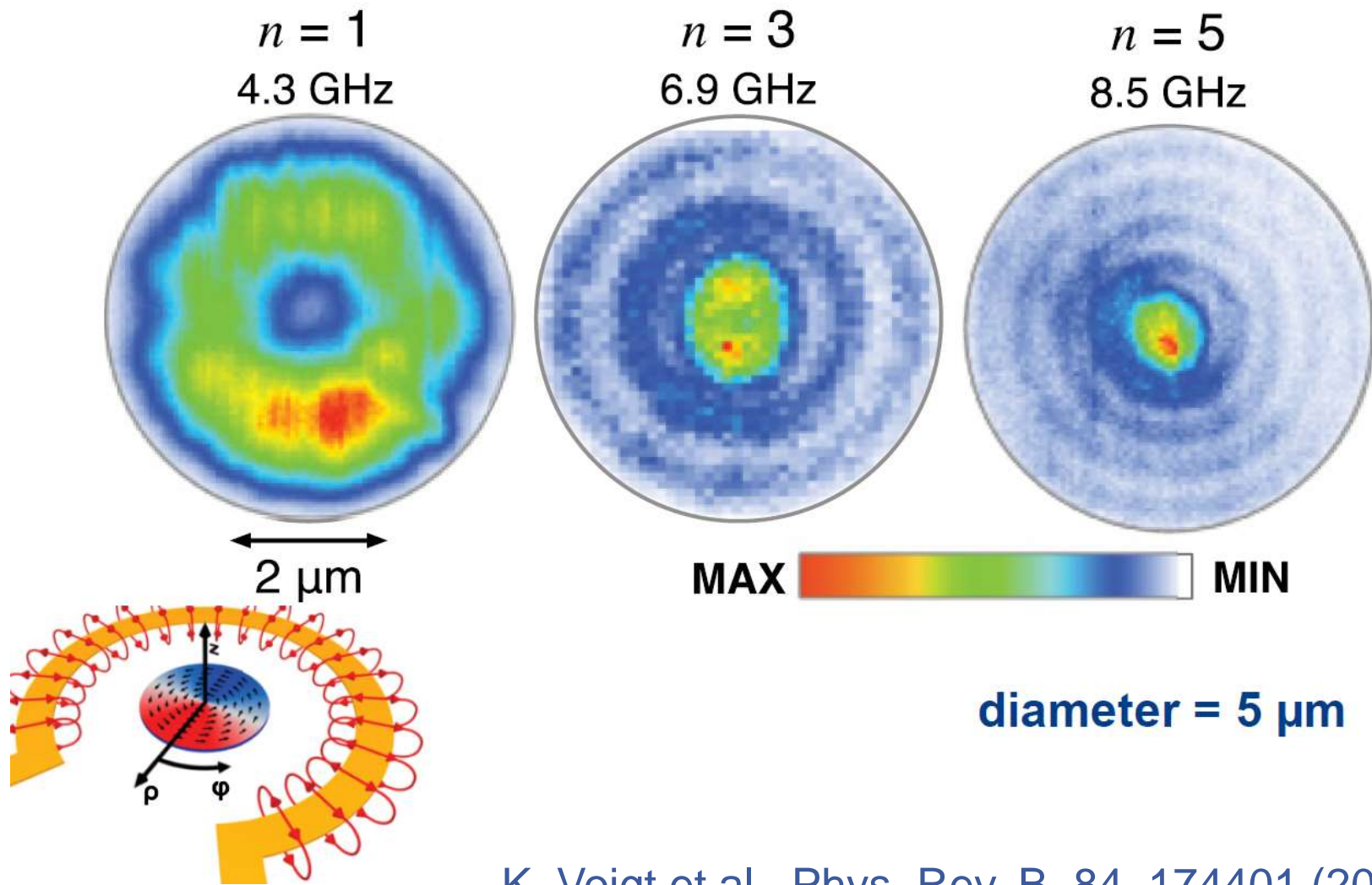
15 repeats of Pt(2.7 nm)/Co₆₀Fe₂₀B₂₀(0.8 nm)/MgO(1.5 nm)

Material from S. Eisebitt, Max-Born-Institut, Germany

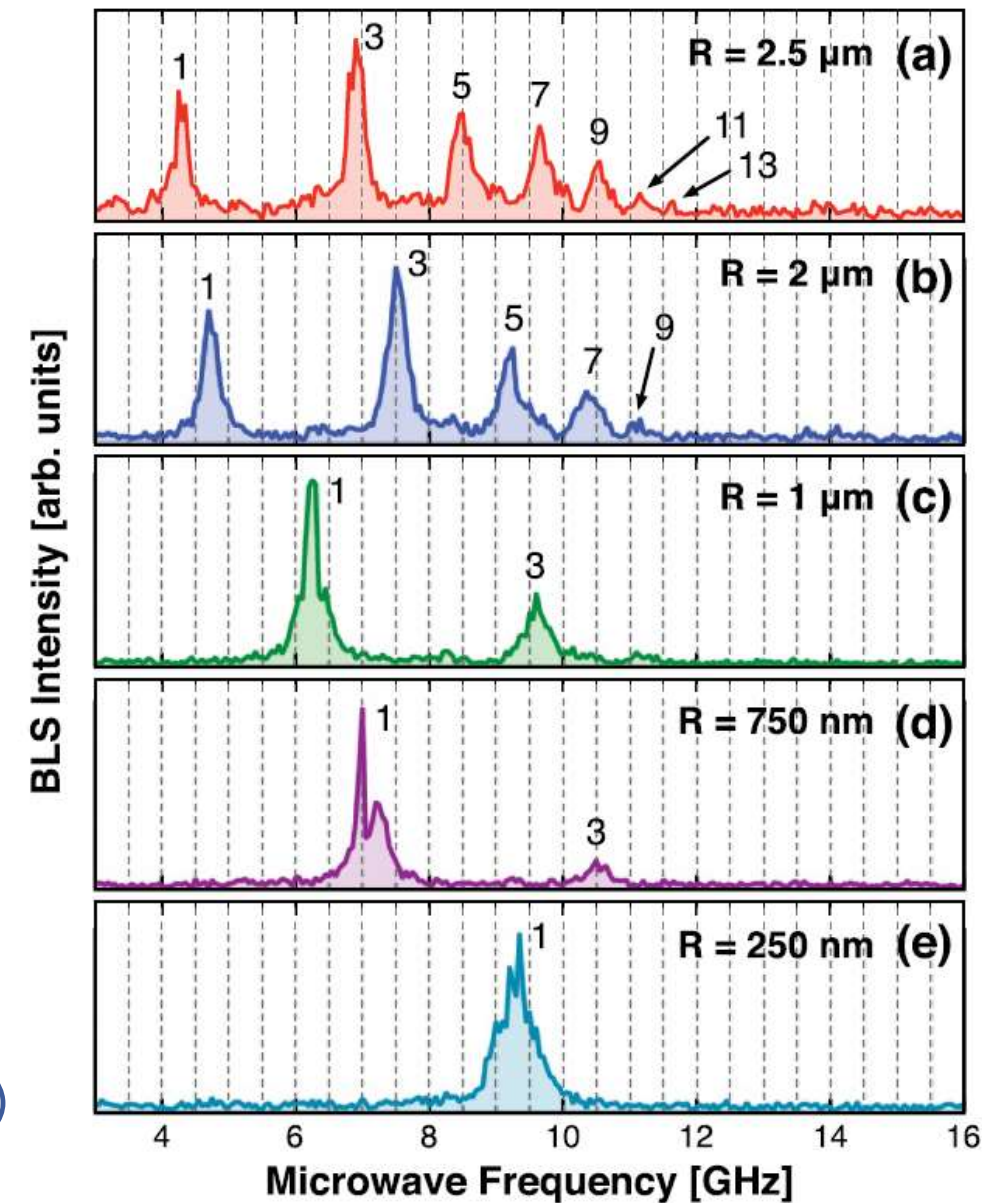


Material from H. Schultheiss, HZDR, German

Brillouin light scattering microscopy



K. Voigt et al., Phys. Rev. B. 84, 174401 (2011)



Imaging of spin-wave phenomena (up to THz!).

Material from H. Schultheiss, HZDR, Germany



... papers, papers, papers ...

- McCord, Jeffrey. "Progress in magnetic domain observation by advanced magneto-optical microscopy." *Journal of Physics D: Applied Physics* 48.33 (2015): 333001.
- Fischer, Peter, and Hendrik Ohldag. "X-rays and magnetism." *Reports on Progress in Physics* 78.9 (2015): 094501.
- Krishnan, Kannan M. *Fundamentals and applications of magnetic materials*. Oxford University Press, 2016.
- A. Hubert, R. Schäfer. *Magnetic domains: the analysis of magnetic microstructures*. Springer Science & Business Media, 2008.